UNIVERSITÉ DE STRASBOURG

ÉCOLE DOCTORALE SCIENCES DE LA TERRE ET DE L'ENVIRONNEMENT

UMR7516

THÈSE présentée par :

Pauline CHENIN

soutenue le : 22 **Janvier 2016**

pour obtenir le grade de : **Docteur de l'université de Strasbourg**

Discipline/ Spécialité : Sciences de la Terre

Unravelling the impact of inheritance on the Wilson Cycle: A combined mapping and numerical modelling approach applied to the North Atlantic rift system

THÈSE dirigée par :

M. MANATSCHAL Gianreto	Professeur de l'Université de Strasbourg

RAPPORTEURS :

M. ANDERSEN Torgeir B.	Professeur de l'Université d'Oslo
M. SCHMALHOLZ Stefan	Professeur de l'Université de Lausanne

AUTRES MEMBRES DU JURY :

M. DEWEY John F.	Professeur émérite de l'Université d'Oxford
M. SKOGSEID Jakob	Docteur, Statoil ASA Stavanger

École doctorale des Sciences de la Terre (ED 413)
Institut de physique du Globe de Strasbourg (UMR 7516)

THÈSE

Pour l'obtention du grade de

DOCTEUR DE L'UNIVERSITÉ DE STRASBOURG

Faculté des Sciences de la Terre

Présentée par

Pauline CHENIN

Unravelling the impact of inheritance on the Wilson Cycle: A combined mapping and numerical modelling approach applied to the North Atlantic rift system

Directeur de thèse : **Pr. Gianreto MANATSCHAL**
En collaboration avec : **Pr. Luc L. LAVIER**

Soutenue le 22 Janvier 2016
Devant la Commission d'Examen

Pr. Torgeir B. ANDERSEN	University of Oslo	Rapporteur, Président du Jury
Pr. Stefan SCHMALHOLZ	Université de Lausanne	Rapporteur (excusé)
Pr. Othmar MUNTENER	Université de Lausanne	Rapporteur remplaçant
Pr. John F. DEWEY	University of Oxford	Examinateur
Dr. Jakob SKOGSEID	Statoil ASA Stavanger	Examinateur
Pr. Luc L. LAVIER	University of Texas at Austin	Invité (excusé)
M. Duncan ERRATT	ExxonMobil Leatherhead	Invité
Pr. Karel SCHULMANN	Université de Strasbourg	Invité

Remerciements

En premier lieu, je tiens à remercier du fond du coeur mon superviseur Gianreto Manatschal, pour m'avoir confié ce sujet et accompagné dans cette entreprise. Tu as su me guider, tout en me laissant la liberté de façonner une thèse qui me ressemble. Je te suis infiniment reconnaissante pour ta disponibilité et ton écoute, ainsi que pour les connaissances, conseils et encouragements que tu m'as prodigués tout au long de ces trois années.

Je souhaite aussi exprimer ma gratitude à Luc Lavier pour avoir rendu possible ma visite à *l'Institute for Geophysics* de l'Université du Texas à Austin, et pour le temps qu'il m'a consacré sur place. Ma reconnaissance va également à Suzon Jammes pour son accueil chaleureux, tant du point de vue professionnel que personnel. Ce séjour de 7 mois a été financé par la commission franco-américaine dans le cadre d'une bourse Fulbright. Je remercie les différents acteurs de ce programme de m'avoir permis de vivre une aventure extraordinairement enrichissante aux Etats-Unis.

Les recherches menées au cours de cette thèse s'inscrivent dans le cadre du projet CEIBA (*Center of Excellence in Basin Analysis*) financé par la compagnie Exxon-Mobil. Je remercie Garry Karner, porteur et ardent défenseur du projet, ainsi que Christopher Johnson, pour leur regard critique et constructif sur mon travail aux cours de nos réunions annuelles.

Je tiens également à témoigner ma gratitude aux autres participants du projet CEIBA, en particulier à Othmar Müntener et Suzanne Picazo pour les nombreux échanges scientifiques que nous avons eu, ainsi qu'à Daniel Stöckli et Emily Cooperdock dont les commentaires ont, eux aussi, fertilisé les discussions au sein du projet.

Je suis reconnaissante envers Karel Schulmann pour les discussions que nous avons eu au sujets des Variscides, et pour les conseils qu'il m'a donné face à la complexité de cet orogène.

Je remercie également Julie Tugend pour sa relecture critique de mon manuscrit, ainsi que Benoît Petri, Isabelle Haupert, Morgane Gillard et Michael Nirrengarten pour les discussions scientifiques (ou pas) que nous avons eu au cours de ces années passées ensemble.

Enfin, je souhaite témoigner ma gratitude aux membres de mon entourage qui, en se montrant attentionnés, positifs et secourables, ont largement contribué au ravissement qu'ont été, pour moi, ces trois années. En particulier, un grand merci aux "auteurs de l'auteur" pour la relecture de ce "charabia scientifique" qu'est le résumé en français du manuscrit et pour l'organisation sans faille du pot de thèse. Merci aussi, à ma "petite" soeur pour sa relecture du résumé français et ses coups de pouces sur le plan graphique.

Contents

Résumé détaillé **1**

1 Etat de l'art et limites actuelles 3
2 Objectifs de cette thèse 7
3 Choix de la zone d'étude 10
4 Choix des méthodes 10
5 Contexte géologique de la zone d'étude : 12
5.1 La fragmentation de Rodinia 12
5.2 Les orogenèses Calédonienne et Varisque 12
5.2.1 Océans et continents impliqués 12
5.2.2 Orogenèses et effondrements post-orogéniques 16
5.3 Les système de rift Alpin et Nord Atlantique 18
5.4 L'orogenèse Alpine en Europe de l'Ouest 21
5.4.1 Les Alpes *sensu stricto* 21
5.4.2 Les Pyrénées 21
6 Synthèse 22
6.1 Chapitre I 22
6.2 Chapitre II 31
6.3 Chapitre III 38
7 Discussion 43
8 Conclusions & Perspectives : Vers un modèle général 49
Références bibliographiques 51

General introduction **65**
1 State of the art and unanswered questions 67
2 Aim of this thesis 71
3 Choice of the study area 73
4 Choice of the methods 75

General geological setting **77**
1 General overview 79
2 Pre-orogenic paleogeography 81
2.1 The Iapetus Ocean 83
2.2 The Tornquist Seaway 84
2.3 The Rheic Ocean 84
2.4 The Saxothuringian ‘ocean’ 85
2.5 The Medio-European ‘ocean’ 86
2.6 The Rhenohercynian ‘ocean’ 86
3 The Caledonides and the Variscides 87
3.1 The Caledonian orogeny and collapse 87
3.2 The Variscan orogeny and collapse 90
4 The Alpine Tethys and North Atlantic rift systems 92
5 The Alpine orogeny in Western Europe 96
5.1 The Alps *sensu stricto* 96
5.2 The Pyrenees 96

I Orogenic inheritance and the North Atlantic rift **101**
Abstract 103
1 Introduction 105
2 Geological setting 105
3 Mapping inheritance 106
3.1 Definition 106
3.2 Selection criteria and limitations 108
3.3 Mapping method 110
3.4 Inheritance map: highlights 111
4 Mapping rift domains 111
4.1 Definition 111
4.2 Mapping method and limitations 111
4.3 Rift domains map: highlights 114
5 Mapping rift timing 114

5.1 Definition . . . 114
5.2 Mapping method and limitations . . . 115
5.3 Rift timing maps: highlights . . . 117
6 Discussion . . . 117
6.1 Maps analysis and comparison . . . 117
6.2 Areas for further research . . . 118
7 Conclusion . . . 119

II Margins in orogens **123**
Abstract . . . 125
1 Introduction . . . 127
2 Characteristics of rifted margins . . . 128
2.1 First-order architecture . . . 129
2.2 Dimensions and maturity of rift systems . . . 130
2.3 First-order lithological architecture . . . 135
3 First-order architecture of collisional orogens . . . 137
4 Discussion . . . 141
4.1 ‘Narrow oceans’ and ‘magma-poor’ subduction . . . 141
4.2 Characteristics of ‘narrow’ versus ‘wide’ oceans . . . 142
4.3 Subduction of narrow ‘oceans’ and subsequent orogeny . . . 142
4.4 Impact on the magmatic budget of subsequent extension . . . 144
5 Conclusion . . . 146

III Underplating and subsequent rifting **151**
Abstract . . . 153
1 Introduction . . . 155
2 Geological setting . . . 157
2.1 Orogenic collapse in Western Europe . . . 157
2.2 Architecture of the post-collapse Variscan lithosphere . . . 157
2.3 The Alpine Tethys and North Atlantic rift systems . . . 158
3 Numerical modeling study . . . 159
3.1 The thermo-mechanical code FLAC . . . 159
3.2 Model design . . . 162
4 Results . . . 164
4.1 Reference model . . . 164
4.2 Impact of the thermal state . . . 167
4.2.1 Model results . . . 167

4.2.2 Summary 172
4.3 Impact of the rheological composition 172
4.3.1 Model results 172
4.3.2 Summary 176
5 Discussion 177
5.1 Cooled underplating: a barrier to rifting? 177
5.2 Hot underplating: a prefered location for extension? 178
5.3 Underplating: a trigger to multiple necking instabilities? 178
6 Conclusion 180

Synthesis & Discussion **183**
7 Synthesis 185
7.1 Chapter I 185
7.2 Chapter II 194
7.3 Chapter III 201
8 General discussion 206

Conclusion & Perspectives **213**

General references **217**

ANNEX **253**

A Inheritance and the structure of hyperextended rift systems **253**
Abstract 255
1 Introduction 257
2 Defining inheritance in rift systems and rifted margins 258
2.1 Inheritance 258
2.1.1 Thermal inheritance 259
2.1.2 Compositional inheritance 260
2.1.3 Structural inheritance 260
2.2 Hyperextended, magma-poor and polyphase rift systems 261
2.2.1 Magma poor vs. magma-rich rift systems 261
2.2.2 Polyphase rifting 262
2.2.3 3D evolution of rift systems 264
3 The role of inheritance in structuring rift systems 264
3.1 Influence of inheritance on a large-scale 265
3.1.1 Variscan processes controlling crustal inheritance 265

3.1.1.1 Pre- and syn-Variscan structures 265
3.1.1.2 Late- and post-Variscan structures 267
3.1.2 Variscan processes controlling mantle inheritance 268
3.1.2.1 Pre- to syn-Variscan inheritance 268
3.1.2.2 Post-Variscan to early rift inheritance 269
3.1.3 Control of inheritance on rift evolution 271
3.2 Control of orogenic inheritance on a regional-scale 272
3.2.1 Inheritance vs. rift-induced processes 272
3.2.2 Inheritance and rifted margin segmentation 276
3.3 Control of inheritance on a local-scale 279
3.3.1 Pre-rift structures and detachment faulting 279
3.3.2 Pre-rift salt and detachment faulting 282
4 Rifting and thermal state: a modelling approach 285
4.1 Modelling approach 285
4.2 Modelling results 288
4.3 Implications 289
5 Discussion 297
5.1 Relative role of inheritance vs. rift-induced processes 297
5.2 The role of inheritance within an evolving rift system 298
6 Conclusion 303
References 307

B Mapping orogenic inheritance in Western Europe 317
1 The Caledonian orogenic domain 319
2 The Variscan orogenic domain 319
3 The Alpine orogenic domain 320
4 The extent of post-orogenic underplating 321
5 Summary: Palaeozoic and Mesozoic orogenic inheritance 321

C Mapping rift sub-domains in the North Atlantic region 325
1 Initial objectives 327
2 Method actually developed 329
2.1 Filtered Bouguer anomaly map 329

D Numerical modelling: test on parameters 335
1 Wavelength of the necking instability 337
2 Impact of fault strength 338

3 The impact of large-scale mantle density contrasts 340

E Numerical modelling: other lithospheric architectures 343

1 An alternative Variscan lithosphere architecture 345

2 Caledonian architecture 348

References Annex 2 – 5 351

List of Figures

Résumé détaillé **1**

1	Le Cycle de Wilson classique	4
2	La zone d'étude: l'Atlantique Nord	11
3	Paléo-geographie Paléozoïque globale	13
4	Les orogènes Calédoniens et Varisques	14
5	Les lithosphères Calédonienne et Varisque	17
6	Paléo-geographie Mésozoïque globale	19
7	Le système de rift Téthysien	19
8	Le système de rift Nord Atlantique	20
9	L'héritage orogénique en Europe de l'ouest	24
10	Les principaux domaines de rift dans l'Atlantique Nord	27
11	L'évolution temporelle du système de rift Nord Atlantique	29
12	L'architecture premier ordre des marges hyper-étendues	32
13	Architecture premier ordre des orogènes matures et immatures	36
14	Architecture des modèles numériques	38
15	Résumé des résultats de modélisation numérique	40
16	Sous-plaquage et systèmes de rift en Europe de l'Ouest	42
17	Carte tectonique synthétique de l'Atlantique Nord	45
18	Les "Cycle de Wilson" proposés dans cette étude	50

General introduction **65**

1	The original Wilson Cycle	68
2	The study area: the North Atlantic	74

General geological setting **77**

1 Global Palaeozoic palaeogeography 80
2 The main structures of the Caledonian and Variscan orogens . . . 82
3 The Caledonian and Variscan orogenies 88
4 The Caledonian and Variscan lithospheres 91
5 Global Mesozoic paleogeography 93
6 The Tethyan rift system 93
7 The North Atlantic rift system 94
8 Architecture of the Alpine and Pyrenean orogens 97

Chapter I **103**

I.1 Geological setting of the North Atlantic 107
I.2 Orogenic inheritance in Western Europe 109
I.3 Main rift domains in the North Atlantic 112
I.4 Timing of the main rifting events in the North Atlantic 116

Chapter II **125**

II.1 Definition of margins distal sub-domains 128
II.2 Statistical analysis of rift sub-domains width 136
II.3 First-order architecture of hyperextended rifted margins 138
II.4 First-order architecture of collisional orogens 140
II.5 First-order architecture of mature and immature orogens 145

Chapter III **153**

III.1 Rifts and underplating in the North Atlantic region 156
III.2 Architecture of the numerical models 164
III.3 ‘Christmas trees’ of the numerical models 166
III.4 Results of Models 1–4 168
III.5 Results of Models 1–4: second invariant of strain 169
III.6 Results of Models 1–4: stress intensity 170
III.7 Results of Models 5–8 173
III.8 Results of Models 5–8: second invariant of strain 174
III.9 Results of Models 5–8: stress intensity 175

Synthesis & Discussion **183**
1 Orogenic inheritance in Western Europe 187
2 Rift domains in western Europe 191
3 Timing of rift in Western Europe 193
4 First-order architecture of hyperextended rifted margins 196
5 First-order architecture of mature and immature orogens 199
6 Architecture of the numerical models 202
7 Synthesis of the results of the numerical modelling 204
8 Underplating and rift systems in Western Europe 205
9 Synthetic tectonic map of the North Atlantic 208

Conclusion & Perspectives **213**
1 The 'Wilson Cycle' end-members proposed in this study 214

ANNEX **253**

Annex 1 **253**

A1 Definition of inheritance 259
A2 Architecture and evolution of magma-poor and magma-rich rifted margins 263
A3 Orogenic lithosphere in Western Europe 266
A4 Composition of subcontinental mantle 270
A5 Architecture of necking domains in Iberia 274
A6 Rift domains in the southern North Atlantic 277
A7 Inversion of rift-related normal faults in the Alps 280
A8 Relationships between pre-rift salt & extensional detachment faults 283
A9 Numerical models design 287
A10 High temperature model: viscosity 290
A10 High temperature model: strain rate 291
A11 Medium temperature model: viscosity 292
A11 Medium temperature model: strain rate 293
A12 Low temperature model: viscosity 294
A12 Low temperature model: strain rate 295
A13 Final topography of the three models 296
A14 Tectonic evolution of magma-poor rifted margins 300

Annex 2 **317**

B1 Definition of orogenic inheritance 319
B2 Caledonian inheritance in Western Europe 320
B3 Variscan inheritance in Western Europe 320
B4 Alpine inheritance in Western Europe 321
B5 Extent of underplating in Western Europe 322
B6 Orogenic inheritance in western Europe 323

Annex 3 **325**

C1 Initial definition of rift domains 327
C2 Map of the initial rift domains in the North Atlantic 328
C3 Map of former rift domains in the Alps 330
C4 New definition of rift domains 331
C5 Cross sections used in the mapping 331
C6 Filtered Bouguer gravity anomaly map 332
C7 Magnetic anomaly map EMAG2 332

Annex 4 **335**

D1 Wavelength of the necking instability for Moho at 500°C 337
D2 Models with weak faults 339
D3 Models with stronger faults 340
D4 The impact mantle density contrasts 341

Annex 5 **343**

E1 Alternative Variscan numerical model 346
E2 Results of Model 3 (Chapter III) 347
E3 A numerical model for Caledonian lithosphere 349

Résumé détaillé

1 Etat de l'art et limites actuelles

L'importance de l'héritage géologique dans le contrôle des processus tectoniques reste, aujourd'hui encore, très discutée. Intuitivement, on pourrait s'attendre à ce que, dans un matériel hétérogène soumis à des contraintes, les zones de faiblesse localisent la déformation de manière privilégiée. Il paraîtrait alors raisonnable de supposer que, lors d'un épisode d'extension de grande échelle, les rifts s'ouvrent au niveau des anciennes sutures ou zones de déformation majeure. Parallèlement, tout océan est voué à disparaître par subduction, soit spontanément car devenu gravitairement instable, soit du fait d'un forçage externe (Nikolaeva *et al.*, 2010; Stern, 2004). La lithosphère océanique étant nettement plus dense que la lithosphère continentale, la fermeture de ces océans doit logiquement s'achever par la collision de leurs marges opposées, c'est-à-dire à l'endroit même de leur ouverture.

Ce paradigme, connu sous le nom de *Cycle de Wilson* (Figure 1), a été établi à partir de l'étude des paléo-assemblages faunistiques dans l'Atlantique Nord (Wilson, 1966). En effet, la comparaison entre les anciennes espèces présentes sur les continents américain et européen et leur évolution au cours du temps ont permis de démontrer qu'un ancien océan, aujourd'hui connu sous le nom de Iapetus, séparait l'Amérique du Nord de l'Europe de façon quasi analogue à l'Atlantique Nord actuel entre le Paléozoïque inférieur et le Paléozoïque supérieur. Cet océan n'existait plus entre le Paléozoïque supérieur et Mésozoïque inférieur, à l'époque où la *Pangée* regroupait l'ensemble des continents. La fermeture de l'océan Iapetus est à l'origine de l'orogenèse Calédonienne dont les traces sont encore visibles de nos jours le long des côtes est nord-américaines et groenlandaises, ainsi qu'à l'ouest de la Norvège et au nord-ouest du Royaume-Uni (Ziegler, 1988).

Néanmoins, cette hypothèse est mise à mal en de nombreux endroits, notamment en Europe de l'Ouest où la plupart des sutures Varisques n'ont pas été affectées au cours des phases d'extension Mésozoïques, ni lors du développement du rift Nord Atlantique, ni de celui de la Tethys Alpine. De plus, Krabbendam et Barr (2000) ont souligné que, sur les 25 000 km de rift que comptait l'ancien supercontinent Gondwana, seuls 45% sont parallèles à d'anciennes sutures, et plus de 20 000 km d'anciennes zones orogéniques n'ont pas été réactivées lors des épisodes d'extension subséquents. Ces observations prouvent que l'héritage orogénique n'est pas systématiquement réutilisé au cours des phases de déformation postérieures et interrogent quant aux autres facteurs susceptibles de contrôler la localisation des processus tectoniques.

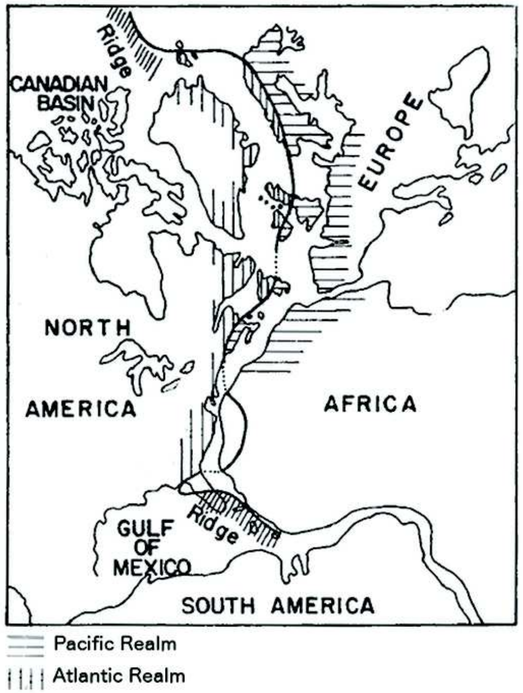

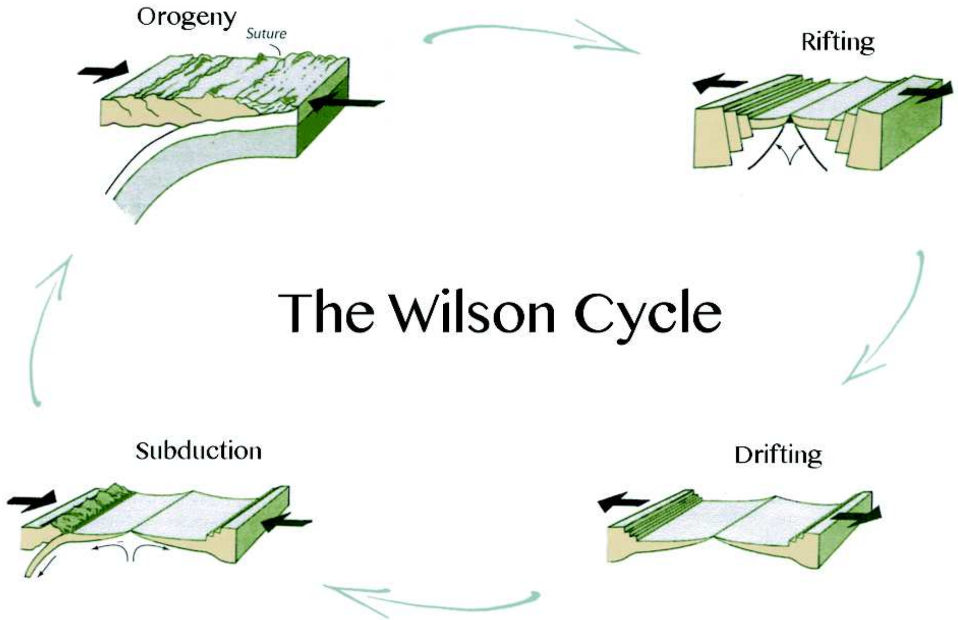

Figure 1 – A gauche : Distribution actuelle des paléo-assemblages faunistiques Pacifiques et Atlantiques dans la région de l'Atlantique Nord (Wilson, 1966) ; A droite : Schématisation du Cycle de Wilson (modifié d'après Allègre et Dars, 2009)

L'influence de l'héritage sur le Cycle de Wilson peut être analysée selon deux axes de recherche principaux : **(1) Comment les structures et hétérogénéités causées par les orogenèses contrôlent-elles les épisodes de rift subséquents ?** et **Comment l'architecture structurale et lithologique des systèmes de rift influence-t-elle les orogenèses ?**

1) Des orogènes aux rifts

Les processus orogéniques et post-orogéniques créent des linéaments majeurs, ainsi que des hétérogénéités lithologiques et thermiques conséquentes. Cet héritage orogénique est susceptible d'influencer significativement les épisodes d'extension subséquents. En effet, la réactivation d'anciennes failles de chevauchement est souvent invoquée pour expliquer la localisation et l'orientation de failles normales plus récentes. Par exemple, la zone de faille de Møre–Trøndelag est décrite comme une structure faible, possiblement formée au cours du Protérozoïque, ayant joué en compression lors de l'orogenèse Calédonienne, ayant été réactivée en extension lors de l'effondrement post-orogénique de la chaîne, avant d'être utilisée à nouveau lors du rifting Mésozoïque de l'Atlantique Nord (e.g. Doré *et al.*, 1997, et références y contenues). A plus grande échelle, Withjack *et al.* (2012) ont décrit l'ensemble du système de rift de la côte Est nord-américaine comme étant situé au niveau des ceintures de plissement et chevauchement d'orogènes Paléozoïques ou antérieurs. Selon ces auteurs, les failles bordières des bassins de rift avortés sont d'anciennes structures orogéniques. Par contre, les failles internes à ces bassins, dont les tailles sont nettement inférieures, ont des orientations beaucoup plus variées.

Bien que cette problématique ait été abondemment étudiée par la communauté scientifique, les investigations menées simultanément à différentes échelles n'ont pas permis de faire émerger une règle universelle quant aux interactions entre l'héritage orogénique et systèmes de rift (e.g. Manatschal *et al.*, 2015, Annex A). De plus, de nombreux paramètres entrent en jeu lors de la réactivation de structures héritées, à commencer par l'orientation de celles-ci par rapport à la contrainte tectonique, l'intensité de cette contrainte – à laquelle s'ajoute une éventuelle pression de fluide (Sibson, 1985), ainsi que la rhéologie du matériel environnant (Chenin et Beaumont, 2013).

Par ailleurs, l'effondrement gravitaire de certains orogènes de collision est accompagné d'une importante activité magmatique. C'est vraisemblablement le cas de l'orogène Varisque en Europe de l'Ouest, ainsi que dans la Province de Basin and Range à l'ouest des Etats-Unis, où la croûte inférieure sismiquement très réflective a été interprétée comme un sous plaquage de corps magmatiques mafiques pouvant aller jusqu'à 10 km d'épaisseur (Rey, 1993). En effet, lors d'un effondrement post-orogénique riche en magma, la relaxation thermique entraîne la fusion partielle de la croûte continentale inférieure, qui se répercute dans les niveaux sus-jacents par la mise en place de nombreuses intrusions plus ou moins acides (Schaltegger, 1997; Costa and Rey, 1995 ; voir aussi Petri, 2014 pour une synthèse). De plus, l'éventuel délaminage de la racine crustale cause une remontée quasi adiabatique de l'asthénosphère sous-jacente, et par conséquent sa fusion partielle, qui se traduit par un sous-plaquage mafique de la croûte continentale (Mckenzie et Bickle, 1988; Rey, 1993). Celui-ci fera office de croûte inférieure une fois la lithosphère ré-équilibrée isostatiquement, après son refroidissement et son érosion. Cependant, les conséquences lithologiques et thermiques d'un tel magmatisme de grande ampleur n'ont, jusqu'à présent, jamais été prises en compte dans l'analyse des épisodes extensifs subséquents.

2) Des rifts aux orogènes

Il semble légitime de supposer que l'architecture des systèmes extensifs a une incidence sur les caractéristiques des orogenèses résultant de leur fermeture. Cette hypothèse est étayée par le contraste entre les orogènes Calédonien et Varisque, dont les configurations géographiques pré-orogéniques diffèrent largement. En effet, alors que la première résulte principalement de la fermeture d'un océan de grande envergure (l'océan Iapetus), la seconde est issue de la fermeture d'une série de bassins océaniques de petites tailles (les océans Rhénohercynien, Saxothuringien et Médio-Européen), en plus de celle d'un océan majeur (l'océan Rhéique ; voir Matte (2001) pour une synthèse).

Or la diversité morphologique, mais aussi lithologique et thermique des systèmes de rift est indiscutable, comme l'illustrent les bassins de rift avortés tels que Rockall ou Porcupine, à l'opposé des océans matures comme l'Atlantique ou le Pacifique. Néanmoins, les spécificités des systèmes extensifs impliqués dans les orogenèses de collision sont encore rarement prises en considération lors de l'analyse de celles-ci. Cela vient potentiellement du fait que, malgré des descriptions morphologiques qualitatives des systèmes de rift de plus en plus poussées (e.g. Minshull, 2009; Reston, 2009; Sutra et al., 2013), il n'en existe, à ce jour, aucune étude quantitative. De plus, aucune synthèse quant à l'architecture lithologique des marges à l'échelle lithosphérique n'a jusqu'à présent été proposée. Par ailleurs, hormis quelques études récentes et très locales (Butler, 2013; Butler *et al.*, 2006; Mohn *et al.*, 2014; Tugend *et al.*, 2015, et références y contenues), les orogènes sont aujourd'hui essentiellement considérés comme le résultat de processus tectono-magmatiques induits par la subduction, sans tenir compte des caractéristiques initiales des marges impliquées. A l'opposé, les orogènes issus de la fermeture de bassins océaniques étroits, qui n'impliquent que des processus de subduction transitoires, n'ont jusqu'à présent reçu que peu d'attention de la part de la communauté scientifique.

De nombreux auteurs se sont attelés à démontrer (Audet et Bürgmann, 2011; Tommasi et Vauchez, 2001; Vauchez *et al.*, 1997) ou tempérer (Krabbendam et Barr, 2000; Manatschal *et al.*, 2015) le contrôle qu'exercent les structures et/ou hétérogénéités pré-existantes sur les épisodes tectoniques subséquents, tant en contexte extensif (e.g. Cappelletti *et al.*, 2013; Chenin et Beaumont, 2013; Manatschal *et al.*, 2015) que compressif (Butler *et al.*, 2006; Mohn *et al.*, 2014, 2011). De ces travaux, il ressort que l'héritage exerce indiscutablement un certain contrôle sur les processus tectoniques, mais que cette influence dépend de nombreux facteurs tels que l'échelle considérée, la nature des hétérogénéités, la rhéologie des couches qui les contiennent, l'état thermique du système dans son ensemble, la composition du manteau, ainsi que les processus syn-tectoniques susceptibles de modifier les caractéristiques physico-chimiques et thermiques de l'ensemble du système. De plus, comme l'héritage lié aux phases d'extension est susceptible d'influencer les orogenèses subséquentes et *vice-versa*, l'impact de l'héritage tectonique devrait être étudié en tenant compte de l'ensemble des étapes du Cycle de Wilson, ce qui n'a, jusqu'à présent, jamais été fait.

2 Objectifs de cette thèse

L'objectif de cette thèse est double. Il s'agit, dans un premier temps, de comprendre l'influence de l'héritage sur les processus tectoniques à grande échelle, et ce tout au long du Cycle de Wilson. Dans un deuxième temps, il s'agit de tester la crédibilité des hypothèses émises et d'apprécier l'évolution du système au premier ordre et de façon semi-quantitative. Il est important de noter que, dans ce travail, les termes *grande échelle* et *premier ordre* sont utilisés pour qualifier des structures, des hétérogénéités lithologiques ou thermiques, ainsi que des processus physiques ou chimiques qui se reflètent à une échelle supérieure au déca-kilomètre.

La problématique relative à l'impact de l'héritage sur le Cycle de Wilson peut être divisée en deux axes de recherche :

1) Impact de l'héritage orogénique sur les systèmes de rift

Dans le premier chapitre de cette thèse, j'examine comment l'héritage orogénique Calédonien et Varisque contrôle l'architecture et le budget magmatique du système de rift Nord Atlantique à grande échelle. Ma démarche consiste, dans un premier temps, à développer des méthodes de cartographie fiables permettant de compiler les structures et hétérogénéités majeures laissées par les orogenèses, l'architecture premier ordre des systèmes de rift, et l'âge des évènements tectoniques majeurs liés au rift. Cette étape me permet, dans un deuxième temps, de construire une analyse rigoureuse en confrontant des éléments cohérents et pertinents à l'échelle considérée. Mon approche est guidée par les questions suivantes :

- **Comment définir et cartographier l'héritage orogénique à grande échelle ?**
- **Comment définir et cartographier l'architecture des systèmes de rift à grande échelle?**
- **Comment caractériser et cartographier l'évolution temporelle premier ordre d'un système de rift ?**
- **Quelles sont les relations entre l'héritage orogénique et l'architecture et l'évolution temporelle des systèmes de rift ?**

2) Impact de l'architecture des systèmes de rift sur les orogènes

Dans le deuxième chapitre de cette thèse, je cherche à évaluer l'impact de l'architecture et de la lithologie des systèmes de rift hyper-étendus, en particulier de leurs marges, sur les orogenèses de collision. Dans un premier temps, j'effectue une étude statistique des dimensions des domaines marginaux décrits par Sutra et al. (2013), à partir de coupes sismiques. Ceci me permet de décrire quantitativement l'architecture structurale premier ordre des rifts hyper-étendus. Parallèlement, j'examine la lithologie de la lithosphère continentale, ainsi que les transformations qu'elle subit au cours du rifting, et de la lithosphère océanique. Ceci me permet de synthétiser l'architecture lithologique premier ordre des bassins de rift hyper-étendus. J'analyse ensuite comment ces spécificités se reflètent dans les orogènes en concentrant mon étude sur la fermeture de bassins de rift étroits, afin de m'affranchir des altérations induites par les processus de subduction prolongée tels que le magmatisme d'arc. Pour récapituler, ma démarche consiste à élucider :

- **Quelles sont les caractéristiques structurales des "océans étroits" et des océans "larges" et comment les quantifier ?**
- **Quelles sont les caractéristiques lithologiques des "océans étroits" et des océans "larges" ?**
- **Quelles sont les différences architecturales majeures entre les "océans étroits" et les océans "larges" ?**
- **Comment les spécificités des marges se reflètent-elles lors d'une orogenèse issue de la fermeture d'un "océan étroit" ? Quelles sont les différences par rapport à une orogenèse résultant de la subduction d'un océan "large" ?**

A partir des tentatives de réponse à ces questions, la prochaine étape consiste à tester la crédibilité des hypothèses émises. Pour cela, j'intègre les résultats obtenus dans les premiers chapitres de ma thèse dans des modèles numériques, de sorte à les étudier les processus en jeu de manière semi-quantitative, et ce à une échelle et une résolution similaires à celles considérées jusque là. Ici, j'étudie en particulier l'effet de l'héritage laissé par un effondrement post-orogénique riche en magma sur une phase d'extension subséquente.

3) Modélisation l'impact du sous-plaquage sur un rift subséquent

Dans le troisième chapitre de cette thèse j'étudie les conséquences du sous-plaquage de corps mafiques au niveau de la croûte continentale inférieure et de l'appauvrissement en éléments incompatibles du manteau sous-jacent sur un système de rift subséquent. J'utilise le code thermo-mécanique FLAC (Cundall, 1989; Lavier et Manatschal, 2006; Tan *et al.*, 2012) pour tester l'effet d'hétérogénéités lithologiques et thermiques de grande échelle sur une lithosphère orogénique en extension, et ce sous différentes conditions thermiques. En particulier, j'examine :

- **Comment un sous-plaquage mafique de la croûte continentale et/ou une zone de manteau appauvri à l'aplomb d'une ancienne zone de suture orogénique influencent-ils l'architecture et l'évolution d'un système de rift subséquent ?**
- **Comment l'état thermique de la lithosphère et du corps sous-plaqué se répercute-t-il sur les processus d'extension ?**
- **Est-il-possible d'appliquer ces résultats à l'analyse du système de rift Nord Atlantique au niveau de la lithosphère Varisque sous-plaquée ?**

3 Choix de la zone d'étude

Mon étude se concentre sur l'Atlantique Nord, entre la zone de fracture de Açores–Gibraltar et la latitude 70°N. Cette région est particulièrement intéressante, car elle contient deux domaines orogéniques distincts aux histoires géologiques contrastées – à savoir les Calédonides au nord et les Variscides au sud – tous deux affectés par un même épisode de rift au Mésozoïque (Figure 2).

De plus, les nombreuses études géologiques et géophysiques publiques dont a bénéficié cette région, tant sur terre qu'en mer, ont permis de constituer une base de données conséquente avec une couverture appréciable. Celle-ci inclut : des grilles topographiques et gravimétriques (e.g. Sandwell and Smith, 2009; Smith and Sandwell, 1997), des grilles d'intensité des anomalies magnétiques (e.g. EMAG2 by Maus et al., 2009), ainsi que des grilles d'épaisseur sédimentaire (e.g. Whittaker *et al.*, 2013) à l'échelle globale ; des cartes géologiques et structurales d'échelle régionale à locale ; et localement, des campagnes sismiques réflexion et/ou réfraction (voir Artemieva et Thybo (2013) pour synthèse), ainsi que des campagnes de forage et de dragage (par exemple DSDP, ODP).

Cet ensemble de données actuelles est complété par des études thermo-chronologiques et paléo-magnétiques, qui ajoutent des contraintes temporelles au système. Celles-ci ont permis l'établissement de reconstructions paléo-géographiques et cinématiques d'échelle régionale à globale (entre autres Gaetani *et al.*, 2003; Tait *et al.*, 2000; Torsvik, 1998; Torsvik et Cocks, 2013).

4 Choix des méthodes

Les méthodes utilisées pour répondre aux problèmes soulevés doivent à la fois être applicables à grande échelle, donner des résultats fiables quant aux processus premier ordre, et se satisfaire des données publiques disponibles.

La cartographie apparaît être un outil adapté pour synthétiser les structures et hétérogénéités premier ordre à grande échelle. Comme de telles cartes n'existent pas à ce jour, je me suis attelée à développer des méthodes afin de cartographier l'héritage orogénique, ainsi que l'architecture et l'évolution temporelle des systèmes de rift, et à les appliquer dans la région de l'Atlantique Nord. Dans un premier temps, j'ai défini des critères de sélection pour limiter ma compilation aux caractéristiques premier ordre pertinentes pour mon étude. Puis j'ai déterminé les observables à partir desquels je pourrais construire une méthode de cartographie fiable. Finalement, je me suis appuyée à la fois sur l'observation de coupes sismiques, l'analyse de don-

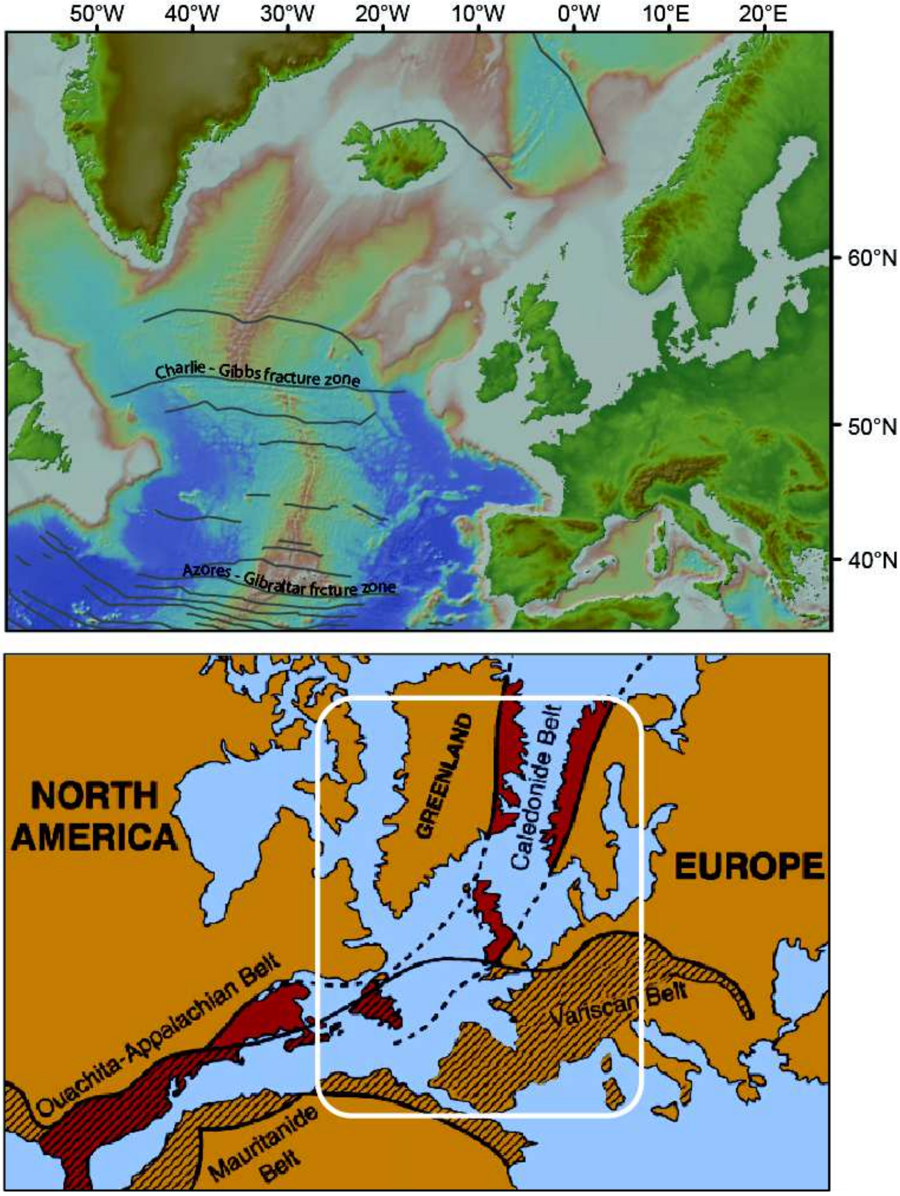

Figure 2 – En haut : Localisation de la zone étudiée (image de Geomap app) ; En bas : Etendue des orogènes Calédonien et Varisque dans la configuration paléo-géographique de la fin de Paléozoïque (modifiée d'après Nance *et al.*, 2010).

nées de gravimétrie et de magnétisme terrestre, ainsi que sur un travail de synthèse bibliographique.

Par ailleurs, la modélisation numérique offre la possibilité d'analyser l'évolution structurale, lithologique et thermique premier ordre de systèmes géologiques simplifiés d'échelle lithosphérique. En l'occurrence, cette méthode est un complément idéal au travail de cartographie décrit précédemment, car elle est particulièrement fiable à des échelles et résolutions similaires. De plus, la relative simplicité et rapidité de mise en place des expériences permet d'analyser aisément l'influence d'un grand nombre de paramètres.

5 Contexte géologique de la zone d'étude :

5.1 Du Protérozoïque au Paléozoïque : la fragmentation de Rodinia

Suite à la fragmentation du supercontinent Rodinia au cours du Néoprotérozoïque ($\sim$ 800 Ma), la géographie de l'ère Paléozoïque est dominée par quatre continents principaux – à savoir Gondwana, Laurentia, Baltica et Siberia – séparés par trois océans majeurs baptisés Panthalassa, Iapetus et Rhéique (Cocks et Torsvik, 2005). La subduction puis la fermeture de ces océans ont mené à la ré-agglomération de l'ensemble des continents sous la forme du supercontinent *Pangée* à la fin du Paléozoïque (Figure 3 ; voir Torsvik *et al.* (2012) pour une synthèse). En Europe de l'Ouest, cette phase de collision s'est traduite par les orogenèses Calédonienne au Siluro-Dévonien, et Varisque au Carbonifère Supérieur (Krawczyk *et al.*, 2008; Kröner *et al.*, 2008, et références y contenues).

5.2 Les orogenèses Calédonienne et Varisque

5.2.1 Océans et continents impliqués

Les orogenèses Calédonienne et Varisque ont impliqué trois continents majeurs, à savoir : (1) Laurentia $\simeq$ le craton Nord Américain + le Groenland + la partie nord du Royaume-Uni (voir Cocks et Torsvik (2011) pour une synthèse) ; (2) Baltica $\simeq$ le craton Est-Européen (qui comprend le nord de l'Europe entre la *Trans-European suture zone* et l'Oural, et entre la chaîne de Timan et la Mer Noire et la Mer Caspienne) + les différents terrains accrétés au nord, jusqu'à Svalbard (voir Cocks et Torsvik (2005) pour une synthèse) ; et (3) Gondwana $\simeq$ l'Afrique + l'Amérique du Sud + l' Australie + l'Antarctique + l'Inde+ la péninsule Arabique + le reste de l'Europe + la Nouvelle Ecosse et l'ouest de la Terre Neuve (voir Torsvik et Cocks (2011) pour une synthèse). Une quatrième plaque plus petite, baptisée Avalonia

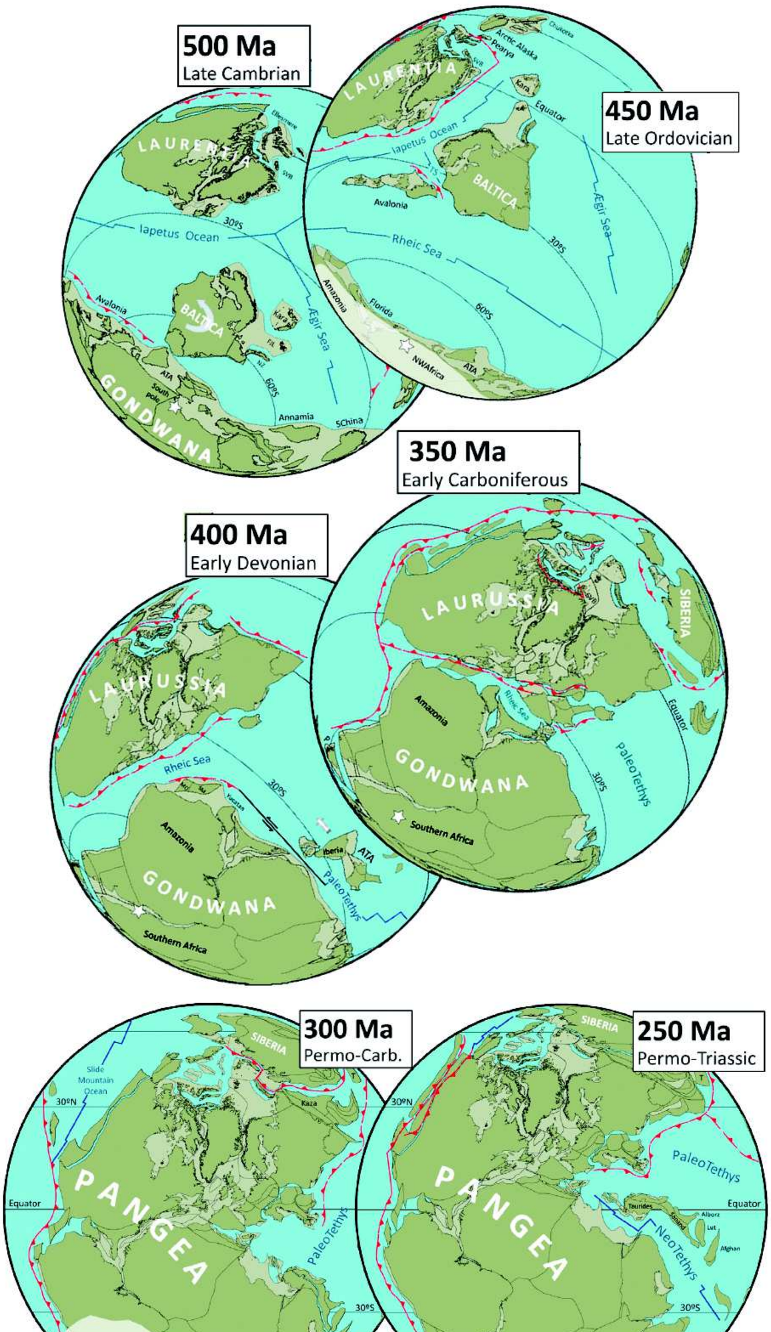

Figure 3 – Reconstruction paléo-géographique globale entre le Cambrian Inférieur et le Trias Inférieur d'après Torsvik *et al.* (2012). TS = Tornquist Seaway.

($\simeq$ l'Europe de l'ouest, y compris le sud du Royaume-Uni, la Belgique et l'Allemagne du Nord + la Nouvelle Ecosse et l'ouest de la Terre Neuve ; voir Cocks *et al.* (1997) pour une synthèse), s'est détachée du supercontinent Gondwana à la fin du Cambrien, laissant au niveau de sa marge nord une série de blocs continentaux peu amincis séparés par des bassins de rift étroits ($\sim$ 500–1 000 km ; (voir Kröner et Romer (2013); Torsvik et Cocks (2011) pour une synthèse). Dans ce mémoire, je fais référence à ce groupe de micro-continents/rubans continentaux sous le nom de "Gondwana-derived terranes assemblage".

Trois océans principaux séparaient ces continents, à savoir : (1) l'océan Iapetus entre Laurentia, Baltica et Avalonia (Mac Niocaill *et al.*, 1997; McKerrow et Cocks, 1976; Torsvik, 1998 ; voir Figure 3 entre 500 et 450 Ma), dont la largeur dépassait largement le millier de kilomètres (3 300 km selon van Staal *et al.*, 2012) ; (2) la Mer de Tornquist entre Avalonia et Baltica (voir Figure 3 à 450 Ma), de l'ordre de 500–1 000 km de large (Cocks et Fortey, 1982; McKerrow *et al.*, 2000a; Torsvik et Rehnström, 2003) ; (3) l'océan Rhéique entre Avalonia et le "Gondwana-derived terranes assemblage" (Cocks et Fortey, 1982; von Raumer *et al.*, 2003, e.g.), dont la largeur dépassait 2 000 km (> 4 000 km selon Nance et Linnemann, 2008).

D'autre part, plusieurs océans de tailles plus modestes (< 500–1 000 km ; McKerrow *et al.*, 2000a) séparaient probablement les différents micro-continents ou blocs de croûte continentale plus ou moins amincie du "Gondwana-derived terranes assemblage", à savoir les "océans" Rhénohercynien, Saxothuringien et Médio-Européen (voir Franke (2006) pour une synthèse).

Figure 4 – a) Reconstruction paléo-géographique de l'Atlantique Nord avant le rifting Mésozoïque mettant en évidence des différents continents, micro-continents et *terranes* impliqués dans les orogenèses Calédonienne et Varisque (d'aprèsvan Staal *et al.*, 2012). b) Reconstruction paléo-géographique de l'Atlantique Nord à la fin du Permien montrant l'étendue des orogènes Calédonien et Varisque dans la région de l'Atlantique Nord (d'après Nance *et al.*, 2010). c) Principales structures orogéniques des Calédonides et des Variscides et configuration paléo-géographique possible de l'Europe de l'Ouest au Permien (à 270 Ma). 1, suture de Iapetus arc magmatique Ordovicien ; 2, Avalonia ; 3, Armorica ; 4, nappe ophiolitique ancrée dans la suture de Galicia–Southern Brittany ; 5, nappes de Schistose dans le sud des Variscides ; 6, "foredeep basin" Carbonifère (Viséen à Westphalien) ; 7, vergence principale des nappes. CCSZ: Coïmbra–Cordoba Shear Zone; Beja S: suture Beja (d'après Matte, 2001).

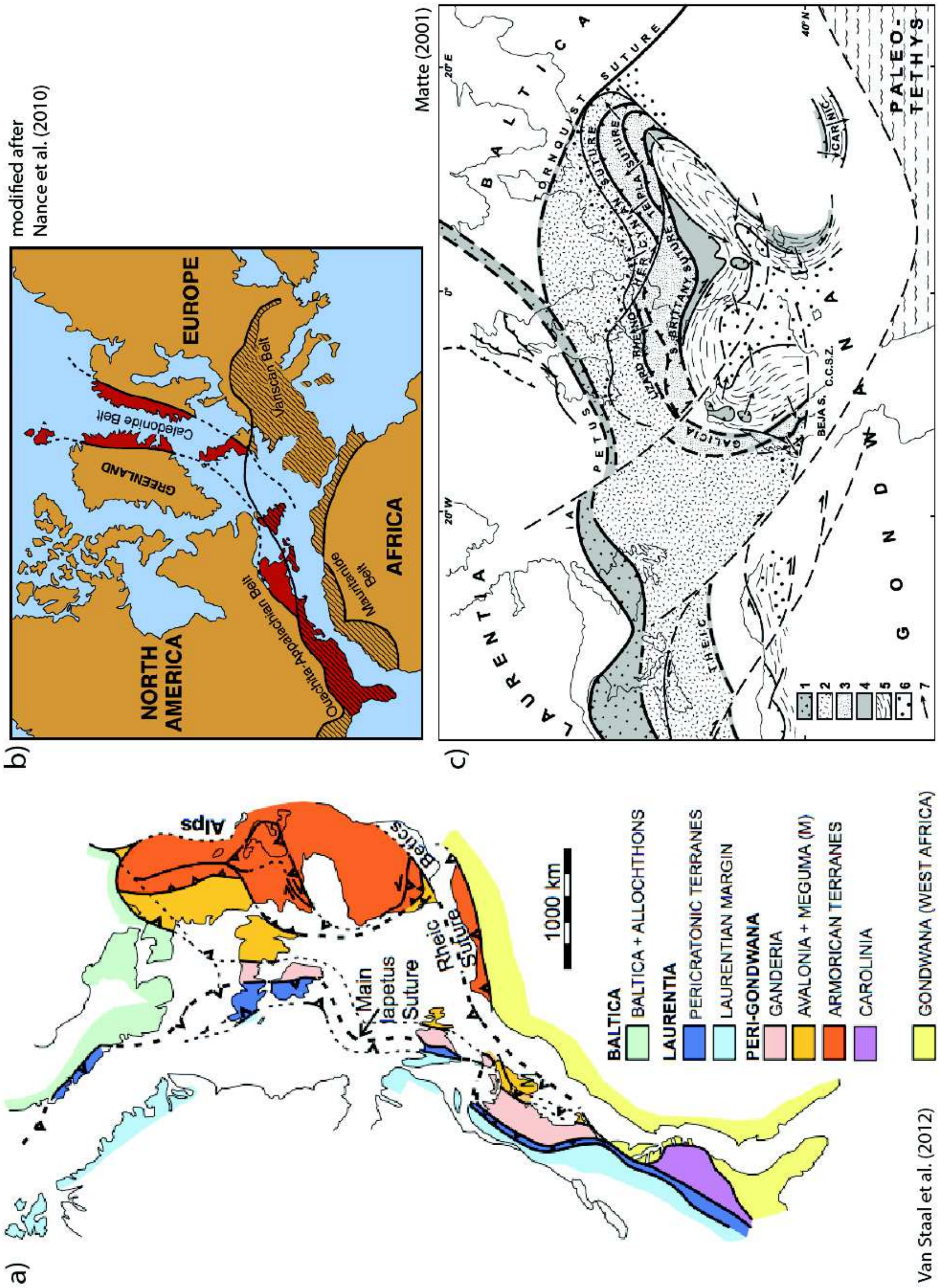
a)
Van Staal et al. (2012)
Alps
Betics
Main Iapetus Suture
Rheic Suture
1000 km
BALTICA
BALTICA + ALLOCHTHONS
LAURENTIA
PERICRATONIC TERRANES
LAURENTIAN MARGIN
PERI-GONDWANA
GANDERIA
AVALONIA + MEGUMA (M)
ARMORICAN TERRANES
CAROLINIA
GONDWANA (WEST AFRICA)
b)
modified after
Nance et al. (2010)
NORTH AMERICA
EUROPE
AFRICA
GREENLAND
Caledonide Belt
Variscan Belt
Ouachita-Appalachian Belt
Mauritanide Belt
c)
Matte (2001)
LAURENTIA
BALTICA
GONDWANA
PALEO-TETHYS
TORNQUIST SUTURE
IAPETUS
RHEIC
GALICIA
S. BRITTANY SUTURE
BEJA S.
C.C.S.Z.
CARNIC
20°W
0°
20°E
40°N

5.2.2 Orogenèses et effondrements post-orogéniques

L'orogenèse Calédonienne est le résultat de la fermeture de la Mer de Tornquist entre Baltica et Avalonia à la fin de l'Ordovicien, et de celle de l'Océan Iapetus entre Balonia (= Baltica + Avalonia) et Laurentia au Silurien Inférieur (Figure 4 ; voir Krawczyk *et al.* (2008) pour une synthèse). La chaîne Calédonienne est à la fois un orogène d'accrétion et de collision selon la définition d'Isozaki (1997) et Cawood *et al.* (2009). Elle peut être divisée en trois domaines de complexité variable.

D'un côté, les Calédonides Scandinaves résultent de la fermeture du large océan Iapetus au Silurien Inférieur avec une accrétion minime d'arcs magmatiques, et de la collision entre le bouclier Baltique et celui de Laurentia (van Staal *et al.*, 2012; Roberts, 2003 ; voir la Figure 4 a, b et c). Elle est caractérisée par une paire de ceintures métamorphiques parallèles exposées en Norvège (Murphy *et al.*, 2010, et références y contenues) : d'un côté, la ceinture haute pression/basse température représente le prisme d'accrétion, qui se compose d'un empilement de nappes plus ou moins allochtones ; de l'autre, la ceinture de basse pression/haute température résulte de l'arc magmatique formé lors de la subduction de l'océan Iapetus (Rey *et al.*, 1997, et références y contenues).

D'un autre côté, les Calédonides Britanniques et Appalachiennes sont nettement plus complexes car elles ont impliqué la collsion, l'accrétion et/ou l'obduction de nombreux arcs magmatiques, terranes et micro-continents tout au long de l'Ordovicien (Krawczyk *et al.*, 2008; McKerrow *et al.*, 2000b; van Staal *et al.*, 2012, 1998; Winchester *et al.*, 2002 ; voir la Figure 4 a, b et c). De ce fait, cet orogène est largement de type "accrétion" selon la définition d'Isozaki (1997) et Cawood *et al.* (2009), et n'est pas construite en paire de ceintures métamorphiques parallèles.

Finalement, les Calédonides Polonaises sont issues de la fermeture de l'océan Tornquist au Siluro-Dévonien (Figure 4 c). Cette partie de l'orogène est très mal connue car enfouie sous une épaisse couverture sédimentaire Mésozoïque et affectées à la fois par l'orogenèse Varisque et le rifting Mésozoïque (Krawczyk *et al.*, 2008; Meissner *et al.*, 1994; Pharaoh, 1999 ; voir aussi Dadlez, 2000 pour une synthèse). La localisation de l'ancienne marge de Balltica est encore incertaine (Trans-European Suture Zone ? Linéament de l'Elbe ?). Cependant, l'absence de structure orogénique majeure et d'assemblage haute pression suggère que la collision était relativement "douce", sans doute gouvernée par une convergence largement décrochante (Dadlez, 2000; Torsvik et Rehnström, 2003).

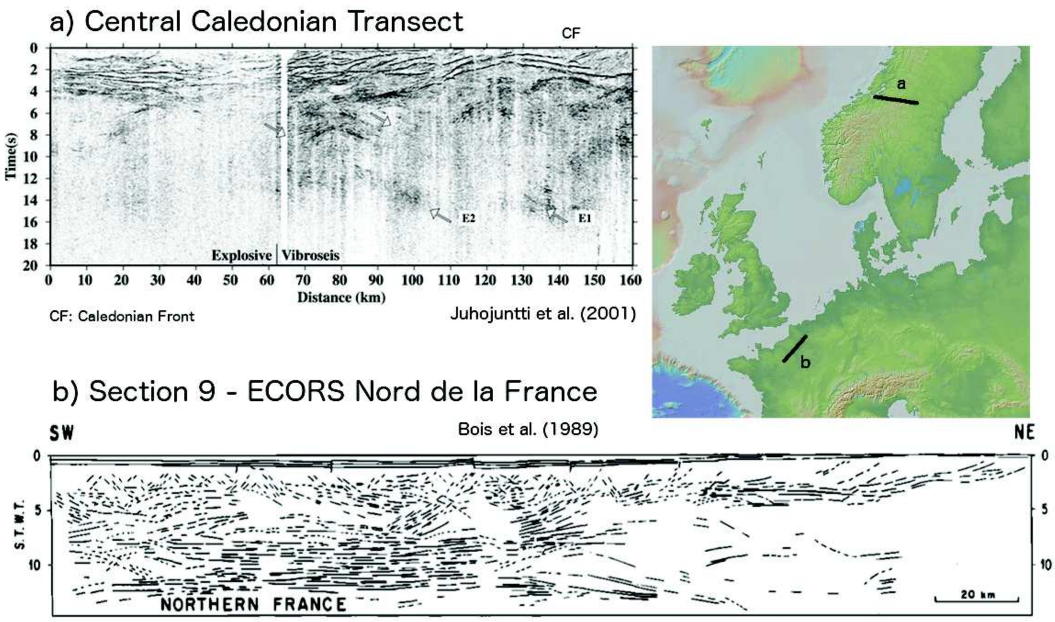

Figure 5 – Coupes sismiques au travers de (a) l'orogène Calédonien (Juhojuntti *et al.*, 2001) ; et (b) de l'orogène Varisque (Bois *et al.*, 1989).

A l'opposé, l'orogenèse Varisque résulte essentiellement de la fermeture de la série de bassins de rift étroits le long de la marge nord-gondwanienne – à savoir les *océans* Rhénohercynien, Saxothuringien et Médio-Européen ; voir Franke (2006) – en plus de celle du vaste Océan Rhéique (Kröner et Romer, 2013). L'architecture de la chaîne Varisque diffère largement des orogènes classiques, dans le sens où il s'agit d'un collage de blocs continentaux peu déformés, séparés par d'intenses zones de déformation (voir Kröner et Romer (2013) pour une synthèse). Seule la subduction de l'océan Rhéique a formé un arc magmatique, aujourd'hui exposé dans le *Mid-German Crystalline Rise*, et l'ensemble de l'orogène est dépourvu de prisme d'accrétion de taille significative (Franke, 2006, et références y contenues).

Lorsque la convergence a cessé à la fin du Carbonifère, les reliefs d'Europe de l'Ouest se sont effondrés sous leur propre poids. Cet effondrement, essentiellement réalisé via la formation de failles normales et de failles de détachement, s'est déroulé sans manifestation magmatique significative au nord du linéament de l'Elbe (Andersen, 1998; Fossen *et al.*, 2014; Meissner, 1999). Par contre, au niveau de l'orogène Varisque, il a été suivi d'une intense activité magmatique, qui s'est traduite par un sous-plaquage mafique pouvant aller jusqu'à une dizaine de kilomètres d'épaisseur au niveau de la croûte continentale inférieure, et par la mise en place d'intrusions plus ou moins acides dans les niveaux sus-jacents (Bois *et al.*, 1989; Meissner, 1999; Schaltegger, 1997; Schuster et Stüwe, 2008; Costa and Rey, 1995; Petri, 2014). De ce fait, les structures orogéniques ont été largement effacées dans le domaine Varisque d'Europe de l'ouest, alors qu'elles sont relativement bien préservées dans la lithosphère Calédonienne dépourvue d'activité magmatique post-orogénique (Figure 5).

5.3 Les système de rift Alpin et Nord Atlantique

La fragmentation de la Pangée a débuté au Jurassique inférieur avec l'ouverture de l'Atlantique Central et sa propagation vers l'est, connue comme le système de rift de la Tethys Alpine (Figures 6 and 7 ; Domeier *et al.*, 2012; Schmid et al., 2004, et références y contenues). Celle-ci qui comprenait "l'océan" Liguro-Piémontais et une possible branche nommée "océan" Valaisan, formée au Jurassique Supérieur (Figure 7 ; Stampfli *et al.* (1998); Schmid et al. (2004), et références y contenues). Simultanément, La Néothethys se propageait vers l'ouest, le long du front Varisque sud, de telle sorte que les deux systèmes étaient possiblement reliés dès la fin du Jurassique (Frizon de Lamotte et al., 2011).

Parallèlement, au Jurassique Inférieur, des bassins de l'ordre de 8 km de profondeur se formaient en réponse à une phase d'extension dans la partie nord de l'Atlantique Nord (Doré *et al.*, 1999). Roberts *et al.* (1999) ont interprété cet évènement comme la propagation vers le sud du système de rift Arctique, qui se prolongeait jusque dans la Mer du Nord, et, de manière plus éparse, dans les bassins de Jeanne d'Arc, de Porcupine et de Galice (Figures 6 and 8).

Le système de rift de la Tethys Alpine a été abandonné et inversé à partir du Crétacé, et la convergence résultante entre l'Afrique et l'Europe a mené aux orogenèses Alpine et Pyrénéenne. Parallèlement, le rift Arctique et celui de l'Atlantique Central sont devenus coalescents au large du Royaume-Uni (Figure 8 ; Doré *et al.*, 1999).

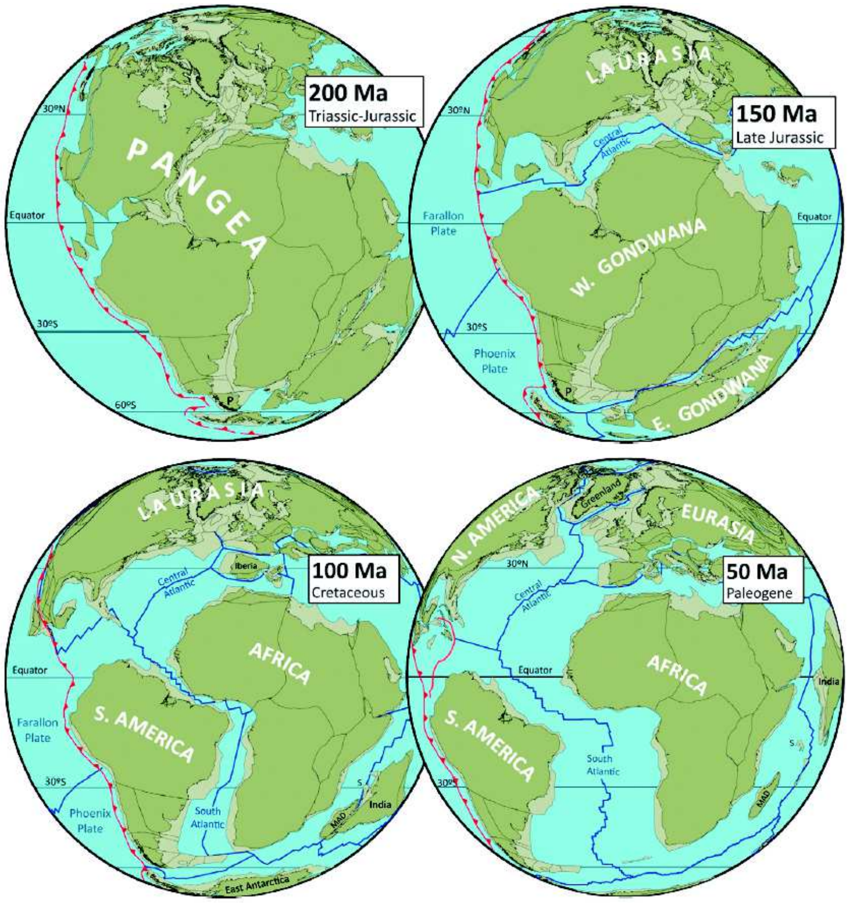

Figure 6 – Reconstruction paléo-géographique globale entre la fin du Trias et le début du Cénozoïque d'après Torsvik *et al.* (2012).

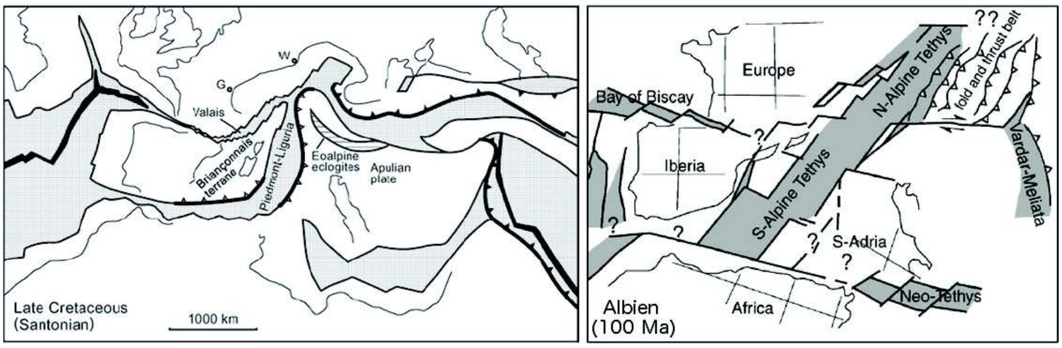

Figure 7 – Configuration possible du système de rift de la Tethys Alpine pendant (à gauche) le Crétacé Supérieur d'après Schmid et al. (2004) ; et (à droite) à l'Albien d'après Manatschal et Müntener (2009).

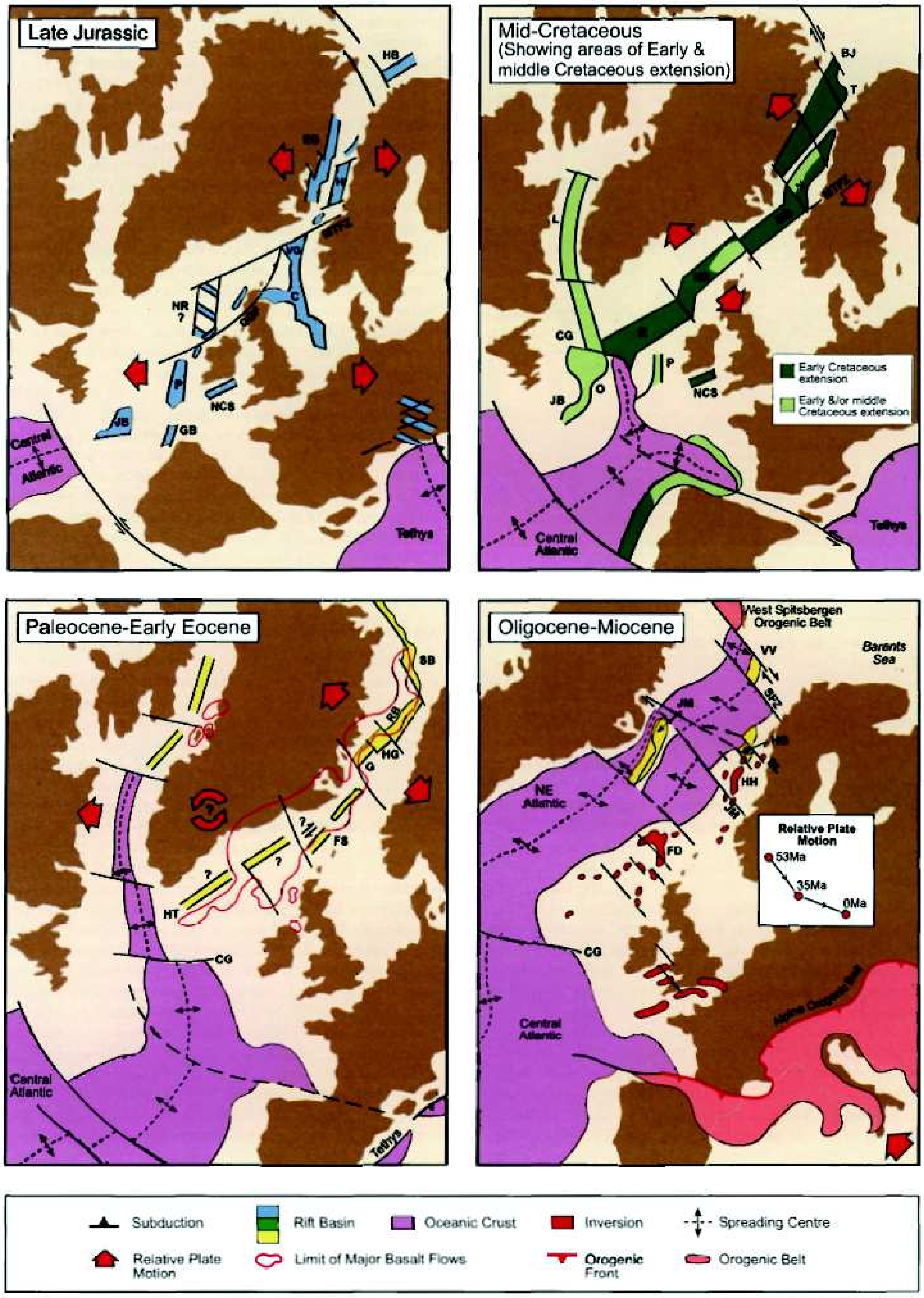
Late Jurassic
HB
NR
?
P
NCS
GB
JB
Central Atlantic
Tethys
Mid-Cretaceous
(Showing areas of Early & middle Cretaceous extension)
BJ
T
L
CG
JB
O
P
NCS
Early Cretaceous extension
Early &/or middle Cretaceous extension
Central Atlantic
Tethys
Paleocene-Early Eocene
SB
HG
FS
HT
CG
Central Atlantic
Tethys
Oligocene-Miocene
West Spitsbergen Orogenic Belt
Barents Sea
VV
NE Atlantic
HH
FD
CG
Central Atlantic
Relative Plate Motion
53Ma
35Ma
0Ma
Alpine Orogenic Belt
Subduction
Rift Basin
Oceanic Crust
Inversion
Spreading Centre
Relative Plate Motion
Limit of Major Basalt Flows
Orogenic Front
Orogenic Belt

Figure 8 – Evolution premier ordre du système de rift Nord Atlantique entre le Trias Inférieur et le début du Miocène (d'après Doré *et al.*, 1999). BL : Bivrost Lineament ; BJ : Bjørnøya Basin ; C : Central Graben ; CG : Charlie–Gibbs Fracture Zone ; EG : East Greenland Rift ; FD : Faeroes Dome ; FS : Faeroe-Shetland Basin ; G : Gjallar Ridge ; GB : Galicia Bank Basin ; GGF : Great Glen Fault ; H : Halten Terrace ; HG : Hel Graben ; HH : Helland-Hansen Arch ; HT : Hatton Trough ; JM : Jan Mayen ; L : Labrador Sea ; MTFZ : Møre–Trødelag Fracture Zone ; MB : Møre Basin ; NCS : North Celtic Sea ; NR : North Rockall Trough ; O : Orphan Basin ; P : Porcupine Basin ; R : Rockall Trough ; R : Røst Basin ; SB : Svorestnaget Basin ; T : TromsøBasin ; V : Vestfjorden Basin ; VG : Vøring Graben ; VV : Vestbakken Volcanic Province

5.4 L'orogenèse Alpine en Europe de l'Ouest

5.4.1 Les Alpes *sensu stricto*

Dans le cas des Alpes, la phase de collision principale a débuté au cours de l'Eocène, à $\sim$ 35 Ma (Schmid *et al.*, 2008). Au premier ordre, cet orogène peut être décrit comme un épais prisme d'accrétion asymétrique, plus développé du côté européen (Dal Piaz *et al.*, 2003). Leurs parties externes sont formées de massifs cristallins, qui représentent les anciennes marges continentales de la Tethys Alpine, alors que la partie interne est composée d'un empilement complexe de débris plus ou moins distaux (Mohn *et al.*, 2014). Les assemblages de haute pression sont relativement courants dans la chaîne de montagne (Chopin, 1987; Meyre et Pusching, 1993; Thöni et Jagoutz, 1993), mais aucun indice de magmatisme volumineux, ni aucun assemblage métamorphique de haute température contemporain de la fermeture de l'"océan" ne suggère l'existence d'un arc volcanique. Il faut noter qu'en détail, les Alpes sont structuralement relativement complexes, dans le sens où leur construction résulte de la collision de plusieurs micro-plaques, et qu'elle a impliqué des mouvements décrochants subséquents (Mohn *et al.* (2011) ; voir Handy *et al.* (2010) pour une synthèse).

5.4.2 Les Pyrénées

Parallèlement, la convergence entre l'Afrique et l'Europe s'est traduite par l'initiation d'une subduction dans le Golfe de Gascogne et la fermeture des bassins de rifts hyper-étendus entre La France et l'Espagne (Tugend et al., 2014b, et références y contenues). Le climax de la phase compressive a eu lieu entre l'Eocène à l'Oligocène (Muñoz, 2002). La chaîne pyrénéenne peut être décrite comme un prisme d'accrétion asymétrique, plus développé dans sa partie méridionale (Casteras, 1933; Mattauer, 1968). Tout comme dans les Alpes, les parties externes sont composées des anciennes marges continentales, et la partie interne est composée d'une accumulation de débris plus ou moins distaux (Tugend et al., 2014b). Cet orogène est dépourvu à la fois d'assemblage haute pression et d'indice suggérant l'existence d'un arc magmatique.

6 Synthèse

Dans cette section je discute, chapitre par chapitre, comment les données produites et les conclusions tirées de leur analyse permettent de répondre à la problématique de ma thèse (c.f. section 2).

6.1 Chapitre I

Dans le premier chapitre de ma thèse, je définis et j'identifie, à l'échelle de l'Atlantique Nord, l'héritage orogénique, l'architecture des domaines de rift et l'âge des évènements de rift majeurs.

Comment définir et cartographier l'héritage orogénique à grande échelle ?

Dans cette étude, je définis l'*héritage* comme la différence entre une lithosphère idéale, dont les propriétés physiques sont latéralement homogènes, et une lithosphère réelle (Figure 9 a). Suivant cette philosophie, l'héritage comprend à la fois les hétérogénéités structurales, lithologiques et thermiques (voir en Annexe A pour une discussion plus poussée de la notion d'héritage).

Du fait de leur différente histoire géologique, je distingue trois domaines orogéniques dans la région de l'Atlantique Nord, à savoir les domaines Calédonien, Varisque et Alpin (voir l'Annexe B pour la composante Alpine). Je définis un domaine orogénique comme la zone délimitée par la trace actuelle de ses fronts de déformation à la surface de la Terre. Il faut noter que cette aire ne reflète qu'une étendue minimale de l'orogène, puisque les structures orogéniques ont certainement été, au moins partiellement, érodées. Cependant, elle reste une approximation raisonnable à l'échelle considérée.

Pour chaque domaine, je cartographie les structures et hétérogénéités orogéniques premier ordre correspondantes. Je sélectionne comme pertinents et cartographiables, les sutures orogéniques, les failles majeures, les bassins d'avant-pays, les arcs magmatiques, les corps sous-plaqués et les intrusions magmatiques de grande taille, ainsi que les zones de manteau appauvri qui leurs sont associées (voir le Chapitre I section 3 pour une discussion).

Les cartes réalisées dans le cadre de cette étude sont présentées sur la Figure9 (b). Elles mettent en évidence que le système de rift Nord Atlantique suit partiellement les sutures correspondant aux anciens océans majeurs Iapetus (Calédonien) et Rhéique (Varisque). Par contre, le rift abandonne la suture de l'océan (Calédonien)

Tornquist, de taille plus modeste, et ignore celles des océans (Varisques) "étroits" Rhénohercynien, Saxothuringien et Médio-Européen (< 500–1 000 km ; McKerrow *et al.*, 2000a).

Comment définir et cartographier l'architecture des systèmes de rift à grande échelle?

Afin de mettre en évidence l'architecture premier ordre des systèmes de rift, je distingue trois domaines principaux, à savoir les domaines *proximal*, *distal* et *océanique* (Figure 10 a). Je définis ceux-ci en me basant sur des critères morphologiques simplifiés à partir de ceux définis par Sutra et al. (2013), qui ont l'avantage d'être identifiables sur des coupes sismiques. D'autre part, j'utilise des données de gravimétrie et de magnétisme, afin de corréler les limites de ces différents domaines entre les coupes sismiques.

Dans le domaine proximal, la croûte continentale n'est que peu, voire pas amincie ($\sim$ 30–35 km), et le toit du socle est parallèle au Moho. La limite entre le domaine proximal et le domaine distal correspond au *point d'étranglement* ("necking point" sur la Figure 10 a), qui marque le début de l'approfondissement du toit du socle et de la remontée du Moho (à noter que cette dernière n'est visible que sur les coupes sismiques "en profondeur"). De manière générale, cette limite est également nettement visible sur les cartes d'anomalie de Bouguer dont les basses fréquences ont été éliminées avec un filtre passe-haut (voir en Annexe C). Cette méthode permet de supprimer le signal dû aux variations de densité du manteau, qui ont de grandes longueurs d'ondes, et ainsi de faire ressortir le signal haute fréquence lié aux variations de l'architecture crustale. Une carte de l'anomalie de Bouguer filtrée est donc un outil efficace pour extrapoler le point d'étranglement entre les coupes sismiques, à condition qu'il n'y ait pas d'additions magmatiques significatives, ou que leur signal gravimétrique ait été corrigé.

La limite entre le domaine distal et le domaine océanique est défini comme le *point de rupture lithosphérique* ("lithospheric breakup point" sur la Figure 10 a), et correspond au début de l'accrétion océanique en régime stationnaire. Sur les coupes sismiques, cette limite se traduit par une inflexion dans la profondeur du toit du socle entre, d'un côté, une surface plus ou moins chaotique soulignée d'un Moho discontinu (Whitmarsh *et al.*, 2001) et dont les dépôts sédimentaires sont syntectoniques (ou appartiennent à la séquence "sag" ; voir Haupert *et al.*, sous presse), et de l'autre, une croûte océanique homogène de $\sim$ 6 à 7 km/2 sTWT d'épaisseur, couverte par des dépôts sédimentaires passifs. Il faut noter que l'inflexion du toit

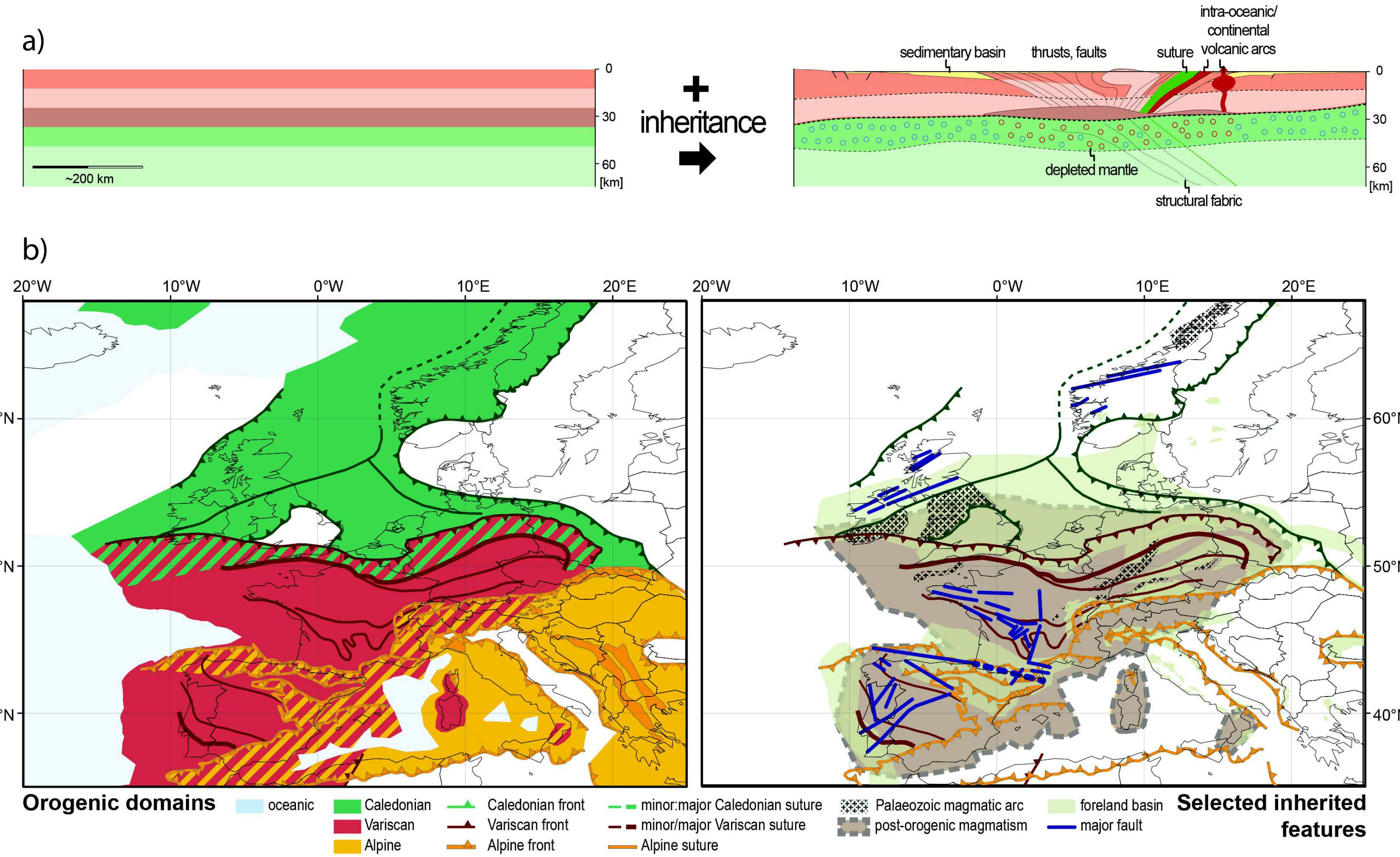

Figure 9 – (a) Définition schématique de la notion d'héritage ; (b) Cartes des domaines orogéniques (à gauche) et des structures et hétérogénéités héritées correspondantes (à droite) en Europe de l'Ouest.

du socle peut se faire, soit vers le haut, soit vers le bas, selon le budget magmatique associé à la rupture lithosphérique : la transition entre un manteau exhumé et une croûte océanique stationnaire se traduit par une inflexion vers le haut car la densité du manteau exhumé est supérieure à celle d'une croûte océanique de type "Penrose" (Anonymous, 1972). A l'inverse, la transition entre une marge riche en magma et une croûte océanique stationnaire s'exprime par une inflexion vers le bas.

Comme le plancher océanique créé à l'axe de la dorsale enregistre le champ magnétique contemporain, le point de rupture lithosphérique peut, *a priori*, être extrapolé entre les coupes sismiques à partir des cartes d'anomalies magnétiques. Néanmoins, cette méthode n'est pas applicable dans le cas où l'accrétion océanique aurait débuté pendant la période dite "calme", c'est-à-dire sans inversion du champ magnétique.

Il faut mentionner que les additions magmatiques de grande ampleur associées à la rupture lithosphérique dans l'Atlantique Nord perturbent à la fois le signal sismique, gravimétrique et magnétique, rendant l'identification des domaines de rift délicate dans cette région. Afin de localiser les zones où les limites des domaines de rift sont discutables, j'ai reporté ces additions magmatiques sur ma carte des domaines de rift (Figure 10 b).

Il convient également de noter que, en théorie, il serait possible de cartographier les domaines de rift avec une plus grande résolution, par exemple en distinguant les différents sous-domaines décrits par Sutra et al. (2013) au sein du domaine distal. Cependant, ceci nécessiterait des coupes sismiques de haute qualité et résolution, données encore rares dans le domaine public, ainsi qu'un développement plus poussé des méthodes pour corréler ces sous-domaines dans l'espace (voir en Annexe C). En effet, la méthode utilisée par Tugend *et al.* (2015) pour identifier les domaines et sous-domaines de rift en Ibérie et dans le Golfe de Gascogne ne sont pas directement applicables dans la partie septentrionale de l'Atlantique Nord, à cause du brouillage induit par les additions magmatiques, tant dans le signal sismique que gravimétrique.

La carte des domaines de rift réalisée dans le cadre de cette étude est présentée en Figure 10 (b). Elle met en évidence que : (1) les domaine distaux ne sont pas forcément associés à la rupture lithosphérique (par exemple, la Mer du Nord et les bassins de Porcupine, Hatton, Rockall et Orphan) ; (2) les marges conjuguées de la partie méridionale de l'Atlantique Nord ont des domaines distaux de largeurs comparables. Au contraire, le domaine distal de la marge Est est significativement plus large que son conjugué Ouest dans la partie septentrionale de l'Atlantique Nord.

De plus, le domaine distal de la marge Est contient des rubans de croûte continentale peu amincie (Rockall, Hatton and Porcupine banks), contrairement à son conjugé ; (3) les additions magmatiques dans la partie septentrionale de l'Atlantique Nord sont largement limitées au domaine distal ; en particulier leur limite la plus distale correspond généralement au point de rupture lithosphérique.

Comment caractériser et cartographier l'évolution temporelle premier ordre d'un système de rift ?

Afin de caractériser l'évolution temporelle des systèmes de rift, je me concentre sur deux évènements majeurs, à savoir : (1) le début de l'étranglement, c'est-à-dire la transition entre la phase d'étirement ("stretching mode") et d'amincissement ("thinning mode") ; et (2) la rupture lithosphérique, c'est-à-dire la transition entre la phase d'hyper-extension/exhumation et le début de l'accrétion océanique stationnaire (voir Lavier et Manatschal (2006) pour une discussion des différent modes de déformation). En d'autre termes, je cherche à dater la formation du point d'étranglement et du point de rupture lithosphérique décrits dans la section précédente.

L'extension d'une lithosphère contenant des hétérogénéités, à la fois dans la croûte et le manteau lithosphérique, forme initialement des bassins de rift au niveau des zones de faiblesse crustales (voir les modèles numériques de Chenin et Beaumont, 2013). Dans la nature, ceci se traduit par une extension très distribuée dans les premiers stades du rifting (e.g. Bertotti, 1991; Tankard et Welsink, 1989). Parallèlement, des failles/zones de cisaillement se développent au niveau des zones de faiblesse du manteau supérieur et de la croûte inférieure. Comme ces couches sont les plus rigides de la lithosphère (Maggi *et al.*, 2000), la croissance des instabilités d'amincissement ("necking instabilites") est très rapide (Zuber *et al.*, 1986), trop rapide pour que la diffusion thermique compense l'advection de chaleur qui en résulte. L'étranglement est donc un processus d'affaiblissement qui s'auto-renforce (Buck *et al.*, 1999) et résulte rapidement en la localisation de la déformation. Le début de l'étranglement s'exprime, en surface, par la transition entre une extension initialement très distribuée et une extension focalisée sur un nombre réduit de failles qui accommodent une importante déformation (Mohn *et al.*, 2012). L'abandon simultané de tous les futurs bassins proximaux est enregistré par la formation de la discordance d'étranglement ("necking unconformity") dans le domaine proximal, qui sépare les dépôts syn-tectoniques des dépôts passifs (voir l'insert de droite sur la Figure 11 a).

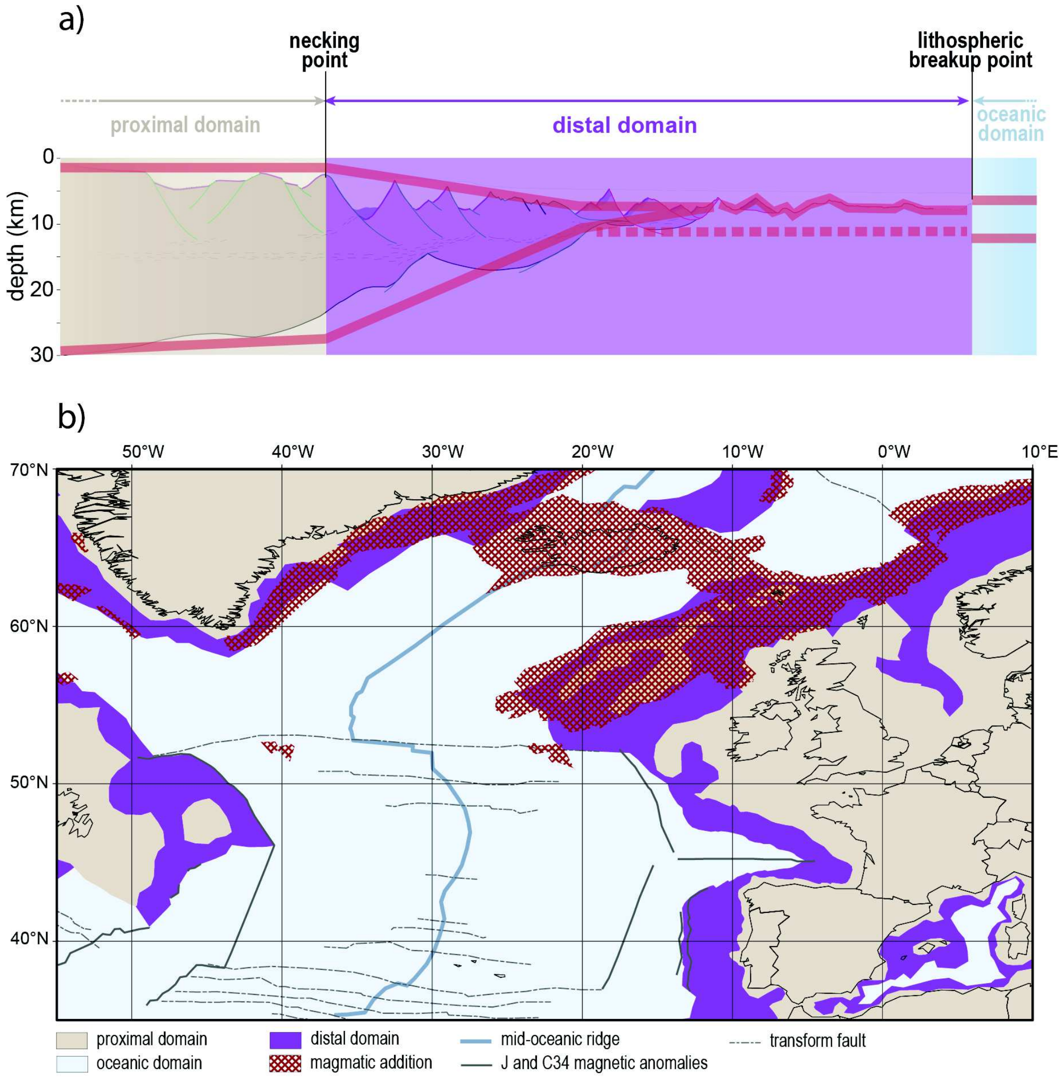

Figure 10 – (a) Definition des domaines de rift, simplifiée d'après Sutra et al. (2013), et leur morphologie premier ordre (lignes rouges). La ligne rouge en pointillée représente le Moho sismique dans les régions où il diffère du Moho pétrologique. (b) Carte des domaines de rift et des additions magmatiques liées à la rupture lithosphérique dans l'Atlantique Nord.

Si l'extension se poursuit, la croûte est progressivement amincie jusqu'à une épaisseur nulle, jusqu'à ce que l'accrétion océanique débute (= la "rupture lithosphérique"). L'extension cesse alors d'être accommodée par la déformation de matériel préexistant et est comblée par l'accrétion de matériel néo-formé (i.e. la croûte océanique). De ce fait, le passage de l'hyper-extension à l'accrétion océanique est enregistré par la transition entre des dépôts sédimentaires syn-tectoniques et un remplissage passif, tout comme le début de l'étranglement (voir l'insert de droite sur la Figure 11 a). Cependant, cette discordance liée à la rupture lithosphérique est plus jeune que celle liée au début de l'étranglement, et existe uniquement dans le domaine distal.

Il convient cependant de noter que, bien que le terme "discordance" soit abondamment utilisé dans la littérature pour référer à l'enregistrement sédimentaire de la rupture lithosphérique, sa pertinence reste un abondant sujet de débat. En effet, la fin de l'enregistrement sédimentaire syn-tectonique n'est pas forcément contemporaine de la rupture lithosphérique, car une phase d'exhumation du manteau peut avoir lieu entre temps ("phase sag" ; voir Haupert *et al.*, sous presse). De plus, la phase d'exhumation peut être marquée par les jeux successifs de différentes failles de détachement, dont chacun forme une discordance comparable aux autres, mais dont les âges diffèrent (Gillard *et al.*, 2015). Toutes ces discordances sont antérieures à la rupture lithosphérique. Par conséquent, pour déterminer l'âge de la rupture lithosphérique, il est nécessaire de sélectionner la dernière/plus distale des discordances. Une autre possibilité consiste à utilier les premiers sédiments déposés sur la croûte océanique stationnaire, or ceux-ci ne sont pour ainsi dire jamais datés. Pour dater la rupture lithosphérique, le proxy le plus accessible reste donc l'âge de la première anomalie magnétique du plancher océanique, à condition que l'accrétion océanique n'ait pas débuté au cours d'une période sans inversion du champ magnétique.

La carte des âges résultant de la compilation de données publiques selon cette philosophie est présentée en Figure 11 (b). Elle met en évidence qu'une phase d'étranglement a affecté aussi bien le sud que le nord de l'Atlantique Nord au Jurassique. Cependant, la rupture lithosphérique s'est faite plus tôt dans la partie méridionale (Crétacé) que dans la partie septentrionale (Eocène). De ce fait, le laps de temps entre l'étranglement et la rupture continentale est significativement plus long dans le sud (> 80 Myr) que dans le nord (< 45 Myr) de l'Atlantique Nord.

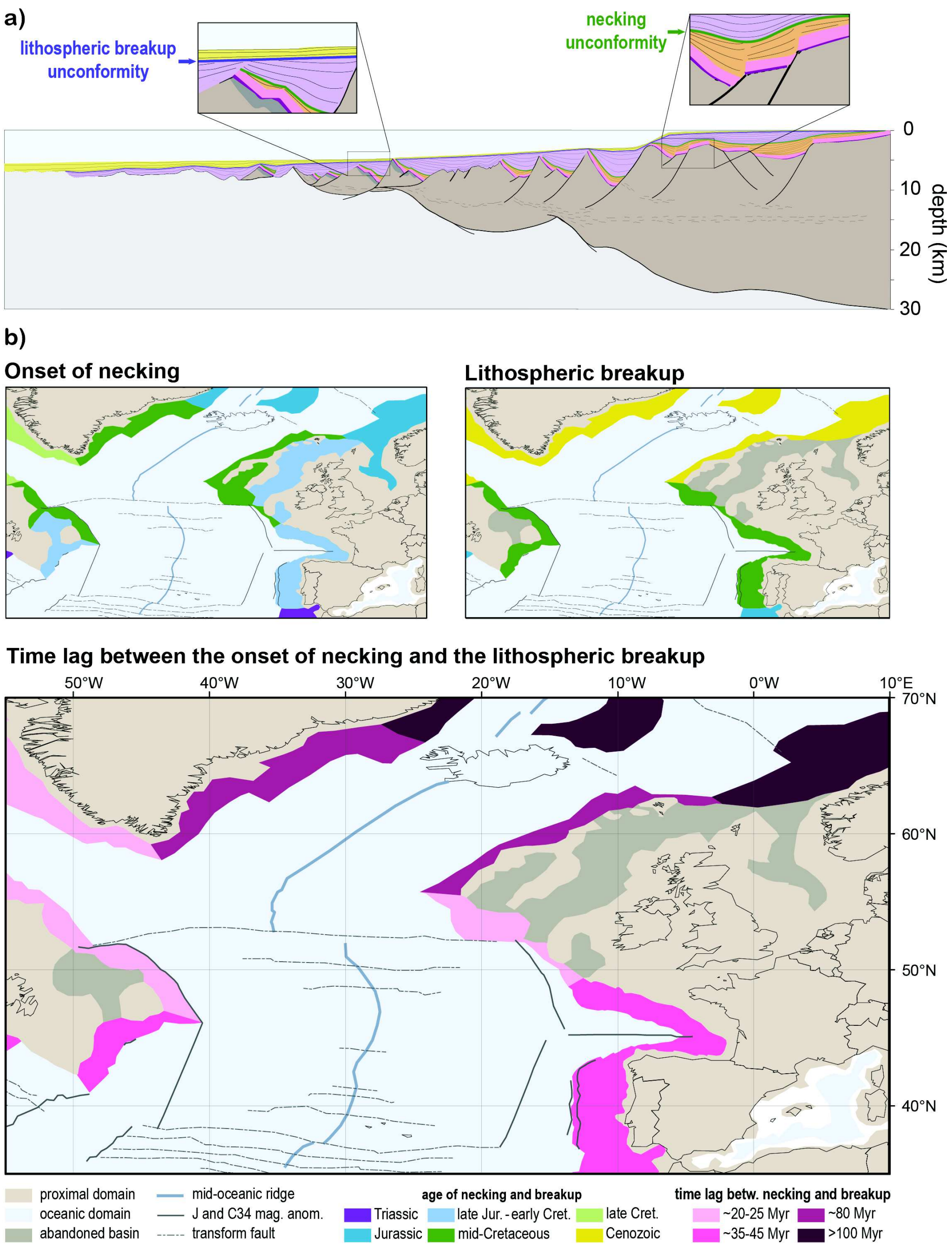

Figure 11 – Enregistrement sédimentaire de l'évolution temporelle du système de rift de l'Atlantique Nord : a) Enregistrement sédimentaire du début de l'étranglement (insert de droite) et de la rupture lithosphérique (insert de gauche) ; b) Carte du l'âge du début de l'étranglement (en haut à gauche), de la rupture lithosphérique (en haut à droite), et du laps de temps entre ces deux évènements (en bas)

Quelles sont les relations entre héritage orogénique et architecture et évolution temporelle des systèmes de rift ?

La comparaison des différentes cartes présentées ci-dessus met en évidence que les caractéristiques du système de rift Nord Atlantique changent abruptement et significativement de part et d'autre du front de déformation Varisque. En effet, le rift traverse l'orogène Calédonien et en réactive les structures héritées au nord, alors qu'au sud, il évite les sutures situées au coeur de l'orogène Varisque d'Europe de l'Ouest. De plus, la transition entre le début de l'étranglement et la rupture lithosphérique est longue (> 80 Myr), polyphasée et forme une succession de bassins de rift avortés au nord, contrairement au sud où elle est significativement plus courte (< 50 Myr) et apparemment continue. Par ailleurs, la rupture lithosphérique est accompagnée d'un important magmatisme au nord, alors qu'elle se fait de façon apparemment a-magmatique au sud.

Il est intéressant de noter que la zone de fracture de Charlie-Gibbs semble prolonger au large le front de déformation Varisque ou la suture Rhéique, ou encore, selon Buiter et Torsvik (2014), la suture de l'océan Iapetus. Elle correspond également à une limite relativement nette entre des provinces riches en magma au nord et pauvres en magma au sud, de façon analogue à la zone de transfert du Colorado dans l'Atlantique Sud (Franke *et al.*, 2010).

Par ailleurs, Roberts *et al.* (1999) ont décrit les premiers stades de l'ouverture de l'Atlantique Nord comme la propagation vers le nord d'un système de rift de l'Atlantique Central qui se terminait initialement dans le bassin de Porcupine, et d'un système de rift Arctique qui se propageait vers le sud, jusque dans la Mer du Nord. Ces deux branches ont été abandonnées au Crétacé Supérieur, suite à quoi les deux systèmes sont devenus coalescents au large du Royaume-Uni. Ici encore, le front de déformation Varisque est précisément situé à l'extrémité de chacun de ces rifts. Cette observation supporte également l'hypothèse que le front Varisque est limite majeure.

Cependant, quel que soit le domaine orogénique qu'il affecte, le système de rift Nord Atlantique réactive, au moins partiellement, les sutures correspondant aux anciens océans majeurs (> 2,000 km), à savoir les océans Iapetus et Rhéique, alors que les sutures correspondant aux anciens océans étroits (< 500–1,000 km ; la Mer de Tornquist et les "océans" Rhénohercynien, Saxothuringien and Médio-Européen) n'ont quasiment pas été affectées, ni lors du rifting de la Tethys Alpine, ni lors de celui de l'Atlantique Nord.

6.2 Chapitre II

Dans le second chapitre de ma thèse, je caractérise l'architecture structurale et lithologique premier ordre des systèmes de rift hyper-étendus, et j'étudie comment elles se répercutent dans les orogenèses de collision. J'utilise le terme *hyper-étendu* pour caractériser des systèmes de rift qui sont allés au-delà du *couplage* entre croûte et manteau (Doré et Lundin, 2015; Sutra et al., 2013). Je me focalise, en particulier, sur les orogènes résultant de la fermeture d'océans "étroits" (c'est-à-dire des systèmes de rift hyper-étendus dont la largeur est inférieure à < 300 km – voir plus loin pour une discussion de cette valeur) premièrement pour m'affranchir de la complexité associée aux subductions prolongées (formation d'arcs magmatiques et/ou avant-arcs, arrière-arcs), et deuxièmement parce que l'impact de l'héritage lié au rift sur de tels systèmes n'a été que peu étudié jusqu'à présent. Il convient de noter que je qualifie de "matures" les systèmes de rift comportant un système d'accrétion stationnaire et auto-entretenu, à l'opposé des systèmes de rift "immatures" dont le développement n'a pas dépassé le stade de l'hyper-extension ou de l'exhumation.

Quelles sont les caractéristiques structurales des "océans" étroits et des océans larges, et comment les quantifier ?

Afin de caractériser l'architecture des systèmes de rift (Figure 12 a), je distingue trois sous-domaines au sein du domaine distal, en me basant sur les critères morphologiques décrits par Sutra et al. (2013) : (i) le domaine d'étranglement (*necking domain*), caractérisé par un amincissement abrupt de la croûte continentale de 30–35 km à ~ 10 km, qui se traduit par un approfondissement du toit du socle associé à une remontée du Moho sur les coupes sismiques migrées en profondeur ; (ii) le domaine hyper-étendu (*hyperextended domain*) où la croûte continentale est atténuée jusqu'à une épaisseur nulle. La transition entre le domaine d'étranglement et le domaine hyper-étendu se reflète dans la réduction du pendage du Moho sur les coupes sismiques en profondeur ; (iii) un domaine d'exhumation (*exhumation domain*) peut éventuellement exister dans les marges dites "pauvres en magma", lorsque du manteau sous-continental est exhumé au niveau du plancher océanique et/ou lorsqu'un un système d'accrétion encore balbutiant forme une croûte océanique "embryonnaire" (à l'opposé d'une croûte océanique stationnaire de type "Penrose" ; voir Anonymous, 1972). Sur les coupes sismiques, le domaine d'exhumation apparaît comme une surface relativement irrégulière dépourvue de Moho – ou avec un Moho discontinu en présence d'une activité magmatique embryonnaire (Whitmarsh *et al.*, 2001).

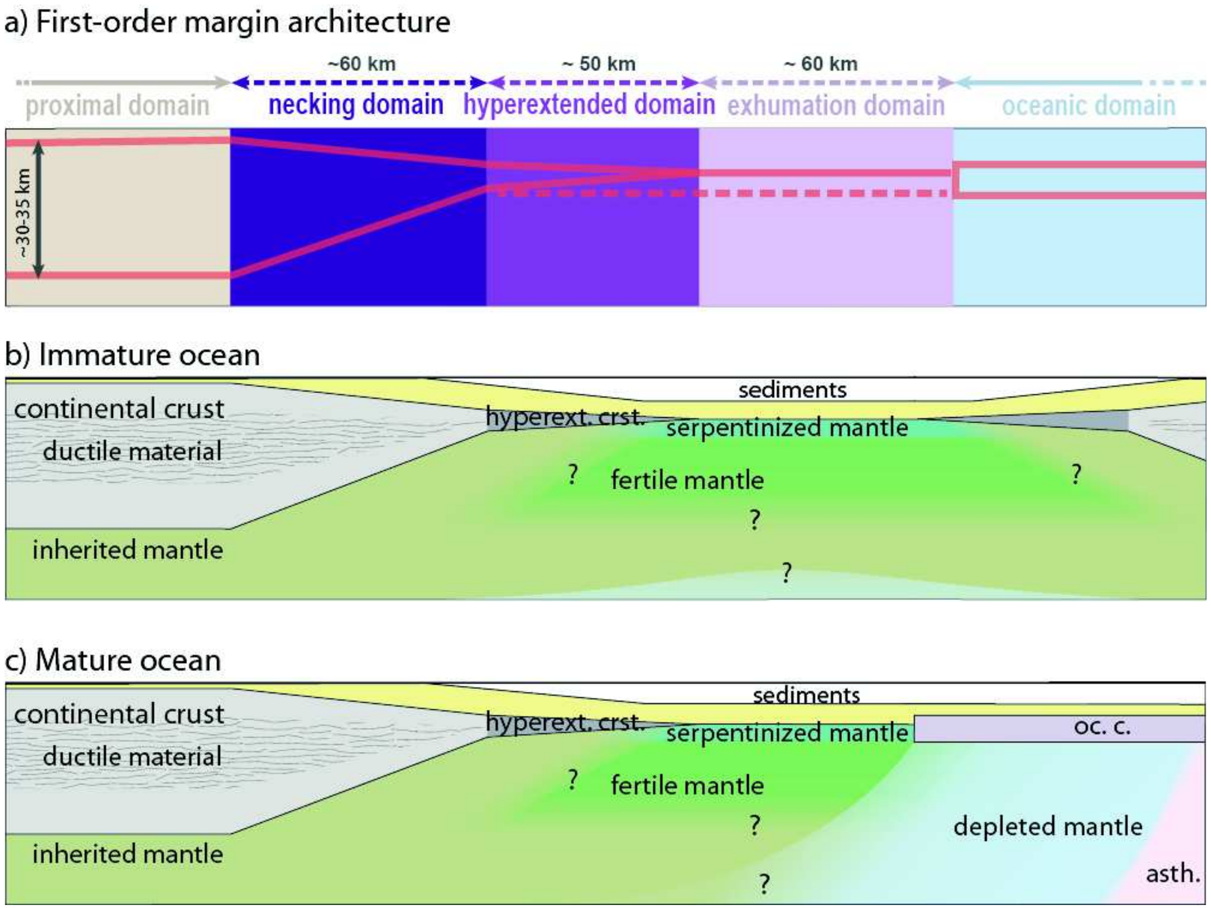

Figure 12 – (a) Architecture structurale premier ordre d'une marge hyper-étendue ; (b) Architecture lithologique premier ordre d'un océan immature ; (c) Architecture lithologique premier ordre d'un océan mature. hyp. c. : croûte continentale hyper-étendue ; oceanic c. croûte océanique ; depl. m. : manteau appauvri ; asth. : manteau asthénosphérique. Voir dans le texte pour discussion.

Les analyses statistiques effectuées sur une sélection de coupes sismiques (c.f. Figure II.2 (a) dans le Chapitre II) montrent que, malgré une variation considérable de la longueur totale des marges selon les systèmes de rift, la longueur du domaine hyper-étendu semble relativement constante (50 km en moyenne). Au contraire, les domaines d'étranglement et d'exhumation ont des dimensions nettement plus variables, bien que leur longueur moyenne soit comparable ($\sim$ 60 km).

Le fait que le domaine hyper-étendu ait une longueur relativement constante pourrait s'expliquer par la théorie du prisme critique de Coulomb, comme proposé par Nirrengarten *et al.* (subm.). En effet, le matériel composant le domaine hyper-étendu est complètement cassant (Sutra et Manatschal, 2012; Sutra et al., 2013 ; Figure 12) et repose sur un décollement à faible coefficient de friction (i.e. une faille de détachement mantellique). Lorsqu'un tel système est soumis à de l'extension, il se déforme de façon similaire à un prisme critique de Coulomb, dont les caractéristiques dépendent à la fois des paramètres de friction du matériel et de la pression de fluides (Dahlen, 1984; Davis *et al.*, 1983). A l'opposé, la déformation dans les domaines d'étranglement et d'exhumation du manteau est essentiellement contrôlée par l'architecture et/ou la rhéologie héritée(s) de la croûte et/ou du manteau, comme proposé par Manatschal *et al.* (2015) – voir en Annexe A.

Par ailleurs, aucune corrélation n'apparaît, entre la longueur des sous-domaines distaux et la longueur totale du domaine distal (voir Figure II.2 (b) dans le Chapitre II). La longueur du domaine d'étranglement et celle du domaine hyper-étendu apparaissent également indépendantes de la maturité du système de rift (voir Figure II.2 (d) dans le Chapitre II).

Quelles sont les caractéristiques lithologiques des "océans" étroits et des océans larges ?

Dans le domaine proximal et dans le domaine d'étranglement, ni la composition de la croûte, ni celle du manteau ne sont significativement modifiées lors de l'extension. Par conséquent, tous deux préservent l'essentiel de leurs caractéristiques héritées. De façon générale, la croûte peut être rapprochée d'un matériel quartzo-feldspathique, et le manteau dit "hérité" d'une péridotite de composition moyenne de 35–65% olivine, 7–30 % clinopyroxène, 25–30% orthopyroxène, $\sim$ 1% spinelle (Picazo *et al.*, 2015, in prep.). Il faut cependant noter que, lors de l'extension, le matériel ductile est progressivement éliminé jusqu'à disparaître totalement au niveau du point de couplage ("coupling point" sur la Figure 12 ; voir Pérez-Gussinyé *et al.*, 2003; Sutra et al., 2013 et Manatschal *et al.*, 2015 en Annexe A).

A l'inverse, les interactions fluides–roches forment une quantité notable de minéraux hydratés dans le domaine hyper-étendu (séricite et illite dans les reliquats de croûte continentale ; serpentine dans la partie superficielle du manteau ; Pinto, 2014). Bien que la croûte hyper-étendue ne soit jamais complètement altérée, sa rhéologie est contrôlée par la phase la plus faible si elle est en quantité suffisante (Jammes *et al.*, 2013, subm.). De ce fait, la croûte continentale hyper-étendue ainsi que les 6 km superficiels du manteau se comportent, au premier ordre, comme un matériel de type phyllosilicate.

Par ailleurs, l'amincissement de la croûte à 10 km ou moins conduit à la fusion partielle du manteau asthénosphérique sous-jacent. Ce magma n'est pas immédiatement extrait, mais "imbibe" le manteau lithosphérique sus-jacent (Müntener *et al.*, 2010, 2004; Piccardo *et al.*, 2014). La composition moyenne d'un tel manteau "enrichi" est d'environ 51% olivine, 16% clinopyroxène, 25% orthopyroxène, 7% plagioclase,1% spinelle, et sa densité est notablement plus faible que celle d'un manteau hérité moyen ($\sim$ 3,250 kg.m^{-3} comparé à $\sim$ 3,300 kg.m^{-3} ; Picazo *et al.*, 2015, in prep.).

Si l'extension se poursuit jusqu'à la rupture lithosphérique et qu'un système d'accrétion stationnaire est mis en place, ce dernier forme une croûte océanique mafique et homogène, tant du point de vue de sa composition (environ 50% plagioclase et 50% pyroxène) que de son épaisseur ($\sim$ 6–7 km ; Anonymous, 1972). Les processus de fusion partielle dont est issue la croûte océanique extraient les éléments les plus incompatibles de l'asthénosphère, et la percolation de ce magma au travers du manteau lithosphérique sus-jacent en lessive également une quantité non négligeable. Ces processus laissent un manteau "appauvri" dont la composition moyenne est de 57% olivine, 13% clinopyroxène, 28% orthopyroxène, 2% spinelle (Picazo *et al.*, 2015, in prep.) sur une épaisseur d'environ 70 km (Müntener, communication personnelle). La densité de ce manteau appauvri similaire à celle du manteau hérité moyen ($\sim$ 3,300 kg.m^{-3} ; Picazo *et al.*, 2015, in prep.).

La Figure 12 synthétise l'architecture d'un système de rift non-volcanique immature (b) ; et mature (c).

Quelles sont les différences premier ordre entre les "océans" étroits et les océans larges ?

Les études statistiques présentées dans le Chapitre II laissent penser que les "océans" de moins de 350–400 km de large sont généralement dépourvus de système d'accrétion auto-entretenu – donc de croûte océanique stationnaire – et que leur plancher est formé soit de croûte continentale amincie, soit de manteau exhumé et/ou de croûte océanique embryonnaire. A l'inverse, les océans de grande taille (> 1 000 km) ont généralement atteint une telle envergure du fait d'un système d'accrétion mature produisant une croûte océanique stationnaire. Par conséquent, le manteau sur lequel reposent les "océans" étroits a probablement conservé la composition fertile acquise lors de l'hyper-extension, alors que celui des océans matures est vraisemblablement appauvri, comparable à celui des rides médio-océaniques.

D'un autre côté, comme il n'y a pas de différence statistique entre l'architecture des marges d'un système de rift étroit/immature et d'un océan de grande envergure/mature, je propose que, au premier ordre, la seule différence entre ces deux extrêmes soit l'existence d'une croûte océanique stationnaire reposant sur un manteau appauvri (comparer les schémas (b) et (c) de la Figure 12).

Comment les spécificités des marges se reflètent-elles lors d'une orogenèse subséquente à la fermeture d'un océan étroit ? Quelles sont les différences par rapport à une orogenèse conséquente à la subduction d'un océan large ?

Au cours de la subduction d'un océan étroit, le pendage de la plaque plongeante reste relativement faible (Billen, 2008; Stevenson et Turner, 1977; Tovish *et al.*, 1978). De ce fait, il est peu probable que la subduction s'auto-entretienne (Gurnis *et al.*, 2004; Hall *et al.*, 2003), et un système de convection vigoureux de petite échelle a peu de chance de se mettre en place dans le coin mantellique (Peacock *et al.*, 1994), au contraire de ce qui est observé dans le cas de subductions prolongées. De plus, la subduction d'un "océan" étroit n'est pas assolée à une activité magmatique significative, car sa courte durée ne permet pas à une quantité suffisante d'éléments volatiles d'atteindre une profondeur assez grande pour permettre la fusion partielle du coin mantellique (Gaetani et Grove, 1998; Peacock, 1991; Rüpke *et al.*, 2004). En conséquence, l'hydratation est vraisemblablement le processus dominant dans le coin mantellique.

Par ailleurs, du fait de son faible pendage, la plaque plongeante exerce une traction vers le bas relativement faible, et les éventuels flux convectifs du manteau ont une faible emprise sur le slab, rendant la formation d'un bassin d'arrière-arc et le magmatisme qui lui est associé improbables (Heuret et Lallemand, 2005; Uyeda, 1981). Par conséquent, le manteau lithosphérique sous-jacent aux orogènes résultants de la fermeture d'océans étroits est vraisemblablement relativement fertile et hydraté (Figure 13 b).

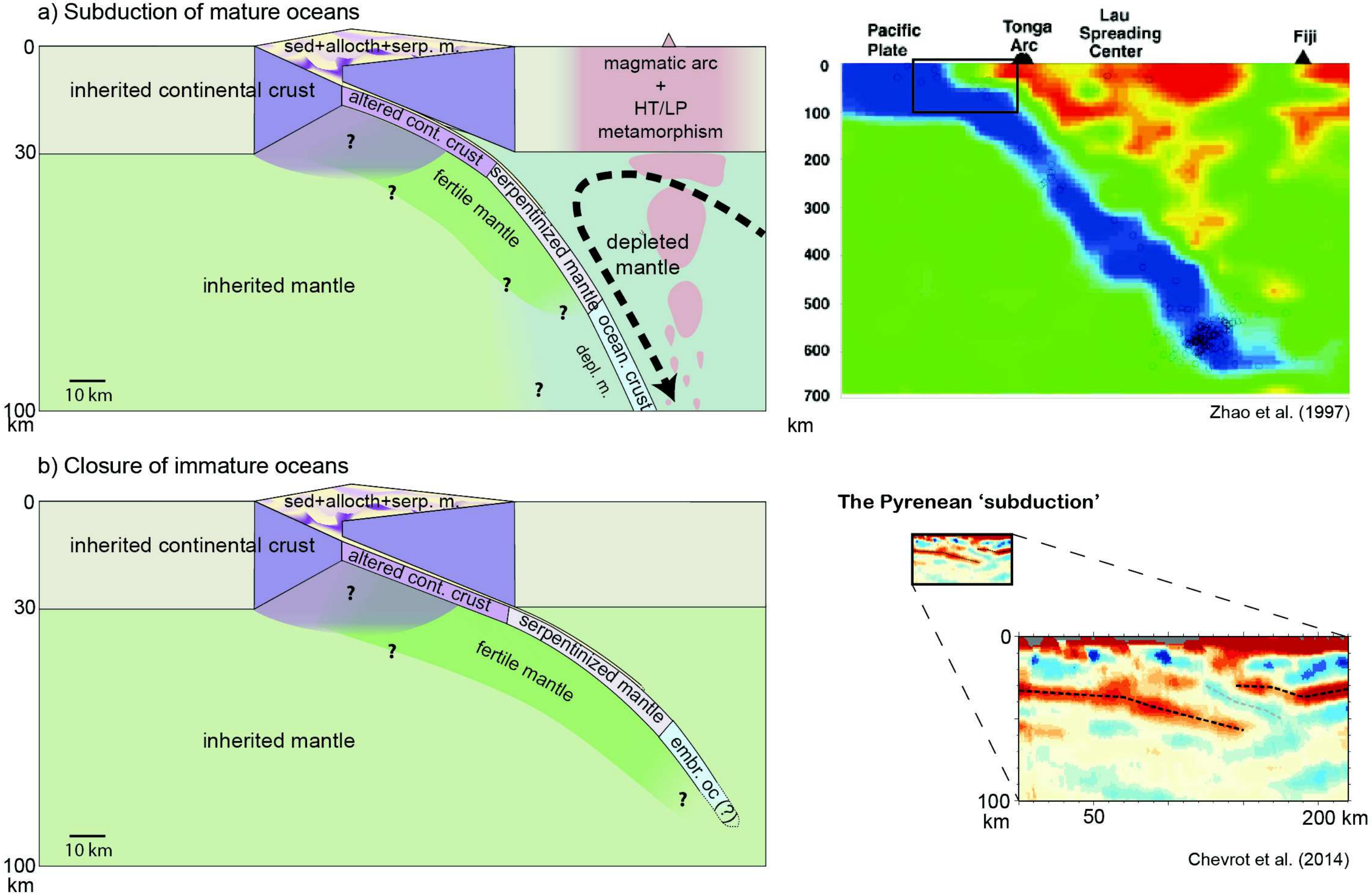

Figure 13 – Tableaux de gauche : Architecture d'un orogène produit par (a) la subduction d'un océan large et mature ; et (b) la fermeture étroit et immature. depl. m.: manteau appauvri ; embr. oc.: croûte océanique embryonnaire ; HT/LP: haut temperature/basse pression ; oc. crust: croûte océanique ; Tableaux de droite : Tomographie sismique au travers de la subduction Pacifique (océan mature) d'après Zhao (1997) et de la "subduction" pyrénéenne (océan immature) d'après Chevrot *et al.* (2015). Les inserts marquent l'échelle des zones représentée sur les tableaux de gauche correspondants.

A l'inverse, la subduction prolongée relative à la fermeture d'un océan large est fortement susceptible de s'auto-entretenir, en particulier à cause de l'éclogitisation progressive de la plaque plongeante (Doin et Henry, 2001). Lors de telles subductions prolongées, une convection vigoureuse se développe généralement dans le coin mantellique, amenant rapidement à grande profondeur une quantité notable d'éléments volatiles issus de la déshydratation du slab (Peacock *et al.*, 1994). La fusion partielle qui en résulte se traduit par la formation d'une épaisse croûte *sialique* (arcs magmatiques) et du métamorphisme de haute température dans le toit de la subuction, et appauvri le coin mantellique en éléments incompatibles (Bonatti et Michael, 1989; Uyeda, 1981). En d'autres termes, ils induisent d'importantes perturbations lithologiques et thermiques, tant dans la croûte que dans le manteau.

De plus, lorsque que plusieurs centaines de kilomètres de croûte océanique sont subductées, la forte traction du slab et possiblement les effet de traction du flux mantellique convectif sur le slab, peuvent induire son retrait, menant à la formation d'un bassin d'arrière arc (Heuret et Lallemand, 2005; Uyeda, 1981). Celle-ci est possiblement associée à de l'accrétion océanique, donc à un appauvrissement du manteau sous-jacent (Figure 13 b). Bien que la convection vigoureuse présente dans le coin mantellique tende à en homogénéiser la composition, un appauvrissement par rapport au manteau asthénosphérique standard est hautement probable, et a été observé par Woodhead *et al.* (1993) et Martinez et Taylor (2002).

Ainsi, les orogenèse causées par la fermeture d'un océan étroit sont sans doute essentiellement contrôlées par des processus mécaniques, sans modification significative de la composition ou de l'état thermique des marges initiales, et avec une influence notable de l'architecture héritée des marges impliquées. Au contraire, les orogenèses produites par la fermeture d'océans larges seraient significativement contrôlées par des processus induits par la subduction.

La différence de composition mantellique engendrées par la fermeture d'océans larges et étroits pourrait se répercuter dans le budget magmatique des phases d'extension subséquentes, comme un effondrement post-orogénique ou un épisode de rift. En effet, le manteau appauvri sous-jacent aux orogènes matures ne permettrait potentiellement pas une fusion partielle significative, à l'inverse de celui sous des orogènes immatures. Cette hypothèse pourrait expliquer à la fois l'effondrement a-magmatique de la chaîne Calédonienne norvégienne (Fossen *et al.*, 2014; Meissner, 1999), qui résulte de la fermeture du large océan Iapetus (McKerrow et Cocks, 1976), et de l'épisode magmatique majeur associé à l'effondrement de la chaîne Varisque en

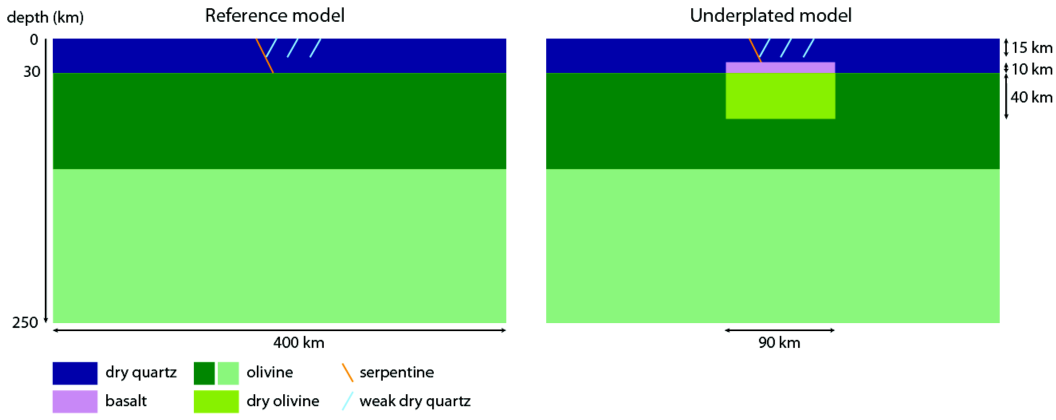

Figure 14 – Architecture lithologique et structurale du modèle de référence (à gauche) et du modèle sous plaqué (à droite). La base de la lithosphère (limite vert foncé/vert clair) est l'isotherme 1 300 °C (pas de changement des paramètres physiques entre les matériaux de part et d'autre de la limite). Sa profondeur varie entre 115 km lorsque le Moho est à 400°C et 85 km quand le Moho est à 500°C.

Europe de l'Ouest (Costa and Rey, 1995), issue de la fermeture des 'océans étroits' Rhénohercynien, Saxothuringien et Médio-Européen (Franke, 2006).

Alternativement, le faible budget magmatique de l'effondrement Calédonien pourrait être expliqué par la composition appauvrie du manteau cratonique sous-jacent aux deux continents impliqués dans la collision, à savoir Baltica et Laurentia (Bernstein *et al.*, 1998; Beyer *et al.*, 2004; Griffin *et al.*, 2003).

6.3 Chapitre III

Dans le troisième chapitre de ma thèse, j'analyse, via la modélisation numérique, l'effet d'un sous-plaquage mafique de la croûte continentale, et de l'appauvrissement du manteau sous-jacent qui en résulte, sur un épisode de rift subséquent. En particulier, j'utilise le code thermo-mécanique FLAC (Cundall, 1989) pour étudier la réactivation de zones de faiblesse au sein d'une croûte quartzique sous-plaquée par une couche basaltique de 10 km d'épaisseur et une zone de manteau appauvri de 70 km d'épaisseur (voir Figure 14).

Comment un sous-plaquage mafique de la croûte continental et/ou une zone de manteau appauvri à l'aplomb d'une ancienne zone de suture orogénique influencent-ils l'architecture et l'évolution d'un système de rift subséquent ? Comment l'état thermique de la lithosphère et du corps sous-plaqué se répercutent-ils sur les processus d'extension ?

Les modèles numériques présentés dans le Chapitre III (voir la Figure 15 pour une synthèse) suggèrent que, dans une lithosphère à l'équilibre thermique, l'existence d'une croûte inférieure juvénile mafique et/ou d'une zone de manteau appauvri à l'aplomb d'une ancienne zone de suture orogénique empêche la réactivation des structures faibles héritées lors de l'extension (Modèles 2–4 et 6–8). Par contre, si les intrusions sont encore significativement plus chaudes que le milieu environnant, elles sont susceptibles de concentrer la déformation, donc de localiser le rift dans l'ancienne zone orogénique (Modèle 5). De plus, les résultats des modèles supportent qu'en présence d'un corps sous-plaqué, plus l'état thermique de la lithosphère est chaud, plus la phase d'extension est longue, comme précédemment démontré pour une lithosphère horizontalement homogène (par exemple Buck *et al.*, 1999).

Par ailleurs, si la lithosphère est suffisamment chaude, l'existence de corps plus résistants de grande dimension dans la croûte inférieure et/ou le manteau lithosphérique peut déclencher la formation d'instabilités d'étranglement régulièrement espacées ("necking instabilities"). Ce phénomène se traduit par la préservation de régions de croûte continentale peu ou pas amincie (y compris la zone sous-plaquée), contiguës à des zones d'étranglement ou hyper-étendues (Modèles 3, 4 et 6–8).

Il est intéressant de noter que, dans le modèle de référence dépourvu de sous-plquage (Modèle 1), l'hyper-extension ne se localise pas au niveau de la zone de suture, bien qu'elle soit l'hétérogénéité avec la rhéologie la plus faible et la plus grande envergure (Figure 14). En effet, l'extension se focalise sur les deux "failles" antithétiques qui lui sont adjacentes, alors qu'elles sont plus résistantes et n'affectent que la partie la plus superficielle de la croûte continentale. Ceci peut s'expliquer par le fait que l'amincissement de la lithosphère s'initie au centre de la zone de rift, et comme la remontée de l'asthénosphère devient rapidement un processus actif qui s'auto renforce, elle contrôle la localisation de la rupture lithosphérique finale. Il convient également de noter que, dans ce modèle, l'asymétrie des marges semble essentiellement contrôlée par la distribution initiale des zones de faiblesse.

Bien entendu, d'autres facteurs tels que l'intensité de l'affaiblissement des failles au cours de la déformation, ou encore la différence de densité entre le manteau appauvri et le manteau standard peuvent potentiellement avoir une influence notable sur la déformation. Or ces paramètres sont, à l'heure actuelle, encore largement méconnus. Pour ces raisons, j'ai réalisé quelques modèles pour tester leur influence. Les résultats de ces expériences sont présentés en Annexe D, sections 2 et 3.

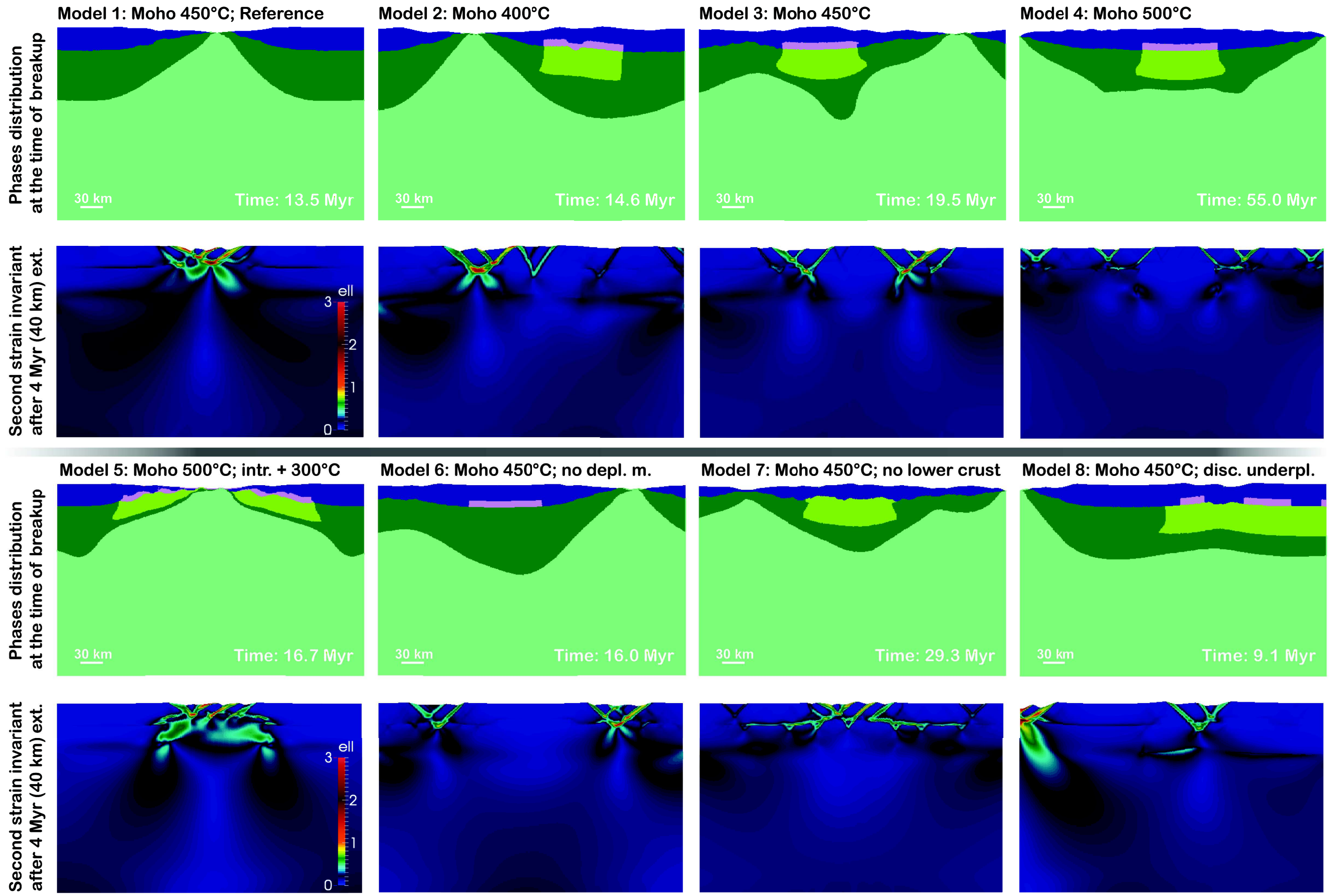

Figure 15 – Synthèse des 8 modèles numériques présentés dans le Chapitre III. Tableaux du haut : distribution des différents matériaux au moment de la "rupture lithosphérique" ; Tableaux du bas : second invariant du tenseur de déformation après 4 Myr (40 km) d'extension.

Est-il-possible d'appliquer ces résultats à l'analyse du rift Nord Atlantique au niveau de la lithosphère Varisque sous-plaquée ?

D'un côté, les résultats présentés dans le paragraphe précédant pourraient expliquer pourquoi le système de rift de la Tethys Alpine et la partie méridionale de l'Atlantique Nord contournent le coeur sous-plaqué de l'orogène Varisque en Europe de l'ouest, alors que la partie septentrionale du rift Nord Atlantique coupe l'orogène Calédonien et suit grossièrement la suture de l'ancien océan Iapetus dans la région dépourvue d'activité magmatique post-orogénique significative (Figure 16 ; Fossen *et al.*, 2014; Meissner, 1999). De plus, le développement vers le sud du Graben Central (Mer du Nord) et la propagation vers le nord du bassin de Porcupine (sud-ouest du Royaume-Uni) semblent tous deux se terminer là où commence le sous-plaquage post-orogénique de la lithosphère (Figure 16). Ces observations laissent également penser qu'une lithosphère sous-plaquée pourrait être une barrière à la propagation des rifts.

D'un autre côté, le fait que, dans le modèle de référence dépourvu de sous-plaquage, le rift ne se localise pas au niveau de la suture mais entre deux failles de la ceinture de plissement-chevauchement adjacente peut être rapproché du comportement du rift Nord Atlantique septentrional. En effet, entre la Norvège et le Groenland, la suture de l'océan Iapetus a été réactivée lors de l'extension, mais la rupture lithosphérique en est décalée. Cette dernière se localise au sein de la ceinture de plissement-chevauchement (Figure 16).

Par ailleurs, les instabilités d'étranglement déclenchées par la présence de sous-plaquage pourrait expliquer la formation de rubans de croûte continentale peu ou pas amincie au large de la péninsule ibérique et de la Terre-Neuve (Galicia Bank and Flemish Cap, respectivement), ainsi que les bassins avortés de Porcupine et de la Mer Celtique. En effet, la partie sud de l'Atlantique Nord s'est développée à la limite de la lithosphère Varisque sous-plaquée, comme le suggère la croûte mafique pré-rift visible sur les coupes sismiques établies dans ces régions (e.g. Díaz et Gallart, 2009; Freeman *et al.*, 1988; Van Avendonk *et al.*, 2009). De plus, une zone de manteau appauvri, vraisemblablement issue d'un arc magmatique formé lors de la subduction de l'océan Iapetus, a été mise en évidence au large de la Terre-Neuve (Müntener and Manatschal, 2006). Toutes ces hétérogénéités plus résistantes pourraient avoir déclenché le boudinage de la croûte continentale, comme illustré par les modèles 2 à 4 et 6 à 8.

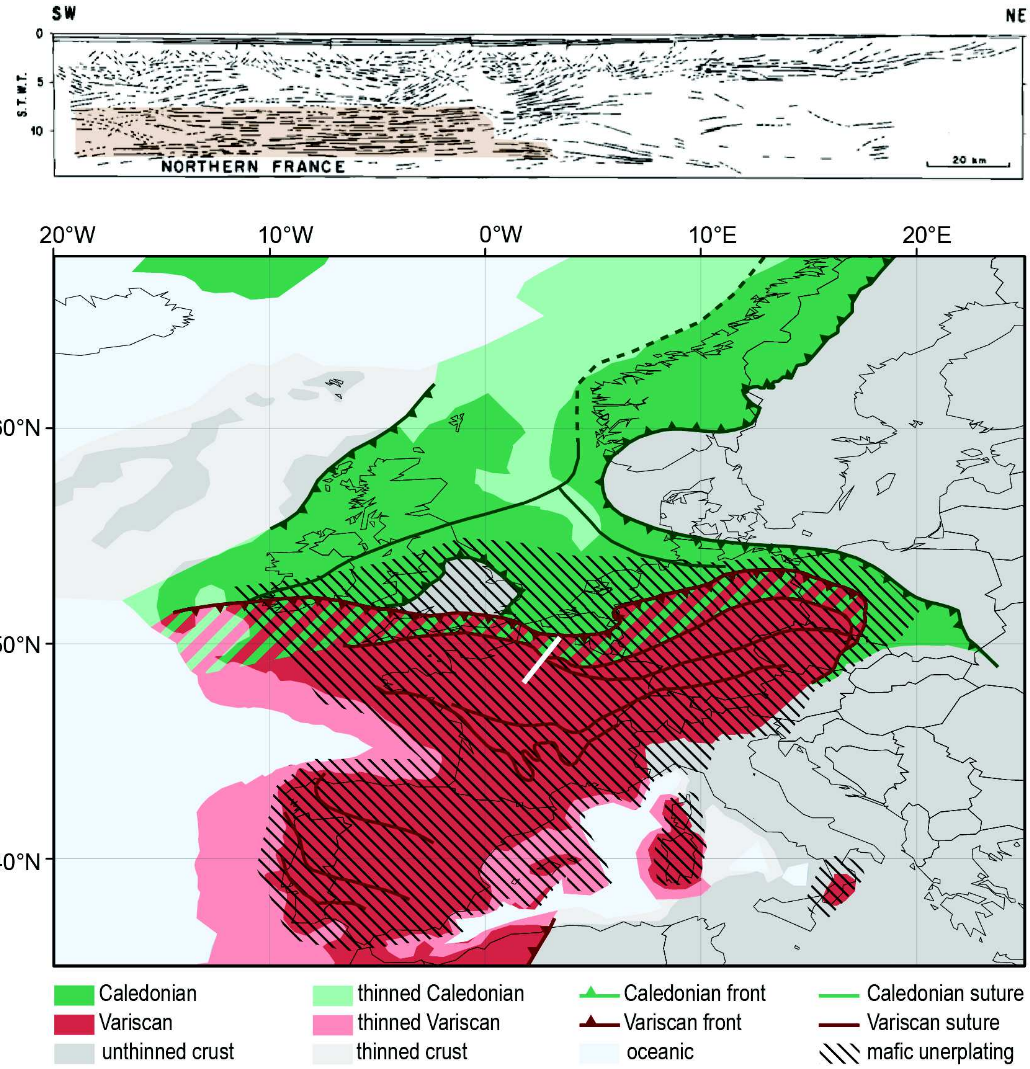

Figure 16 – En haut : Coupe sismique au travers de l'orogène Varisque d'après Bois *et al.* (1989) – voir la carte en dessous pour sa localisation ; En bas : Carte montrant l'étendue des domaines orogéniques Calédonien et Varisque, du sous-plaquage mafique Permien, et du système de rift Mésozoïque de l'Atlantique Nord. Les données sur lesquelles est basée l'estimation de l'étendue du sous-plaquage sont décrites en Annexe B, section 4.

Par contre, aucun indice ne suggère la présence de sous-plaquage post-orogénique plus au nord, alors que les rubans de croûte peu amincie sont toujours présents (Hatton et Rockall banks). Dans ces régions, c'est possiblement l'extension polyphasée, ponctuée par des périodes de relaxation qui pourraient être à l'origine de la formation de ces bassins de rift avortés. En effet, lors de l'extension, la partie inférieure de la croûte amincie est remplacée par du manteau qui, une fois refroidi, est nettement plus résistant à la déformation. Lors d'un épisode subséquent, l'extension tendra donc à se localiser ailleurs (Buck *et al.*, 1999).

Une explication alternative pourrait s'appuyer sur l'existence de zones de manteau appauvri résultant d'arcs magmatiques (et/ou avant-arcs, arrière-arcs) associés à la subduction de l'océan Iapetus, analogues à celles mise en évidence lors de la campagne de dragage au large de la Terre-Neuve Müntener and Manatschal (2006). Comme l'illustre le Modèle 7, une telle architecture rhéologique est favorable au développement d'instabilités d'étranglement régulièrement espacées. Cependant, cette hypothèse est difficile à tester car il n'existe aucun échantillon du manteau sous-jacent à Rockall Bank ou Hatton Bank.

7 Discussion

Le rôle de l'héritage dans le contrôle des processus tectoniques est une question de longue date en Sciences de la Terre. En particulier, on peut se demander si le Cycle de Wilson, théorie selon laquelle les océans tendent à s'ouvrir et se refermer le long des même lignes, ne serait pas une conséquence de l'héritage laissé par les processus de rift et/ou les orogenèses. Pour répondre à cette question, l'étude du système de rift Nord Atlantique est particulièrement adaptée, car il affecte simultanément deux domaines orogéniques aux histoires géologiques contrastées.

Impact de l'héritage orogénique

La comparaison des cartes présentées dans le Chapitre I démontrent que, dans l'Atlantique Nord, les caractéristiques du système de rift diffèrent largement selon le domaine orogénique qu'il affecte. En effet, l'extension se fait de manière prolongée et polyphasée, en réactivant largement les structures orogéniques antérieures dans la partie Calédonienne, au nord de la zone de fracture de Charlie–Gibbs. Au contraire, la rupture lithosphérique est achevée à la suite un épisode d'extension relativement court, qui évite la plupart des anciennes sutures orogénique dans la partie Varisque de l'Europe de l'Ouest située entre les zones de fractures Charlie–

Gibbs et Açores–Gibraltar. De plus, la rupture lithosphérique est accompagnée par une activité magmatique intense au nord de la zone de fracture Charlie–Gibbs, alors qu'elle s'effectue sans manifestation magmatique significative au sud. Ces observations supportent l'hypothèse que **l'héritage orogénique influence fortement les épisodes de rift subséquents, mais peut se refléter différemment selon les caractéristiques des orogenèses antérieures**.

Impact de l'état thermique de la lithosphère

Un premier facteur qui pourrait expliquer cette diversité est l'état thermique de la lithosphère, qui dépend entre autres du temps de latence entre l'épisode orogénique et le début de l'extension. Dans la région de l'Atlantique Nord, $\sim$ 200 Myr se sont écoulés entre la fin des Calédonides et le début de l'étranglement en Atlantique Nord septentrional, alors que ce temps est de 100 Myr entre la fin des Variscides et le début de l'étranglement dans l'Atlantique Nord méridional. Or, comme décrit par Buck (1991) et réaffirmé dans le Chapitre III, des temps de latence plus courts – donc des états thermiques plus chauds – entraînent des épisodes de rift plus longs et caractérisés par une déformation plus distribuée. Ces affirmations sont en opposition avec les caractéristiques des rifts observées dans ces régions.

Impact de l'intensité du magmatisme post-orogénique

L'intensité du magmatisme post-orogénique est un autre facteur pouvant expliquer la différence de comportement du rift Nord Atlantique entre la lithosphère Calédonienne et Varisque. En effet, alors que l'effondrement de l'orogène Calédonien a été essentiellement contrôlé par des processus mécaniques, celui de la chaîne Varisque a été accompagné par une intense activité magmatique qui s'est traduite par la mise en place d'une croûte inférieure mafique pouvant atteindre10 km d'épaisseur sous une grande partie de l'Europe de l'Ouest (Costa and Rey, 1995; Rey, 1993 ; voir la Figure 16). Les différentes plaques lithosphériques ont vraisemblablement été soudées, et le manteau sous-jacent témoigne d'un appauvrissement en éléments incompatibles notable (Picazo *et al.*, 2015, in prep.).

Comme le retour à l'équilibre thermique d'une lithosphère s'achève généralement en moins de 100 Myr (Jaupart et Mareschal, 2007), les variations latérales de température au sein de la lithosphère Varisque étaient probablement insignifiantes au moment de l'étranglement, bien que son état thermique ait sans doute été encore relativement chaud (température du Moho jusqu'à $\sim$ 600°C selon Müntener and

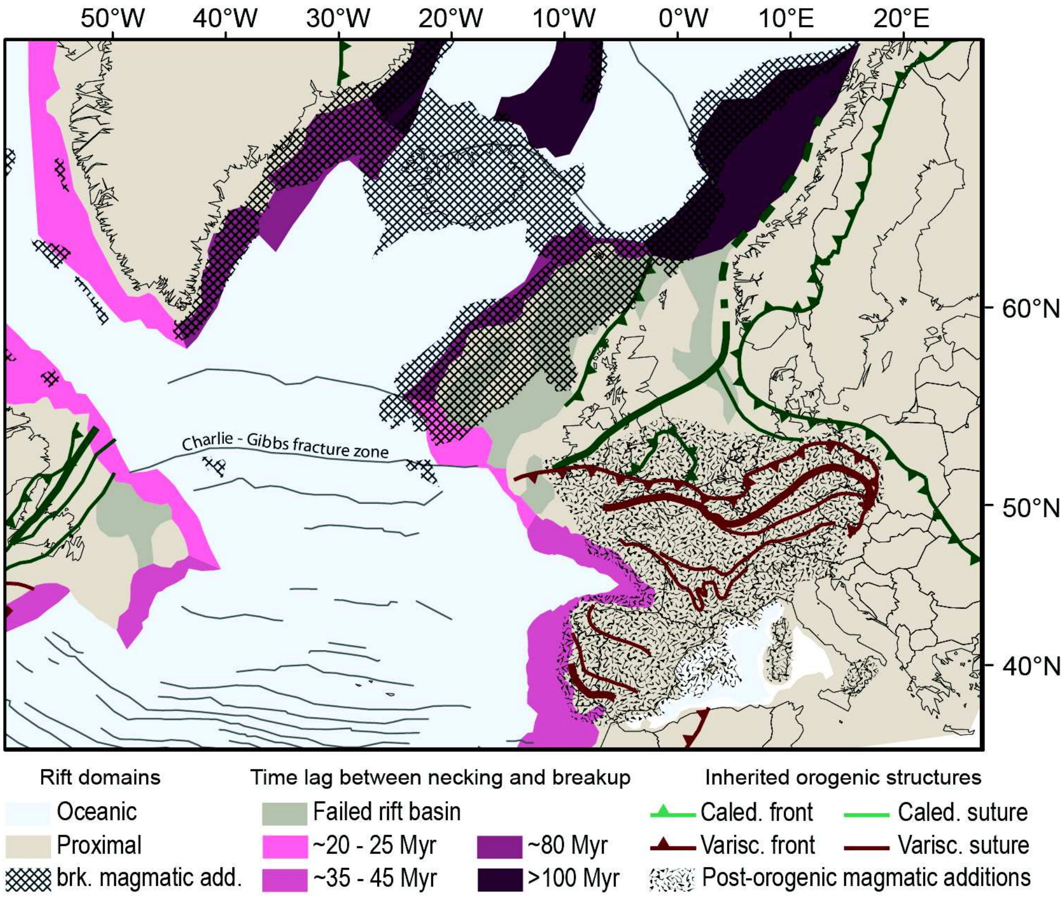

Figure 17 – Carte de l'Atlantique Nord synthétisant les domaines de rift majeurs, les additions magmatiques liées à la rupture continentale ou postérieures, les structures orogéniques Calédonienne et Varisque de premier ordre, les régions affectées par une intense activité magmatique post-orogénique et l'écart de temps entre l'étranglement et la rupture lithosphérique.

Manatschal, 2006). Dans ce contexte, les modèles numériques présentés dans le chapitre III laissent supposer que **l'important sous-plaquage de la lithosphère Varisque peut avoir joué un rôle de barrière au développement des rifts de la Tethys Alpine et de l'Atlantique Nord le long des sutures orogéniques en Europe de l'Ouest**.

De plus, à la fois la propagation vers le sud du système de rift Arctique dans la Mer du Nord, et la propagation vers le nord de l'Atlantique Nord dans le bassin de Porcupine semblent se terminer là où commence le sous-plaquage (voir la Figure 17). En effet, la présence d'une couche à forte réflectivité sismique à la base de la croûte continentale a été mise en évidence lors de la campagne sismique BIRPS dans le sud de la Mer du Nord ainsi qu'au sud-ouest du Royaume-Uni (Bois *et al.*, 1990; Blundell et al., 1991). Cette observation étaye également l'hypothèse que le sous-plaquage est une barrière à la propagation des rifts.

Impact de la paléo-géographie

Les cadres paléo-géographiques contrastés qui précèdent aux orogenèses Calédonienne et Varisque ont vraisemblablement eu une influence considérable sur leurs caractéristiques structurales, lithologiques et thermiques respectives. Ces spécificités se sont vraisemblablement ensuite répercutées dans les épisodes de rift subséquents.

L'orogenèse Calédonienne est essentiellement issue de la fermeture d'un océan de grande envergure entre deux continents majeurs, à savoir Laurentia et Baltica (Roberts, 2003). Il est important de noter que ces deux continents sont en grande partie composés d'un coeur cratonisé le long duquel différents *terranes* ont été accrétés (Cocks et Torsvik, 2005, 2011). A l'opposé, l'orogenèse Varisque s'est en grande partie formée par l'accrétion de différents micro-continents et/ou rubans continentaux le long de la marge sud d'Avalonia, suite à la fermeture de plusieurs "océans étroits". Par la suite, la fermeture du large océan Rhéique a mené à la collision entre cet "agrégat" et le continent Gondwana (Franke, 2006). Or, comme souligné dans le Chapitre II, des différences majeures peuvent être attendues entres des orogènes "matures" (i.e. issus de la fermeture d'océans larges) et des orogènes "immatures" (i.e. produits par la fermeture d'océans étroits, < 300 km).

Les orogenèses immatures sont essentiellement contrôlées par des processus mécaniques, sans modification significative de l'architecture thermique, de la lithologie ou de la composition dans les premiers stades de la collision continentale. Au contraire, la composition et l'état thermique des orogènes matures sont notablement affectés par les processus magmatiques et métamorphiques associés aux subductions prolongées. En conséquence le toit des subductions matures aura été thermiquement affaibli de façon notoire (Gerya et Meilick, 2011), et la composition du coin mantellique aura été relativement appauvrie au moment de la collision continentale (voir dans la Chapitre II).

D'ailleurs, les différences de composition mantellique entre les orogènes matures et immatures pourraient vraisemblablement se refléter dans l'intensité du magmatisme associé à leur éventuel effondrement post-orogénique. En effet, le manteau relativement appauvri sous les orogènes matures ne permettrait pas une fusion partielle suffisante pour être exprimée en surface. Par conséquent, l'effondrement apparaîtrait dépourvu d'activité magmatique. Au contraire, on peut légitimement suspecter que le manteau peu ou pas appauvri sous-jacent aux orogènes immatures soit aisément fusible, donc propice à la production d'une importante quantité de magma. Ce raisonnement pourrait à la fois expliquer l'effondrement a-magmatique de la chaîne Calédonienne, et l'intense activité magmatique associée à l'effondrement de la chaîne Varisque.

Alternativement, l'absence de magmatisme lors de l'effondrement de la chaîne Calédonienne pourrait s'expliquer par le gradient géothermique faible, l'épaisseur importante, et l'intense appauvrissement du manteau caractérisants les lithosphères cratoniques impliquées dans les Calédonides (Bernstein *et al.*, 1998; Beyer *et al.*, 2004; Griffin *et al.*, 2003). Au contraire, la composition du manteau lithosphérique des micro-continents impliqués dans la collision Varisque est vraisemblablement beaucoup plus fertile.

Il est cependant important de noter que la fermeture d'un seul océan étroit ne créé pas forcément une topographie assez conséquente pour que son retour à l'équilibre isostatique nécessite un effondrement orogénique de grande ampleur. De ce fait, les effondrements post-orogéniques accompagnés d'épisodes magmatiques conséquents pourraient être restreints aux subductions multiples d'océans étroits – comme dans le cas des Variscides – ou éventuellement aux subductions prolongées caractérisées par une convection assez intense pour que le coin mantellique soit réhomogénéisé efficacement avec l'asthénosphère (fertile) environnante. Cependant, cette hypothèse est difficile à tester, d'une part parce que le cas des Variscides semble rare, sinon unique, et d'autre part car peu de croûtes inférieures sous-plaquées suite à un effondrement post-orogénique ont été incontestablement identifiées jusqu'à présent.

L'architecture des océans étroits/immatures par rapport aux océans larges/matures

Puisque les orogenèses immatures sont essentiellement contrôlées par des processus mécaniques, l'héritage lié au rift joue vraisemblablement un rôle important dans leur développement. De ce fait, il est indispensable de connaître l'architecture des systèmes de rift afin de comprendre les processus orogéniques.

Les études statistiques sur les dimensions des systèmes de rift menées dans le Chapitre II suggèrent l'existence de plusieurs caractéristiques communes à l'ensemble des marges riftées. En effet, au premier ordre, la plupart des marges sont caractérisées par une succession similaire de domaines comparables (Péron-Pinvidic *et al.*, 2013; Sutra et al., 2013 ; voir la Figure 10). De plus, la largeur et la rhéologie du domaine hyper-étendu semblent relativement constantes entre les différentes marges étudiées, et ce indépendamment de largeur totale du domaine distal ou de la maturité du système de rift. En conséquence, on peut légitimement supposer que le domaine hyper-étendu est contrôlé par des processus identiques dans tous les systèmes de rift (voir dans le Chapitre II ; Manatschal *et al.*, 2015; Sutra et Manatschal, 2012, Nirrengarten *et al.*, subm.).

Au contraire, les dimensions et les caractéristiques rhéologiques du domaine proximal et du domaine d'étranglement sont nettement plus variables, vraisemblablement car elles sont essentiellement contrôlées par l'héritage orogénique (Manatschal *et al.*, 2015). Il convient de noter que le domaine d'exhumation n'existe que dans les marges dites "pauvres en magma", et ne peut, par conséquent, pas être considéré comme caractéristique des marges riftées.

Il est intéressant de noter que, d'après les observations décrites dans les paragraphes précédents, c'est la "variabilité" (dans l'architecture et la lithologie) qui semble caractériser les domaines de rift contrôlés par l'héritage, alors que les caractéristiques des domaines contrôlés par les processus *induits par l'extension* sont beaucoup plus constantes. Parallèlement, les processus *induits par la subduction* semblent relativement constants parmi les subductions matures (i.e. formation d'arcs magmatiques, métamorphisme de haute température/basse pression dans le toit de la subduction ; voir Uyeda, 1981), alors que rien ne peut être prédit dans le cas des subductions transitoires d'océans étroits. De ce fait, on peut s'attendre à nettement plus de variabilité dans le cas d'orogènes immatures que dans le cas d'orogènes matures.

8 Conclusions & Perspectives : Vers un modèle général

L'héritage tectonique semble grandement affecter l'ensemble du Cycle de Wilson, et de diverses façons selon la taille et la maturité des océans impliqués. Il pourrait par conséquent être intéressant de distinguer deux cas extrêmes de Cycle de Wilson (Figure 18) : d'un côté, la fermeture d'un océan étroit et immature conduirait à une subduction transitoire et une orogenèse essentiellement contrôlée par des processus mécaniques. Dans ce cas, les caractéristiques initiales des marges (héritage) seraient des facteurs de contrôle dominants dans l'architecture des orogènes résultants, laissant présager une grande variabilité.

A l'opposé, la fermeture d'un océan mature/de grande envergure se fait au cours d'une subduction prolongée, vraisemblablement associée à la formation d'arcs magmatiques (et potentiellement aussi des avant-arcs et/ou arrière-arcs) et à un appauvrissement du manteau en éléments incompatibles. Comme ces processus modifient notablement la lithologie et l'état thermique, à la fois de la croûte et du manteau, l'orogenèse est probablement significativement contrôlée par les conséquences des processus induits par la subduction. De ce fait, les différents orogènes de ce type ont de fortes chances de montrer une certaine uniformité d'architecture.

De plus, du fait de l'appauvrissement du manteau résultant de la formations d'arcs, avant-arcs et/ou arrière-arcs, le budget magmatique disponible dans le manteau au moment de l'effondrement post-orogénique est susceptible d'être relativement faible au niveau d'un orogène mature – à moins qu'une convection vigoureuse n'ait homogénéisé le coin mantellique. A l'inverse le budget magmatique est susceptible d'être beaucoup plus important au niveau d'un orogène immature, car le manteau n'a pas été appauvri lors de la subduction. Or un sous-plaquage mafique de grande ampleur est susceptible de faire barrière à la propagation d'un rift, donc de contrôler si un futur océan s'ouvrira ou non au niveau d'une ancienne zone orogénique. Cependant, des études plus poussées sont nécessaires afin d'approuver ou de rejeter ces hypothèses.

En prenant du recul, une autre question fondamentale apparaît : pourquoi existe-t-il aussi bien des bassins de rifts étroits et immatures que des océans larges et matures ? Malgré les preuves irréfutables que le développement de certains systèmes de rift s'arrête au stade de l'hyper-extension, les facteurs qui contrôlent la mise en place d'un système d'accrétion océanique stationnaire restent, jusqu'à présent, largement méconnus.

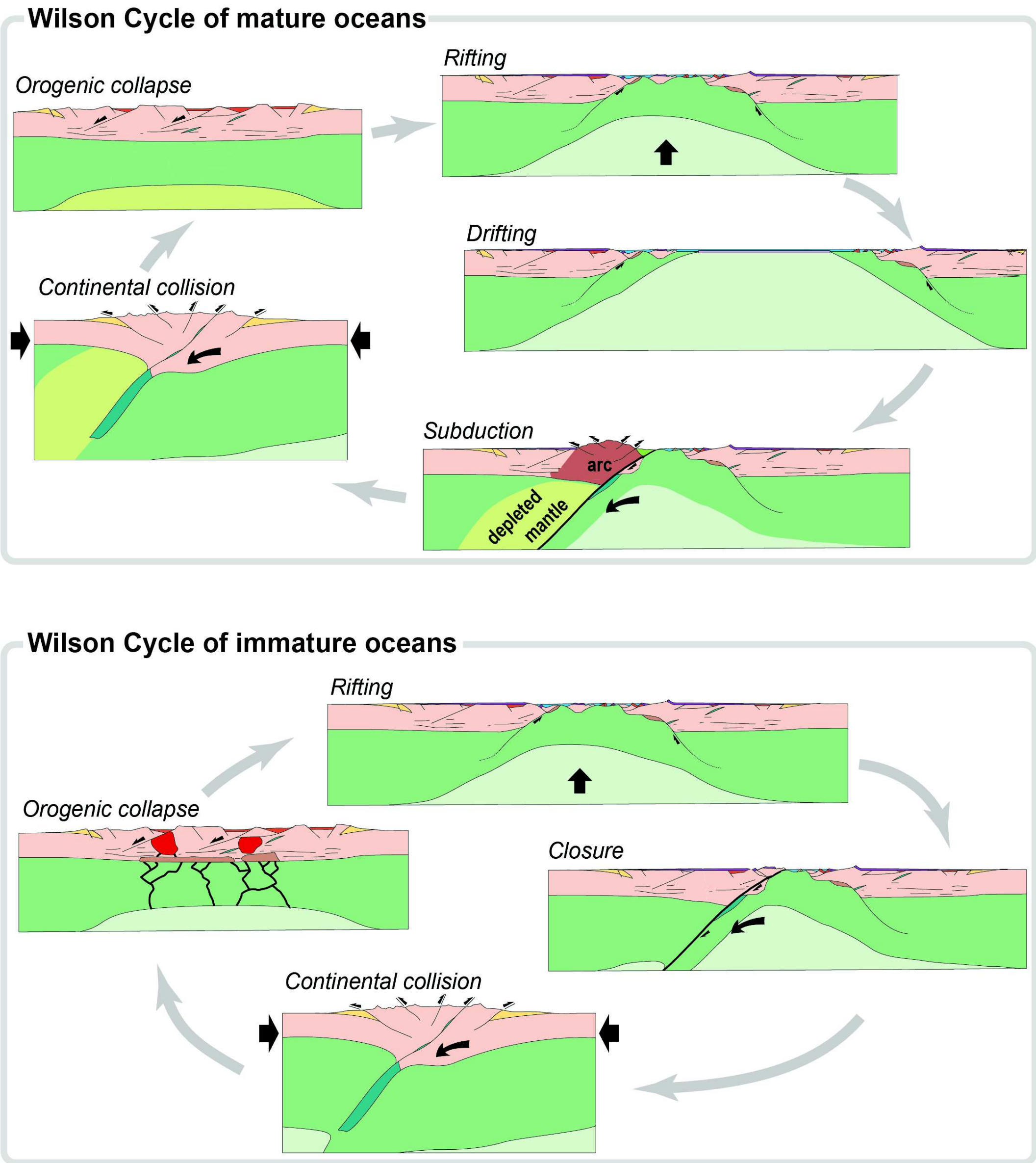

Figure 18 – Illustration des deux "Cycle de Wilson" proposés dans cette étude (modifié d'après Petri, 2014).

Références bibliographiques

Allègre, C. et Dars, R. (2009). *La géologie, passé, présent et avenir de la Terre*. Pour la Science, belin édition.

Andersen, T. B. (1998). Extensional tectonics in the Caledonides of southern Norway, an overview. *Tectonophysics*, 285:333–351.

Anonymous (1972). Penrose field conference on ophiolites. *In Penrose Field Conference on ophiolites*, volume 17, pages 24–25. Geotimes.

Artemieva, I. M. et Thybo, H. (2013). EUNAseis: A seismic model for Moho and crustal structure in Europe, Greenland, and the North Atlantic region. *Tectonophysics*, 609:97–153.

Audet, P. et Bürgmann, R. (2011). Dominant role of tectonic inheritance in supercontinent cycles. *Nature Geoscience*, 4(3):184–187.

Bernstein, S., Kelemen, P. B. et Brooks, C. (1998). Depleted spinel harzburgite xenoliths in Tertiary dykes from East Greenland: Restites from high degree melting. *Earth and Planetary Science Letters*, 154(1-4):221–235.

Bertotti, G. (1991). Early Mesozoic extension and Alpine shortening in the western Southern Alps: The geology of the area between Lugano and Menaggio (Lombardy, Northern Italy). *Mem. Soc. Geol. Padova*, 43:17–123.

Beyer, E. E., Brueckner, H. K., Griffin, W. L., O'Reilly, S. Y. et Graham, S. (2004). Archean mantle fragments in Proterozoic crust, Western Gneiss Region, Norway. *Geology*, 32(7):609–612.

Billen, M. I. (2008). Modeling the Dynamics of Subducting Slabs. *Annual Review of Earth and Planetary Sciences*, 36(1):325–356.

Blundell, D. J., Hobbs, R. W., Klemperer, S. L., Scott-Robinson, R., Long, R. E., West, T. E. et Duin, E. (1991). Crustal structure of the central and southern North Sea from BIRPS deep seismic reflection profiling. *Journal of the Geological Society*, 148(3):445–457.

Bois, C., Lefort, J.-P., Le Gall, B., Sibuet, J.-C., Gariel, O., Pinet, B. et Cazes, M. (1990). Superimposed Variscan, Caledonian and Proterozoic features inferred from deep seismic profiles recorded between southern Ireland, Southwestern Britain and western France. *Tectonophysics*, 177(1-3):15–37.

Bois, C., Pinet, B. et Roure, F. (1989). Dating lower crustal features in france and adjacent areas from deep seismic profiles. *Geophysical Monograph Series*, 51:17–31.

Bonatti, E. et Michael, P. J. (1989). Mantle peridotites from continental rifts to ocean basins to subduction zones. *Earth and Planetary Science Letters*, 91(3-4):297–311.

Buck, R., Lavier, L. L. et Poliakov, A. N. B. (1999). How to make a rift wide. *Philosophical Transactions of the Royal Society A: Mathematical, Physical and Engineering Sciences*, 357(1753):671–693.

Buck, W. R. (1991). Modes of continental lithospheric extension. *Journal of Geophysical Research*, 96(B12):20,161–20,178.

Buiter, S. J. H. et Torsvik, T. H. (2014). A review of Wilson Cycle plate margins: A role for mantle plumes in continental break-up along sutures? *Gondwana Research*, 26(2):627–653.

Butler, R. W. H. (2013). Area balancing as a test of models for the deep structure of mountain belts, with specific reference to the Alps. *Journal of Structural Geology*, 52(1):2–16.

Butler, R. W. H., Tavarnelli, E. et Grasso, M. (2006). Structural inheritance in mountain belts: An Alpine-Apennine perspective. *Journal of Structural Geology*, 28(11):1893–1908.

Cappelletti, A., Tsikalas, F., Nestola, Y., Cavozzi, C., Argnani, A., Meda, M. et Salvi, F. (2013). Impact of lithospheric heterogeneities on continental rifting evolution: Constraints from analogue modelling on South Atlantic margins. *Tectonophysics*, 608(0316):30–50.

Casteras, M. (1933). Recherches sur la structure du versant nord des Pyrénées centrales et orientales. *Bulletin du Service de la Carte Géologique de France*, 37:25.

Cawood, P. A., Kröner, A., Collins, W. J., Kusky, T. M., Mooney, W. D. et Windley, B. F. (2009). Accretionary orogens through Earth history. *Geological Society, London, Special Publications*, 318(1):1–36.

Chenin, P. et Beaumont, C. (2013). Influence of offset weak zones on the development of rift basins: Activation and abandonment during continental extension and breakup. *Journal of Geophysical Research*, 118(4):1698–1720.

Chevrot, S., Sylvander, M., Diaz, J., Ruiz, M., Paul, A., Cougoulat, G., Péquegnat, C., Wolyniec, D., Delmas, P., Grimaud, F., Benahmed, S., Pauchet, H., de Saint Blanquat, M., Lagabrielle, Y. et Manatschal, G. (2015). The Pyrenean architecture as revealed by teleseismic P-to-S converted waves recorded along two dense transects. *Geophysical Journal International*, 200(1):1096–1107.

Chopin, C. (1987). Very-High-Pressure Metamorphism in the Western Alps: Implications for Subduction of Continental Crust [and Discussion]. *Philosophical Transactions of the Royal Society A: Mathematical, Physical and Engineering Sciences*, 321(1557):183–197.

Cocks, L. R. M. et Fortey, R. A. (1982). Faunal evidence for oceanic separations in the Palaeozoic of Britain. *Journal of the Geological Society*, 139(4):465–478.

Cocks, L. R. M., McKerrow, W. S. et van Staal, C. R. (1997). The margins of Avalonia. *Geological Magazine*, 134(5):627–636.

Cocks, L. R. M. et Torsvik, T. H. (2005). Baltica from the late Precambrian to mid-Palaeozoic times: The gain and loss of a terrane's identity. *Earth-Science Reviews*, 72:39–66.

Cocks, L. R. M. et Torsvik, T. H. (2011). The Palaeozoic geography of Laurentia and western Laurussia: A stable craton with mobile margins. *Earth-Science Reviews*, 106:1–51.

Costa, S. et Rey, P. (1995). Lower crustal rejuvenation and growth during post-thickening collapse: Insights from a crustal cross section through a Variscan metamorphic core complex. *Geology*.

Cundall, P. A. (1989). Numerical experiments on localization in frictional materials. *Ingenieur-Archiv*, 59(2):148–159.

Dadlez, R. (2000). Pomeranian Caledonides (NW Poland), fifty years of controversies: a review and a new concept. *Geological Quartely*, 44(3):221–236.

Dahlen, F. A. (1984). Noncohesive critical Coulomb wedges: An exact solution. *Journal of Geophysical Research*, 89(B12):10125.

Dal Piaz, G. V., Bistacchi, A. et Massironi, M. (2003). Geological outline of the Alps. *Episodes*, 26(3):175–180.

Davis, D., Dahlen, F. A. et Suppe, J. (1983). Mechanics of fold-and-thrust belts and accretionary wedges Cohesive Coulomb theory. *Journal of Geophysical Research*, 88(B2):1153–1172.

Díaz, J. et Gallart, J. (2009). Crustal structure beneath the Iberian Peninsula and surrounding waters: A new compilation of deep seismic sounding results. *Physics of the Earth and Planetary Interiors*, 173(1-2):181–190.

Doin, M.-P. et Henry, P. (2001). Subduction initiation and continental crust recycling : the roles of rheology and eclogitization. *Tectonophysics*, 342:163–191.

Domeier, M., Van Der Voo, R. et Torsvik, T. H. (2012). Paleomagnetism and Pangea: The road to reconciliation. *Tectonophysics*, 514-517:14–43.

Doré, A. G., Lundin, E. R., Fichler, C. et Olesen, O. (1997). Patterns of basement structure and reactivation along the NE Atlantic margin. *Journal of the Geological Society*, 154:85–92.

Doré, A. G., Lundin, E. R., Jensen, L. N., Birkelan, Ø., Eliassen, P. E. et Fichler, C. (1999). Principal tectonic events in the evolution of the northwest European Atlantic margin. *In* Fleet, A. J. et Boldy, S. A. R., éditeurs : *Petroleum Geology of Northwest Europe: Proceedings of the 5th Conference*, pages 41–61. The Geological Society, London.

Doré, T. et Lundin, E. (2015). Hyperextended continental margins – Knowns and unknowns. *Geology*, 43(1):95–96.

Fossen, H., Gabrielsen, R. H., Faleide, J. I. et Hurich, C. A. (2014). Crustal stretching in the Scandinavian Caledonides as revealed by deep seismic data. *Geology*, 42(9):791–794.

Franke, D., Ladage, S., Schnabel, M., Schreckenberger, B., Reichert, C., Hinz, K., Paterlini, M., de Abelleyra, J. et Siciliano, M. (2010). Birth of a volcanic margin off Argentina, South Atlantic. *Geochemistry, Geophysics, Geosystems*, 11(2):n/a–n/a.

Franke, W. (2006). The Variscan orogen in Central Europe: construction and collapse. *Geological Society, London, Memoirs*, 32(1):333–343.

Freeman, B., Klemperer, S. L. et Hobbs, R. W. (1988). The deep structure of northern England and the Iapetus Suture zone from BIRPS deep seismic reflection profiles. *Journal of the Geological Society*, 145(5):727–740.

Frizon de Lamotte, D., Raulin, C., Mouchot, N., Wrobel-Daveau, J.-C., Blanpied, C. et Ringenbach, J.-C. (2011). The southernmost margin of the Tethys realm during the Mesozoic and Cenozoic: Initial geometry and timing of the inversion processes. *Tectonics*, 30(3):1–22.

Gaetani, G. A. et Grove, T. L. (1998). The influence of water on melting of mantle peridotite. *Contributions to Mineralogy and Petrology*, 131(4):323–346.

Gaetani, M., Dercourt, J. et Vrielynck, B. (2003). The Peri-Tethys Programme: achievements and results. *Episodes*, 26(2):79–93.

GERYA, T. V. et MEILICK, F. I. (2011). Geodynamic regimes of subduction under an active margin: effects of rheological weakening by fluids and melts. *Journal of Metamorphic Geology*, 29:7–31.

GILLARD, M., AUTIN, J., MANATSCHAL, G., SAUTER, D., MUNSCHY, M. et SCHAMING, M. (2015). Tectonomagmatic evolution of the final stages of rifting along the deep conjugate Australian-Antarctic magma-poor rifted margins: Constraints from seismic observations. *Tectonics*, 34:753–783.

GRIFFIN, W., O'REILLY, S., ABE, N., AULBACH, S., DAVIES, R., PEARSON, N., DOYLE, B. et KIVI, K. (2003). The origin and evolution of Archean lithospheric mantle. *Precambrian Research*, 127(1-3):19–41.

GURNIS, M., HALL, C. et LAVIER, L. (2004). Evolving force balance during incipient subduction. *Geochemistry, Geophysics, Geosystems*, 5(7).

HALL, C. E., GURNIS, M., SDROLIAS, M., LAVIER, L. L. et MÜLLER, R. (2003). Catastrophic initiation of subduction following forced convergence across fracture zones. *Earth and Planetary Science Letters*, 212(1-2):15–30.

HANDY, M. R., M. SCHMID, S., BOUSQUET, R., KISSLING, E. et BERNOULLI, D. (2010). Reconciling plate-tectonic reconstructions of Alpine Tethys with the geological-geophysical record of spreading and subduction in the Alps. *Earth-Science Reviews*, 102(3-4):121–158.

HAUPERT, I., MANATSCHAL, G., DECARLIS, A. et UNTERNEHR, P. (in press.). Upper-plate magma-poor rifted margins: stratigraphic architecture and structural evolution. *Marine and Petroleum Geology*.

HEURET, A. et LALLEMAND, S. (2005). Plate motions, slab dynamics and back-arc deformation. *Physics of the Earth and Planetary Interiors*, 149(1-2 SPEC. ISS.):31–51.

ISOZAKI, Y. (1997). Contrasting two types of orogen in Permo-Triassic Japan: Accretionary versus collisional. *The Island Arc*, 6:2–24.

JAMMES, S., LAVIER, L. L. et REBER, J. E. (2013). Effect of polymineralic crustal composition on deformation processes. *In AGU Fall Meeting Abstracts*, page 2519.

JAUPART, C. et MARESCHAL, J. C. (2007). Heat flow and thermal structure of the lithosphere. *Treatise on Geophysics*, 6:217–251.

JUHOJUNTTI, N., JUHLIN, C. et DYRELIUS, D. (2001). Crustal reflectivity underneath the Central Scandinavian Caledonides. *Tectonophysics*, 334(3-4):191–210.

KRABBENDAM, M. et BARR, T. D. (2000). Proterozoic orogens and the break-up of Gondwana: why did some orogens not rift? *Journal of African Earth Sciences*, 31(1):35–49.

Krawczyk, C. M., McCann, T., Cocks, L. R. M., England, R. W., McBride, J. H. et Wibraniec, S. (2008). Caledonian tectonics. *In* McCann, T., éditeur : *The Geology of Central Europe, Volume 1: Precambrian and Palaeozoic*, pages 303–381. The Geological Society, London.

Kröner, U., Mansy, J. L., Mazur, S., Aleksandrowski, P., Hann, H. P., Huckriede, H., Lacquement, F., Lamarche, J., Ledru, P., Pharaoh, T. C., Zedler, H., Zeh, A. et Zulauf, G. (2008). Variscan tectonics. *In* McCann, T., éditeur : *The Geology of Central Europe, Volume 1: Precambrian and Palaeozoic*, chapitre 11, pages 599–664. the Geological Society, London.

Kröner, U. et Romer, R. (2013). Two plates – Many subduction zones: The Variscan orogeny reconsidered. *Gondwana Research*, 24(1):298–329.

Lavier, L. L. et Manatschal, G. (2006). A mechanism to thin the continental lithosphere at magma-poor margins. *Nature*, 440(7082):324–328.

Mac Niocaill, C., Van der Pluijm, B. A. et Van der Voo, R. (1997). Ordovician paleogeography and the evolution of the Iapetus ocean. *Geology*, 25(2):159–162.

Maggi, A., Jackson, J. A., Priestley, K. et Baker, C. (2000). A re-assessment of focal depth distributions in southern Iran, the Tien Shan and northern India: do earthquakes really occur in the continental mantle? *Geophysical Journal International*, 143(3):629–661.

Manatschal, G., Lavier, L. et Chenin, P. (2015). The role of inheritance in structuring hyperextended rift systems: Some considerations based on observations and numerical modeling. *Gondwana Research*, 27(1):140–164.

Manatschal, G. et Müntener, O. (2009). A type sequence across an ancient magma-poor ocean–continent transition: the example of the western Alpine Tethys ophiolites. *Tectonophysics*, 473:4–19.

Martinez, F. et Taylor, B. (2002). Mantle wedge control on back-arc crustal accretion. *Nature*, 416(6879):417–420.

Mattauer, M. (1968). Les traits structuraux essentiels de la chaîne pyrénéenne. *Revue de Géologie Dynamique et de Géographie physique*, 10:3–11.

Matte, P. (2001). The Variscan collage and orogeny (480- 290 Ma) and the tectonic definition of the Armorica microplate: a review. *Terra Nova*, 13:122–128.

Maus, S., Barckhausen, U., Berkenbosch, H., Bournas, N., Brozena, J., Childers, V., Dostaler, F., Fairhead, J. D., Finn, C., von Frese, R. R. B., Gaina, C., Golynsky, S., Kucks, R., Lühr, H., Milligan, P., Mogren, S., Müller, R. D., Olesen, O., Pilkington, M., Saltus, R., Schreckenberger, B., Thébault, E. et Caratori Tontini, F. (2009). EMAG2: A 2-arc min resolution Earth Magnetic Anomaly Grid compiled from satellite, airborne, and marine magnetic measurements. *Geochemistry, Geophysics, Geosystems*, 10(8): n/a–n/a.

Mckenzie, D. et Bickle, M. J. (1988). The volume and composition of melt generated by extension of the lithosphere. *Journal of Petrology*, 29(3):625–679.

McKerrow, W. S. et Cocks, L. R. M. (1976). Progressive faunal migration accross the Iapetus Ocean. *Nature*, 263:304–306.

McKerrow, W. S., Mac Niocaill, C., Ahlberg, P. E., Clayton, G., Cleal, C. J. et Eagar, R. M. C. (2000a). The Late Palaeozoic relations between Gondwana and Laurussia. *Geological Society, London, Special Publications*, 179(1):9–20.

McKerrow, W. S., Mac Niocaill, C. et Dewey, J. F. (2000b). The Caledonian Orogeny redefined. *Journal of the Geological Society*, 157(6):1149–1154.

Meissner, R. (1999). Terrane accumulation and collapse in central Europe: seismic and rheological constraints. *Tectonophysics*, 305(1-3):93–107.

Meissner, R., Sadowiakl, P. et Thomas, S. A. (1994). East Avalonia, the third partner in the Caledonian collisions: evidence from deep seismic reflection data. *Geologische Rundschau*, 83(1):186–196.

Meyre, C. et Pusching, A. R. (1993). High-pressure metamorphism and deformation at Trescolmen, Adula nappe, Central Alps. *Schweizerische Mineralogische und Petrographische Mitteilungen*, 73(2):277–283.

Minshull, T. A. (2009). Geophysical characterisation of the ocean–continent transition at magma-poor rifted margins. *Comptes Rendus Geoscience*, 341(5):382–393.

Mohn, G., Manatschal, G., Beltrando, M. et Haupert, I. (2014). The role of rift-inherited hyper-extension in Alpine-type orogens. *Terra Nova*, 26(5):347–353.

Mohn, G., Manatschal, G., Beltrando, M., Masini, E. et Kusznir, N. (2012). Necking of continental crust in magma-poor rifted margins: Evidence from the fossil Alpine Tethys margins. *Tectonics*, 31(1):TC1012.

Mohn, G., Manatschal, G., Masini, E. et Müntener, O. (2011). Rift-related inheritance in orogens: a case study from the Austroalpine nappes in Central Alps (SE-Switzerland and N-Italy). *International Journal of Earth Sciences*, 100(5): 937–961.

Muñoz, J. A. (2002). The Pyrenees. *In* Gibbons, W. et Moreno, M. T., éditeurs : *The Geology of Spain*, pages 370–385. Journal of the Geological Society.

Müntener, O. et Manatschal, G. (2006). High degrees of melt extraction recorded by spinel harzburgite of the Newfoundland margin: The role of inheritance and consequences for the evolution of the southern North Atlantic. *Earth and Planetary Science Letters*, 252:437–452.

Müntener, O., Manatschal, G., Desmurs, L. et Pettke, T. (2010). Plagioclase Peridotites in Ocean-Continent Transitions: Refertilized Mantle Domains Generated by Melt Stagnation in the Shallow Mantle Lithosphere. *Journal of Petrology*, 51(1-2):255–294.

Müntener, O., Pettke, T., Desmurs, L., Meier, M. et Schaltegger, U. (2004). Refertilization of mantle peridotite in embryonic ocean basins: trace element and Nd isotopic evidence and implications for crust,Äìmantle relationships. *Earth and Planetary Science Letters*, 221:293–308.

Murphy, J. B., Keppie, J. D., Nance, R. D. et Dostal, J. (2010). Comparative evolution of the Iapetus and Rheic Oceans: A North America perspective. *Gondwana Research*, 17:482–499.

Nance, R. D., Gutiérrez-Alonso, G., Keppie, J. D., Linnemann, U., Murphy, J. B., Quesada, C., Strachan, R. A. et Woodcock, N. H. (2010). Evolution of the Rheic Ocean. *Gondwana Research*, 17:194–222.

Nance, R. D. et Linnemann, U. (2008). The Rheic Ocean: Origin, Evolution, and Significance. *GSA Today*, 18(12):4.

Nikolaeva, K., Gerya, T. V. et Marques, F. O. (2010). Subduction initiation at passive margins: Numerical modeling. *Journal of Geophysical Research: Solid Earth*, 115(3):1–19.

Nirrengarten, M., Manatschal, G., Yan, X., Kusznir, N. et Millot, B. (subm.). Application of the critical Coulomb wedge theory to hyper-extended, magma-poor rifted margins. *Earth and Planetary Science Letters*.

Peacock, S. M. (1991). Numerical Simulation of Subduction Zone Pressure-Temperature-Time Paths: Constraints on Fluid Production and Arc Magmatism. *Philosophical Transactions of the Royal Society of London A: Mathematical, Physical and Engineering Sciences*, 335(1638):341–353.

Peacock, S. M., Rushmer, T. et Thompson, A. B. (1994). Partial melting of subducting oceanic crust. *Earth and Planetary Science Letters*, 121(1-2):227–244.

Pérez-Gussinyé, M., Ranero, C. R. et Reston, T. J. (2003). Mechanisms of extension at nonvolcanic margins: Evidence from the Galicia interior basin, west of Iberia. *Journal of Geophysical Research*, 108(B5).

Péron-Pinvidic, G., Manatschal, G. et Osmundsen, P. T. (2013). Structural comparison of archetypal Atlantic rifted margins: A review of observations and concepts. *Marine and Petroleum Geology*, 43:21–47.

Petri, B. (2014). *Formation et exhumation des granulites permiennes.* Thèse de doctorat, Université de Strasbourg.

Pharaoh, T. C. (1999). Palaeozoic terranes and their lithospheric boundaries within the Trans-European Suture Zone (TESZ): a review. *Tectonophysics*, 314:17–41.

Picazo, S., Müntener, O. et Manatschal, G. (2015). Recognizing mantle domains related to an extensional cycle: the record from Western Europe. *In AGU Fall Meeting Abstracts*, San Francisco.

Piccardo, G. B., Padovano, M. et Guarnieri, L. (2014). The Ligurian Tethys: Mantle processes and geodynamics. *Earth-Science Reviews*, 138(October):409–434.

Pinto, V. H. (2014). *Linking tectonic evolution with fluid history in hyperextended rifted margins: Examples from the fossil Alpine and Pyrenean rift systems and the present-day Iberia rifted margin.* Thèse de doctorat, Université de Strasbourg.

Reston, T. J. (2009). The structure, evolution and symmetry of the magma-poor rifted margins of the North and Central Atlantic: A synthesis. *Tectonophysics*, 468(1-4):6–27.

Rey, P. (1993). Seismic and tectono-metamorphic characters of the lower continental crust in Phanerozoic areas: a consequence of post-thickening extension. *Tectonics*, 12(2):580–590.

Rey, P., Burg, J.-P. et Casey, M. (1997). The Scandinavian Caledonides and their relationship to the Variscan belt contractional tectonics. *In* Burg, J.-P. et Ford, M., éditeurs : *Orogeny trough time*, pages 179–200. Geological Society Special Pubication No. 121, London.

Roberts, D. (2003). The Scandinavian Caledonides: event chronology, palaeogeographic settings and likely modern analogues. *Tectonophysics*, 365:283–299.

Roberts, D. G., Thompson, M., Mitchener, B., Hossack, J., Carmichael, S. et Bjørnseth, H.-M. (1999). Palaeozoic to Tertiary rift and basin dynamics: mid-Norway to the Bay of Biscay – a new context for hydrocarbon prospectivity in the deep water frontier. *In* Fleet, A. J. et Boldy, S. A. R., éditeurs : *Petroleum Geology of Northwest Europe: Proceedings of the 5th Conference*, pages 7–40. The Geological Society, London.

Rüpke, L. H., Morgan, J. P., Hort, M. et Connolly, J. A. D. (2004). Serpentine and the subduction zone water cycle. *Earth and Planetary Science Letters*, 223(1-2):17–34.

Sandwell, D. T. et Smith, W. H. F. (2009). Global marine gravity from retracked Geosat and ERS-1 altimetry: Ridge Segmentation versus spreading rate. *Journal of Geophysical Research*, 114(B01411).

Schaltegger, U. (1997). Magma pulses in the Central Variscan Belt: episodic melt generation and emplacement during lithospheric thinning. *Terra Nova*, 9(5/6): 242–245.

Schmid, S. M., Bernoulli, D., Fügenschuh, B., Matenco, L., Schefer, S., Schuster, R., Tischler, M. et Ustaszewski, K. (2008). The Alpine-Carpathian-Dinaridic orogenic system: correlation and evolution of tectonic units. *Swiss Journal of Geosciences*, 101:139–183.

Schmid, S. M., Fgenschuh, B., Kissling, E., Schuster, R. et Fügenschuh, B. (2004). Tectonic map and overall architecture of the Alpine orogen. *Eclogae Geologicae Helvetiae*, 97:93–117.

Schuster, R. et Stüwe, K. (2008). Permian metamorphic event in the Alps. *Geology*, 36(8):603–606.

Sibson, R. H. (1985). A note on fault reactivation. *Journal of Structural Geology*, 7(6):751–754.

Smith, W. H. F. et Sandwell, D. T. (1997). Global seafloor topography from satellite altimetry and ship depth soundings. *Science*, 277:1957–1962.

Stampfli, G., Mosar, J., Marquer, D., Marchant, R., Baudin, T. et Borel, G. (1998). Subduction and obduction processes in the Swiss Alps. *Tectonophysics*, 296(1-2):159–204.

Stern, R. J. (2004). Subduction initiation: spontaneous and induced. *Earth and Planetary Science Letters*, 226:275–292.

Stevenson, D. J. et Turner, J. S. (1977). Angle of subduction. *Nature*, 270(5635): 334–336.

Sutra, E. et Manatschal, G. (2012). How does the continental crust thin in a hyperextended rifted margin? Insights from the Iberia margin. *Geology*, 40(2): 139–142.

Sutra, E., Manatschal, G., Mohn, G. et Unternehr, P. (2013). Quantification and restoration of extensional deformation along the Western Iberia and Newfoundland rifted margins. *Geochemistry, Geophysics, Geosystems*, 14(8):2575–2597.

Tait, J., Schätz, M., Bachtadse, V. et Soffel, H. (2000). Palaeomagnetism and Palaeozoic palaeogeography of Gondwana and European terranes. *Geological Society, London, Special Publications*, 179(1):21–34.

Tan, E., Lavier, L. L., Van Avendonk, H. J. A. et Heuret, A. (2012). The role of frictional strength on plate coupling at the subduction interface. *Geochemistry, Geophysics, Geosystems*, 13(10):n/a–n/a.

Tankard, A. J. et Welsink, H. J. (1989). Mesozoic extension and styles of basin formation in Atlantic Canada. *In* Tankard, A. J. et Balkwill, H. R., éditeurs : *Extensional tectonics and stratigraphy of the North Atlantic margins; Am. Assoc. Petroleum Geol. Mem. 46*, pages 175–195.

Thöni, M. et Jagoutz, E. (1993). Isotopic constraints for eo-Alpine high-P metamorphism in the Austroalpine nappes of the Eastern Alps: bearing on Alpine olrogenesis. *Schweizerische Mineralogische und Petrographische Mitteilungen*, 73(2):177–189.

Tommasi, A. et Vauchez, A. (2001). Continental rifting parallel to ancient collisional belts: an effect of the mechanical anisotropy of the lithospheric mantle. *Earth and Planetary Science Letters*, 185:199–210.

Torsvik, T. H. (1998). Palaeozoic palaeogeography: A North Atlantic viewpoint. *GFF*, 120:109–118.

Torsvik, T. H. et Cocks, L. R. M. (2011). The Palaeozoic palaeogeography of central Gondwana. *Geological Society London Special Publication*, 357:137–166.

Torsvik, T. H. et Cocks, L. R. M. (2013). New global palaeogeographical reconstructions for the Early Palaeozoic and their generation. *Geological Society, London, Memoirs*, 38(1):5–24.

Torsvik, T. H. et Rehnström, E. F. (2003). The Tornquist Sea and Baltica–Avalonia docking. *Tectonophysics*, 362(1-4):67–82.

Torsvik, T. H., Van der Voo, R., Preeden, U., Mac Niocaill, C., Steinberger, B., Doubrovine, P. V., van Hinsbergen, D. J., Domeier, M., Gaina, C., Tohver, E., Meert, J. G., McCausland, P. J. A. et Cocks, L. R. M. (2012). Phanerozoic polar wander, palaeogeography and dynamics. *Earth-Science Reviews*, 114:325–368.

Tovish, A., Schubert, G. et Luyendyk, B. P. (1978). Mantle flow pressure and the angle of subduction: Non-Newtonian corner flows. *Journal of Geophysical Research*, 83(B12):5892.

Tugend, J., Manatschal, G. et Kusznir, N. (2015). Spatial and temporal evolution of hyperextended rift systems: implication for the nature, kinematics and timing of the Iberian-European plate boundary. *Geology*, 43(1):15–18.

Tugend, J., Manatschal, G., Kusznir, N. J., Masini, E., Mohn, G. et Thinon, I. (2014). Formation and deformation of hyperextended rift systems: Insights from rift domain mapping in the Bay of Biscay-Pyrenees. *Tectonics*, 33(7):1239–1276.

Uyeda, S. (1981). Subduction zones and back arc basins - A review. *Geologische Rundschau*, 70(2):552–569.

Van Avendonk, H. J., Lavier, L. L., Shillington, D. J. et Manatschal, G. (2009). Extension of continental crust at the margin of the eastern Grand Banks, Newfoundland. *Tectonophysics*, 468(1-4):131–148.

van Staal, C. R., Barr, S. M. et Murphy, J. B. (2012). Provenance and tectonic evolution of Ganderia: Constraints on the evolution of the Iapetus and Rheic oceans. *Geology*, 40(11):987–990.

van Staal, C. R., Dewey, J. F., Niocaill, C. M. et McKerrow, W. S. (1998). The Cambrian-Silurian tectonic evolution of the northern Appalachians and British Caledonides: history of a complex, west and southwest Pacific-type segment of Iapetus. *Geological Society, London, Special Publications*, 143(1):197–242.

Vauchez, A., Barruol, G. et Tommasi, A. (1997). Why do continents break-up parallel to ancient orogenic belts? *Terra Nova*, 9(2):62–66.

von Raumer, J. F., Stampfli, G. M. et Bussy, F. (2003). Gondwana-derived microcontinents – the constituents of the Variscan and Alpine collisional orogens. *Tectonophysics*, 365:7–22.

Whitmarsh, R. B., Manatschal, G. et Minshull, T. a. (2001). Evolution of magma-poor continental margins from rifting to seafloor spreading. *Nature*, 413(6852):150–154.

Whittaker, J. M., Goncharov, A., Williams, S. E., Müller, R. D. et Leitchenkov, G. (2013). Global sediment thickness data set updated for the Australian-Antarctic Southern Ocean. *Geochemistry, Geophysics, Geosystems*, 14(8):3297–3305.

Wilson, J. T. (1966). Did the Atlantic close and then re-open? *Nature*, 211:676–681.

Winchester, J. A., Pharaoh, T. C. et Verniers, J. (2002). Palaeozoic amalgamation of Central Europe: an introduction and synthesis of new results from recent geological and geophysical investigations. *In* Winchester, J. A., Pharaoh, T. C. et Verniers, J., éditeurs : *Palaeozoic Amalgamation of Central Europe*, volume 201, pages 1–18. Geological Society, London, Special Publications, 201.

Withjack, M. O., Schilsche, R. W. et Olsen, P. E. (2012). Development of the passive margin of eastern North America: Mesozoic rifting, igneous activity, and breakup. *In* Roberts, D. G. et Bally, A. W., éditeurs : *Regional Geology and Tectonics: Phanerozoic Rift Systems and Sedimentary Basins*, chapitre 13, pages 301–335. Elsevier.

Woodhead, J., Eggins, S. et Gamble, J. (1993). High field strength and transition element systematics in island arc and back-arc basin basalts: Evidence for multiphase melt extraction and a depleted mantle wedge. *Earth and Planetary Science Letters*, 114(4):491–504.

Zhao, D. (1997). Depth Extent of the Lau Back-Arc Spreading Center and Its Relation to Subduction Processes. *Science*, 278(5336):254–257.

Ziegler, P. A. (1988). Evolution of the Arctic-North Atlantic and the Western Tethys. *American Association of Petroleum Geologists Memoir*, 43:164–196.

Zuber, M. T., Parmentier, E. M. et Fletcher, R. C. (1986). Extension of continental lithosphere - A model for two scales of Basin and Range deformation. *Journal of Geophysical Research*, 91(4):4826–4838.

General introduction

1 State of the art and unanswered questions

The importance of inheritance in the control of tectonic processes is a long-standing question in Earth Sciences. Intuitively, one could expect that, when a heterogeneous material is submitted to stress, deformation would localize preferentially at weak spots. Thus, one may reasonably presume that, in large-scale extensional settings, rifts would develop at former sutures or major deformation structures. Respectively, every oceanic basin will sooner or later undergo subduction, either spontaneously because it has become gravitationally unstable, or due to external forcing (Nikolaeva et al., 2010; Stern, 2004). As oceanic lithosphere is denser than continental lithosphere, closure should terminate by the collision of the continental margins on either sides of the rift basin, that is at the very location of the initial breakup.

This paradigm known as *the Wilson Cycle* (Figure 1) was established based on the analysis of paleo faunal assemblages in the North Atlantic (Wilson, 1966). The distribution and evolution of the Pacific and Atlantic faunal Realms in North-America and Western Europe show that a former ocean, namely the Iapetus Ocean, separated the two continents from lower to middle Palaeozoic times, while it didn't exist from late Palaeozoic to middle Mesozoic anymore. The closure of this ocean caused the Caledonian Orogeny, whose remnants are exposed in Western Norway and Northwest United Kingdom on one side, and Greenland and North America on the other (e.g. Gee et al., 2008; Mac Niocaill et al., 1997; Ziegler, 1988).

However, the theory of the Wilson Cycle is challenged in numerous places, for instance in Western Europe where most of the Variscan sutures were not reactivated during the Mesozoic extensional phases, neither by the North Atlantic, nor by the Alpine Tethys rift system. Furthermore, Krabbendam and Barr (2000) highlighted that, of the 25,000 km of the rifted margins of the Gondwana supercontinent, only 45% are parallel to former sutures, and more than 20,000 km of pre-existing orogens did not rift. These observations prove that orogenic inheritance is not necessarily reactivated during subsequent extensional phases and begs the question about what may truly control the localization and details of tectonic systems.

Understanding the impact of inheritance throughout the Wilson Cycle requires to answer two key questions: **(1) How do orogenic structures and heterogeneities control subsequent rifting?** and **(2) How does the structural and lithological architecture of rift systems impact orogeny?**

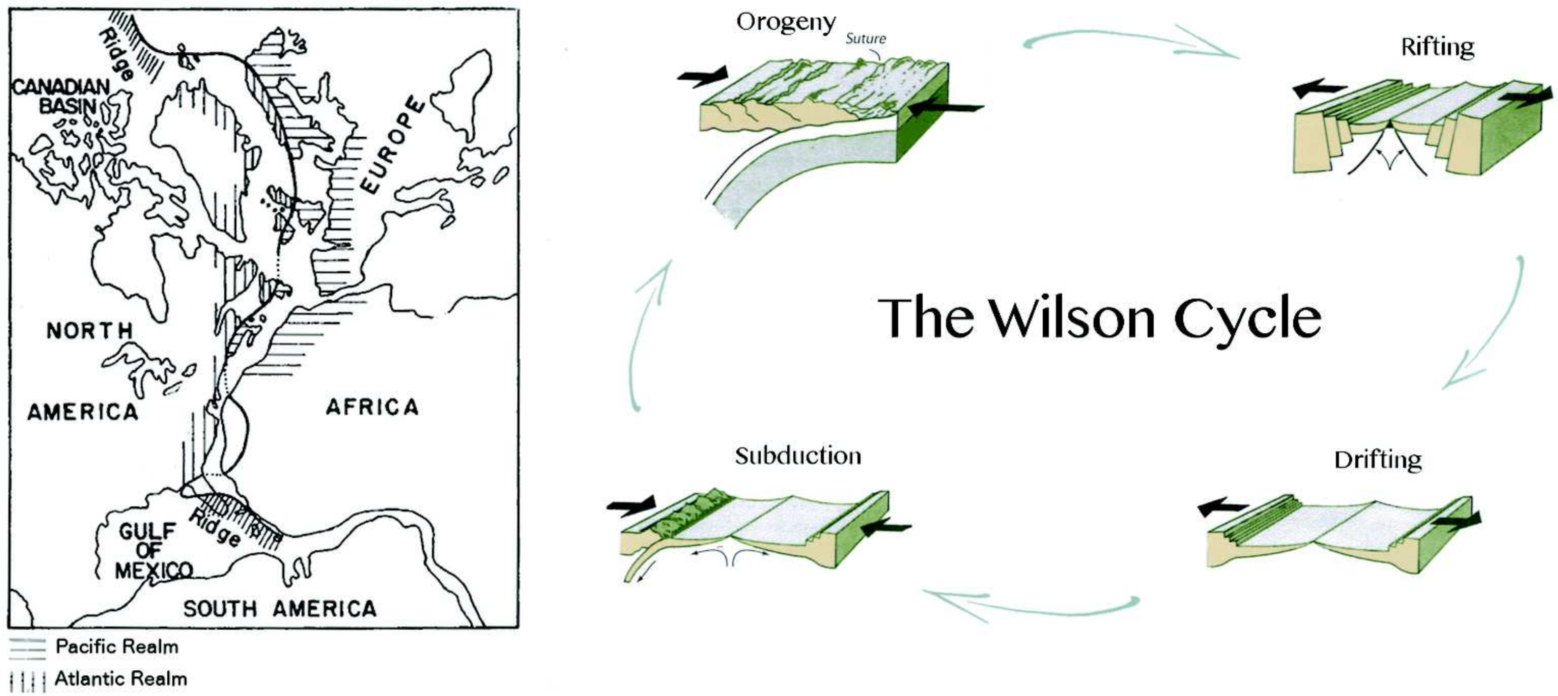

Figure 1 – Left: Distribution of the Pacific and Atlantic faunal realms in the North Atlantic region (Wilson, 1966); Right: Illustration of the Wilson Cycle paradigm modified after Allègre and Dars (2009).

1) From orogens to rifts

Orogenic and post-orogenic processes leave pervasive structures and first-order lithological and thermal heterogeneities, which could presumably control subsequent extension in a meaningful way (Dewey et al., 1993; Tommasi and Vauchez, 2001; Vanderhaeghe and Teyssier, 2001; Vauchez et al., 1997). For instance, thrust faults are often cited as a preferential location for the development of subsequent normal faults. The Møre–Trøndelag Fault Zone along western Norway is an illustrative example. It is described as a line of weakness, possibly initially formed during the Proterozoic. It was used as a thrust fault during the Caledonian orogeny and reactivated as a normal fault during both the orogenic collapse of the range and the Mesozoic extensional phase (e.g. Doré et al., 1997, and references therein). On a broader scale, Withjack et al. (2012) described the whole eastern North American rift system as located along former orogenic belts from Palaeozoic or older orogens, with the main border-faults of the 'failed' rift basins being reactivated orogenic structures. However, according to the same authors, the orientation of the smaller-scale faults within these basins is much more variable.

Although the impact of orogenic inheritance on subsequent rifting has been extensively studied by the scientific community, the investigations carried out at different scales did not bring to light a unique rule governing the interplay between them (e.g. Direen et al., 2008; Dunbar and Sawyer, 1989; Krabbendam, 2001; Krabbendam and Barr, 2000; Lundin and Doré, 2011; Ring, 1994; Tommasi and Vauchez, 2001; Vauchez et al., 1997; see Manatschal et al., 2015 in Annex A for a review). Indeed, several parameters come into play in the reactivation of inherited faults, in particular their orientation with respect to the stress direction (e.g. Ring, 1994), the intensity of the stress and fluid pressure (Sibson, 1985), and the rheology of the encompassing material (Chenin and Beaumont, 2013).

Besides, the post-orogenic collapse of some mountain ranges is associated with a major magmatic event, which modifies significantly the thermal state and the lithology of the lithosphere. For instance, seismic sections through the Variscan and the Basin and Range provinces display an up to 10 km thick, highly reflective lower crust, which has been interpreted as massive mafic underplating (Bussy et al., 2000; Rey, 1993). Indeed, the isostatic re-equilibration following an orogenic collapse may induce the uplift, and consequently the partial melting, of the underlying asthenosphere. The resulting melts may accumulate at the base of the continental crust, forming a mafic lower crust devoid of inheritance (Costa and Rey, 1995; Mckenzie and Bickle, 1988; Rey, 1993). In addition, the thermal relaxation of the orogen may induce widespread partial melting of the lower crust, which translates into more or less acidic intrusions in the overlying crustal levels (Dewey, 1988; Schaltegger, 1997; Vanderhaeghe and Teyssier, 2001; see Petri, 2014 for a review). However, the thermal and lithological consequences of such major magmatic events have no been integrated in the analysis of subsequent extensional events so far.

2) From rifts to orogens

The structural and lithological architecture of extensional systems may significantly impact the orogenic systems produced by their closure (e.g. Butler et al., 2006; Jammes et al., 2014, 2009; Mohn et al., 2014; Tugend et al., 2015, 2014). This assumption is supported by the contrasting architectures of the Caledonian and Variscan orogens, which have contrasting pre-orogenic settings. Indeed, the Caledonides resulted mainly from the closure of the wide (> 3,000 km) Iapetus Ocean (Mac Niocaill et al., 1997; McKerrow and Cocks, 1976; van Staal et al., 2012), whereas the Variscides were essentially produced by the closure of several narrow 'oceans' (< 500–1,000 km), in addition to the suturing of the wide Rheic Ocean (> 2,000 km; Franke, 2006; McKerrow et al., 2000a; Nance et al., 2010).

Present-day rift basins show a large diversity in size and seafloor characteristics, as evidenced by the existence of 'failed' rift basins such as the Rockall Trough and the Porcupine Basin, as opposed to the wide Atlantic and Pacific oceans. However, the specificities of extensional systems are rarely taken into account in the analysis of orogens. One possible reason may be that, although rifted margins benefit from even more accurate morpho-structural descriptions (e.g. Minshull, 2009; Reston, 2009; Sutra et al., 2013), no analysis of the width of the marginal domains and no synthesis of the lithospheric-scale lithology of rift systems have been published to date. Furthermore, except from a few recent studies, which have been limited to the Alps and Pyrenees (Butler, 2013; Butler et al., 2006; Mohn et al., 2014; Tugend et al., 2014), orogens have usually been considered as controlled by the processes associated with protracted, steady-state subduction, without taking into account the initial characteristics of the margins (Uyeda, 1981). Thus, the mechanical processes at play during orogenesis and the potential impact of rift-inherited structures have usually been overlooked in the analyse of orogens, even when they results from transitional, short-lived subduction processes.

Numerous authors attempted to demonstrate (Audet and Bürgmann, 2011; Tommasi and Vauchez, 2001; Vauchez et al., 1997) or temper (Krabbendam and Barr, 2000; Manatschal et al., 2015) the importance of inheritance in controlling tectonic processes, both in extensional (e.g. Cappelletti et al., 2013; Chenin and Beaumont, 2013; Manatschal et al., 2015; Tugend et al., 2014, and references therein) and compressional settings (e.g. Butler et al., 2006; Jammes and Huismans, 2012; Jammes et al., 2014; Mohn et al., 2014, 2011; Tugend et al., 2014, and references therein). From this work, it stands out that inheritance has definitely some control on tectonic processes, however its impact depends on numerous factors such as the scale under consideration, the nature of the heterogeneities, the rheology of the encompassing material, the thermal state, the composition of the mantle, and all the syn- and post-tectonic processes, which may modify the physico-chemical and thermal properties of the whole evolving system. Moreover, rift-related inheritance is likely to influence subsequent orogenic phases and *vice-versa*. Thus, the impact of tectonic inheritance should be studied taking all the steps of the Wilson Cycle into account, which has not been done so far.

2 Aim of this thesis

The objective of my PhD thesis is twofolds: first, I aim to better understand the interactions between large-scale inheritance and tectonic processes throughout the Wilson Cycle. Second, I seek to test the credibility of the assumptions I draw and appraise the first-order evolution of the system in a semi-quantitative way. Note that, in this work, I use the terms 'first-order' and 'large-scale' to describe structures, lithological and thermal heterogeneities, as well as tectonic processes, which express at a scale beyond the deca-kilometer. The problematic relative to the impact of inheritance on the Wilson Cycle can be broken into two research axes:

1) Impact of orogenic inheritance on rift systems

Through the first chapter of my thesis, I investigate how large-scale Caledonian and Variscan orogenic inheritance may control the first-order architecture and magmatic budget of the North Atlantic rift system. To do this, I develop mapping methods to compile (a) the large-scale orogenic structures/heterogeneities; (b) the architecture of rift systems; and (c) the timing of major rift events. This allows me to undertake a rigorous analysis by comparing datasets that are coherent at the scale under consideration. My approach is guided by the following questions:

- **How to define and map orogenic inheritance on a large-scale?**
- **How to define and map the first-order structural architecture of rift systems?**
- **How to define and map the timing of major rifting events?**
- **How does orogenic inheritance impact the first-order architecture and evolution of rift systems?**

2) Impact of rift systems architecture on orogens

Through the second chapter of my thesis, I attempt to unravel the first-order impact of the structural and lithological architecture of rift systems – in particular of their margins – on collisional orogens. I first undertake a statistical study on the dimensions of the marginal domains defined by Sutra et al. (2013) for a selection of natural rift systems that reached at least the stage of hyperextension (Doré and Lundin, 2015). Besides, I examine the lithology of both continental and oceanic lithospheres, as well as how rift-induced processes may modify them. Second, I analyze how these specificities are expressed during orogenesis. I focus my study on the closure of 'narrow oceans', first to avoid complexity induced by long-lasting subduction processes (e.g. arc-, forearc- and/or backarc magmatism and compressional or extensional deformation), and second because the impact of inheritance in such collisional systems remain little studied to date. To summarize, my approach consists in answering to the following questions:

- **What is the first-order structural architecture of 'narrow' and 'wide oceans' and how to described it quantitatively?**
- **What is the lithospheric-scale lithological architecture of 'narrow' and 'wide oceans'?**
- **What are the first-order differences in the architecture of 'narrow' and 'wide oceans'?**
- **How do the specificities of rifted margins impact orogenies following the closure of 'narrow oceans'? What are the differences compared to orogenies subsequent to the closure of 'wide oceans'?**

Based on these results, my next step aims to test some of the assumptions drawn from their analysis and to appreciate more quantitatively the interplay between inheritance and tectonic processes. Here, I use numerical modelling to analyze at a similar scale and resolution as my previous mapping, the impact of major post-orogenic magmatism on subsequent extension.

3) Numerical modelling: Impact of underplating on later rifting

In the third chapter of my thesis, I study, via numerical modelling, how mafic underplating of the lower crust and associated underlying mantle depletion may impact a subsequent rifting event. I use the thermo-mechanical numerical code FLAC (Cundall, 1989; Lavier and Manatschal, 2006; Tan et al., 2012) to test the effect of large-scale lithological and thermal heterogeneities on an extending lithosphere under different thermal states. In particular, I investigate:

- **How does mafic underplating of the continental crust and/or mantle depletion beneath a former orogenic suture impact the architecture and evolution of a subsequent rift system?**
- **How does the thermal state of such a lithosphere influence extensional processes?**
- **Is it possible to apply these results to the analysis of the North Atlantic rift system over the underplated Variscan lithosphere?**

3 Choice of the study area

My study focuses on the North Atlantic, between the Azores–Gibraltar fracture zone and latitude N 70° (Figure 2). This region is of particular interest, since it includes two distinct orogenic domains with contrasting geological histories, namely the Caledonian orogen to the north and the Variscan orogen to the south, both overprinted by a same episode of rifting during the Mesozoic (c.f. section *General geological setting* for a synthesis).

Besides, numerous geological and geophysical public studies, both offshore and onshore, offer an extended and well-stocked database. These include: global-scale topographic and gravimetric grids (Sandwell and Smith, 2009; Smith and Sandwell, 1997), magnetic anomaly grids (e.g. EMAG2 by Maus et al., 2009) and total sediment thickness grids (e.g. Whittaker et al., 2013); regional- to local-scale geological and structural maps; local refraction and reflection seismic surveys (see Artemieva and Thybo, 2013 for a review), as well as dredging and drilling surveys (for example DSDP, ODP).

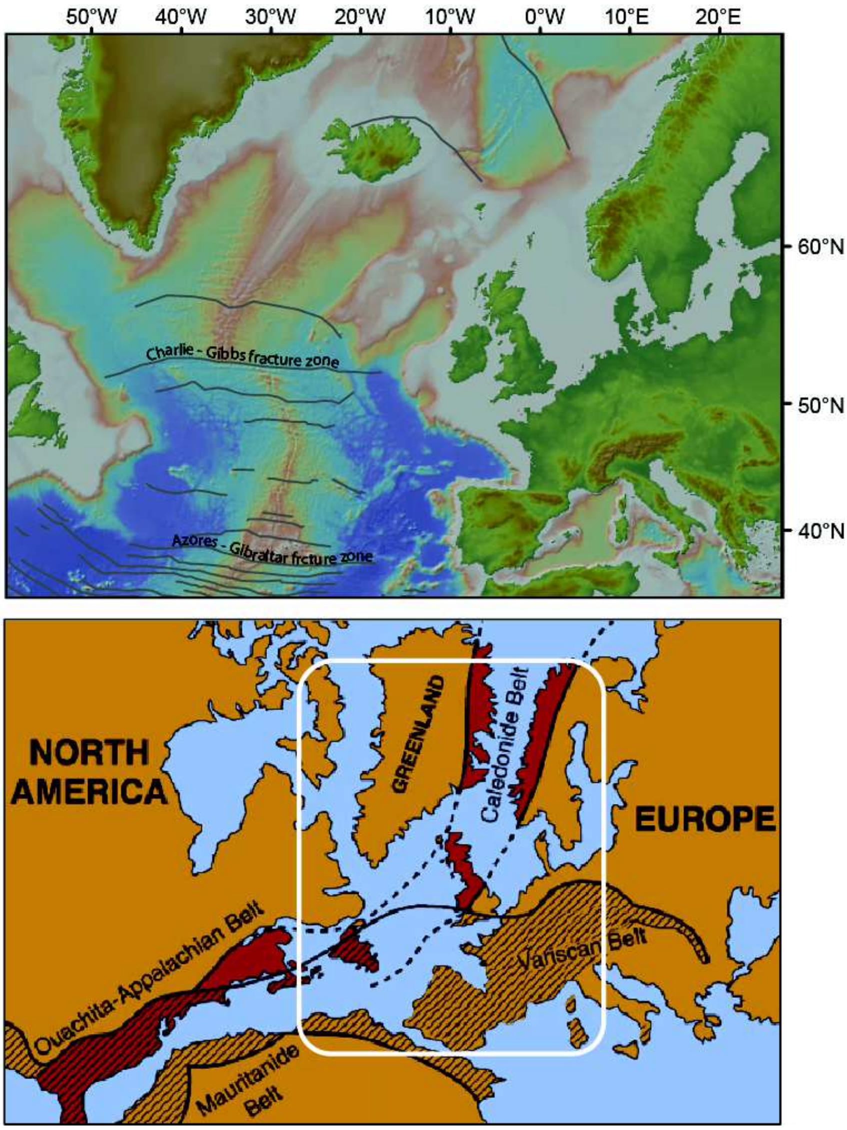

Figure 2 – Top: Present-day location of the study area (from Geomap app); Bottom: Paleogeography of the North Atlantic region after the termination of the Caledonian and Variscan orogenies in latest Palaeozoic and extent of both orogens (modified after Nance et al., 2010).

This dataset of present-day measurements is complemented by thermo-chronological and paleomagnetic studies, which add time constraints and allow for paleogeographic and cinematic reconstructions, from the local- to the global scale (amongst others Gaetani et al., 2003; Tait et al., 2000; Torsvik, 1998; Torsvik and Cocks, 2013b).

4 Choice of the methods

The methods used to answer the problematic must, all at once: be practicable at large-scale, provide reliable results with respect to the first-order processes, and be applicable with the available public data.

Mapping appears as an appropriate method to synthesize the first-order structures, heterogeneities and processes on a large-scale. As such maps do not exist at present, I undertake to develop methods to map orogenic inheritance, as well as the architecture and timing of hyperextended rift systems at the scale of the North Atlantic region. First, I define selection criteria in order to restrict my collection to the first-order characteristics. Second, I determine on which observable features I could rely to create a reliable mapping method. In the end, I base my work on the observation of seismic sections, the analysis of gravimetric and magnetic data and on published scientific literature (see Chapter I for a detailed description of this work).

Besides, numerical modelling enables to analyze the lithospheric-scale structural, lithological and thermal evolution of simplified geological systems. This method complements the mapping approach particularly well, since it is particularly reliable at a similar scale and resolution. Indeed, it allows to design experiments integrating the first-order structures and heterogeneities that have been highlighted by the mapping work, and to compare the structural, lithological and thermal evolution of the modelled rift systems with structural and thermo-chronological data from actual rift systems. Moreover, because the modelling experiments are relatively simple and quick to implement, this tool allows for the testing of numerous parameters (see Chapter III for a description of the numerical code).

General geological setting

1 General overview

Following the breakup of the supercontinent Rodinia in early Neoproterozoic (∼ 800 Ma), Palaeozoic paleogeography is dominated by four main continents – namely Gondwana, Laurentia, Baltica and Siberia – separated by three major oceans that are the Panthalassa, Iapetus and Rheic oceans (Jurdy et al., 1995; Torsvik et al., 2012; Veevers, 2004; see Figure 1). The expansion and subsequent subduction of these oceans brought about drifting of the continents, and eventually their convergence and merging into the supercontinent Pangea in latest Palaeozoic (see Torsvik et al., 2012, for a review). In particular in Western Europe, the successive collisions resulted in the Cambro-Ordovician Caledonian orogeny (Krawczyk et al., 2008; McKerrow et al., 2000b) and the Late Carboniferous Variscan orogeny (Kröner et al., 2008; Kröner and Romer, 2013; Matte, 2001; Rast, 1988; Warr, 2009). It is worth noting that the configuration of Pangea in Early Permian is still debated (the *Pangea A* versus *Pangea B* controversy), but the scientific community is almost unanimous about a *Pangea A* configuration in Early Jurassic (Domeier et al., 2012; Muttoni et al., 2003).

Breakup of Pangea began in latest Triassic–earliest Jurassic (Frizon de Lamotte et al., 2015; Veevers, 2004) with the opening of the Central Atlantic Ocean and Alpine Tethys rift system on one side (Schettino and Turco, 2009; Schmid et al., 2004, and references therein), and significant thinning ('necking'; see Sutra et al., 2013) in the northern North Atlantic on the other (Doré et al., 1999; Roberts et al., 1999). The Alpine Tethys rift was abandoned and inverted from Late Cretaceous time onward, giving rise to the Alpine and Pyrenean orogens. At the same time, the southern and northern parts of the North Atlantic rift system became coalescent offshore Western Europe (Doré et al., 1999; Roberts et al., 1999).

As the primary objective of my thesis is to unravel the potential links between inheritance and tectonic systems systems in Western Europe, I summarize in this chapter the major orogenic and rifting events, which affected this region. I first give an overview of the pre-, syn- and post-orogenic framework of the Caledonides and Variscides. In particular, I emphasize the dimensions of the rift basins involved in these orogenies, and the both rift-related and orogenic processes that left long-lasting large-scale inheritance. Second, I review briefly the development of the Alpine Tethys and North Atlantic rift systems, with special focus on their location and timing. Finally, I summarize the construction of the Alpine and Pyrenean orogens and highlight their first-order architecture.

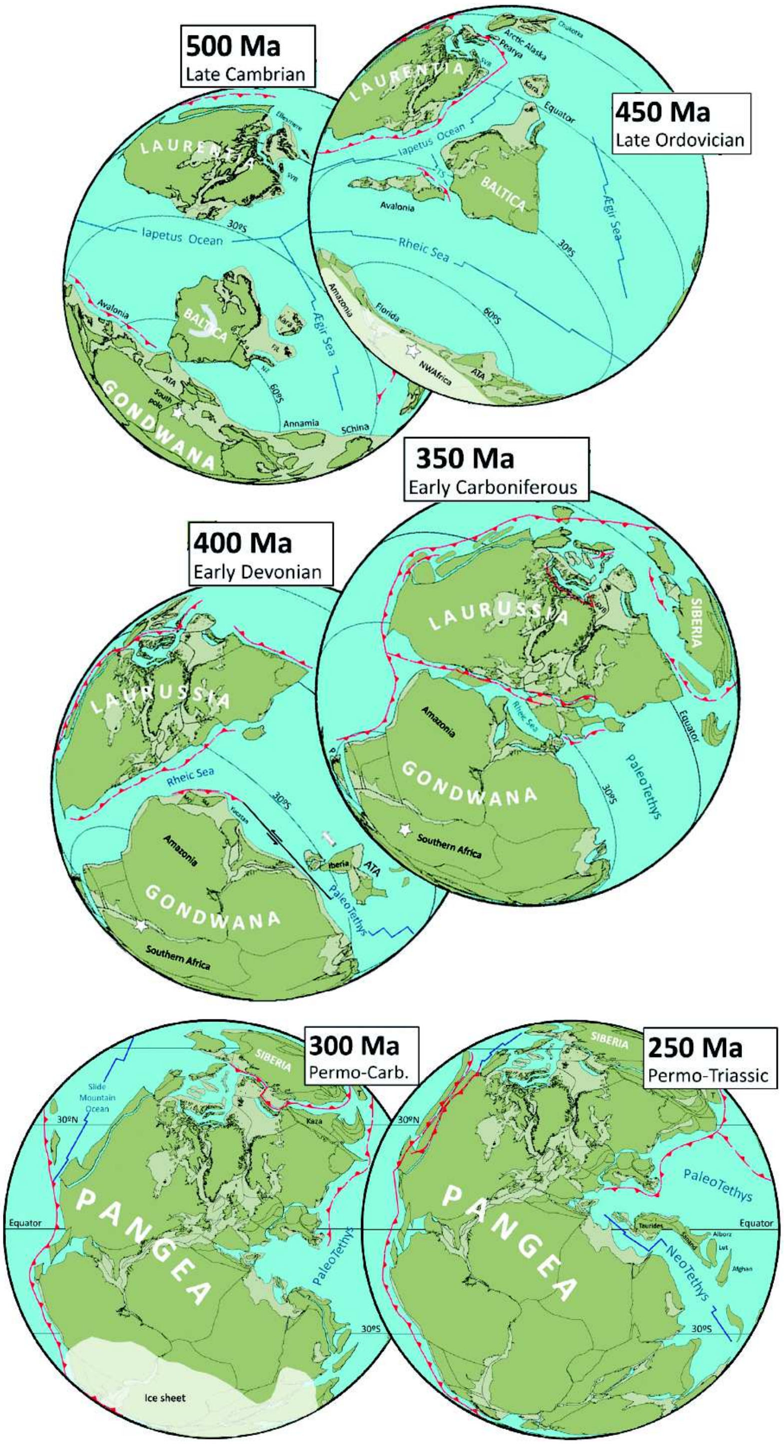

Figure 1 − Global paleogeographic reconstruction from late Cambrian to Early Triassic after Torsvik et al. (2012). TS = Tornquist Seaway.

2 Pre-orogenic paleogeography

The construction of the Caledonian and Variscan orogens involved three major continents of lower Palaeozoic time (see Figure 1 at 450 Ma), namely: (1) Laurentia $\simeq$ the North American craton + Greenland + northern United Kingdom (see Cocks and Torsvik (2011) for a review); (2) Baltica $\simeq$ the East European craton, including Northern Europe from the trans-European suture zone to the Urals mountains, and from the Timan Range to the Black Sea and Caspian Sea, + the various accreted terranes to the north, up to Svalbard (see review by Cocks and Torsvik, 2005); and (3) Gondwana $\simeq$ Africa + South America + Australia + Antarctica + India+ Arabia + the remaining parts of Europe + Nova Scotia and western Newfoundland (see reviews by Torsvik and Cocks, 2011, 2013a). A fourth smaller plate named Avalonia ($\simeq$ Nova Scotia and Western Newfoundland + southern United Kingdom, Northern France + Belgium and Northern Germany; see review by Cocks et al., 1997) rifted off from Gondwana in late Cambrian, leaving the series of barely thinned continental terranes (now forming Southwestern Europe), separated by narrow rift basins at the northern edge of the supercontinent (Kröner and Romer, 2013; Matte, 2001; Stampfli et al., 2002). This group of micro-continents and/or continental ribbons has various names in the literature, depending on which terranes it includes. It is called *Armorica* by Matte (2001) and *Armorican Spur* by Kröner and Romer (2013); it comprises the *Armorican Terrane Assemblage* + numerous other terranes rifted off at different times for Torsvik and Cocks (2011), and it corresponds to the western part of the Hun Superterrane defined by Stampfli et al. (2002). In the following, I refer to the group of continental ribbons fringing the northern margin of Gondwana – except Avalonia – as the 'Gondwana-derived terranes assemblage'.

All these continents were separated by oceans of different sizes. On the one hand, three major oceans dominated the Palaeozoic paleogeography, in particular the Iapetus ocean between Laurentia and Baltica + Avalonia, and the Rheic ocean between Avalonia and the Gondwana-derived terranes assemblage. On the other hand, one most likely 'second-order' ocean, known as the Tornquist Seaway, separated Baltica from Avalonia. Finally, several minor 'oceanic basins' such as the Rhenohercynian, Saxothuringian and Medio-European 'oceans' isolated the different components of the Gondwana-derived terranes assemblage (Franke, 2006; Matte, 2001; McKerrow et al., 2000a). Note, however, that the precise paleogeographic configuration of Palaeozoic time is still a matter of many debates, in particular the number and size of oceans and (micro-) continents involved. In the next sections, I attempt to summarize the knowns and unknowns about each of these basins.

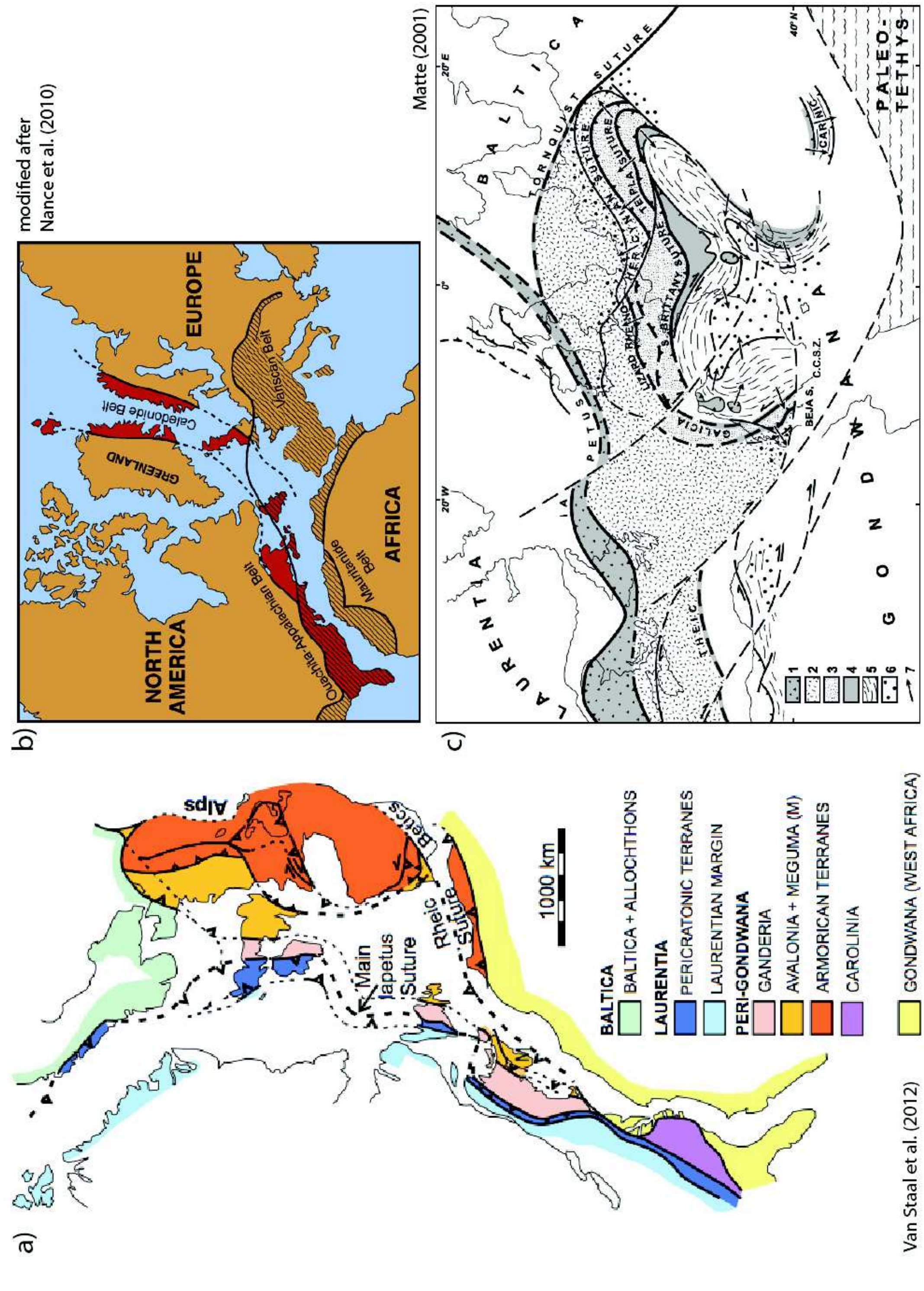

a)
Main Iapetus Suture
Rheic Suture
Alps
Betics
1000 km
BALTICA
BALTICA + ALLOCHTHONS
LAURENTIA
PERICRATONIC TERRANES
LAURENTIAN MARGIN
PERI-GONDWANA
GANDERIA
AVALONIA + MEGUMA (M)
ARMORICAN TERRANES
CAROLINIA
GONDWANA (WEST AFRICA)
Van Staal et al. (2012)
b)
NORTH AMERICA
EUROPE
AFRICA
GREENLAND
Caledonide Belt
Variscan Belt
Ouachita-Appalachian Belt
Mauritanide Belt
modified after
Nance et al. (2010)
c)
LAURENTIA
BALTICA
GONDWANA
IAPETUS
THEIC
GALICIA
PALEO-TETHYS
TORNQUIST SUTURE
BRITTANY SUTURE
BEJA S.
C.C.S.Z.
Matte (2001)

Figure 2 – a) Possible paleogeography of the North Atlantic prior to the Mesozoic rifting highlighting the main terranes involved in the Caledonian and Variscan orogenies (from van Staal et al., 2012). b) Possible paleogeography of the North Atlantic highlighting the extent of the Caledonian and Variscan orogens (modified after Nance et al., 2010). c) Main structures of the Caledonian and Variscan orogens and possible paleogeographic configuration of Western Europe in Permian time (at 270 Ma). 1, Iapetus suture and Ordovician island arc; 2, Avalonia; 3, Armorica; 4, ophiolitic nappes rooted in the Galicia–Southern Brittany suture; 5, Schistose nappes in the southern Variscides; 6, Carboniferous (Visean to Westphalian) foredeep basins; 7, main vergence of nappes. CCSZ: Coïmbra–Cordoba Shear Zone; Beja S: Beja Suture (from Matte, 2001).

2.1 The Iapetus Ocean

The Iapetus ocean (Figure 1 at 500 Ma and Figure 2) opened as a result of Late Proterozoic–Early Cambrian polyphase rifting between the large continental masses of Laurentia, Baltica and Gondwana (Mac Niocaill et al., 1997; McKerrow and Cocks, 1976; Murphy et al., 2010 and references therein; see Figure 1 at 500 Ma). Mantle-bearing mélanges exposed on the Norwegian margin may be remnants of a former hyperextended domain of the Baltic margin (Andersen et al., 2012), however the existence of magmatic provinces and dyke swarms supports a magmatic breakup, possibly related to a mantle plume (Murphy et al., 2010, and references therein). More recently, Abdelmalak et al. (2015) suggested that the former margin of Baltica may have comprised both magma-poor and magma-rich segments.

Based on paleomagnetic data, van Staal et al. (2012) suggested that the Iapetus Ocean reached a maximum width of less than 3,300 km during the Cambrian. By that time, Pacific-type subductions and associated magmatic arcs and backarc basins developed approximately at the same time along both the Laurentian and Gondwanan passive margins, as evidenced by supra-subduction ophiolitic complexes (Murphy et al., 2010 and references therein; van Staal et al., 1998). Intra-oceanic subduction and subsequent arc-continent collision as well as subduction-flip did presumably occur, as evidenced by obducted magmatic arcs and the complex tectono-magmatic record on both the Laurentian and Avalonian margins (Andréasson et al., 2003; Mac Niocaill et al., 1997). The final collision between Laurentia and Balonia (= Baltica + Avalonia) was achieved in Llandovery at about 435 Ma (Andréasson et al., 2003; McKerrow, 1988). Remnants of one of the corresponding foreland basins can be traced in Central Sweden (Gee et al., 2012).

2.2 The Tornquist Seaway

The existence of the Tornquist Seaway between Avalonia and Baltica ('TS' on Figure 1 at 450 Ma and Figure 2 c) was initially inferred by Cocks and Fortey (1982) from the study of paleo-faunas. This ocean may have opened at about 600 Ma during the Neoproterozoic, roughly at the same time as the Iapetus Ocean (McKerrow et al., 2000a). Although protuberant geological record is missing or buried under a thick sedimentary cover, most authors agree on a Late Ordovician (Cocks and Fortey, 1982; Torsvik and Rehnström, 2003) or Early Silurian (Soper et al., 1992) closure. However, the direction of the subduction is a matter of debate: Poprawa et al. (1999) suggest a subduction of Eastern Avalonia beneath Baltica, while Torsvik and Rehnström (2003); van Staal et al. (1998) claim the converse is true, supported by the evidence for arc magmatism on the Avalonian margin, presumably related to the subduction of the Tornquist Seaway (Pharaoh, 1999). As for Hoffmann and Franke (1997), subduction flipped from initially south-directed beneath Avalonia to north-directed beneath Baltica.

The maximum width of the Tornquist Seaway is still very poorly constrained: On the one hand, as paleomagnetic data do not point to a significant distance between these two continents, it is usually not regarded as a wide ocean; however East–West extent is undetectable from paleomagnetic data, unlike North–South extent (Torsvik and Rehnström, 2003). On the other hand, the faunal provinciality between Avalonia and Baltica indicates that the Tornquist Seaway was at least 500–1,000 km wide (Cocks and Fortey, 1982; McKerrow et al., 2000a).

2.3 The Rheic Ocean

The Rheic ocean (Figures 1 at 450 Ma and Figure 2) opened during Late Cambrian–Early Ordovician and separated a series of terranes, which includes the microplate Avalonia, from Northern Gondwana (Linnemann et al., 2008; Murphy et al., 2006, 2010; Nance et al., 2010; van Staal et al., 2012; von Raumer and Stampfli, 2008, and references therein). Rifting was associated with bimodal magmatism (Linnemann et al., 2008; Nance et al., 2010). According to some authors, rifting was facilitated by slab pull of the northwestward-subducting Iapetus slab beneath Laurentia (Nance et al., 2010). However, others argue that rifting initially started as a continental backarc basin associated to the subduction of the Iapetus ocean beneath northern Gondwana, as evidenced by supra-subduction ophiolites (Arenas et al., 2007; Martínez Catalán et al., 1997, 2007; van Staal et al., 2012, 1998). The onset of steady-state seafloor spreading was triggered by a magmatic pulse dated at 490–485 Ma, (Linnemann et al., 2008). During its drifting stage, the Rheic Ocean widened quickly (5–8 $cm.yr^{-1}$ or more according to Murphy et al., 2010; Nance et al., 2010), and may have become as wide as 4,000 km in the Silurian (Nance et al., 2010). Its closure started in Early Devonian at approximately 440 Ma and was achieved by continental collision in Late Devonian $\sim$ 370 Ma (Martínez Catalán et al., 1997), apparently without forming a significant accretionary wedge (Murphy et al., 2010). Subduction polarity is much debated, for instance Franke (2000) considered it was essentially north-directed beneath Laurentia and Avalonia, Matte (2001) suggested it was south-directed beneath the Gondwana-derived terranes assemblage and according to Nance et al. (2010) subduction occurred on both sides. Most authors agree on the major magmatic arc now exposed in the Mid German Crystalline Rise to be related to the closure of the Rheic Ocean (Franke, 2000), however according to Oncken et al. (2000), the latter was formed consequently to the closure of the Rhenohercynian 'ocean'. For most authors, the Rheic suture in Western Europe runs south of United Kingdom, across northern France and central Germany and ends in the Bohemian Massif in Czech Republic (Cocks et al., 1997; Nance and Linnemann, 2008; Pharaoh, 1999; see Figure 2). Note that on Figure 2 (c), its suture is merged with the Lizard-Rhenohercynian suture.

2.4 The Saxothuringian 'ocean'

The existence of the Saxothuringian 'ocean' within the Gondwana-derived terrane assemblage (labelled 'Tepla Suture' on Figure 2 c) is inferred from allochthonous MORB basalts, allochthonous eclogites and paleomagnetic data (Franke, 2006; Franke et al., 1995; Tait et al., 1995). It opened in Cambro-Ordovician but did most likely not evolved into a mature ocean. Because it was never a significant biogeographic barrier, some authors argue that it was probably $<$ 500–1,000 km wide (McKerrow et al., 2000a). However, its width and lateral extent are very poorly known (Schulmann et al., 2009). Its subduction commenced at $\sim$ 400 Ma and brought about continental collision at 380 Ma (Franke, 2006). According to Žák et al. (2009) the Central Bohemia plutonic complex is a large magmatic arc formed as a result of the closure Saxothuringian ocean and continental collision between the Saxothuringian and Tepla-Barrandian Terranes. However, Keppie et al. (2010) interpreted the corresponding high pressure and ophiolites as extrusion of the Rheic ocean in the overriding Gondwana-derived plate.

2.5 The Medio-European 'ocean'

The existence of the Medio-European 'ocean' (also referred to as the Massif Central, Theic, Proto-Tethys, Galicia–Southern-Brittany and Moldanubian ocean) within the Gondwana-derived terranes assemblage ('Galicia–S. Brittany Suture' on Figure 2 c) is still controversial (Matte, 2001). Although it is inferred from ophiolites (Matte, 2001) and high pressure rocks (Franke, 2006), several authors argue that the ophiolites are actually remnants of the Rheic ocean, either strike-slipped slices, allochtonous nappes or extrusion of subducted material in the upper (Gondwanan) plate (see Keppie et al., 2010; Martínez Catalán et al., 2007).

The Medio-European 'ocean' is undetectable from both paleomagnetic and biostratigraphic data, thus, if it existed, it was most likely relatively narrow (< 500–1,000 km; Faure et al., 2009; McKerrow et al., 2000a; Robardet, 2003). Its precise configuration and evolution are very poorly constrained and its width may have varied significantly along strike, since the Gondawana-derived terranes assemblage was most likely comprised of a discontinuous series of micro-continents and/or continental ribbons (see section 2). Nevertheless, some lines of evidence point to a Late Cambrian opening, at latest, and a Middle- to Late-Devonian closure (Faure et al., 2009; Franke, 2006; McKerrow et al., 2000a). Its subduction may have locally formed magmatic arcs, for instance the Somme Unit in French Morvan (Faure et al., 2009) and the Central Bohemian Plutonic Complex in Central Europe (Schulmann et al., 2009), as evidenced by the magmatic rocks of calc-alkaline geochemical affinities.

2.6 The Rhenohercynian 'ocean'

The existence of the narrow (< 500–1,000 km) Rhenohercynian 'ocean' (Figure 2 c), undetectable from both paleomagnetic and biostratigraphic data, was inferred from ophiolites and volcanic records (Franke, 2006, and references therein). This oceanic basin opened during the Emsian (∼ 400 Ma) following a phase of magma-poor rifting in the latest stage, or shortly after, the closure of the Rheic Ocean (Franke, 2006, and references therein). The geodynamic cause for the development of this basin is not understood yet, as it opened in a setting of convergence but not in the position of a backarc basin (Franke, 2000). In any case, the Rhenohercynian 'ocean' was very short-lived, since subduction was already going on in mid-Fransien (∼ 380 Ma) and brought about continental collision from latest Devonian–earliest Carboniferous onward (Franke, 2006). It closure did not produce a proper magmatic arc, although it may have contributed to some of the Mid-German Crystalline Rise magmatism (Franke, 2006; Oncken et al., 2000).

3 The Caledonides and the Variscides

3.1 The Caledonian orogeny and collapse

The Caledonian orogeny includes all the Cambrian to Devonian tectonic events related to the closure of the Tornquist Seaway between Baltica and Avalonia, and to the closure of the Iapetus ocean between Laurentia and Baltica (McKerrow et al., 2000b). On a first-order, one can distinguish three zones characterized by different levels of complexity.

On the one hand, the Scandinavian–Greenland Caledonides resulted from the Lower Silurian suturing of the Iapetus Ocean between the two large Laurentian and Baltic cratonic shields, with only limited accretion of magmatic arcs or terranes (Figure 2 a and b; Figure 3 a; Roberts, 2003; van Staal et al., 2012). This typical *collisional orogen* (Cawood et al., 2009; Isozaki, 1997) is characterized by paired high pressure/low temperature (high P/low T) and high temperature/low pressure (high T/low P) metamorphic belts exposed in Norway (Murphy et al., 2010, and references therein): The high P/low T metamorphic belt, which is comprised of stacked thin and far-travelled thrust nappes, represents the accretionary wedge. On the other hand, the high T/low P metamorphic belt is a result of the arc magmatism associated with the subduction of the Iapetus Ocean (Rey et al., 1997, and references therein).

On the other hand, the British–Appalachian Caledonides are much more complex, since they involved the collision, accretion and/or obduction of several arcs (Penobscot, Taconic, Notre Dame, Popelogan–Vicoria and Gander arcs) and microcontinents (in particular Avalonia and Ganderia), as well as the closure of several backarc basins (for instance the *Baie Verte oceanic tract*) throughout the Ordovician (Krawczyk et al., 2008; McKerrow et al., 2000b; van Staal et al., 2012, 1998; Winchester et al., 2002; see Figure 2 a and Figure 3 b). These individual orogenic events are referred to as the Penobscotian, Grampian–Taconic, Humberian orogenies (McKerrow et al., 2000b; van Staal et al., 1998). Therefore, in this region, the orogen is largely of *accretionary-type*, in addition to *collisional-type* according to the definition of Isozaki (1997) and Cawood et al. (2009). Thus, it does not show the typical orogenic architecture with paired high P/low T and high T/low P metamorphic belts.

Finally, the North-German–Polish Caledonides resulted from the Late Ordovician–Early Silurian closure of the Tornquist Seaway (Figure 2 a and c). Yet, little is known about the architecture and evolution of this orogenic event, because the corresponding area is both buried beneath a thick Mesozoic sedimentary cover and overprinted by subsequent tectonic events (Variscan deformation to the South-East (Krawczyk et al., 2008) and Mesozoic extensional events in the North Sea; Meissner et al. (1994); Pharaoh (1999); see also Dadlez (2000) for a review). Whether the margin of Baltica is located at the Trans-European Suture Zone or at the Elbe Line is therefore not clear yet. However, the lack of protuberant orogenic structures and high pressure rocks assemblages in this region suggests a 'soft' continental collision between Avalonia and Baltica, essentially governed by strike-slip convergence (Dadlez, 2000; Torsvik and Rehnström, 2003).

After the termination of convergence in the Devonian, the Caledonian range underwent a phase of extensional collapse essentially achieved through mechanical deformation and without significant magmatic activity North of the Elbe lineament (Fossen et al., 2014; Meissner, 1999). During the collapse, orogenic structures were usually reactivated in extension in the internal part and in compression in the external part of the orogen, in order to accommodate the flow of material from the thickened lithosphere toward regions of lower potential energy (Andersen, 1998). This led to the formation of intracontinental basins in Norway (Séranne and Seguret, 1987), East Greenland (Strachan, 1994) and northern Britain (Coward et al., 1989). Extensional structures include normal faults and long-offset detachment faults, which are usually limited to upper- and middle-crustal levels (Andersen, 1998, and references therein). These extensional detachment faults may have allowed for rapid thinning of the crust, resulting in exhumation of deep crustal levels typically showing eclogite to amphibolite metamorphic facies (Andersen, 1998). At deeper levels, extensional collapse manifested as ductile flow of the thermally weakened lower crust (Rey et al., 2001). Despite this significant tectonic event, seismic data suggest that many of the orogenic and post-orogenic structures such as sutures, major faults and fold-and-thrust belts, are relatively well-preserved within the lithosphere, especially in the external domain (Figure 4 a; Juhojuntti et al., 2001; Meissner, 1999; Meissner et al., 1994).

Figure 3 – a) The Scandinavian Caledonides: Details of the Baltic margin (top) prior to the final suturing of the Iapetus Ocean (bottom) from Roberts (2003). Upm. A. = Uppermost Allochthon; U. A. = Upper Allochton; M. A. = Middle Allochthon; L. A. = Lower Allochthon. b) Detail of the different orogenic events along the eastern margin of Laurentia (top) before the final closure of the Iapetus Ocean (bottom) after Van Staal and Barr (2012). AAT: Annieopsquotch Accretionary Tract; BVOT: Baie Verte Oceanic Tract; LBOT: Lush Bight Oceanic Tract; LRF: Lloyd's River Fault; PVA: Popelogan–Victoria Arc; RIL: Red Indian Line. c) Schematic view of the successive tectonic events, which led to the Variscan orogeny of Western Europe (from Franke, 2000). Franconia, Saxo-Thuringia, Bohemia and Moldanubia are components of the Gondwana-derived terranes assemblage.

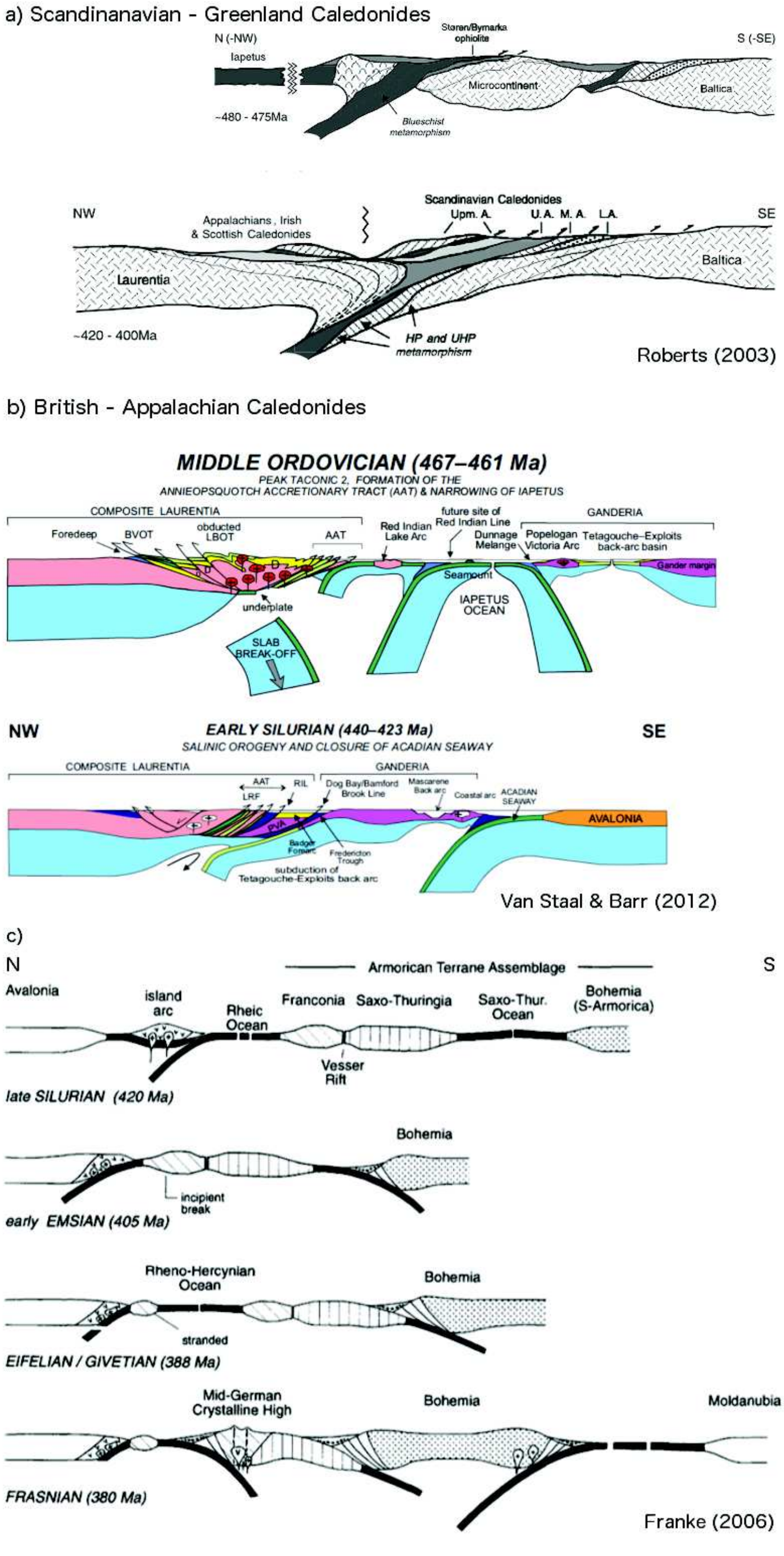
a) Scandinanavian - Greenland Caledonides
N (-NW)
Iapetus
Støren/Bymarka ophiolite
S (-SE)
Microcontinent
Baltica
~480 - 475Ma
Blueschist metamorphism
NW
Appalachians , Irish & Scottish Caledonides
Scandinavian Caledonides
Upm. A.
U. A.
M. A.
L.A.
SE
Laurentia
Baltica
~420 - 400Ma
HP and UHP metamorphism
Roberts (2003)
b) British - Appalachian Caledonides
MIDDLE ORDOVICIAN (467–461 Ma)
PEAK TACONIC 2, FORMATION OF THE ANNIEOPSQUOTCH ACCRETIONARY TRACT (AAT) & NARROWING OF IAPETUS
COMPOSITE LAURENTIA
Foredeep
BVOT
obducted LBOT
AAT
Red Indian Lake Arc
future site of Red Indian Line
Dunnage Melange
GANDERIA
Popelogan Victoria Arc
Tetagouche–Exploits back-arc basin
Gander margin
Seamount
underplate
IAPETUS OCEAN
SLAB BREAK-OFF
NW
EARLY SILURIAN (440–423 Ma)
SALINIC OROGENY AND CLOSURE OF ACADIAN SEAWAY
SE
COMPOSITE LAURENTIA
GANDERIA
AAT
RIL
LRF
Dog Bay/Bamford Brook Line
Mascarene Back arc
Coastal arc
ACADIAN SEAWAY
AVALONIA
Badger Forearc
Fredericton Trough
subduction of Tetagouche-Exploits back arc
Van Staal & Barr (2012)
c)
N
Armorican Terrane Assemblage
S
Avalonia
island arc
Rheic Ocean
Franconia
Saxo-Thuringia
Saxo-Thur. Ocean
Bohemia (S-Armorica)
Vesser Rift
late SILURIAN (420 Ma)
Bohemia
incipient break
early EMSIAN (405 Ma)
Rheno-Hercynian Ocean
Bohemia
stranded
EIFELIAN / GIVETIAN (388 Ma)
Mid-German Crystalline High
Bohemia
Moldanubia
FRASNIAN (380 Ma)
Franke (2006)

3.2 The Variscan orogeny and collapse

The Variscides of Western Europe are a complex collage of little deformed basement blocks separated by high strain zones containing more or less evidence for subduction processes (see Kröner and Romer, 2013 for a review; Figures 2 c and 3 c). According to most authors, the westernmost part of the European orogen resulted from both the closure of the large Rheic Ocean and the suturing of several narrow (< 500–1,000 km) 'oceans', namely the Rhenohercynian, Saxothuringian and Medio-European 'oceans' (Franke, 2006; Matte, 1991; McKerrow et al., 2000a; von Raumer et al., 2003; Warr, 2009). However, there is much more debate on the eastern part, especially in the Bohemian massif (Kroner and Romer, 2014; Schulmann et al., 2014a,b).

Collision with the mainland of Gondwana culminated in Visean time at ~ 340 Ma, and from then on, convergence was accommodated by transpressional strike-slip movements related to escape tectonics (Kröner and Romer, 2013; Martínez Catalán et al., 2007, and references therein). Thus, the Variscan orogen does not show the typical high P/low T and high T/ low P paired metamorphic belt architecture. Furthermore, except from the large magmatic complexes now exposed in the Mid-German Crystalline Rise and in Central Bohemia, there is very limited evidence for arc magmatism in the orogen, even for the subduction of the Rheic Ocean (Franke, 2006; Pereira et al., 2012).

Shortly after the termination of convergence in latest Carboniferous–earliest Permian, the Variscan range underwent a phase of crustal extension, which formed intracontinetal basins over most of Western Europe (McCann et al., 2006; Ziegler and Cloetingh, 2004). This event was followed by a major magmatic event, which caused widespread, more or less acidic intrusions in the middle crust and up to 10 km thick mafic underplating of the continental crust (Bois et al., 1989; Costa and Rey, 1995; Petri, 2014; Rey, 1993; Schaltegger, 1997; Schuster and Stüwe, 2008).

For most authors, these events reflect the collapse of the Variscan range following the termination of convergence. Indeed, the high topography of the orogen may have become gravitationally unstable once compression ceased, especially because of the thermal weakening induced by crustal thickening (Burg et al., 1994; Dewey, 1988; Dörr and Zulauf, 2010; Rey, 1993). Note however, that according to Henk (1997), gravitational collapse alone cannot account for the amount of Permo-Carboniferous crustal thinning observed in Central Europe, and the latter must have been aided by stress field re-organisation. In this view, Ziegler (1988) and Stampfli and Borel

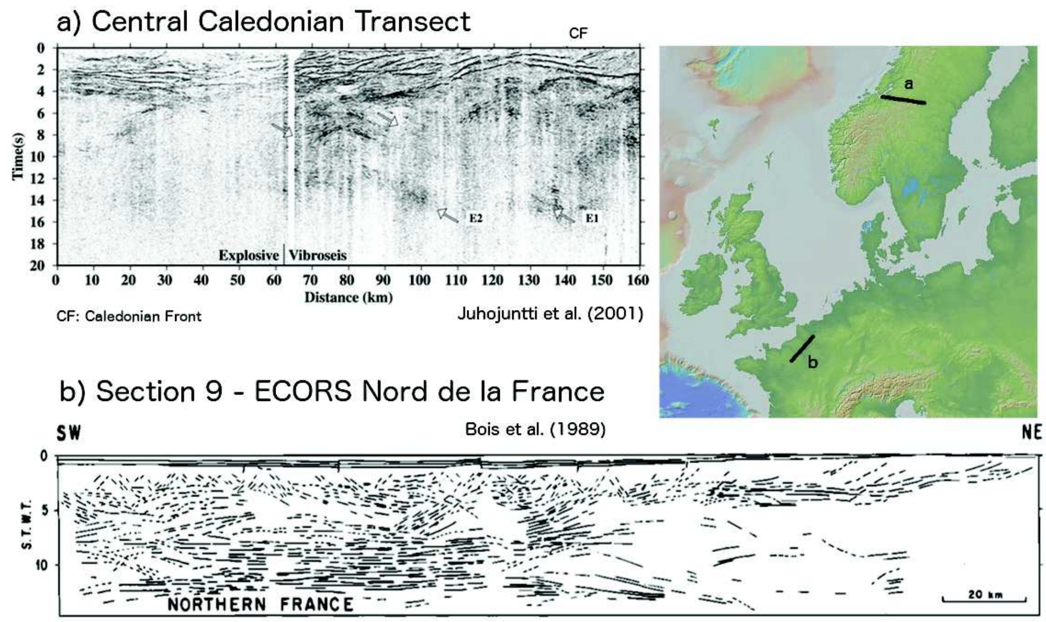

Figure 4 – Seismic sections through the former (a) Scandinavian Caledonian orogen (Juhojuntti et al., 2001) and through the (b) Variscan orogen of Western Europe (Bois et al., 1989) – see map for approximate location. Note that orogenic structures are erased in the Variscan lower crust (section b) whereas they are well-preserved in the entire Caledonian continental crust (section a).

(2002), amongst others, proposed that backarc extension associated to slab rollback in the Paleotethys contributed to the extensional setting in Western Europe.

By contrast, Franke (2014) argues that high reliefs were scarce in the Variscan range, thus it can't have collapsed. In his view, the lithospheric thinning and the important phase of heating are related to mantle activity caused by the Tethyan rift.

Thermal and isostatic re-equilibration of the lithosphere was achieved during the Permian and the Triassic through extension, uplift and erosion. By that time, the continental crust was about 30–35 km thick with a rejuvenated lower crust devoid of orogenic structural inheritance (Figure 4 b; Bois et al., 1989; Meissner, 1999; Rey, 1993). Moreover, these magmatic processes depleted most likely the underlying mantle in fusible elements and were associated with high grade (granulite facies) metamorphism (Costa and Rey, 1995; Petri, 2014; Rey, 1993; Schaltegger, 1997; Schuster and Stüwe, 2008).

4 The Alpine Tethys and North Atlantic rift systems

The assembly of Pangea had barely been completed, when the supercontinent started to break apart. Putting aside orogenic collapse, extension began to manifest during the Permo-Triassic as erratically oriented basins of moderate depth (< 8 km) scattered along the Caledonian orogenic belt (Doré et al., 1999; Ziegler, 1988).

Indisputable onset of rifting in Western Europe is marked by the Triassic onset of necking in Central Atlantic and its northwestward propagation to the south of Iberia into the Tethyan realm, along the southern front of the Variscan orogen (Figures 5 and 6; Frizon de Lamotte et al., 2011). By the end of Jurassic, both rift systems were linked through the so-called Alpine Tethys, which includes the Piedmont-Liguria and Valais 'Oceans' (Frizon de Lamotte et al., 2011; Schmid et al., 2004; Stampfli et al., 1998, and references therein). Besides, throughout the Jurassic, necking propagated from the Arctic region between Norway and Greenland, down to the North Sea, creating significant accommodation space in the Møre and Vøring basins, in the Vicking Graben and in the Central Trough (Doré et al., 1999; Erratt et al., 1999; Roberts et al., 1999; Ziegler, 1988; see Figure 7).

In Late Jurassic–Early Cretaceous, necking began to propagate northward along southern Iberia and opened the Orphan, Porcupine and Rockall basins, as well as the Bay of Biscay (Enachescu, 2006; Tucholke et al., 2007; Tucholke and Sibuet, 2007; Ziegler, 1988).

During mid-Cretaceous, seafloor spreading had started between Iberia and Newfoundland and in the Bay of Biscay, and necking was propagating northwestward in the Labrador Sea (Chalmers and Pulvertaft, 2001; Sibuet et al., 2007; Ziegler, 1988; Figure 7). By that time, extension had shifted from predominantly E-W directed to NW-SE directed, which may relate to the termination of seafloor spreading in the Tethys and the onset of it subduction at its northern margin (Doré et al., 1999, and references therein). Note that the Bay of Biscay may have been connected to the Alpine Tethys (Manatschal et al., 2011; Schmid et al., 2004) through a series of discontinuous narrow hyperextended rift basins floored with exhumed mantle (the Basque-Cantabrian and Arzacq-Mauléon basins Jammes et al., 2009; Lagabrielle and Bodinier, 2008; Tugend et al., 2014). Although the size of the different rift basins and the maturity of their spreading system remains a matter of debate (see Handy et al., 2010), all these basins and oceans remained most likely relatively narrow ($<$ 400–600 km according to Li et al., 2013; Rosenbaum and Lister, 2005).

Offshore United Kingdom north of the Charlie–Gibbs fracture zone, Cretaceous extension did not localize at the former Jurassic basins, but stepped further north-

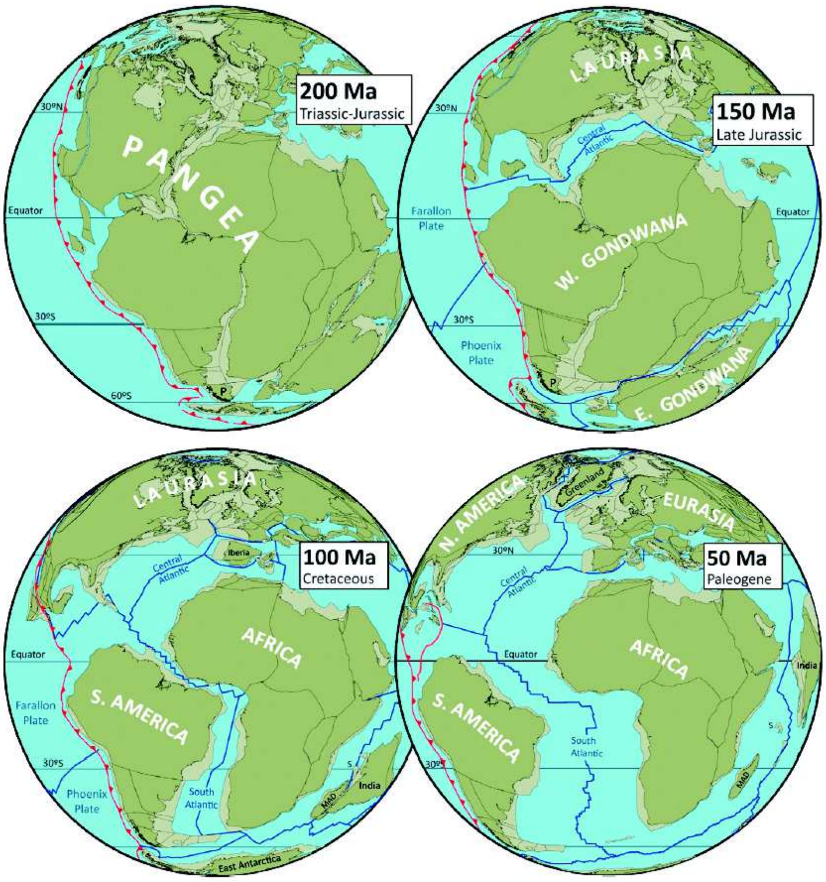

Figure 5 – Global Paleogeographic reconstruction from Late Triassic to Early Cenozoic after Torsvik et al. (2012).

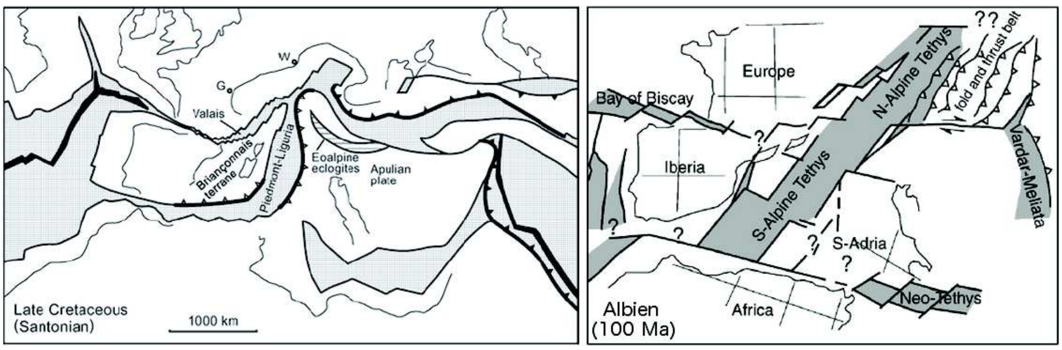

Figure 6 – Possible Late Cretaceous configurations of the Alpine Tethys rift system: left-hand panel after Schmid et al. (2004); right-hand panel after Manatschal et al. (2011).

west in the Hatton Basin and at the locus of the present day ocean (Figure 7; Doré et al., 1999; Lundin and Doré, 1997). Extension in northern North Atlantic may have continued less intensely and more erratically during the Late Cretaceous, until the final rifting and subsequent onset of seafloor spreading was forced by an excess magmatic event during the Eocene (Doré et al., 1999, and references therein). This peak in magmatic activity was most likely related, either to a mantle plume and/or to a more fertile mantle heterogeneity inherited from the previous rift episodes (see Meyer et al., 2007, for a review).

Figure 7 – Late Triassic to Early Miocene first-order direction of extension during the in the North Atlantic region (from Doré et al., 1999). BL: Bivrost Lineament; BJ: Bjørnøya Basin; C: Central Graben; CG: Charlie–Gibbs Fracture Zone; EG: East Greenland Rift; FD: Faeroes Dome; FS: Faeroe-Shetland Basin; G: Gjallar Ridge; GB: Galicia Bank Basin; GGF: Great Glen Fault; H: Halten Terrace; HG: Hel Graben; HH: Helland-Hansen Arch; HT: Hatton Trough; JM: Jan Mayen;L: Labrador Sea; MTFZ: Møre–Trødelag Fracture Zone; MB: Møre Basin; NCS: North Celtic Sea; NR: North Rockall Trough; O: Orphan Basin; P: Porcupine Basin; R: Rockall Trough; R: Røst Basin; SB: Svorestnaget Basin; T: TromsøBasin; V: Vestfjorden Basin; VG: Vøring Graben; VV: Vestbakken Volcanic Province

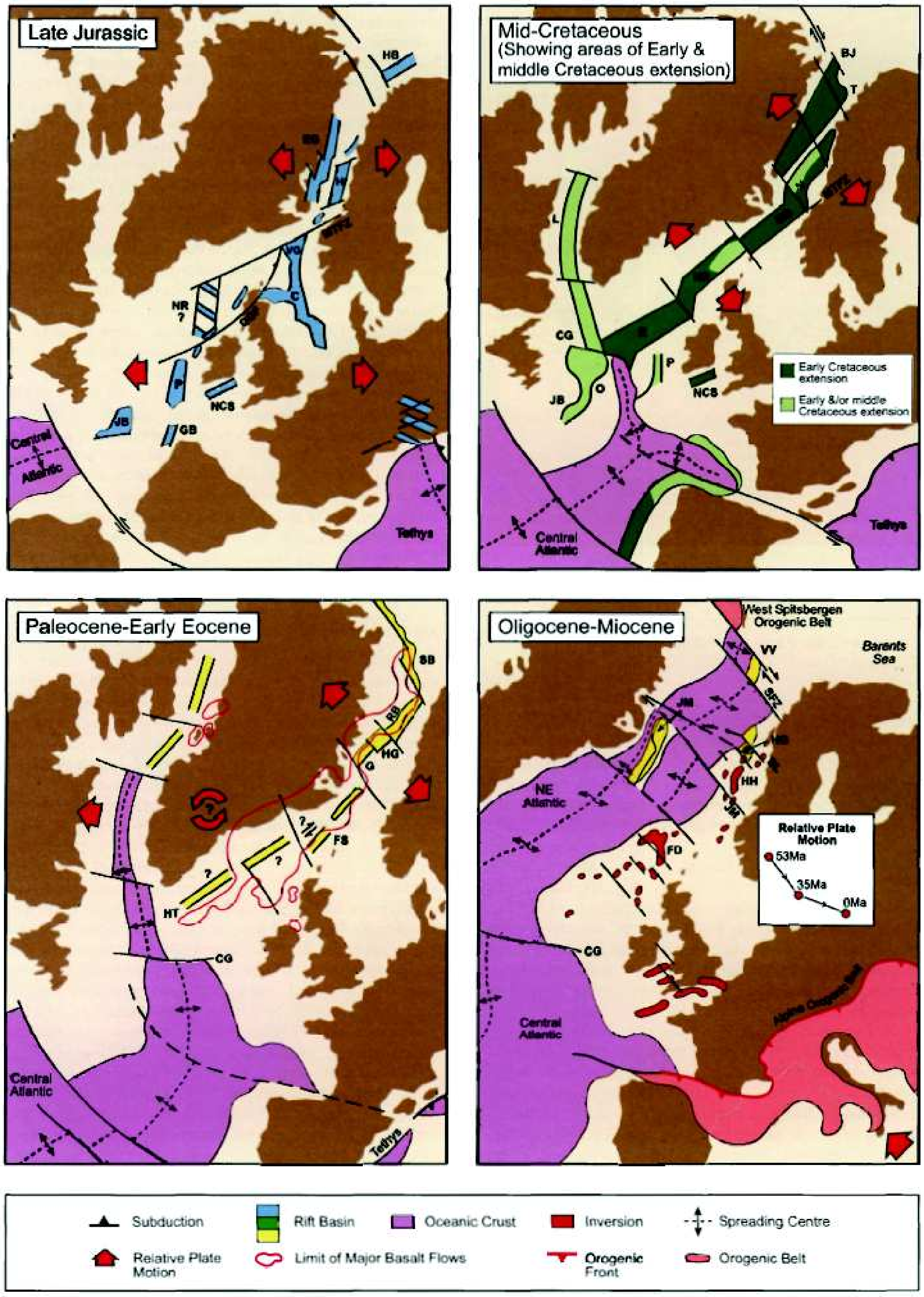
Late Jurassic
HB
VG
NR
?
C
NCS
P
JB
GB
Central
Atlantic
Tethys
Mid-Cretaceous
(Showing areas of Early &
middle Cretaceous extension)
BJ
T
L
CG
P
NCS
JB
O
Early Cretaceous extension
Early &/or middle Cretaceous extension
Central
Atlantic
Tethys
Paleocene-Early Eocene
SB
HG
G
FS
HT
CG
Central
Atlantic
Tethys
Oligocene-Miocene
West Spitsbergen
Orogenic Belt
VV
Barents
Sea
NE
Atlantic
HH
FD
CG
Relative Plate
Motion
53Ma
35Ma
0Ma
Central
Atlantic
Subduction
Rift Basin
Oceanic Crust
Inversion
Spreading Centre
Relative Plate
Motion
Limit of Major Basalt Flows
Orogenic
Front
Orogenic Belt

5 The Alpine orogeny in Western Europe

5.1 The Alps *sensu stricto*

Subduction of the Tethyan rift system began during the Late Cretaceous and brought about convergence between southern Europe and the so-called Apulian/ Adriatic plate, which was comprised of several microplates (see Schmid et al., 2008). The main phase of continental collision commenced during the Eocene, at about 35 Ma, and led to the construction of the Alpine orogen (see Schmid et al., 2008). However the orogenic evolution of the Alpine domain was actually more complex since it was diachronous from East to West and involved as many as seven (micro-) plates (Europe, Africa, Iberia, Adria, Alcapia, Alkapecia, and Tiszia; see Handy et al., 2010). For instance, the eastern Alps display at least one earlier collisional phase known as the Eo-alpine orogeny (from 140 to 84 Ma), produced by the closure of the Meliata Ocean (see Schmid et al., 2008, for a review). Orogenesis was associated with several deformation phases of various orientation (see Mohn et al., 2011, and references therein), major strike-slip movements and significant rotation of the Apulian plate during both Early and Late Cretaceous, all of which contributed to the complex deformation and seafloor spreading patterns (Handy et al., 2010, and references therein).

At present, the Alps are a 1,200 km long and 300 km wide arcuate mountain range. It is made of a thick asymmetric doubly-verging accretionary wedge, more developed on the northwestern (European) side (Dal Piaz et al., 2003). Although the deep structure of the orogen remains a matter of debate (see Figure 8 a), the surface has been extensively mapped and studied since the beginning of the last century. The external parts of the orogen are comprised of crystalline massifs and a thin-skinned fold-and-thrust belt made of carbonate platforms, both of which represent the former continental margins. In contrast, the internal part is a complex stacking of basement remnants, ophilites and pre-, syn- and post-rift sediments (Mohn et al., 2014). The orogen comprises widespread occurrence of high- to ultra high-pressure metamorphic parageneses (Chopin, 1987; Meyre and Pusching, 1993; Thöni and Jagoutz, 1993), but there is no evidence for significant arc-related magmatic activity or high-temperature metamorphism contemporaneous to subduction in the Alps.

5.2 The Pyrenees

Contemporaneously to the Alpine Orogeny, Late Cretaceous northward drifting of Africa brought about an onset of subduction in the Bay of Biscay and the closure

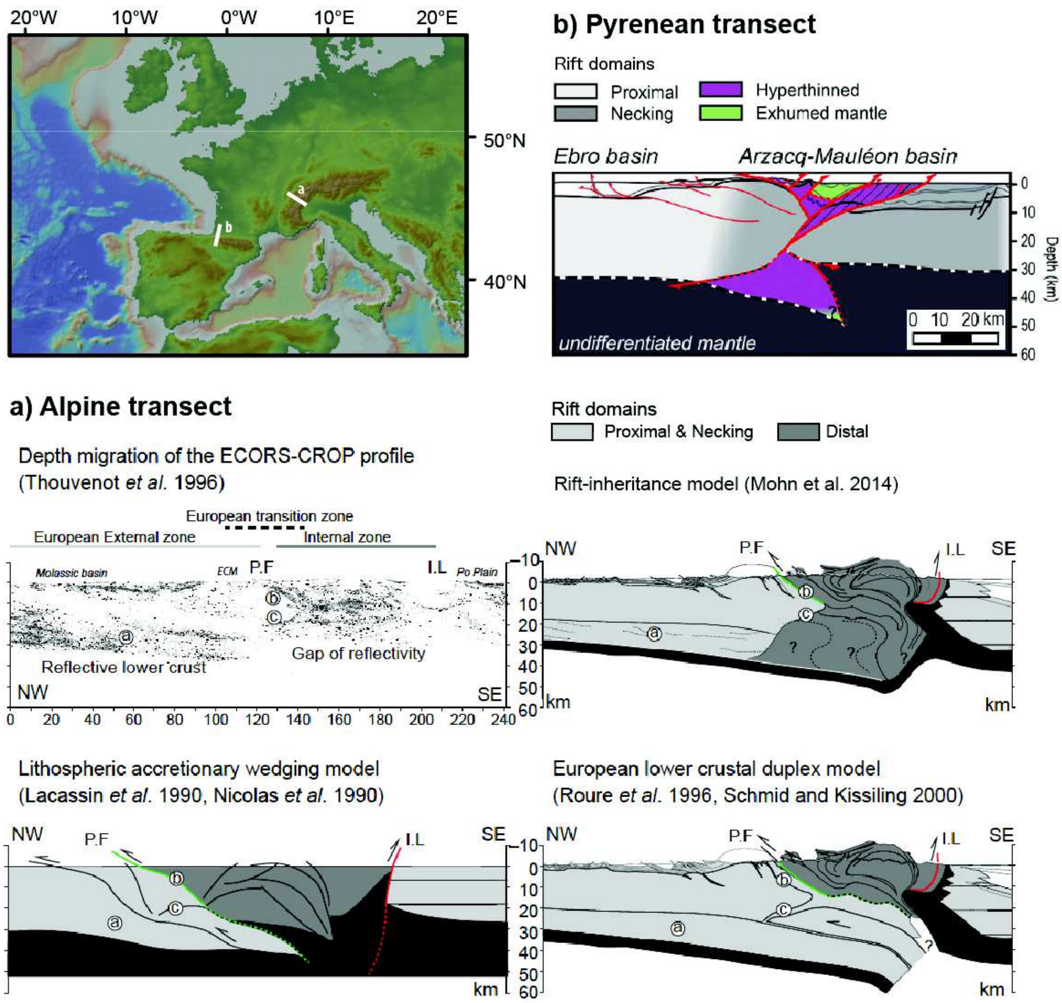

Figure 8 – First-order structural architecture of the (a) Alpine orogen after Mohn et al. (2014) and (b) Pyrenean orogen after Tugend et al. (2014). P.F.: Penninic Front; I.L.: Periadriatic Line.

of the narrow and segmented hyperextended rift system between Iberia and France (Tugend et al., 2014, and references therein). The climax of compression in the Pyrenees is recorded from Eocene to Oligocene (Muñoz, 2002) and the amount of shortening is in the order of 140–200 km (Rosenbaum et al., 2002).

At present, the Pyrenees *sensu stricto* are a 1,000 km long and 150 km wide mountain range made of an asymetrical doubly-verging accretionary wedge more developed on its southern (Iberian) side (Casteras, 1933; Mattauer, 1968, see Figure 8 b). The southern external part of the orogen comprises crystalline massifs, which represent the former continental margins, while the internal part is a complex stacking sampling the former hyperextended and exhumation rift domains (Tugend et al., 2014). The range lacks both high-pressure and high-temperature syn-orogenic rock assemblages, as well as evidence for magmatism related to the orogeny.

Introduction to Chapter I

The first step of my study aims to synthesize the first-order orogenic inheritance, the first-order architecture of rift systems and the timing of major rifting events at the scale of the North Atlantic, in order to highlight potential correlations between them.

Chapter I

Assessing the impact of orogenic inheritance on the architecture, timing and magmatic budget of the North Atlantic rift system: a mapping approach

Pauline Chenin[*,1], Gianreto Manatschal[1], Luc L. Lavier[2] & Duncan Erratt[3]

[1] CNRS - IPGS - EOST, Université de Strasbourg, 1 rue Blessig, 67084 Strasbourg, France
[2] Institute for Geophysics, J.J. Pickle Research Campus, Bldg. 196, 10100 Burnet Rd., Austin, Texas, 78758, USA
[3] ExxonMobil International Ltd, ExxonMobil House, Ermyn Way, Leatherhead, Surrey KT22 8UX, UK
[*] Corresponding author (email: chenin@unistra.fr)

modified after the version Published in *Journal of the Geological Society* on September 2015
Volume 172; issue 6; pages 711–720

Abstract

To investigate the impact of orogenic inheritance on the characteristics of the North Atlantic rift system we develop new mapping methods that highlight the first-order architecture and timing of rifts, as well as the distribution of heterogeneities inherited from the Palaeozoic Caledonian and Variscan orogenies. These maps demonstrates major differences in the behaviour of the North Atlantic rift system relative to both orogens, with the Variscan front appearing to be an important boundary. Indeed, the rift cuts through the Caledonian orogen and parallels its structural grain to the north, while it circumvents the core of the Variscides to the south. In addition, rifting is protracted and polyphase with breakup being magma-rich north of the Variscan front, as opposed to the south where a single, apparently continuous extensional event led to magma-poor breakup in less than 50 Myr. Besides, the North Atlantic rift system reactivates sutures corresponding to large ($> 2{,}000$ km) former oceans, while sutures of small (< 500–$1{,}000$ km) oceanic basins are little affected in both the northern and southern North Atlantic. These observations point to a major influence of orogenic inheritance on the characteristics of rift systems.

Introduction to Chapter II

The previous Chapter underlines the significant variability in the characteristics of the North Atlantic rift system, depending on whether it affects the Caledonian or the Variscan orogenic lithosphere. Yet, one major difference between these two orogenic events is their paleo-geographic settings. Indeed, the Caledonides of Norway–Greenland resulted mainly from the closure of the large Iapetus Ocean, whereas the Variscides of Western Europe were consequent to the closure of several 'narrow' oceans, in addition to the suturing of the wide Rheic Ocean.

Therefore, the next step of my study aims to highlight the specificities of both 'narrow/immature' and 'wide/mature' extensional systems, and how they may influence subsequent orogenic processes.

Chapter II

The role of the initial architecture of rifted margins in orogenesis related to the closure of 'narrow' oceans

Pauline Chenin[*,1], Gianreto Manatschal[1], Othmar Müntener[2]
Suzanne Picazo[2], Garry D. Karner[3], Christopher Johnson[3] &
Marc Ulrich[1]

[1] CNRS - IPGS - EOST, Université de Strasbourg, 1 rue Blessig, 67084 Strasbourg, France
[2] Institut des sciences de la Terre (ISTE), Géopolis, CH-1015 Lausanne, Schwitzerland
[3] ExxonMobil Upstream Research Company, PO Box 2189, Houston, TX 77252, USA
[*] Corresponding author (email: chenin@unistra.fr)

Abstract

Orogens resulting from the closure of 'narrow oceans' such as the Alps or the Pyrenees usually lack voluminous syn-subduction and syn-orogenic magmatism. Such orogenies may be controlled by mechanical processes in which the initial architecture of the original rifted margins may strongly control the architecture of the orogen. In this paper, we investigate how rift-related inheritance may impact the crustal geometry and mantle geochemistry of orogens related to the closure of 'narrow oceans', and compare them to orogenies resulting from the closure of 'wide/mature oceans'. We first characterize the large-scale structural and lithological architecture of rifted margins for both 'narrow' and 'wide oceans' based on a worldwide compilation of examples. Second, we investigate how these characteristics may be expressed during a subsequent orogeny.

Our results show that 'narrow oceans' are usually devoid of mature spreading systems forming steadily Penrose-type oceanic crust, in contrast to 'wide oceans'. However, there is statistically no difference in the architecture of their margins, thus the main difference between 'narrow' and 'wide oceans' is whether their margins are separated by a significant amount of normal oceanic crust and underlying depleted mantle. Moreover, due to the lack of significant magmatism during the closure of 'narrow oceans', the mantle wedge is likely to remain relatively fertile compared to the wedge above long-lasting subductions of 'wide oceans'. This difference in mantle composition may dictate the magmatic budget of subsequent orogenic collapse or rifting event.

1 Introduction

Collisional orogens are usually regarded as a result from the telescoping of former rifted margins following subduction of a wide oceanic domain (e.g. Ernst, 2005; Uyeda, 1981; Willett et al., 1993). Such long-lasting, Pacific-type subduction systems are typically associated with the formation of volcanic arcs and high temperature/low pressure metamorphism in the hanging wall (Ernst et al., 1970; Miyashiro, 1961, 1967), both of which strongly modify the architecture, lithology and thermal state of the initial margin. Therefore, at least one side of the orogens following the closure of 'wide oceans' may be significantly overprinted by subduction-induced processes. This may explain why, except for a few recent studies (Beltrando et al., 2014; Butler, 2013; Butler et al., 2006; Mohn et al., 2014, 2011; Tugend et al., 2015, and references therein), little attention has been paid to the potential impact of the initial architecture of the intervening rifted margins. However, orogens such as the Alps, the Pyrenees and the central part of the Variscides supposedly result from the closure of 'narrow', possibly 'embryonic' oceans (i.e. devoid of a mature seafloor spreading system) and lack evidence for both voluminous arc magmatism and high temperature metamorphism contemporaneous with the subduction (Jammes et al., 2009; Matte, 2001; Müntener et al., 2010). Consequently, their construction was most likely controlled by mechanical process where the architecture state of the initial margins dictated largely the crustal geometry and mantle geochemistry.

Narrow/embryonic oceans are ubiquitous on Earth at present, for instance the Porcupine Basin, the Rockall Trough and the Flemish Pass in the North Atlantic (Table II.1). Such basins were most likely also common in the past, as exemplified by the Rhenohercynian, Saxothuringian and Medio-European 'oceans' in the Variscan area (see Franke, 2006; McKerrow et al., 2000a), thus, a significant number of present-day orogens may result from the closure of comparable 'narrow oceans'. Therefore, understanding how rift inheritance influences orogenic systems is of primary importance for the understanding of collisional orogens, in general.

In this paper, we define 'narrow oceans' as rift systems that reached at least the stage of hyperextension (see Doré and Lundin (2015) for the definition of *hyperextension*), but remained less than ~ 300 km wide (the reasons for this limit are discussed below). We also distinguish between 'mature' oceans, which comprise a self-sustaining, steady-state seafloor spreading system, and 'immature/embryonic' oceans, whose development stopped at the stage of hyperextension. We investigate how first-order rift-related inheritance of narrow oceans may influence orogens resulting from their closure, and compare these 'immature' orogens with 'mature'

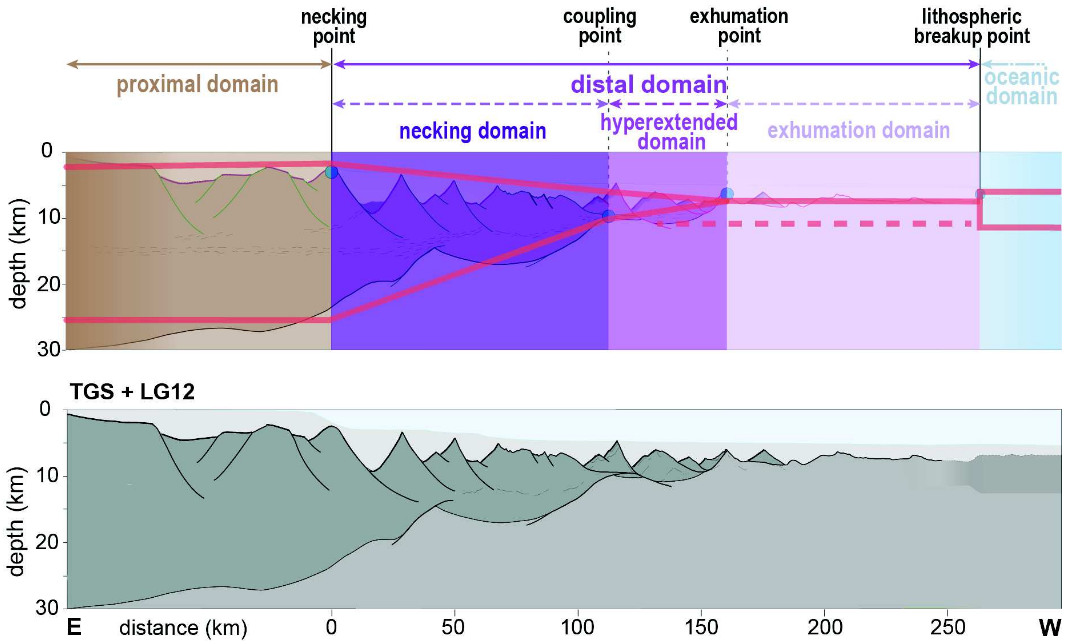

Figure II.1 – Definition of the distal sub-domains comprising hyperextended rifted margins after Sutra et al. (2013) and Chenin et al. (2015). Their first-order morphology is highlighted with red lines. The dotted line represents the 'seismic Moho' (i.e. a sharp increase in P velocity from < 7 km.s^{-1} to > 7.8 km.s^{-1}; see Mengel and Kern, 1992), where it differs from the 'petrologic Moho' (i.e. the crust–mantle boundary).

orogens produced by the closure of wide/mature oceans. We first characterize the large-scale structural and lithological architecture of both narrow and wide oceans based on a worldwide compilation of examples. Second, we investigate how these specificities may be expressed during orogenesis. We focus on collisional orogens resulting from the closure of narrow oceans, first to avoid the complex overprint induced by the magmatic processes associated to long-lasting subduction, and second because the impact of rift-related inheritance in such orogenic systems remains little studied to date. Third, we estimate the maximum width of a basin system which, when subducted, will fail to produce significant magmatic activity. Finally, we discuss how orogens following from the subduction of narrow oceans may differ from those produced by the closure of wide oceans.

2 Characteristics of rifted margins

Recent studies suggest that most rifted margins whose necking and hyperextension were magma-poor display a similar succession of comparable marginal domains (Figure II.1), regardless of whether or not they achieved lithospheric breakup and steady-state seafloor spreading (Péron-Pinvidic et al., 2013; Sutra et al., 2013). In this section, we characterize the first-order architecture and lithology of such rift systems and appraise the width of their distal sub-domains based on natural examples.

2.1 First-order architecture

In order to characterize the architecture of rifted margins, Sutra et al. (2013) distinguished several domains based on morphological criteria (Figure II.1). On the one hand, the *proximal domain* corresponds to un-thinned or minor extended ($\sim$ 30–35 km thick) continental crust and is characterized by parallel, roughly flat basement and Moho topographies. On the other hand, the *oceanic domain* is made of homogeneous, Penrose-type oceanic crust, typically about 6–7 km thick. Here again, basement and Moho are parallel. The *distal domain*, between them, records most of the rift-related deformation.

The distal domain can be divided into several sub-domains (Figure II.1), namely: (a) a *necking domain* characterized by the abrupt thinning of the continental crust from $\sim$ 30–35 km down to $\sim$ 10 km, which translates to a deepening of top basement and shallowing of the Moho (the latter only on seismic sections in depth); (b) a *hyperextended domain*, where continental crust is thinned from $\sim$ 10 km down to 0 km. The transition between the necking and hyperextended domain corresponds to a sudden decrease in the dip of the Moho on depth seismic sections; (c) a so-called *exhumation domain* may exist in magma-poor rifted margins when lithospheric subcontinental mantle is exhumed at the seafloor (Boillot et al., 1987; Manatschal and Müntener, 2009; Whitmarsh et al., 2001). Mantle exhumation is associated with serpentinization down to a depth of 4–6 km (Andreani et al., 2007; Boillot et al., 1989; Escartín et al., 2001; Minshull, 2009), and the transition from serpentinized mantle to fresh peridotite is evidenced by a more or less progressive increase in seismic velocity (Horen et al., 1996; Miller and Christensen, 1997; Skelton et al., 2005). Mantle exhumation may also be accompanied with the emplacement of discontinuous extrusive magmatic rocks from a 'stuttering spreading system', which is characterized by incomplete development of oceanic layers 2 and 3, found in normal oceanic crust (e.g. Bronner et al., 2011; Desmurs et al., 2002; Jagoutz et al., 2007; Müntener et al., 2004). Note that allochthonous blocks of continental crust may be found on top of the serpentinized exhumed mantle of the exhumation domain. Thus, on seismic sections, the exhumation domain usually appears as a more or less corrugated surface devoid of Moho, or with a discontinuous seismic Moho reflector when exhumation is accompanied with magmatism (Whitmarsh et al., 2001). The transition from the exhumation domain into the oceanic domain is highlighted by an abrupt step-up in the basement (Bronner et al., 2011), which reflects the decrease in the density of the lithospheric column resulting from both the production of thicker crust through increased magmatic activity and the decrease in serpentinized mantle layer thickness (Gillard et al., 2015). In contrast, in the case of magma-rich margins, the transition from thickened magmatic crust to steady-state seafloor spreading is expressed as a step-down onto oceanic crust. The first-order morphology of magma-poor rifted margins is highlighted by the red lines on Figure II.1.

2.2 Dimensions and maturity of rift systems

In order to assess the dimensions of rift systems and their distal sub-domains, in addition to their 'maturity', we first compile the width and the lithology of basement rocks for several narrow and wide extensional systems around the world (Table II.1). In this paper, the width of an extensional system refers to the distance between the two conjugate necking points (Figure II.1). Our results suggest that (inactive?) extensional systems narrower than 300 km are usually immature, i.e. devoid of a self-sustained, steady-state spreading system, and are floored with either thinned continental crust, exhumed mantle and/or embryonic oceanic crust (Table II.1).

Second, we measure the width of the distal sub-domains (namely the necking, hyperextended and exhumation domains) for a selection of published seismic sections (Table II.2). For this compilation, we only consider dip seismic lines imaging extensional systems formed in a single, unidirectional and continuous rifting event (i.e. no significant time lag without extension). In addition, we restrict our measurements to domains with minor magmatic additions. Note that we did not include the width of the exhumation domain for rift basins which did not achieve lithospheric breakup, because in this case the full width of the exhumation domain was possibly not realized.

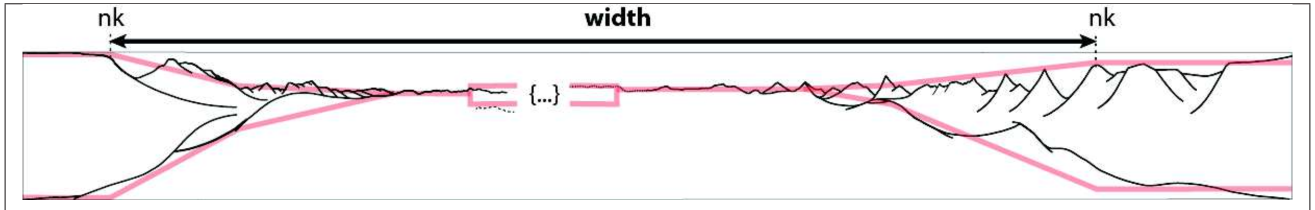

	Width	Basin floor	References
Atlantic Ocean	$\sim$ 3,000 - 5,000 km	oceanic crust	
Porcupine Basin	$<$ 200 km	thinned continental crust (& exhumed mantle?)	Reston et al. (2004)
Rockall Trough	$\sim$ 250 km	thinned continental crust	Klingelhöfer et al. (2005)
Hatton Basin	$\sim$ 200 km	thinned continental crust	Edwards (2002)
Orphan Basin	$\sim$ 400 km	thinned continental crust	Chian et al. (2001)
Northern Red Sea	250–350 km	no or embryonic oceanic crust	Bosworth et al. (2005)
Southern Red Sea	350–450 km	no or embryonic oceanic crust	Bosworth et al. (2005)
Gulf of Aden	$<$ 200 km	(embryonic?) oceanic crust	Bosworth et al. (2005)
Indian Ocean	up to $\sim$ 20,000 km	oceanic crust	
Pacific Oean	up to $\sim$10,000 km	oceanic crust	

Table II.1 – Width and nature of basement floor of several present-day extensional systems. The *width* refers to the distance between the two conjugate necking points (nk).

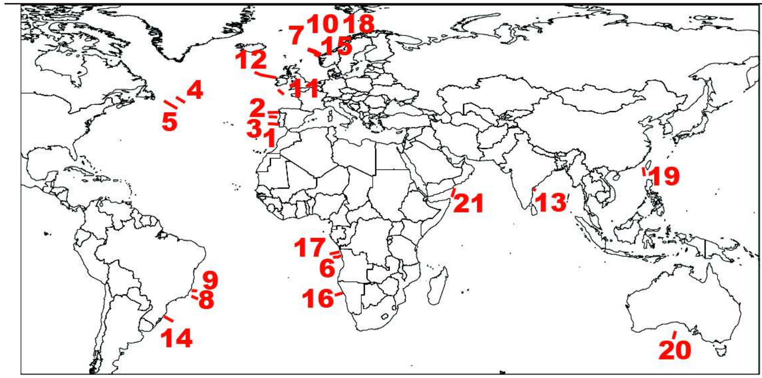

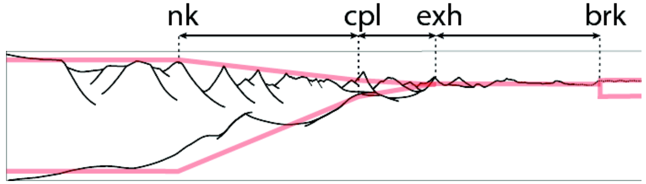

	Section	x(cpl-nk) (km)	x(exh-cpl) (km)	x(brk-exh) (km)	x(brk) (km)	Moho and basement linedrawing
1	IAM5 (Afilhado et al., 2008)	54	64	108	226	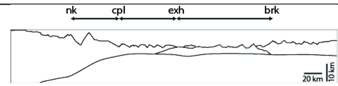
2	ISE1 (Sutra et al., 2013)	208	71	68	347	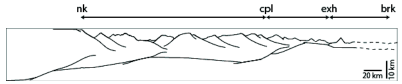
3	TGS+LG12 (Sutra et al., 2013)	100	58	81	239	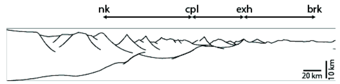
4	SCREECH1 (Sutra et al., 2013)	49	62	30	141	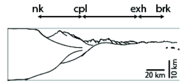
5	SCREECH2 (Sutra et al., 2013)	46	44	90	180	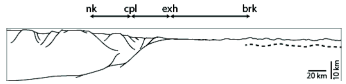
6	Angola (Unternehr et al., 2010)	71			241	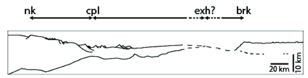

	Section	x(cpl-nk)	x(exh-cpl)	x(brk-exh)	x(brk)	Moho and basement linedrawing
7	Norway (TrII Nirrengarten et al., 2014)	84				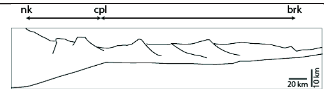
8	Campos Basin (Zalán et al., 2012)	82	58	24	164	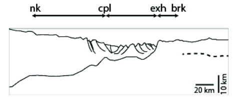
9	Esperito Santo Basin (Zalán et al., 2012)	63	64	39	166	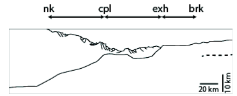
10	Norway (Osmundsen and Ebbing, 2008)	45				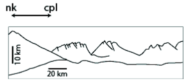
11	E-Porcupine (McDermott et al., 2014)	28	60			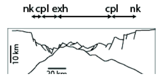
11	W-Porcupine (McDermott et al., 2014)	11	18			
12	E-Rockall (Welford et al., 2010)	72				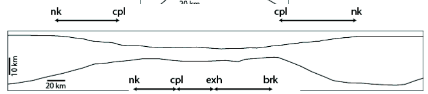
12	W-Rockall (Welford et al., 2010)	87				
13	India (Radhakrishna et al., 2012)	48	42	65	156	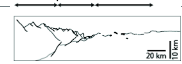
14	S-Pelotas (Stica et al., 2014)	71			155	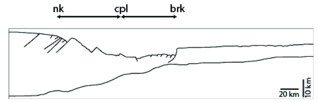
15	Norway (Kvarven, 2013)	43				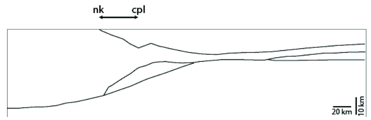
16	Namibia (Gladczenko et al., 1998)	51				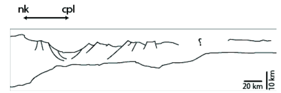

	Section	x(cpl-nk)	x(exh-cpl)	x(brk-exh)	x(brk)	Moho and basement linedrawing
17	Angola (Aslanian et al., 2009)	39			169	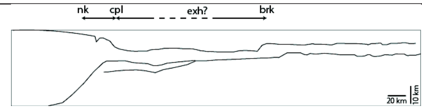
18	Norway (Osmundsen and Ebbing, 2008)	31				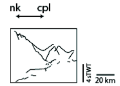
19	China Sea (Lester et al., 2014)	43	39	69	151	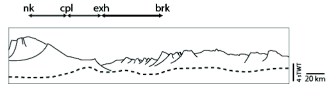
20	South Australia (Direen et al., 2008)			79		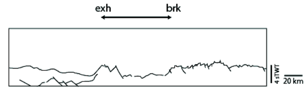
21	Aden (Leroy et al., 2010)	13	39	19	70	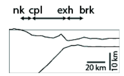

Table II.2 – Width of the distal sub-domains for several hyperextended to oceanic rift systems. nk: necking point; cpl: coupling point; exh: exhumation point; brk: breakup point (see Figure II.1)

The total width of continental margins ranges from about 130 to 350 km, with an average of 200 km (Figure II.2 a and c). Of all the distal sub-domains, the necking domain has the highest variability in width, ranging from 10 to 210 km (average $\sim$ 60 km, median $\sim$ 50 km; standard deviation 40 km; see Figure II.2 c). In contrast, the width of the hyperextended domain seems more constant, comprised between 20 and 70 km, with an average of 50 km (median $\sim$ 60 km; standard deviation 15 km). The width of the exhumation domain varies between about 20 km to 110 km, with an average of 60 km, a median of $\sim$ 70 km and a standard deviation of $\sim$ 30 km. Furthermore, Figure II.2 (b) indicates that no correlation exists between the width of any of the distal sub-domains and the total width of the distal domain.

Figure II.2 (d) suggests that the width of both the necking and hyperextended domains is unrelated to the maturity of the rift system, thus to whether the rift system is a 'narrow' or a 'wide' ocean. Therefore, the structural architecture of the hyprextended margins of immature oceans is statistically not different from that of mature oceans.

2.3 First-order lithological architecture

Although rifting affects an initially more or less horizontally homogeneous lithosphere, tectonic processes and local fluid-rock interactions (including mag- ma) may increasingly modify the lithology and thermal state, thus the rheology of the intervening lithosphere, as extension progresses.

When rifting is not triggered by magmatism (for instance upwelling of a mantle plume), the lithology of the crust is not significantly modified by extension in the proximal domain and in the necking domain. Therefore, the continental crust of both domains can be approximated by a quartzo-feldspathic material, as usually considered by numerical modellers. Note, however, that the necking domain translates the mechanical attenuation of the ductile layers during extension, so that the crust is fully brittle in the hyperextended domain (Manatschal et al., 2015; Pérez-Gussinyé et al., 2003; Sutra et al., 2013; see Figure II.3b and c). Besides, the subcontinental mantle underlying the proximal and necking domains is not significantly modified either and can be approximated by an average 'inherited mantle' consisting of $\sim$ 35–65% olivine, $\sim$ 7–30 % clinopyroxene,$\sim$ 25–30% orthopyroxene and $\sim$ 1% spinel (Picazo et al., 2015 and *in prep.*).

In contrast, in hyperextended and exhumation domains, fluid-rock interactions form hydrous minerals (Picazo et al., 2013), similarly to the fluid-rock processes observed in present-day mid-oceanic ridges (Bach et al., 2004; Boschi et al., 2006;

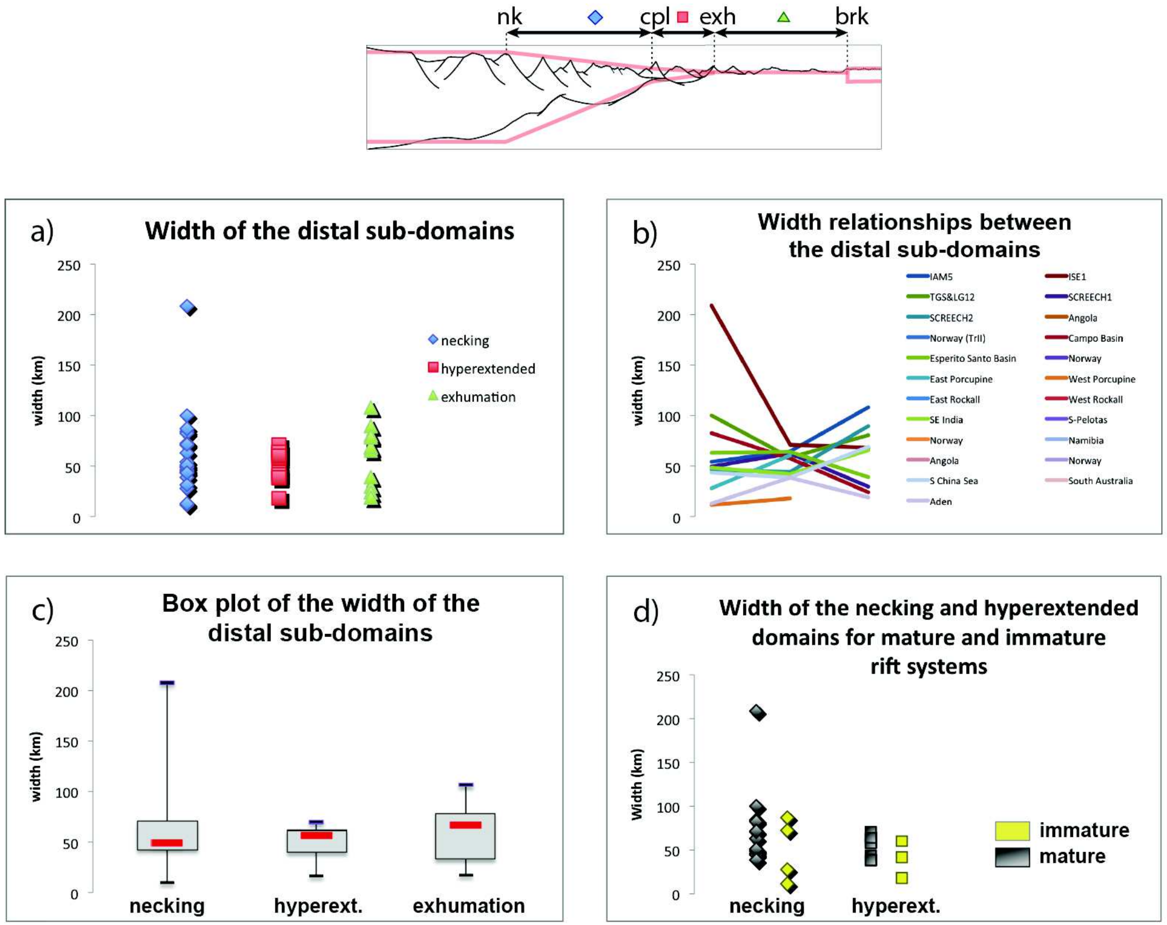

Figure II.2 – Statistical analysis of the width of the different distal sub-domains for our selection of hyperextended rifted margins. (a) Width of the necking, hyperextended and exhumation domains; (b) Width relationships between the distal sub-domains of each margin; (c) Box plot of the width distribution for the necking, hyperextended and exhumation domains; (d) Width of the necking and hyperextended domains for immature and mature oceans.

Mével, 2003; Picazo et al., 2012). Hydrothermal circulation is responsible for the crystallization of hydrous minerals within continental allochthons (e.g. sericite and illite; Pinto (2014) and references therein), as well as in serpentinized peridotite (e.g. serpentinite, chlorite, talc; see Christensen, 1970; Früh-Green et al., 2004; Hess, 1955; Picazo et al., 2013). Therefore, the rheology of the hyperextended continental crust and the top 4–6 km of lithospheric mantle in the exhumation domain can be approximated by a phyllosilicate-type rheology (Figure II.3 b and c).

Significant crustal thinning is also associated with partial melting of the asthenosphere (Latin and White, 1990). The resulting melts are initially not, or only little extracted, but impregnate the overlying lithospheric mantle (Müntener et al., 2010). From a depth of $\sim$ 30 km to the base of the continental crust, the subcontinental mantle underlying the hyperextended crust displays a 'fertile' composition of 51% olivine, 16% clinopyroxene, 25% orthopyroxene, 7% plagioclase and 1% spinel on average (Picazo et al., 2015 and *in prep.*). The density of the fertile mantle is significantly lower than that of the average inherited mantle ($\sim$ 3,250 kg.m^{-3} compared to $\sim$ 3,330 kg.m^{-3}; Picazo et al., 2015 and *in prep.*). Thus, immature rift systems whose development stopped at the stage of hyperextension are likely to retain this fertile mantle composition (Figure II.3 b).

In contrast, during lithospheric breakup, melt starts to be extracted and a sustainable magmatic system is established marking the onset of steady-state seafloor spreading. The resulting basaltic oceanic crust is homogeneous in both composition ($\sim$ 50 % plagioclase and 50 % pyroxene) and thickness ($\sim$ 6–7 km), as pointed by Anonymous (1972). The process of partial melting associated with the creation of oceanic crust depletes the underlying mantle in the most fusible elements, leaving an average composition of 57% olivine, 13% clinopyroxene, 28% orthopyroxene and 2% spinel (Workman and Hart, 2005; see also Figure II.3 c). This depleted mantle is approximately is slightly lighter than the average inherited mantle ($\sim$ 3,305 kg.m^{-3} compared to 3,330 kg.m^{-3}; Picazo et al., 2015, in prep.). Therefore, we expect the mantle underlying the most distal part of the margins of mature oceans to be depleted in fusible elements, conversely to the mantle underlying immature oceans.

3 First-order architecture of collisional orogens

Every ocean will eventually undergo subduction and be sutured after collision of its continental margins. On a first-order, a collisional orogen can be regarded as a 3-parts system comprising (Figure II.4 a): (1) two buttresses; (2) an accretionary wedge; and (3) a subducted part. Note that the existence of a crustal root beneath

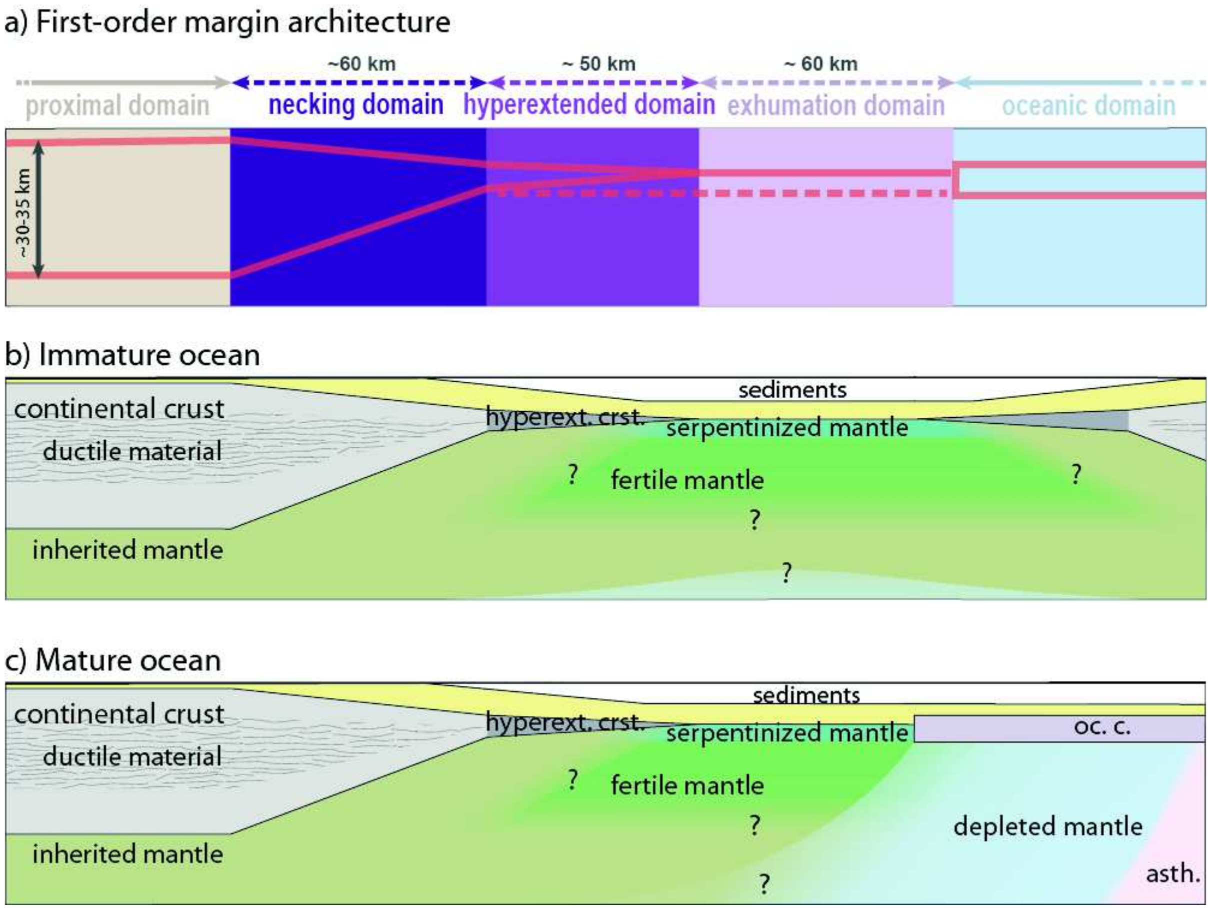

Figure II.3 – (a) First-order structural architecture of rifted margins and average width of the distal sub-domains; (b) First-order lithological architecture of immature/embryonic oceans; (c) First-order lithological architecture of mature oceans. hyp. c.: hyperextended continental crust; oc. c.: oceanic crust; depl. m.: depleted mantle; asth.: asthenospheric mantle. See text for discussion.

orogens is necessary to account for the observed isostasy, however the latter is very poorly constrained, as illustrated by the diversity of interpretations of the deep part of the ECORS-CROP seismic profile (Figure II.4 c).

In this section, we discuss how these different components may relate to specific parts of the initial rift system. In order to avoid the complexity induced by magmatic overprinting, we focus on the well-studied Pyrenean and Alpine orogens, both of which lack voluminous syn-subduction and syn-orogenic magmatism. Moreover, as both are relatively recent, their orogenic architecture is fairly well-preserved.

On the one hand, due to its relatively high density, oceanic lithosphere is usually efficiently subducted. According to Stern (2004), most of the ophiolites preserved within orogens correspond to obducted remnants of buoyant oceanic crust from small and young oceanic basins, usually former forearcs or backarcs. Besides, a significant proportion of sediments is also usually subducted, while the remaining part accumulates in the accretionary prism (Stern, 2011, and references therein). Note that, according to Andersen et al. (2012), some parts of the hyperextended and exhumation domains may be integrated into the accretionary wedge as well, as evidenced by the remnants of exhumed mantle in the Caledonian orogen. This proposition is also verified in the Alps and in the Pyrenees.

On the other hand, both the Alpine and the Pyrenean orogens display a similar architecture, where the external domain is made of little deformed continental basement and the internal part of a complex stacking of material from the distal margin (Beltrando et al., 2014; Casteras, 1933; Jammes et al., 2009; Mattauer, 1968; Schmid et al., 2004). Recent studies (Mohn et al., 2014; Tugend et al., 2015) show consistently that the external parts of the orogen (the buttresses B on Figure II.4), correspond to the necking zones of the former continental margins, and that the accretionary prism (A on Figure II.4) is comprised of thinned continental basement remnants, ophiolites and/or exhumed mantle and thick sequences of highly deformed sediments (Beltrando et al., 2014).

In summary, when the closure of a (narrow) ocean is devoid of significant magmatism, the orogenesis is essentially controlled by mechanical processes and its first-order comprising parts can be related to specific portions of the initial rift system (Figure II.4 a and b), namely: (1) the buttresses to the proximal + necking domains (Figure II.1); (2) the accretionary prism to part of the hyperextended and/or exhumation domains, in addition to part of the overall basin sediments; and (3) the subducted part to most of the hyperextended and exhumation domains, the oceanic lithosphere and part of the distal and oceanic sediments.

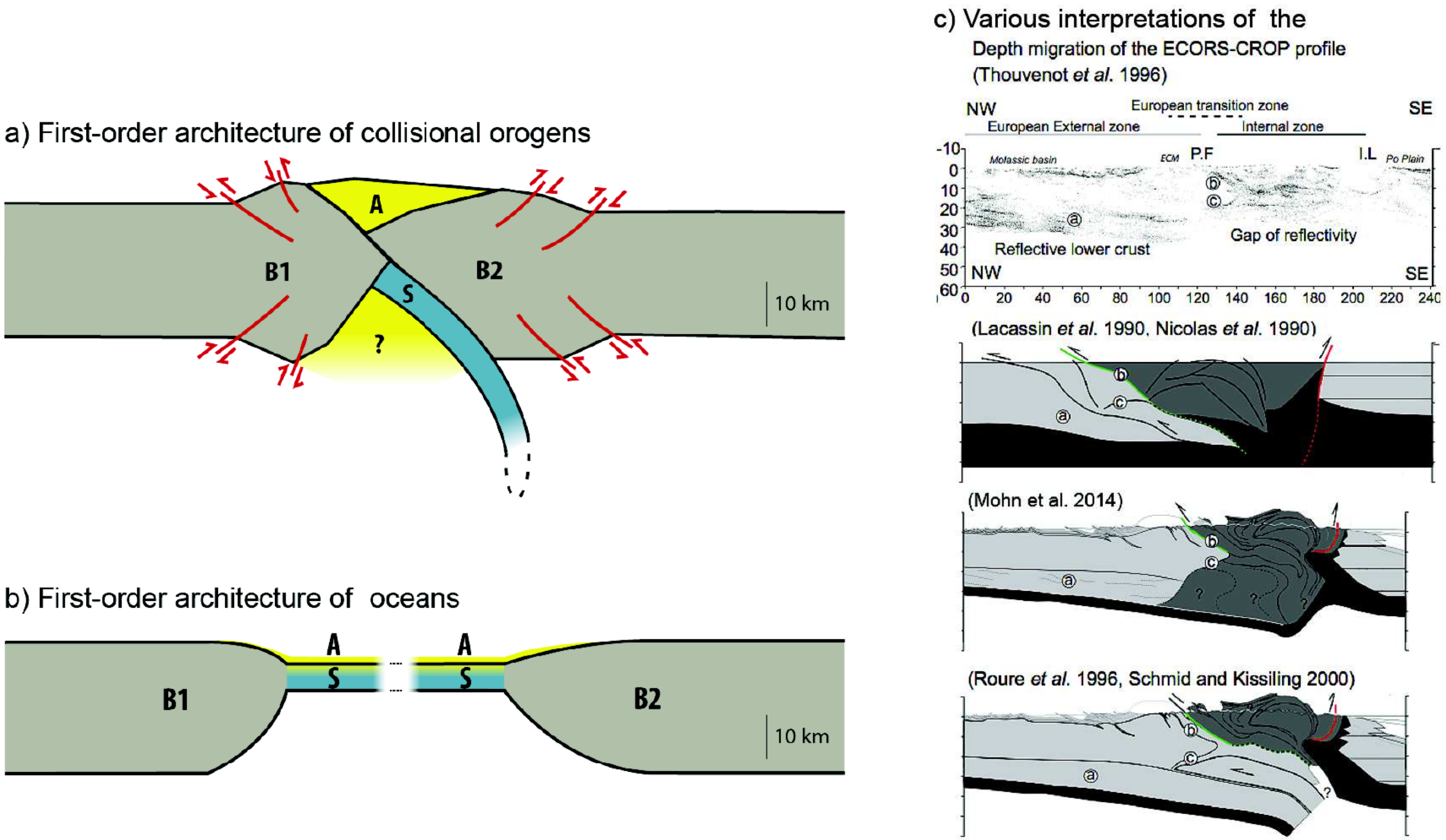

Figure II.4 – First-order architecture of orogens and hyperextended rift basins (a) continental collision involves two buttresses B (external parts of the orogen), an accretionary prism A (internal part of the orogen) and a subducted part S; (b) each element of the orogen can be linked to specific parts of the initial rift basin (see text for discussion). (c) Various interpretations of the deep structure of the ECORS-CROP seismic profile published in Mohn et al. (2014).

4 Discussion

Since the birth of plate tectonics and the understanding of first-order subduction processes, collisional orogens are usually regarded as a result from the telescoping of continental margins after long-lasting subduction of a wide oceanic domain. Such orogens are characterized by paired metamorphic belts, namely a low temperature/high pressure belt corresponding to the accretionary wedge; and a high temperature/low pressure belt related to arc, and potentially backarc magmatism (Brown, 2009; Dewey and Horsfield, 1970; Miyashiro, 1961, and references therein). However, several collisional orogens such as the Alps and the Pyrenees lack voluminous magmatism contemporaneous to subduction, i.e. are devoid of arcs, forearcs and backarcs remnants and of high temperature/low pressure metamorphic assemblages in the upper plate. Yet, both orogens result from the closure of relatively narrow (< 400–600 km), possibly embryonic 'oceans' (Li et al., 2013; Rosenbaum and Lister, 2005), which may be the main cause for the lack of significant magmatic products. Indeed, because significant dehydration of the basaltic crust and serpentinized mantle starts only from a depth of 100–200 km (Peacock et al., 1994; Rüpke et al., 2004), a magmatic arc is unlikely to develop before the slab is subducted to this depth (e.g. England et al., 2004; Jarrard, 1986). Therefore, there must be a critical width for rift systems, below which their subduction is devoid of significant magmatic activity. In such cases, the subsequent orogenies may be essentially controlled by mechanical processes, in which the structural and lithologic architectures of the intervening margins may be the dominant factor in controlling the architecture of the orogen.

4.1 'Narrow oceans' and 'magma-poor' subduction

As slabs subduct with an average dip of 50–60° in the upper mantle (Billen, 2008; Stevenson and Turner, 1977; Tovish et al., 1978), the slab must be at least 130 km long to reach a depth of 100 km. Adding to this twice the length of the necking domain (60 km on average; see section 2.1), which is usually not subducted (section 3), magma generation seems very unlikely during closure of rift systems narrower than 250 km. Furthermore, subduction must last long enough for a sufficient amount of volatiles to reach the right depth and allow partial melting (Gaetani and Grove, 1998; Peacock, 1991). This is consistent with the compilation by Jarrard (1986), which shows that the length of the subducted slab associated with the youngest arc (the Philippines arc, 6 m.y. old) is at least 170 km long. As a consequence, we expect rift basins narrower than 300 km to be devoid of significant magmatism expressed at the surface. In the following, we refer to these as *narrow oceans*, as opposed to *wide oceans*.

Note that, in addition to this so called 'flux melting', arc magma generation can also be largely driven by the decompression melting of the hot asthenosphere rising to compensate the down-dragging of mantle wedge material by the slab (Iwamori, 1998; Jagoutz et al., 2011). Yet, decompression melting becomes important only when a vigorous convection is active in the mantle wedge, which only develops after a significant amount of material has subducted (Conder et al., 2002; Peacock et al., 1994), thus is unlikely during the closure of a narrow ocean.

4.2 Characteristics of 'narrow' versus 'wide' oceans

As highlighted in Table II.1, extensional systems narrower than 300 km are usually devoid of a mature, self-sustaining spreading system, thus of 'normal' oceanic crust. As a result, their seafloor is either comprised of thinned continental crust, exhumed mantle and/or embryonic oceanic crust. On the contrary, mature, steady-state oceanic systems are usually characterized by a homogeneous, Penrose-type oceanic crust. Of course, there is a wide range of oceanic crust types between these 'embryonic' and 'Penrose' end-members. For instance, in ultra-slow spreading systems, a thin (2–5 km thick) 'oceanic crust' comprised of both magmatic and a-magmatic segments may be steadily emplaced for millions of years (Dick et al., 2003). Yet, like normal oceanic crust, oceanic crust from ultra-slow spreading centers is most likely to be efficiently subducted during the closure of wide oceans (Stern, 2004), thus it will *a priori* not influence the subsequent orogeny.

As we demonstrated in section 2.1, there is statistically no relationship between the size or maturity of an extensional system and the architecture of its margins. Therefore, on a first-order, the main difference between narrow and wide oceans is the existence of a significant amount of normal oceanic crust and underlying depleted mantle (Figure II.3 b and c). In contrast, the mantle underlying narrow embryonic oceans is likely to retain its fertile composition resulting from the impregnation by asthenospheric melts during hyperextension.

4.3 Subduction of narrow 'oceans' and subsequent orogeny

During short-lived subduction associated with the closure of narrow 'oceans', the slab remains at relatively shallow angle (Billen, 2008) and no self-sustaining subduction will presumably develop due to insufficient slab pull (Gurnis et al., 2004; Hall et al., 2003). In this context, the development of small-scale convection above the subducting slab is very unlikely (Peacock et al., 1994). Furthermore, the small length of the slab may not allow enough volatiles to reach a sufficient depth for significant partial melting to occur (Grove et al., 2006; Rüpke et al., 2004). In these circumstances, the generation of magma is improbable and hydration of the mantle wedge is likely to be the dominant process (Peacock et al., 1994).

In addition, because of the low dip angle of the slab, both slab pull and the potential effect of mantle flow on the slab are very limited, making the development of backarcs unlikely (Heuret and Lallemand, 2005; Uyeda, 1981). This is supported by the worldwide compilation of backarc deformation style by Heuret and Lallemand (2005), which highlights that no young subduction is associated with strongly extensional backarc settings. Therefore the lithosphere underlying orogens resulting from the closure narrow oceans is likely to be relatively fertile and hydrated (Figure II.5 b).

In contrast, protracted subductions associated with the closure of wide oceans are likely to become self-sustained, in particular due to the eclogitization of the subducting slab, which makes it denser than the encompassing asthenospheric mantle (Aoki and Takahashi, 2004; Doin and Henry, 2001). Long lasting subductions develop usually vigorous convection in the mantle wedge, which drives efficiently volatiles derived from the dehydration of the slab to great depth (Peacock et al., 1994). The resulting partial melting creates thickened sialitic crust at the surface (magmatic arcs), induces high grade metamorphism in the encompassing upper plate and depletes the underlying mantle in fusible elements (Bonatti and Michael, 1989; Uyeda, 1981).

Furthermore, when a significant amount of oceanic lithosphere is subducted, the strong slab pull, and potentially also the effect of dynamic mantle flow dragging on the slab may induce a backward migration of the lower plate with respect to the upper plate (rollback), which may form a backarc basin (Heuret and Lallemand, 2005; Uyeda, 1981). In such cases, extension may be associated with seafloor spreading and underlying mantle depletion as well. Note that, even if the vigorous convection within the mantle wedge may tend to homogenize its composition, a lower mantle fertility is still to be expected beneath orogen resulting from the closure of wide oceans. This assumption is supported by the depleted mantle wedge composition of the Pacific subduction compiled by Woodhead et al. (1993) and the decrease in mantle fertility with increasing distance to the arc region observed in the Lau and Mariana backarc regions (Martinez and Taylor, 2002). Therefore, the thermal and lithological architecture of orogens related to the closure of wide oceans differs much more from that of the initial margins involved compared to orogens produced by the closure of narrow oceans (Figure II.5).

4.4 Impact on the magmatic budget of subsequent extension

The difference in mantle composition resulting from the closure of narrow/ embryonic oceans versus wide oceans may dictate the magmatic budget of subsequent extensional events such as post-orogenic collapse or rifting. Indeed, the depleted mantle beneath orogens related to mature subductions may not allow for voluminous magma production, in contrast to the fertile mantle underlying orogens produced by the closure of narrow oceans. This hypothesis may account for both the a-magmatic collapse of the Norwegian Caledonides and the large amount of magmatism during the Variscan orogenic collapse. Indeed, the Norwegian Caledonides resulted essentially from the closure of the large (> 2,000 km; van Staal et al., 2012) Iapetus Ocean (McKerrow et al., 2000b). The two-sided subduction of the Iapetus ocean formed several magmatic arcs, now exposed in eastern North-America, Western Europe and Norway (Mac Niocaill et al., 1997; McKerrow et al., 2000b). The Caledonian range underwent a phase of orogenic collapse, which was essentially achieved through mechanical deformation, without significant magmatic activity north of the Elbe lineament (Andersen, 1998; Fossen et al., 2014; McClay et al., 1986; Meissner, 1999).

In contrast, the Variscides of Western Europe result from the closure of several narrow ‘oceans’ (Franke, 2006; McKerrow et al., 2000a), in addition to the suturing of the wide (> 2,000 km; Nance and Linnemann, 2008; Torsvik, 1998) Rheic Ocean (see Kröner and Romer, 2013; Matte, 2001 for reviews). Note that only the closure of the Rheic Ocean did presumably form a significant magmatic arc (Franke, 2006). The orogenic collapse of the Variscan range was accompanied by significant magmatic activity, which resulted in widespread, more or less acidic intrusions within the crust, and formed a thick mafic lower crust over most of the orogenic area (Bois et al., 1989; Costa and Rey, 1995; Petri, 2014; Rey, 1993; Schaltegger, 1997).

Alternatively, the low magmatic budget of the Caledonian orogenic collapse may be explained by the depleted composition of the mantle underlying the two continents involved, namely Laurentia and Baltica. Both are comprised of Archean cratonic cores (the North American and East European craton, respectively), which are characterized by a thick, cold and depleted lithospheric mantle (Bernstein et al., 1998; Beyer et al., 2004; Griffin et al., 2003).

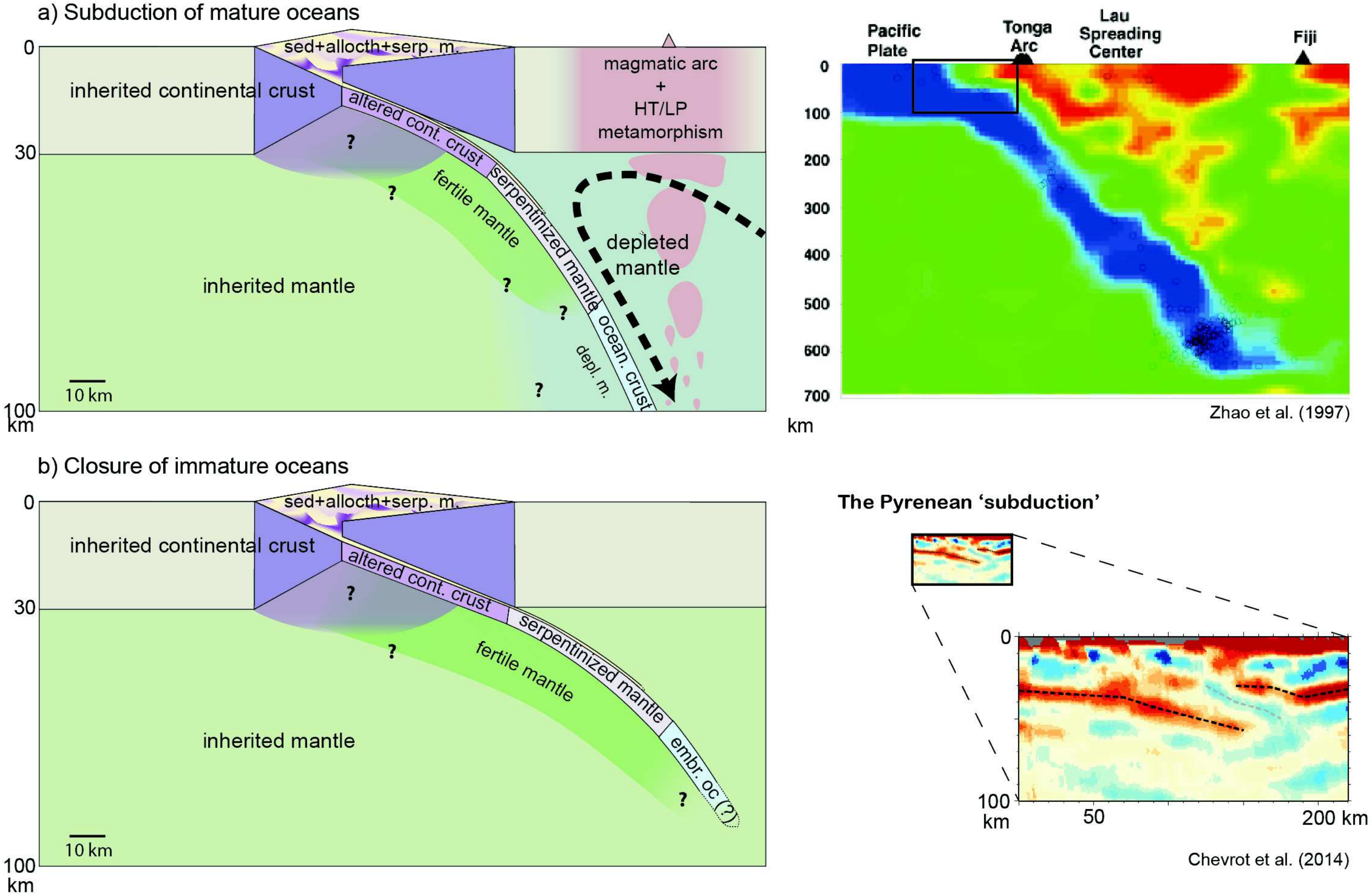

Figure II.5 – Left-hand panels: Architecture of orogens produced by the closure of (a) wide and mature oceans; (b) narrow and immature oceans. depl. m.: depleted mantle; embr. oc.: embryonic oceanic crust; HT/LP: high temperature/low pressure; oc. crust: oceanic crust; Right-hand panels: Seismic tomography across the Pacific subduction (mature ocean) after Zhao (1997) and the Pyrenean 'subduction' (immature ocean) after Chevrot et al. (2015). The inserts highlight the scale of the zone represented on the corresponding left-hand panel.

Note that the importance of the magmatic event associated with a post-orogenic collapse has direct consequences on the characteristics of the lithosphere, since it may erase all the structural inheritance in the lower crust (Bois et al., 1989; Rey, 1993), introduce major compositional and thermal heterogeneities in the upper and middle crust (Costa and Rey, 1995; Vanderhaeghe and Teyssier, 2001), and deplete significantly the underlying mantle. This inheritance is also much likely to be expressed in subsequent tectonic events, for instance influencing the localization and controlling the magmatic budget of later rifting events. In particular, this could account for the differing behaviour of the North Atlantic rift with respect to the Caledonian and Variscan orogenic lithospheres highlighted by Chenin et al. (2015). It could also explain the variability in the behaviour of the Gondwanan rifts with respect to the former orogens affecting the supercontinent (i.e. paralleling, cutting across or avoiding; see Krabbendam and Barr, 2000).

The characteristics of the narrow hyperextended rift systems and wide oceans morphology, lithology, subduction and resulting orogens are summarized in Table II.3 and Figure II.5.

5 Conclusion

In this paper, we show that the distal rift domains, as defined by Sutra et al. (2013), have specific range of width, more or less variable depending on the domain considered. However, both the width of the necking domain and of the hyperextended domain are independent from the total width of the margin (i.e. the distance from the coupling point to the lithospheric breakup point), and of the maturity of the rift system (i.e. whether or not steady-state, self-sustaining seafloor spreading is achieved).

Besides, 'narrow oceans' are usually devoid of mature spreading systems (then called 'immature') in contrast to wide, mature oceans. Therefore the main difference between these end-members is whether their margins are separated by a wide, steady-state oceanic crust. Moreover, narrow and immature 'oceans' are likely to be underlain by fertile mantle resulting from melt impregnation during the phase of hyperextension, conversely to wide and mature oceans, which have a typical mid-oceanic ridge-type, depleted mantle.

During the subduction of narrow oceans, the slab remains presumably at shallow angle (Billen, 2008; Stevenson and Turner, 1977; Tovish et al., 1978). Thus subduction is very unlikely to become self sustained (Gurnis et al., 2004; Hall et al., 2003) or to develop vigorous small-scale convection in the mantle wedge (Peacock et al.,

	Narrow, immature 'oceans'	**Wide, mature oceans**
Spatial extent	$\lesssim$ 350–400 km	$>$ 1,000 km
Oceanic crust	unsteady seafloor spreading $\Rightarrow$ heterogeneous in thickness and composition; no mantle depletion	steady-state seafloor spreading $\Rightarrow$ homogeneous in thickness and composition; depleted underlying mantle
Magmatic activity	none or very little $\Rightarrow$ no mantle depletion	moderate to large $\Rightarrow$ mantle depletion
Subduction geometry	shallow angle	shallow or deep angle
Subduction sustainability	transitory	self-sustained
Mantle wedge convection	minor	vigorous
Magmatic arc	none	yes; new over-thickened crust HT metamorphism and underlying mantle depletion
Backarc basin	none	possible; potential seafloor spreading and underlying mantle depletion
Orogen type	collisional only	accretionary and collisional
Mantle wedge composition	hydrated and fertilized with sediment	depleted in fusible elements
Post-orogenic collapse	possibly magmatic	purely extensional

Table II.3 – Summary of the characteristics of narrow versus wide extensional systems, subduction processes and orogens (see text for discussion).

1994), as opposed to subduction of wide oceans. Furthermore, subduction of narrow oceans does not produce significant magmatic activity, thus no mantle depletion, because not enough volatiles reach a sufficient depth to allow partial melting (Gaetani and Grove, 1998; Peacock, 1991; Rüpke et al., 2004). Therefore, hydration is likely to be the dominant process in the mantle wedge above such transitory subductions.

Conversely, protracted subduction associated with the closure of wide oceans develop vigorous convection in the mantle wedge, forms magmatic arcs, and is potentially associated with seafloor spreading in the backarc region (Peacock et al., 1994; Uyeda, 1981). These processes deplete the underlying mantle in fusible elements, create new crustal material and are associated with high temperature/low pressure metamorphism. As a result, orogenies resulting from the closure of narrow basins may be essentially controlled by mechanical processes, without significant compositional or thermal perturbation, and with a major influence of the inherited characteristics of the intervening margins. In contrast, orogenies consequent to the closure wide oceans may be significantly controlled by subduction-induced processes.

In addition, because of the lack of magmatic activity during the closure of narrow oceans, mantle underlying the resulting orogens may be more fertile compared to mantle underlying orogens consequent to the closure of wide oceans. This may reflect in the magmatic budget of a subsequent extensional event, such as a post-orogenic collapse or an episode of rifting.

Introduction to Chapter III

Chapter I and Chapter II demonstrate that inheritance may significantly control both rifting and orogenic events, and provide some hypotheses about the possible reasons. Based on these considerations, the next step aims to test some of these assumptions and to get some quantitative insight into the interplay between inheritance and tectonic processes.

In Chapter III, I use numerical modelling to analyze the impact of a major post-orogenic underplating on subsequent extensional events.

Chapter III

Impact of mafic underplating and mantle depletion on subsequent extension: a numerical modelling approach

Pauline Chenin[*,1,2], Luc L. Lavier[2], Gianreto Manatschal[1], Othmar Müntener [3] & Suzanne Picazo[3]

[1] CNRS - IPGS - EOST, Université de Strasbourg, 1 rue Blessig, 67084 Strasbourg, France
[2] Institute for Geophysics, J.J. Pickle Research Campus, Bldg. 196, 10100 Burnet Rd., Austin, Texas, 78758, USA
[3] Institut des sciences de la Terre (ISTE), Géopolis, CH-1015 Lausanne, Schwitzerland
[*] Corresponding author (email: chenin@unistra.fr)

Abstract

The orogenic collapse of the Variscan range in Western Europe was accompanied by a major magmatic event during the Permian, which rejuvenated a large fraction of the lower crust by mafic underplating (Costa and Rey, 1995; Petri, 2014; Rey, 1993). The potential impact of such large-scale thermal and/or lithological heterogeneities has rarely been taken into account in the study of subsequent rift systems so far.

In this paper, we investigate through numerical modelling how mafic underplating of the continental crust and/or depletion of the upper mantle beneath a former orogenic area may impact subsequent rifting. Our results suggest that both mafic underplating and mantle depletion may prevent the development of a rift at the overlying inherited weaknesses. Furthermore, the existence of a strong heterogeneity within the lower crust and/or the upper mantle may trigger the boudinage of the continental crust and induce the formation of continental ribbons with multiple rift basins. The wavelength of this necking instability depends on both the thermal state of the lithosphere and the thickness and in-depth location of the strong heterogeneity. We compare our results to the architecture and evolution of the Tethyan and North-Atlantic rift systems with respect to the underplated lithosphere of Western Europe.

1 Introduction

Orogenic processes leave pervasive and long-lasting structural and compositional heterogeneities such as suture zones, faults/shear zones and magmatic additions in both the crust and the mantle. These may behave either as weaknesses, or as strong features. For instance faults have a decreased cohesion and internal angle of friction compared to the unaltered surrounding material; suture zones are largely comprised of weak, hydrated materials (serpentine, argilites, sediments; Hall, 1976; Haynes and McQuillan, 1974); mafic intrusions may represent a thermally weakened region in the early stages of their emplacement, or a strong heterogeneity once they cool down and crystallize.

Intuitively, rifts are expected to take advantage of inherited weaknesses, thus to localize along former orogenic belts (Wilson, 1966). It is the case in northern North Atlantic, where extension followed largely the sutures or fold-and-thrust belt of the Caledonian orogen (see Figure III.1 a and c). However, the Alpine Tethys and southern North Atlantic rift systems are striking counterexamples, since both circumvented the core of the Variscan orogen to the southeast and to the west, respectively (Figure III.1 a and c; see also Chenin et al., 2015). Yet, one major characteristic of the lithosphere of the Western Europe is the existence of widespread magmatic intrusions and underplating of the continental crust, presumably consequent to the orogenic collapse of the Variscan range (Figure III.1 c and d; see Bois et al., 1989; Petri, 2014; Rey, 1993). Since these melts were most likely sourced by the partial melting of the underlying asthenospheric mantle (Costa and Rey, 1995; Gaggero et al., 2007; Petri, 2014; Schaltegger and Brack, 2007; Stahle et al., 2001), the underplated area is presumably underlain by a zone of depleted mantle (McCarthy and Müntener, 2015). In contrast, the continental margins of Norway and Greenland do not show evidence for pre-rift underplating and no significant Permian magmatic activity is recorded north of the Elbe lineament (Fossen et al., 2014; Meissner, 1999).

Through this study, we aim to investigate how magmatic underplating of the continental crust and associated upper mantle depletion may impact subsequent rifting. We design numerical models to compare the evolution of orogenic lithospheres with various distributions of crustal underplating and mantle depletion under different thermal states. We discuss the results in the light of the Tethyan and North-Atlantic rift systems, which benefit from extensive studies on both the characteristics of the orogenic lithospheres and the history of rifting.

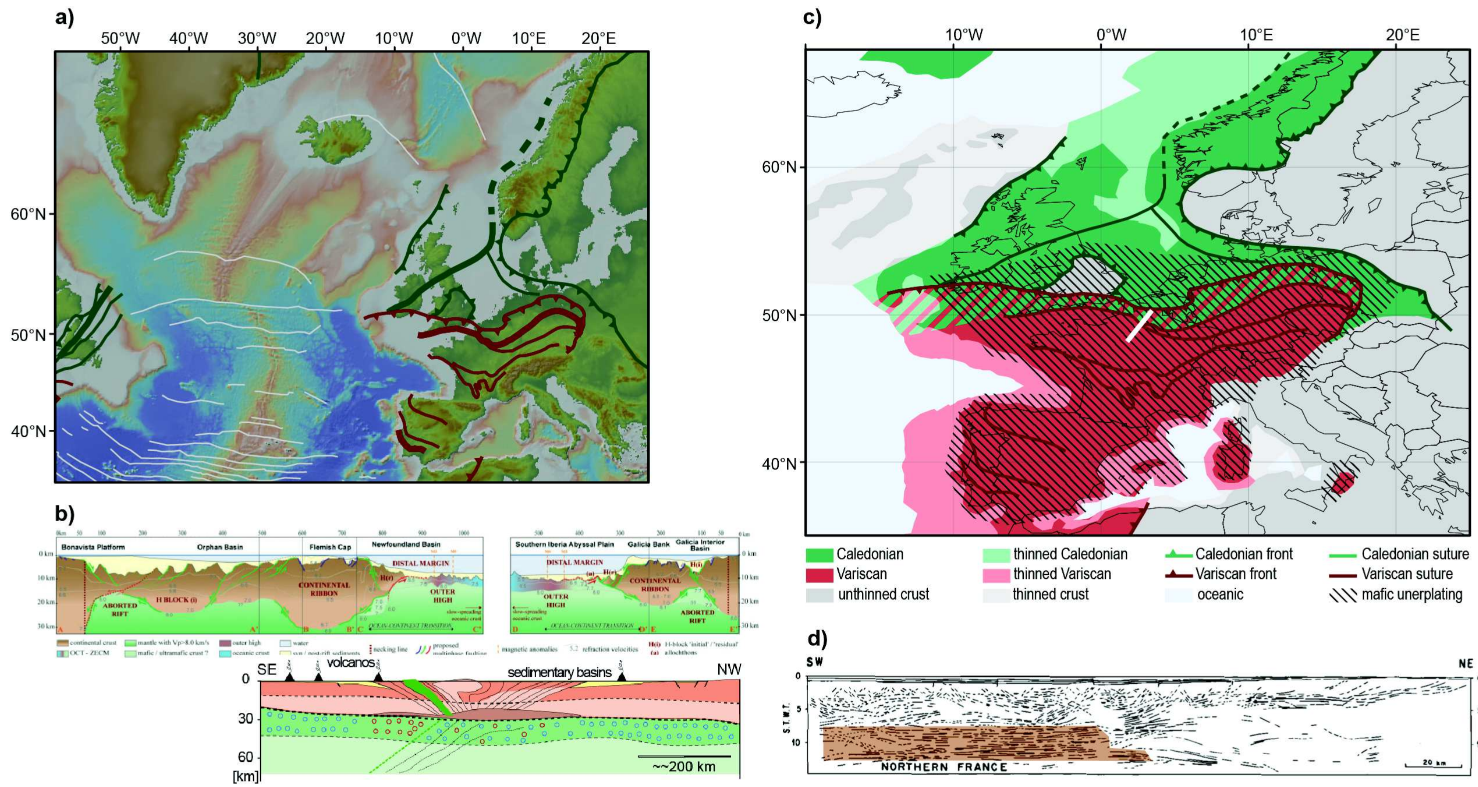

Figure III.1 – a) Map showing the distribution of the major orogenic sutures and deformation fronts from the Caledonian and Variscan orogens in the North Atlantic. b) Top: Synthetic cross-sections of the Iberia–Newfoundland margins, highlighting the Flemish Cap and Galicia Bank continental ribbons (from Péron-Pinvidic and Manatschal, 2010); Bottom: synthetic cross-section of a possible post-orogenic lithosphere after Manatschal et al. (2015). This architecture may approximate that of the Western European lithosphere prior to the onset of rifting. c) Map showing the distribution of orogenic domains, post-orogenic underplating and rift systems in Western Europe. d) Seismic section through the Variscan orogenic area (from Bois et al. (1989); see map (c) for location).

2 Geological setting

2.1 Orogenic collapse in Western Europe

Following the termination of the Palaeozoic Caledonian and Variscan orogenies, most of the resulting mountain ranges of Western Europe collapsed (Dewey, 1988; Dörr and Zulauf, 2010, and references therein). Gravitational re-equilibration of the over-thickened lithosphere was achieved through the formation of normal faults, low-angle detachments and ductile shear zones in the upper- to middle crustal levels (Andersen, 1998, and references therein), and by ductile flow of the thermally weakened lower crust at deeper levels (Rey et al., 2001).

Although this extensional event was largely devoid of magmatic activity in most of the Caledonian region (Fossen et al., 2014; Meissner, 1999), it was accompanied by widespread magmatism in most of the Variscan area of Western Europe (see Figure III.1). Indeed, late- to post-orogenic magmatism and high temperature metamorphism have been documented in Iberia, France, Southern United Kingdom, Western Alps, the Bohemian Massif, Corsica–Sardinia and the Ivrea zone in Northern Italy (Buzzi and Gaggero, 2008; Petri, 2014; Rosas et al., 2008; Schaltegger and Corfu, 1995; Timmerman et al., 2009, in prep.; Augier et al., 2015; Rossi et al., 2015; Vavra et al., 1996). Possible causes for this magmatic event include an uplift of the asthenosphere consequent to the collapse of the Variscan range (Clift et al., 2004; Dewey, 1988; Rey, 1993; Schaltegger and Corfu, 1995) and a thermal event related to the Tethyan rift (Franke, 2014).

2.2 Architecture of the post-collapse Variscan lithosphere

In the Variscan area, the uplift and partial melting of the asthenosphere resulted in rejuvenation of the lower crust by up to 10 km of mafic underplating, but most likely around 6–7 km on average (see the seismic section on Figure III.1; Bois et al., 1989; Rey, 1993) and widespread magmatic intrusions in the upper- and middle-crust (Meissner, 1999; Schaltegger and Corfu, 1995; Schuster and Stüwe, 2008). This major episode of magmatism was fed by the partial melting of the asthenosphere (Costa and Rey, 1995; Petri, 2014), thus, within the orogenic area, we can expect the shallowest part of the former asthenospheric mantle – now integrated in the lithospheric mantle because of the isostatic rebound and thermal equilibration – to be depleted compared to the surrounding lithospheric mantle. Note, however, that the thickness, location and continuity of the depleted mantle are very poorly constrained. As depleted mantle beneath mid-oceanic ridges exists down to depth of 50–200 km

(Anderson, 2006), we regard the depleted mantle source of the underplating as a continuous, 40 km thick layer, with a similar horizontal extent as underplating. These values may be largely underestimated, but provide a lower end-member for our study.

By Permian time, the thick (> 50–60 km) Variscan crust was most likely thinned to about 30–35 km across Western Europe and the lithosphere was thermally and isostatically equilibrated by Late Triassic (Franke, 2006, and references therein). Therefore, on a first-order, the architecture of the Variscan lithosphere can be regarded as the right panel on Figure III.2.

However, the thermal state may have been much higher in the Variscan orogenic area than in the Caledonian area at the onset of *necking* (see Sutra et al. (2013) for a definition of *necking*) during the Jurassic (Doré et al., 1999; Roberts et al., 1999; Ziegler, 1988), with Moho temperature $\sim$ 500–600°C versus 350–500°C, respectively (Čermák and Bodri, 1986; Müntener et al., 2000).

2.3 The Alpine Tethys and North Atlantic rift systems

During the Jurassic, about 100 Myr after the termination of the Variscan orogeny, the orogenic lithosphere of Western Europe started to undergo significant thinning related to the rifting of the Alpine Tethys and North Atlantic oceans (Doré et al., 1999; Roberts et al., 1999; Ziegler, 1988). Although the rift largely followed – at least temporarily – the Caledonian orogenic sutures and/or former fold-an-thrust belts in the northern North Atlantic (Erratt et al., 1999; Williamson et al., 2002; Wilson, 1966), most of the Variscan orogenic structures of Western Europe were only little, if ever, affected. Indeed, the Jurassic Alpine Tethys and the Late Jurassic–Early Cretaceous North Atlantic rift systems developed at the southern and western edges of the underplated orogenic lithosphere, respectively (see Figure III.1; Frizon de Lamotte et al., 2011).

Besides, Chenin et al. (2015) highlighted that rifting in the northern North Atlantic was protracted, polyphase and formed several 'failed' *hyperextended* rift basins (see Doré and Lundin, 2015; Sutra et al., 2013 for a definition of *hyperextended*) separated by continental ribbons (e.g. the Porcupine Basin, Rockall Trough, Hatton Basin offshore United Kingdom; see Doré et al., 1999; Roberts et al., 1999). In contrast, rifting was relatively short in the southern part of the North Atlantic (see Chenin et al., 2015).

3 Numerical modeling study

This study aims to investigate, under various thermal states, how the first-order remnants inherited from a magmatic collapse may impact subsequent rifting. In particular, we use the thermo-mechanical numerical code FLAC to test the effect of a 10 km thick basaltic layer underlain by a 40 km thick zone of depleted mantle beneath a quartzite crust containing weak heterogeneities (see section 2.2).

3.1 The thermo-mechanical code FLAC

For each numerical time step, the modeling involves direct solution of the equation of motion for every grid point including the effects of inertia:

$$\frac{\partial \sigma_{ij}}{\partial x_j} - \rho g_i = \frac{\rho \partial v_i}{\partial t} \tag{III.1}$$

where v_i is the velocity at each grid point, g_i is the acceleration due to gravity, ρ is the mass density and σ_{ij} is the stress in each grid element. In order to approximate quasi-static processes, the effects of inertia must be damped in a way akin to oscillations in a damped oscillator. Starting from a non-equilibrium state, the forces present at each grid point are summed ($f_i = \rho \delta v_i / \delta t$). The corresponding out-of-balance forces and the mass at the grid point give rise to acceleration. The accelerations are integrated to calculate the new velocities that are used to determine the incremental strain, ϵ_{ij} at each grid point. During a single time step, finite rotations also change the stress tensor, which is defined with respect to a fixed frame of reference. Before the incremental strains are determined, the stress tensor is updated to take these rotations into consideration as follows.

$$\sigma_{ij}^{\mathrm{new}} = \sigma_{ij}^{\mathrm{old}} + \left(\omega_{ik}\sigma_{kj} - \sigma_{ik}\omega_{kj}\right)\Delta t \tag{III.2}$$

where Δt is the time step and ω_{ij}, the rotation per unit time, is given in terms of the velocity derivatives by

$$\omega_{ij} = \frac{1}{2}\left(\frac{\partial v_i}{\partial x_j} - \frac{\partial v_j}{\partial x_i}\right) \tag{III.3}$$

By using the constitutive law for elastic, viscous and plastic rheologies the corresponding stress increments are determined from the strain increments, and the forces that they produce on the surrounding grid points are summed to determine the new out-of-balance forces and velocities. This dynamic response is then damped to approach a quasi-static equilibrium. FLAC is a very powerful technique for simulating non-linear rheological behavior at relatively high resolution (the grid size is 1 km) because the explicit time-marching scheme does not require the storage of the large matrices that are needed for implicit methods. The time step of the calculation scales with the elastic-plastic property of our model. If the problem is purely elastic, the time step of the dynamic response scales with the velocity of the elastic wave propagating through the elements. This time step is of the order of a few hundredths of a second. Therefore, the resolution of the domains studied and the timescale needed for our numerical experiments would yield very long run times. In order to decrease the CPU time needed to perform the numerical experiments, we increase the speed of calculation by setting the boundary displacement per time step to a fraction of the grid spacing. To set the boundary displacement, we choose a ratio of boundary velocity to sound velocity of 10^{-6}–10^{-5}. We find that this ratio allows for fast enough runs and at the same time minimizes the error in the strain calculation.

To model the viscous part of the lithosphere, we use the Maxwell viscoelastic constitutive equations relating the deviatoric stress tensor σ_{ij} to the deviatoric strain ϵ_{ii^*}:

$$\frac{\partial \sigma_{ij}}{\partial t} = \frac{E \partial \epsilon_{ij}}{\partial t} - \frac{\sigma \sigma_{ij}}{\tau_M} \qquad \text{(III.4)}$$

where E is Young's modulus and τ_M is the Maxwell time defined as $\tau_M = 2\eta/E$, with η being the effective viscosity defined as:

$$\eta = A^{-1/n} \left(\dot{\epsilon}^{\mathrm{II}}\right)^{-\left(1+\frac{1}{n}\right)} e^{\frac{Q}{nRT}} \qquad \text{(III.5)}$$

where A is the creep law pre-exponent, Q the activation energy, $\dot{\epsilon}^{\mathrm{II}}$ the square root of the second invariant of the strain rate, n the creep law exponent, R the gas constant and T the temperature.

The brittle part of the lithosphere is modeled as an elastoplastic material with a Mohr-Coulomb yield criterion. When the criterion is met the material flows according to non-associative plasticity. This formulation simulates the formation of faults as plastic shear zones.

We model the evolution of the temperature as the model material deforms by using a Lagrangian formulation. We use an explicit finite difference method as used in FLAC. Each time step the flow of heat through each element is calculated using Fourier's law. The corresponding energy is then summed and the temperature is calculated at each grid points using the energy equation:

$$\rho C_p \frac{\partial T}{\partial t} = (k\nabla^2 T) + H \tag{III.6}$$

where T is the temperature, ρ is the density of the material, C_p is specific heat, k is the thermal conductivity tensor, and H is the heat production per unit volume.

The initial mesh of the model is made of quadrilaterals subdivided into two pairs of superimposed constant-strain triangular zones. The use of triangular zones eliminates the problem of "hourglassing" deformation sometimes experienced in finite differences. Since this method is Lagrangian (i.e., the numerical grid follows the deformations), the simulation of large deformation (locally more than 50%) involves re-meshing to overcome the problem of degradation of numerical precision when elements are distorted. We trigger remeshing when one of the triangles in the grid elements is distorted enough that one of its angles becomes smaller than a given value. Every time re-meshing occurs, strains at each grid point are interpolated between the old deformed mesh and the new undeformed mesh using the barycentric coordinates of the nodes and Gauss points of the new elements in the old deformed mesh. The new state of strain is then used with the rheological laws to calculate the stress and resulting out-of-balance forces to start the time step cycle again. Also every time we re-mesh, errors in the interpolation of the state variables result in an increase in the out-of-balance force, and artificial accelerations and oscillations may occur. For this reason the solution may not be in equilibrium immediately after re-meshing. We have tested different criteria to trigger remeshing in order to reduce the oscillations and chose to use a minimum angle of 15° before re-meshing of the grid.

To guarantee that the boundary between the different physical phases in the model (i.e, quartz, plagioclase, olivine) do not diffuse at the time of remeshing we use particles distributed in the grid elements. These particles have both Eulerian and Lagrangian coordinates attached to the elements. When remeshing occurs their Eulerian and barycentric (Lagrangian) coordinates and their physical properties are registered in the old grid. When the new regular grid is formed the Eulerian coordinate of the particles are used to calculate the new barycentric coordinates of the particles in the new grid elements. Then the physical properties are then properly assigned with no spatial diffusion. These particles are also used to track the pressure, strain and temperature history of the different phased through the deformation history. New particles are added or destroyed when needed (i.e. when few particles populate one given grid element or when a particle falls out of the new mesh boundaries after remeshing). Similar remeshing techniques have been developped in previous work showing the efficiency of this method (Babeyko and Sobolev, 2008; Burov and Yamato, 2008; Popov and Sobolev, 2008).

3.2 Model design

The model consists in a 400 km wide per 250 km deep domain (Figure III.2). The horizontal spatial resolution is 1 km and the vertical resolution is 750 m between 0 and 120 km depth, 1 km between 120 and 160 km and 1.8 km between 160 and 250 km. The 30 km thick continental crust is made of dry quartzite (see Table III.1 for the physical parameters corresponding to each material). The lithospheric and asthenospheric mantles are made of olivine with a rheology intermediate between the dry and wet end-members described by Hirth and Kohlstedt (1996), in order to approximate the behavior of an average, relatively fertile mantle. Note that our aim is to investigate the impact of rheological contrasts using plausible rheologies (Figure III.3), rather than to model an actual inherited mantle flow law, which would require additional constrains from field and geochemical studies. The base of the lithosphere corresponds to the 1,300°C isotherm and varies from 115 to 85 km depending on the models, in order to compare the effect of different relaxation time between the orogenic event and the onset of rifting (Artemieva et al., 2006, and references therein). The initial geothermal gradient within the asthenosphere is 0.4°C/km (Hofmeister, 1999; Yamazaki and Karato, 2001) and the basal heat flow is fixed to 12 mW.m^{-2} throughout the experiment.

The underplated material is 10 km thick and has a basalt rheology. The underlying depleted mantle extends down to a depth of 70 km, has a dry olivine rheology, which is stronger than that of the 'standard' mantle (see parameters in Table III.1). The density of the depleted mantle is slightly less than the 'standard' mantle (3,200 kg.m^{-3} v.s. 3,300 kg.m^{-3}, respectively; Picazo et al., in prep).

As orogenic sutures are usually imaged as steep structures, the one in our models is designed as a line dipping at 60°. It follows the antigorite flow law from Amiguet et al. (2014), which represents one of the weakest phases (serpentine) existing in a suture zone. This suture zone crosscuts the whole crust in the reference model devoid of underplating, while it terminates at the top of the basaltic layer in the others, as observed in the Variscan area (see Figure III.1). The other 'faults' represent the thin-skinned orogenic inherited structures(i.e. the fold-and-thrust belt), which extends down to the ductile middle-crust (10 km). These 'faults' have the same rheology as the crust except from their reduced cohesion and angle of friction (Table III.1).

They dip at 30°, which is the value predicted by the Mohr-Coulomb theory for thrust faults. To model fault offset (Lavier et al., 2000), all materials undergo a strain softening process decreasing both their cohesion and internal angle of friction from C_1 to C_2 and from ϕ_1 to ϕ_2 (see Table III.1) until accumulated strain reaches 10%, after which they remains at C_2 and ϕ_2, respectively.

Our reference model (Model 1) has a Moho temperature of 450°C, one suture zone and three faults, but is devoid of both basaltic lower crust and depleted mantle (Figure III.2, left panel). Such a model may represent the first-order architecture of an orogenic lithosphere after an a-magmatic collapse, for instance the Caledonides.

We consider a first series of models (Models 2 to 5) with a similar lithological architecture (Figure III.2, right panel) but different thermal states (Figure III.3). In Models 2 to 4, the lithosphere is initially thermally equilibrated and the temperature of the Moho ranges from 400°C (115 km thick lithosphere, Model 2), to 450°C (100 km thick lithosphere, Model 3) and to 500°C (85 km thick lithosphere, Model 4). These models represent cases where the time lag between the magmatic event and the onset of rifting was sufficient for temperature to to be horizontally re-equilibrated, i.e. $>$ 100 m.y. (Jaupart and Mareschal, 2007).

We also investigate the case when rifting starts over a young lithosphere that has not fully thermally recovered from the magmatic event. For this, we designed Model 5 with an initial Moho at 500°C and the mafic lower crust and underlying depleted mantle are 300°C hotter than the encompassing material.

In the second series of models (Models 2 and 6 to 8), we consider different distributions of crustal and mantle heterogeneities under the same thermal state (Moho 450°C). We compare a model with both crustal underplating and depleted mantle (Model 2) with models with only crustal underplating (Model 6) or only depleted mantle (Model 7). Note that the architecture of Model 7 is presumably common for lithosphere, since the upper mantle is most likely highly heterogeneous (Anderson, 2006, and references therein). For instance, zones of depleted mantle may result from local magmatic events such as volcanic arcs, backarc basins, seamounts, or may they be remnants of a slabs after their break-off.

Because melt extraction from the mantle is likely to be focused to form mafic bodies (Holtzman et al., 2003), mafic underplating may be discontinuous but the deepest underlying mantle is likely to be quite continuously depleted. This is likely to be the first-order architecture of the Variscan lithosphere after its magma-rich orogenic collapse (Petri, 2014; in prep.). Therefore, in Model 8 we investigate the

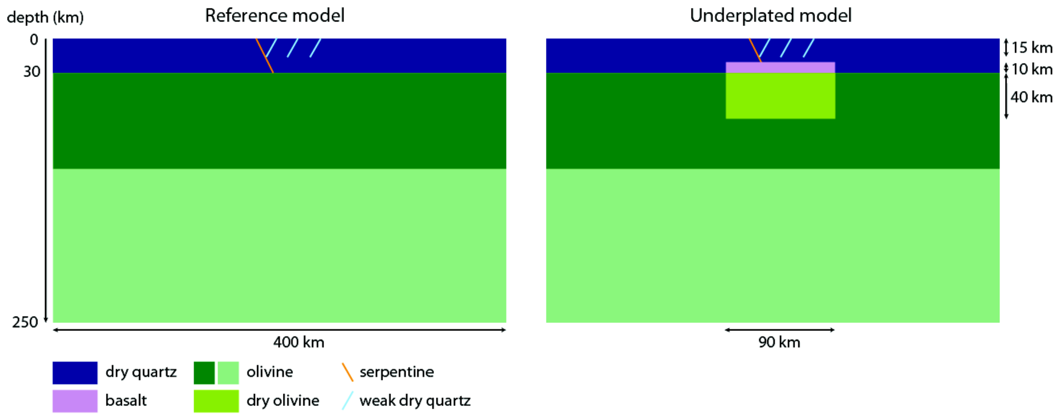

Figure III.2 – Architecture of the reference model (left) and underplated models (right). The base of the lithosphere (ldark green/light green limit) is only a thermal limit, corresponding to the isotherm 1300°C. Its depth varies between 115 km in the model with a Moho at 400°C and 85 km when the Moho is 500°C.

effect of a discontinuous mafic body at the base of the crust underlaid by a continuous depleted mantle.

Note that neither the generation and migration of melts, nor the effect of erosion or sedimentation are modeled in our experiments. Furthermore, each rheological phase is modelled as a homogeneous material with averaged physical properties, which is obviously not geologically realistic. Therefore the absolutes values for basins depth and width, and the timing of rifting should be considered with care and analyzed only by comparison between models.

4 Results

4.1 Reference model

In the reference model without underplating (Model 1 in Figures III.4, III.5 and III.6), the suture zone and the two first adjacent faults are reactivated as soon as extension starts. As a result, a so called ‘H block’ (Lavier and Manatschal, 2006) forms between the suture and the first adjacent fault, and another undeformed block (also referred to as a ‘H block’) is preserved between the two synthetic faults. Both subside as extension progresses, which creates a wide and relatively deep (5 km) basin within the former orogenic area. After 5–6 Myr extension, the crust has been thinned down to about 15 km in both basins. The suture is then abandoned, while deformation remains localized at the two faults. This marks the onset of the so-called ‘thinning phase’, which determines the location of the subsequent breakup.

Layer	Material	ρ (kg.m^{-3})	k (W.m^{-1}.°C)	A (s^{-1}.Mpa^{-n})	n	Q (kJ.mol^{-1})	ϕ_1, ϕ_2 (°)	C_1, C_2 (GPa)
Crust	Quartz	2800	2.2	500	3	300	30, 15	40, 4
Faults	Quartz	2800	2.2	500	3	300	15	4
Suture	Serpentine	2400	3.3	3.98.10e^{-13}	2	27	30, 1	4
Underplating	Basalt	2900	2.2	0.125	3	376	30, 15	40, 4
Mantle	Olivine	3300	3.3	485	3.5	518	30, 15	40, 4
Depl. mantle	Dry olivine	3200	3.3	48.5	3.1	520	30, 15	40, 4

Table III.1 – Material and thermal properties

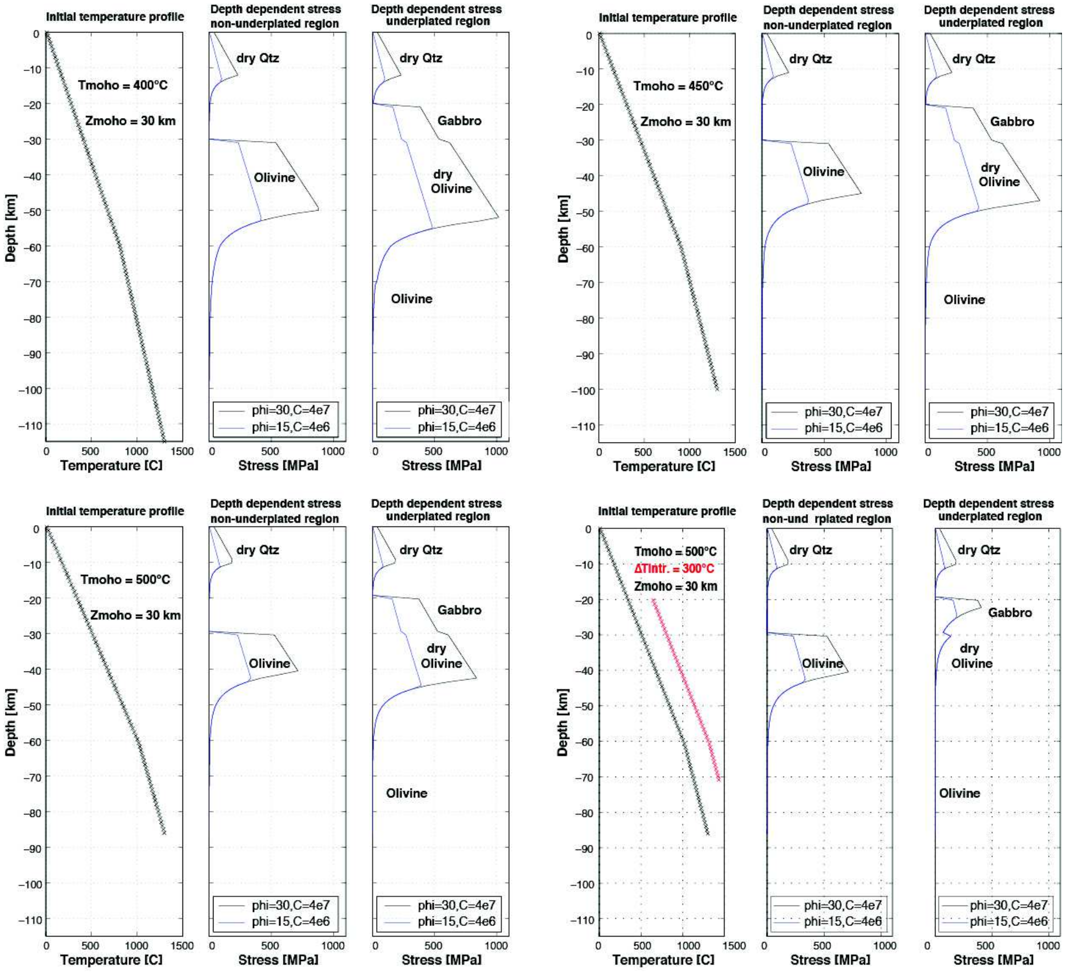

Figure III.3 – Geotherm (left panel) and Depth-dependent stress profile corresponding to the non-underplated (middle panel) and underplated region (right panel) of each model; *phi* refers to the internal angle of friction and C to the cohesion of the materials. All depth-dependent stress profiles are for a reference strain rate of $10^{-15}.s^{-1}$

Thus, in this model, breakup is achieved within the orogenic area, but away from the suture zone.

In the lithospheric mantle deformation remains localized at two shear zones extending from the active crustal shear zones below the orogenic area, while extension is very diffuse in the asthenosphere. Subcontinental lithospheric mantle is exhumed at the seafloor at $\sim$ 11 Myr and 'breakup' (i.e. in our models, when the initial base of the lithosphere reaches the seafloor) is achieved after 13.5 Myr (i.e. 135 km extension). The resulting margins are slightly asymmetric due to the asymmetric distribution of the inherited weaknesses: the left-one is about 130 km wide, while the right one is about 80 km wide.

It is interesting to note that, although the 'suture' has the weakest rheology, it doesn't become the locus of the eventual breakup. Indeed, breakup occurs within the adjacent 'fold-and-thrust belt'. The reason for this is that the extension of the crust is initially accommodated by the suture and the second adjacent conjugate 'fault', which induces the uplift of the underlying asthenosphere between these two structures (see Model 1 in Figures III.4, and III.6). From the moment the rising of the asthenosphere becomes an active upwelling because of its lower density, it controls the location of extension. Note that this configuration of rifting within the fold-and-thrust belt can be compared to the actual location of the North Atlantic rift with respect to the Norwegian–Greenland Caledonides (see Figure III.1).

4.2 Impact of the thermal state

4.2.1 Model results

In Model 2 (Moho at 400°C), the suture zone and the two adjacent faults are initially reactivated and extend down to the uppermost lithospheric mantle, forming a 50 km wide and 1 km deep basin within the orogenic area (Figures III.4, III.5 and III.6). However, these shear zones are abandoned after only 1.5 Myr, while deformation localizes along a pair of conjugate crustal-scale shear zones to the left of the underplated area. Extension remains focused on these shear zones, forming two 'H block'. Deformation in the mantle is focused on the downward continuation of theses faults. As a result, the upwelling of the asthenospheric mantle is very focused and 'breakup' is achieved after only 15 Myr extension, following a very short period of subcontinental lithospheric mantle exhumation ($<$ 2 Myrs).

When the geotherm is higher with a with Moho at 450°C (Model 3 in Figures III.4, III.5 and III.6), the orogenic structures are not significantly reactivated and one set of conjugate shear zones rooted in the uppermost lithospheric mantle

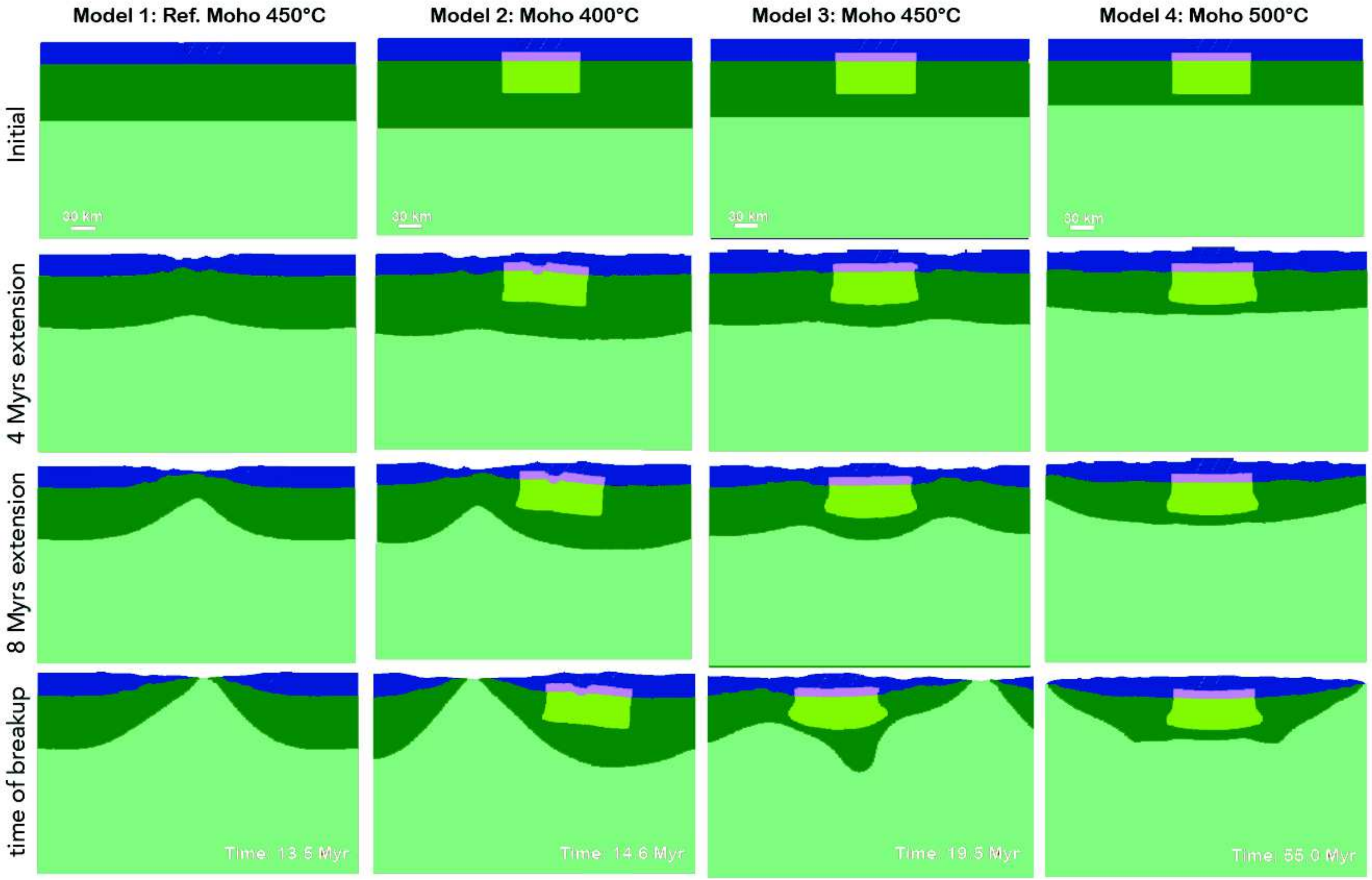

Figure III.4 – Results of the numerical models 1–4 showing the evolution of the rheological phases.

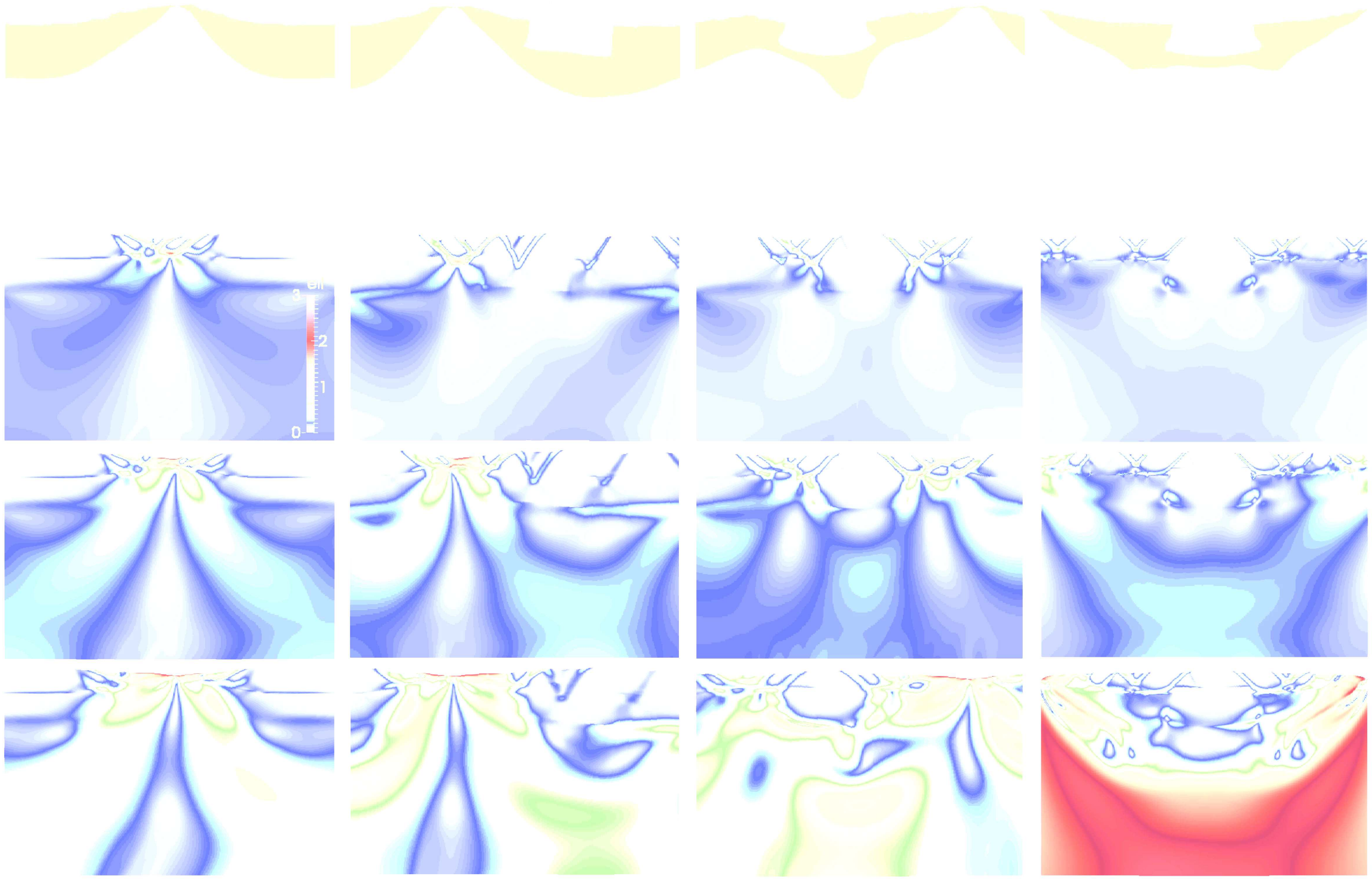

Figure III.5 – Results of the numerical models 1–4 showing phases distribution at the time of 'breakup' and the second invariant of strain at several time steps.

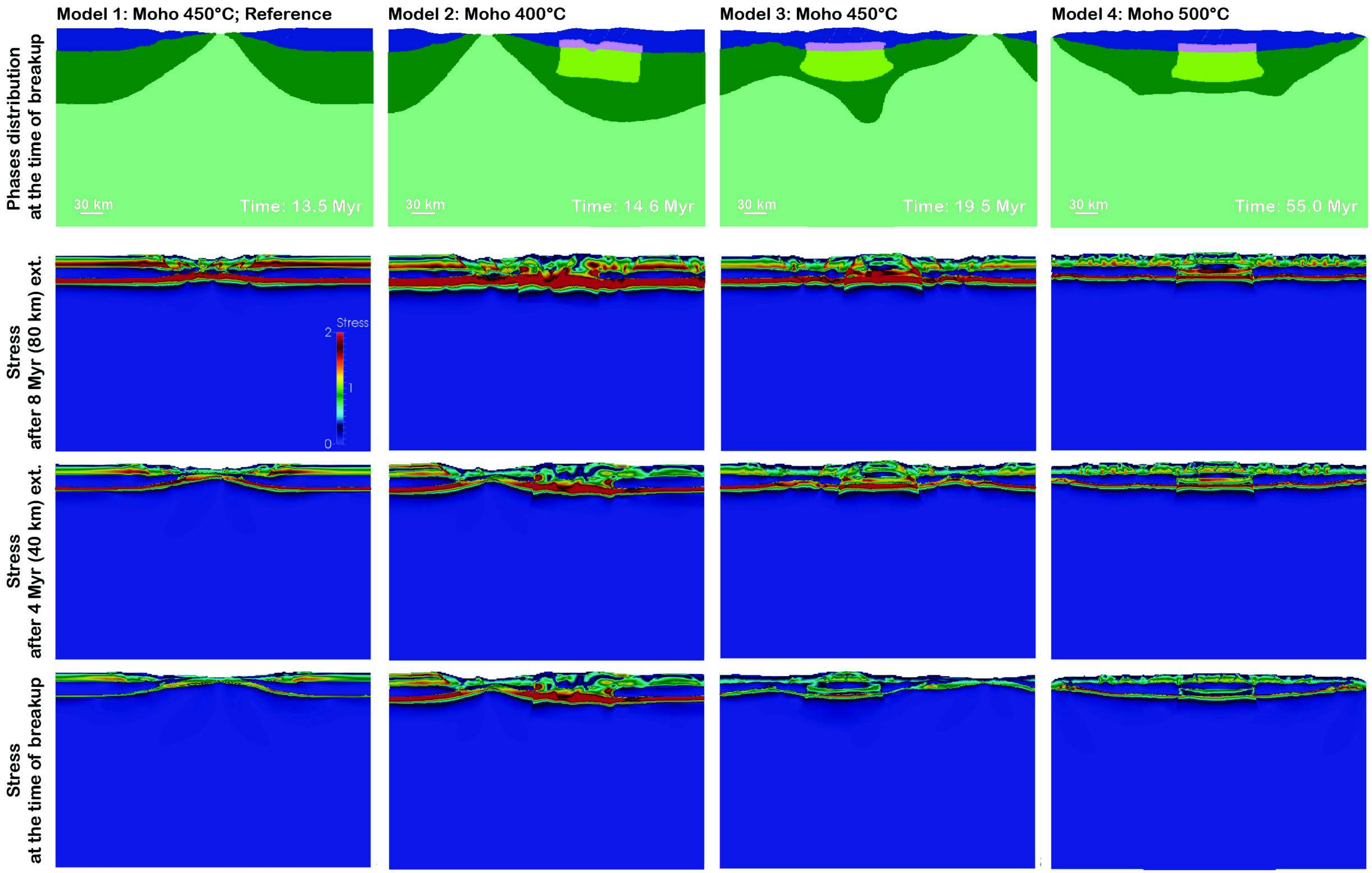

Figure III.6 – Results of the numerical models 1–4 showing phases distribution at the time of 'breakup' and stress intensity at several time steps.

and associated 'H blocks' develop on each side of the underplated area, forming two basins more than 100 km wide. In contrast, the underplated region remains un-thinned, and the underlying lithospheric mantle is even thickened as it starts to dive in the asthenosphere. As a result, the orogenic region is uplifted by about 2 km with respect to the initial base level. After about 12 Myr, the left-hand side basin is abandoned (continental crust is about 15 km thick), while extension localizes on the right-hand side set of shear zones, marking the onset of the thinning phase. 'Breakup' is achieved after approximately 18 Myr after a short period of mantle exhumation ($<$ 3 Myrs). The margins are much wider than in Model 2, and the underplated region may be regarded as a 'continental ribbon' of un-thinned crust separated by two necked domains.

When the thermal state is relatively hot with a with Moho at 500°C (Model 4 in Figures III.4, III.5 and III.6), neither of the orogenic structures are reactivated and two antithetic shear zones rooted at the crust-mantle boundary and associated 'H blocks' form at the edges of the underplated area. A couple of Myr later, these shear zones are abandoned, while two sets of conjugate shear zones rooted in the lower crust form further on each side of the first shear zone with a relatively regular spacing of about 40–50 km. Note that this consistent spacing suggests a 'boudinage' of the crust triggered by a periodic necking instability (Fletcher and Hallet, 1983; Zuber et al., 1986) As a result, several shallow rift basins form synchronously on each side of the orogenic area. The two basins adjacent to the orogenic area are abandoned relatively early (before 5 Myr), while deformation keeps delocalizing outboard from the two more distal basins until focusing at the edges of the model. Conversely, the underplated area remains undeformed, and is uplifted by 2 km with respect to its initial level.

In contrast, when the underplated area and underlying depleted mantle are hotter by 300°C than the encompassing lithosphere (Model 5 in Figures III.7, III.8 and III.9), the inherited structures are immediately reactivated, and keep localizing deformation until the eventual breakup. Extension is accommodated by ductile flow/pure shear in the underlying mafic crust and depleted mantle, and both are thinned, uplifted and eventually exhumed at the seafloor less than 2 Myr before the 'breakup' at about 17 Myr. Note that the mafic crust is more intensely thinned below each inherited weakness, suggesting that at least part of the stress is transmitted from top to base. The final margins are about 110 km and 130 km wide, with the necking points above the edges of the underplated domain.

4.2.2 Summary

In all the models with a thermally equilibrated lithosphere (Models 2, 3 and 4), 'breakup' occurs outside the underplated region, despite the existing weaknesses in the overlying upper crust (Figure III.4). These are barely, or even not reactivated at all, and both the crust and the lithosphere remains un-thinned in the underplated region. In contrast, one or more zones of necking develop on each side and form more or less well-developed rift basins, one of which eventually becomes the locus of thinning, mantle exhumation and eventually 'breakup'. As a result, the underplated region forms a plateau of un- or little thinned continental crust between two necking zones. This process is more obvious when the initial geotherms are higher (here 450°C and 500°C; see in Figures III.5 and III.6).

The contemporaneous development of two (or more) necking zones result presumably from a periodic 'necking instability' as defined by Fletcher and Hallet (1983), triggered by the existence of a strong heterogeneity within a relatively hot lithosphere. Note, however, that we were not able to determine how far away from the underplated region the rift would spontaneously localize if the lithosphere was of infinite length, since even when we increased the model width to 1,000 km, the necking occurs at one or both model edges. This is due to the fact that the model tends to localize close to the boundary where the extension velocity are applied.

In contrast to the initially thermally equilibrated models, rift localizes at the inherited weaknesses underlain by anomalously hot heterogeneities (Model 5 in Figure III.7) and the mafic and depleted mantle are exhumed at the seafloor.

4.3 Impact of the rheological composition

4.3.1 Model results

In the model with a mafic lower crust but no depleted mantle (Model 6 in Figures III.7, III.8 and III.9), the inherited structures are not reactivated, but sets of conjugate shear zones and associated 'H blocks' develop between 20 and 100 km away of each edge of the underplated region. The continental crust is thinned down to about 15 km in the two resulting basins (about 3 km deep), until deformation ceases in the left-hand basin and localizes on the right-hand, marking the onset of the thinning phase. The uplift of the asthenospheric mantle is relatively fast and focused, resulting in 'breakup' after 16 Myr extension, that is less than 3 Myr after subcontinental mantle is exhumed at the seafloor. Note that, in this model as in the comparable model with depleted mantle (Model 3), the lithosphere underlying the orogenic area is thickened as it starts to subside within the asthenosphere.

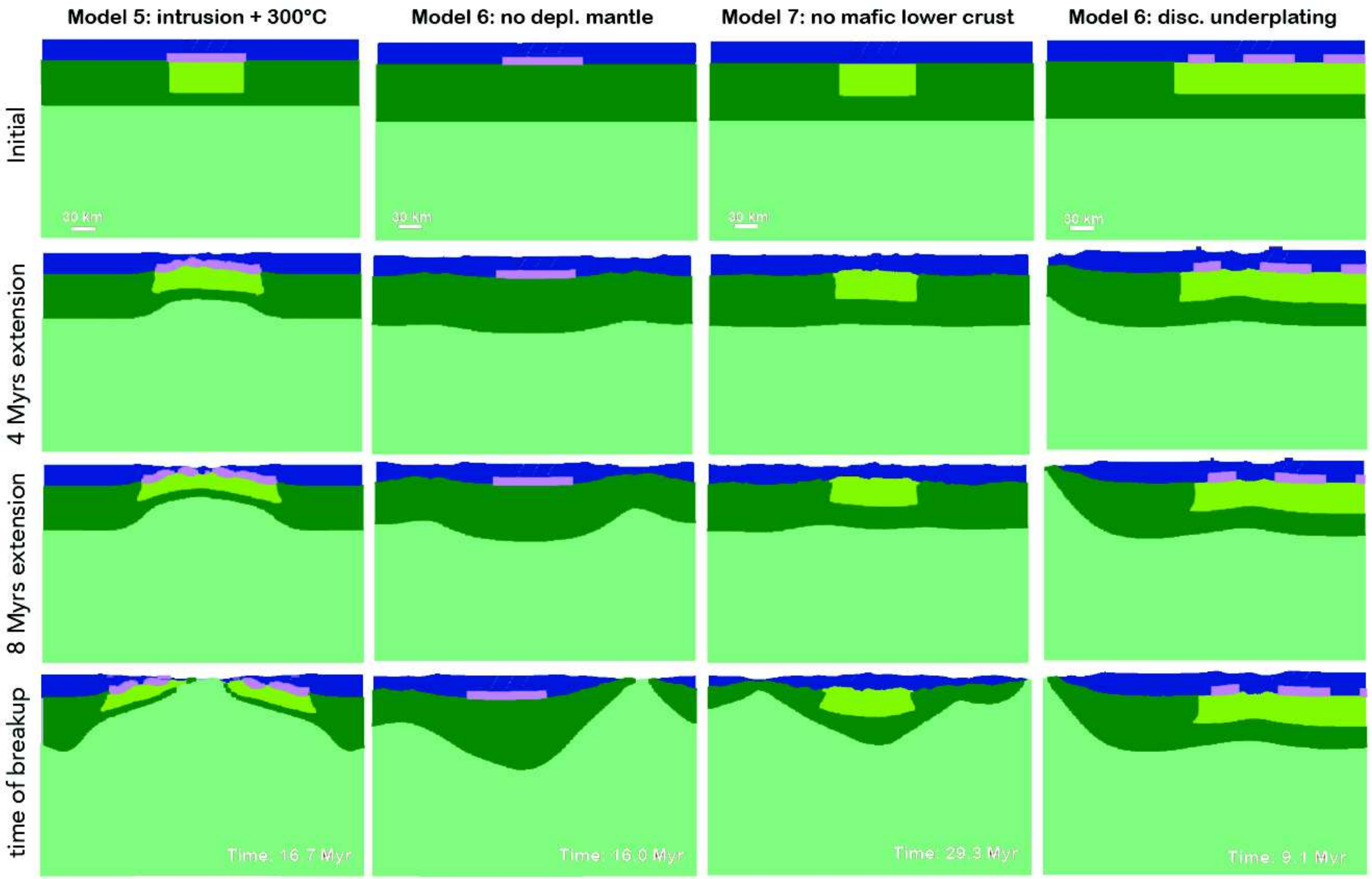

Figure III.7 – Results of the numerical models 5–8 showing the evolution of the rheological phases. depl. m.: depleted mantle; disc. underpl.: discontinuous underplating.

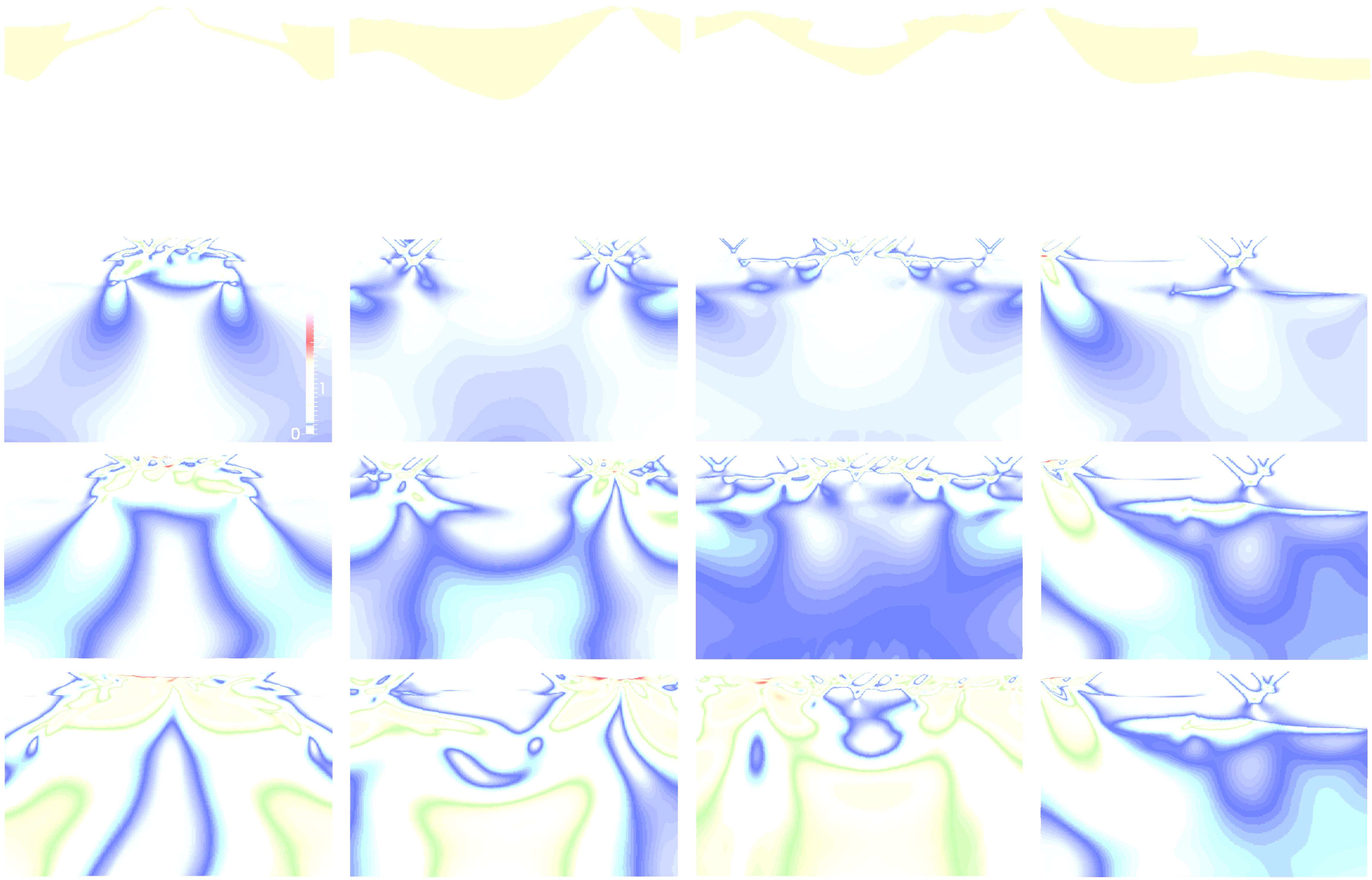

Figure III.8 – Results of the numerical models 5–8 showing phases distribution at the time of 'breakup' and the second invariant of strain at several time steps. depl. m.: depleted mantle; disc. underpl.: discontinuous underplating.

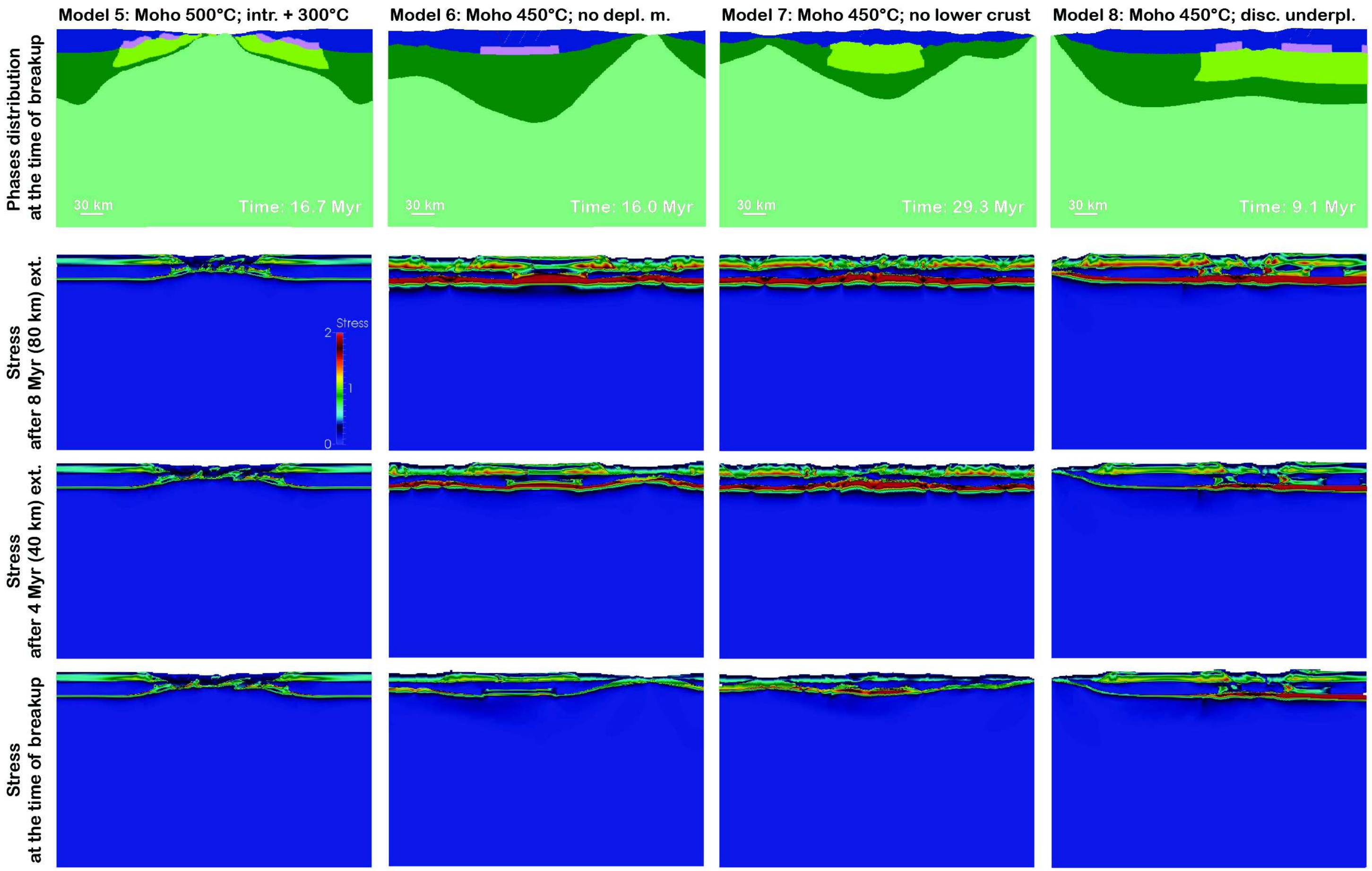

Figure III.9 – Results of the numerical models 5–8 showing phases distribution at the time of 'breakup' and stress intensity at several time steps; depl. m.: depleted mantle. disc. underpl.: discontinuous underplating.

In the model with only depleted mantle (Model 7 in Figures III.7, III.8 and III.9), the inherited weaknesses are initially reactivated and extension is accommodated by a decollement at the crust-mantle boundary and by several small, relatively regularly spaced conjugate shear zones in the uppermost mantle. At about 3 Myr a new set of crustal-scale conjugate shear zones and associated 'H blocks' form about 90 km away from each edge of the underplated area. Deformation remains relatively diffuse, migrating progressively outboard and affecting most of the crust, except in the very center of the underplated area. Thinning of the crust remains very distributed and irregular until extension localizes at the right-hand edge of the model, after about 25 Myr. 'Breakup' is achieved there after 29.5 Myr. Note that, compared to the similar model with only a mafic lower crust (Model 6 in Figures III.8 and III.9), the continental plateau is thinner, lower, and the underlying mantle not thickened as much. In addition, the margin is wider, the aborted rift basin deeper and further from the underplated area, and the lithospheric breakup is achieved much later.

In the model with a discontinuous mafic underplating (Model 8 in Figures III.7, III.8 and III.9), the inherited weaknesses are initially reactivated, forming a 80 km wide and up to 6 km deep, aborted rift basin. However, less than 1 Myr after the onset of extension, another shear zone forms at the left-hand edge of the model, about 120 km away from the underplated region. It localizes rapidly the deformation, as a result, the basin within the orogenic area is abandoned and a very fast and focused asthenospheric upwelling results in 'breakup' after only about 9 Myr extension.

4.3.2 Summary

This series of models with a Moho at 450°C show that areas bearing a mafic lower crust remains un-thinned (Model 3 in Figure III.4 and Models 6, 7 and 8 in Figure III.7), whereas weaknesses located above only depleted mantle undergo some thinning, even if they never become the locus of the eventual 'breakup' (Models 7 and 8). Note that the distance between the necking zones and the edge of the underplated area depends on both the nature/thickness of underplating, as well as on its width (compare Models 3, 6, 7 and 8). Indeed, the necking instabilities develop right above the edges of the underplated region when both a mafic crust and depleted mantle exist (Model 3), 20 km away in Model 6 with only a mafic lower crust, 90 km away when there is only depleted mantle (Model 7), and more than 120 km away when the underplated region is 240 km wide (Model 8).

Besides, deformation remains delocalized much longer when there is only depleted mantle (at least until 26 Myr, while 'breakup' is achieved at about 30 Myr; see Model 7) than in models with a mafic lower crust (until $\sim$ 15 Myr, while 'breakup' at 19.5 Myr in Model 3; until $\sim$ 11 Myr while 'breakup' at 16 Myr in Model 6; and until $\sim$ 4 Myr while 'breakup' at 9 Myr in Model 8). As a result, the margins are much wider and the failed rift basins more numerous.

5 Discussion

5.1 Cooled underplating: a barrier to rifting?

Models 2–4 and 6–8 suggest that, within a thermally equilibrated lithosphere, the existence of a mafic lower crust and associated depleted mantle underneath an orogenic area prevents the reactivation of preexisting weaknesses during an episode of extension. Consequently, rifting and breakup localize away from the former orogenic area, as opposed to what is predicted by the theory of the Wilson Cycle.

This hypothesis may explain why both the Tethyan and southern North Atlantic rift systems circumvented the underplated Variscan lithosphere (Frizon de Lamotte et al., 2011), while the northern North Atlantic rift reactivated the Caledonian Iapetus and Tornquist sutures in regions devoid of significant post-orogenic magmatism (Erratt et al., 1999; Wilson, 1966; see Figure III.1 a and c, and Chenin et al., 2015 for a synthesis). In addition, both the development of the Porcupine basin offshore United Kingdom and of the Central Trough in the North Sea seem to stop close to the edges of the Variscan underplated region (Figure 2 c), supporting the hypothesis that underplating may act as a barrier to future rifting.

It may also explain why, in the Basin and Range province of western United States, present-day extension is localized at the edge of the orogenic area, as highlighted by the distribution of seismic activity published by Bennett (2003). Indeed, although the thick crust in this region was not built from a continental collision, the range underwent a magmatic orogenic collapse comparable to the Variscides, which resulted in the emplacement of an up to 10 km thick magmatic underplating well-imaged on seismic sections (Jarchow et al., 1993; Rey, 1993).

However, the Bay of Biscay is a striking counterexample to this theory, since it opened apparently within a region thought to be underplated. In this case, the strike slip North Pyrenean fault inherited from the late Variscan evolution (Arthaud and Matte, 1977; Burg et al., 1994) may have been reactivated during the initial transtensive, strike-slip opening of the Bay of Biscay (Jammes et al., 2009). Because major strike-slip faults are pervasive structures, which can crosscut the whole lithosphere (Vauchez et al., 1998), the North Pyrenean fault may have remained a weak zone despite the Variscan underplating. In particular, such structures may be particularly sensitive to transcurrent motions.

5.2 Hot underplating: a prefered location for extension?

When magmatic intrusions are not thermally re-equilibrated yet, they may be weaker than the surrounding material. In such cases, rifting may occur atop the underplated area, as illustrated by our Model 5, where the mafic underplating and underlying depleted mantle are 300°C hotter compared to the encompassing lithosphere. This case could be compared to the South China Sea, which was affected by intense subduction- and orogen-related magmatism from Late Jurassic (Li et al., 2007) until Late Cretaceous (Wintsch et al., 2011), prior to rift initiation in Late Cretaceous–Early Paleocene (Holloway, 1982; Lee and Lawver, 1994; Ru and Pigott, 1986). Widespread granitoid intrusions outcrop along the South China Sea margin and seismic imaging shows mafic crustal underplating underlying the whole hyper-extended domain (McIntosh et al., 2014; Nissen et al., 1995). These underplated bodies may be at least partially pre-rift (Nissen et al., 1995). Furthermore, the wide-rift extension style in South China Sea suggests that the geotherm was relatively high at the time of rifting (> 700°C; see Buck et al., 1999; McIntosh et al., 2014).

5.3 Underplating: a trigger to the development of multiple necking instabilities?

Another interesting observation emerging from these models is that, although the evolution of each modeled rift basins is very localized (i.e. achieved through the formation of a so-called ‘H block’; see Lavier and Manatschal, 2006), the existence of thermally re-equilibrated mafic underplating and/or depleted mantle leads to formation of one or more failed rifts and a plateaus of un- or scarcely thinned continental crust over the restricted wavelength of the model box (see Models 2–4 and 6–8 in Figures III.4 and III.7).

In our models with mafic underplating and/or depleted mantle, the lithosphere is significantly thinned and the crust necked in at least two places outside of the underplated area, while the latter remains un- or only little thinned. As a result, one or more ribbons of thicker continental crust form between more or less developed rift basins. This architecture can be compared to the Flemish Cap offshore eastern Canada and the Galicia Bank of Northeast Iberia (see Figure III.1 b). Indeed, both developed from Variscan orogenic lithosphere that experienced the magma-rich orogenic collapse, as attested by the occurrences of pre-rift mafic lower crust (Díaz and

Gallart, 2009; Van Avendonk et al., 2009). Of course, the pre-rift extent and continuity of underplating and possible depleted mantle in Western Europe and Eastern United States are very poorly constrained, however the numerous evidence for Late Palaeozoic magmatism suggest that this event was very widespread. Because melt extraction from the mantle is likely to be focused to form mafic bodies (Holtzman et al., 2003), mafic underplating may be discontinuous but the deepest underlying mantle is likely to be quite continuously depleted. Therefore, our 'geologically most realistic' model to represent the Variscan orogenic lithosphere of Western Europe may be Model 8 (Figures III.8 and III.9).

Note that ribbons of thinned continental crust also exist further north in the North Atlantic (Rockall and Hatton banks, amongst other), although the corresponding lithosphere did not experience significant post-orogenic magmatism (Fossen et al., 2014; Meissner, 1999). In this region, the polyphase extension punctuated by periods of relaxation (Doré et al., 1999) may account for the architecture of this margin. Indeed, during extension, the thinned crust is replaced by lithospheric mantle, which is stronger once it has cooled down. Because such a material is harder to rift, extension will localize elsewhere during the next episode of extension (Buck et al., 1999). An alternative explanation could involve depleted mantle areas representing remnants from magmatic arc, backarc and/or forearc basins associated with the subduction of the Iapetus ocean. Indeed, the depleted subcontinental mantle drilled offshore Newfoundland has been interpreted as residual mantle beneath a volcanic arc related to the subduction of the Iapetus Ocean (Müntener and Manatschal, 2006). This case could be compared to our Model 7 (Figures III.8 and III.9).

The formation of the 'continental ribbons' in our model are very similar to the formation of boudins due to a necking instability. The closest analogue is that of the Basin and Range province in the Western United States, in which multiple fault bounded basins and ranges form due to necking instability in the lithosphere (Buck et al., 2003; Fletcher and Hallet, 1983; Zuber et al., 1986). The necking instabilities are actually initiated by the localization of deformation in the brittle crust and the wavelength, which is of the order of 100 km, is a complex function of the strength contrast between the brittle upper crust, the ductile lower crust and the brittle and ductile mantle lithosphere. This wavelength is acutely perturbed by the weakening and strengthening processes (Buck et al., 1999) occurring during the evolution of the deformation (Buck et al., 2003). In this numerical formulation it is also influenced by the kinematic boundary condition applied on the sides of the models. As a result, one of the necking instability eventually localizes most of the deformation and would form an ocean if the required conditions were present. In fact, both the processes and boundary conditions are similar to the natural conditions since, before extension, the lithosphere is heterogeneous and fragmented in areas with different composition and thermal ages (for instance craton versus young accreted terranes).

In our models, the wavelength of the necking instability, thus the distance between the edge of the underplated region and the locus of 'breakup' is controlled by the thermal state (see Models 2, 3 and 4 in Figures III.5 and III.6), and most likely by the thickness of the strong heterogeneity and its rheology contrast compared to the encompassing material (see Models 2, 6 and 7 in Figures III.4 and III.7). Because rift always localizes at one edge of the model when Moho temperature $\geq 500°C$ for models up to 1,000 km wide, we were not able to determine an empirical relationship (see Annex D section 1). However, as necking is achieved much further from the underplated area when the latter is wider (compare Model 8 to Model 2), we suggest that the width of the strong heterogeneity may control the wavelength of the necking instability.

Note that the necking instability may trigger the thickening of the lithosphere beneath the underplated area (see Model 2), which may eventually dive in the asthenosphere. This observation could be compared to the Rio Grande Rift, where delamination of lithosphere/upper mantle convection is evidenced by seismic tomography (Gao, 2004; van Wijk et al., 2008; Wilson et al., 2005). Indeed, the Rio Grande Rift is adjacent to the Great Plain Craton, whose lithosphere is thicker and stronger (van Wijk et al., 2008). Both the step in lithospheric thickness and the rheological anomaly may account for the development of a necking instability.

6 Conclusion

The main conclusions of this study are: (1) Conversely to what is predicted by the theory of the Wilson Cycle, weaknesses inherited from an orogenic event may not be reactivated during a subsequent extensional event when the orogen underwent a magma-rich orogenic collapse similar to what is observed in the Variscides. (2) Delocalization of extension in multiple basins may be triggered by mantle heterogeneities associated with the collapse of ancient orogenies. Thus, not only the evolution of individual rifts is polyphase (Lavier and Manatschal, 2006), but their eventual evolution from incipient rift to ocean may be controlled by necking instabilities and continental ribbons organizing in, or around mantle heterogeneities. (3) When multiple rift basins form, they geographically organize essentially as a function of the initial thermal state and of the nature/thickness and width of the strong mantle heterogeneities.

Although we do not account for mantle melting and melt migration, the results show that the initial structure of the lithosphere as imposed by different types of orogenies (Variscan versus Caledonian) exert a fundamental control on the evolution of future rifts. It is likely that if extension is accompanied with intense magmatism, rifting would be more localized and the timing of evolution of each basins in a given continental ribbon would be different.

Besides, our numerical models underline the key role of compositional/lithological heterogeneities in both the crust and the mantle. Yet, present-day numerical modelers are essentially using mono-mineralic material with averaged physical properties to model the behaviour of materials comprising heterogeneities at different scales. We therefore stress the importance of integrating this complexity in the design of the rheological phases, as recently undertaken by Jammes et al. (2013), in order to tend toward more geologically realistic results.

Synthesis & Discussion

7 Synthesis

In the following sections, I discuss chapter by chapter, how the data produced and the conclusions drawn from their analysis allow to answer the questions presented in the *General introduction*.

7.1 Chapter I

In the first chapter of my thesis, I define and map large-scale orogenic inheritance, the first-order architecture of rift systems and the timing of major rift events in the North Atlantic region. Note that, in this work, I use the terms 'first-order' and 'large-scale' to describe structures, lithological and thermal heterogeneities, as well as tectonic processes, which express at a scale beyond the deca-kilometer.

How to define and map orogenic inheritance on a large-scale?

In this study, *inheritance* is defined as the deviation between an ideal lithosphere with horizontally homogeneous physical properties ('layer-cake' lithosphere) and a natural lithosphere (Figure 1 (a); see also Annex A for extended definition and discussion). Following this line of thought, inheritance includes structural, thermal and compositional/lithological heterogeneities.

Because of their different geological history, I distinguish between three orogenic domains in the North Atlantic region, namely the Caledonian, Variscan and Alpine domains (see Annex B for the Alpine component). I define an orogenic domain as the area limited by the trace of the corresponding deformation fronts at the present-day surface. Note that this area does not necessary reflect the maximum extent of the orogen, since erosion may have erased part of the orogenic structures, however it remains a reasonable proxy at the scale under consideration.

For each orogenic domain I map, where possible, the corresponding first-order inherited features. I select as relevant and mappable: suture zones, major faults, foreland basins, magmatic arcs, as well as major post-orogenic magmatic intrusions/underplating and associated mantle depletion (see Chapter I, section 3).

Suture zones are definitely the most important inherited structures, since they mark the boundary between former tectonic plates. They are high strain lithospheric-scale structures, comprising usually ophiolites and/or blueschist assemblages (Dewey, 1977; Hall, 1976; Haynes and McQuillan, 1974). Note that major faults, in particular major strike-slip faults, may also crosscut the whole lithosphere (Vauchez et al., 1998), therefore be significant zones of lithospheric weakness.

As foreland basins initially develop below the base level on either sides of an orogen (DeCelles and Giles, 1996), they are *a priori* long-lasting features because they are difficult to erode. Thus, they allow to assess the location and extent of the former orogen quite reliably. Note, however, that as subsequent tectonic movements and/or crustal thickening may cause their uplift and erosion, their present-day extent is only a minimum.

Arc magmatism is characteristic of upper plates above protracted subduction zones. It may either form a new, independent magmatic feature in the framework of an intra-oceanic subduction, for instance the Izu–Bonin-Mariana arc south of Japan; or it may affect the pre-existing overlying margin in the case of a subcontinental subduction, such as along western South America. An intra-oceanic magmatic arc is usually comprised of mafic crustal material underlain by depleted mantle (see Leat and Larter, 2003 for a review). Such arcs may either be preserved in orogens by obduction or integration into the accretionary wedge, as exemplified by the Kohistan Arc in Himalaya (Bard et al., 1980; Burg, 2011; Coward et al., 1986); or it may be subducted. In contrast, arc magmatism over continental lithosphere strongly modifies both the initial thermal and lithological structure of the overlying margin (Gerya and Meilick, 2011), as exemplified in the Andean orogen (Schilling et al., 2006). In this case, because continental crust is note easily subductable, this inheritance is most likely preserved over time.

Similarly, the widespread magmatic intrusions emplaced following the termination of the Variscan orogeny (collapse) strongly modified the thermal state and lithology/composition of both the crust and the mantle (Costa and Rey, 1995; Petri, 2014; Schaltegger, 1997; Vanderhaeghe and Teyssier, 2001). Here, for the sake of simplicity, I assume that this major thermal event resulted in all at once rejuvenation of the lower crust by mafic underplating, more or less acidic magmatic intrusions within the overlying crust and depletion of the underlying mantle over a large part of the Variscan orogenic area, as suggested by the recent studies by Petri (2014) and Petri et al. (subm.). I assess the first-order extent of this region based on seismic data, field studies, drill-holes and xenoliths (see Annex B section 4).

The maps resulting from these compilations are presented in Figure 1 (b). They highlight that: (1) The North Atlantic rift parallels the Caledonian suture of the wide Iapetus Ocean. (2) Conversely, the rift avoids the sutures of the Variscan Rhenohercynian, Saxothuringian and Medio-European ‘narrow oceans’, as well as that of the wide Rheic Ocean in Western Europe.

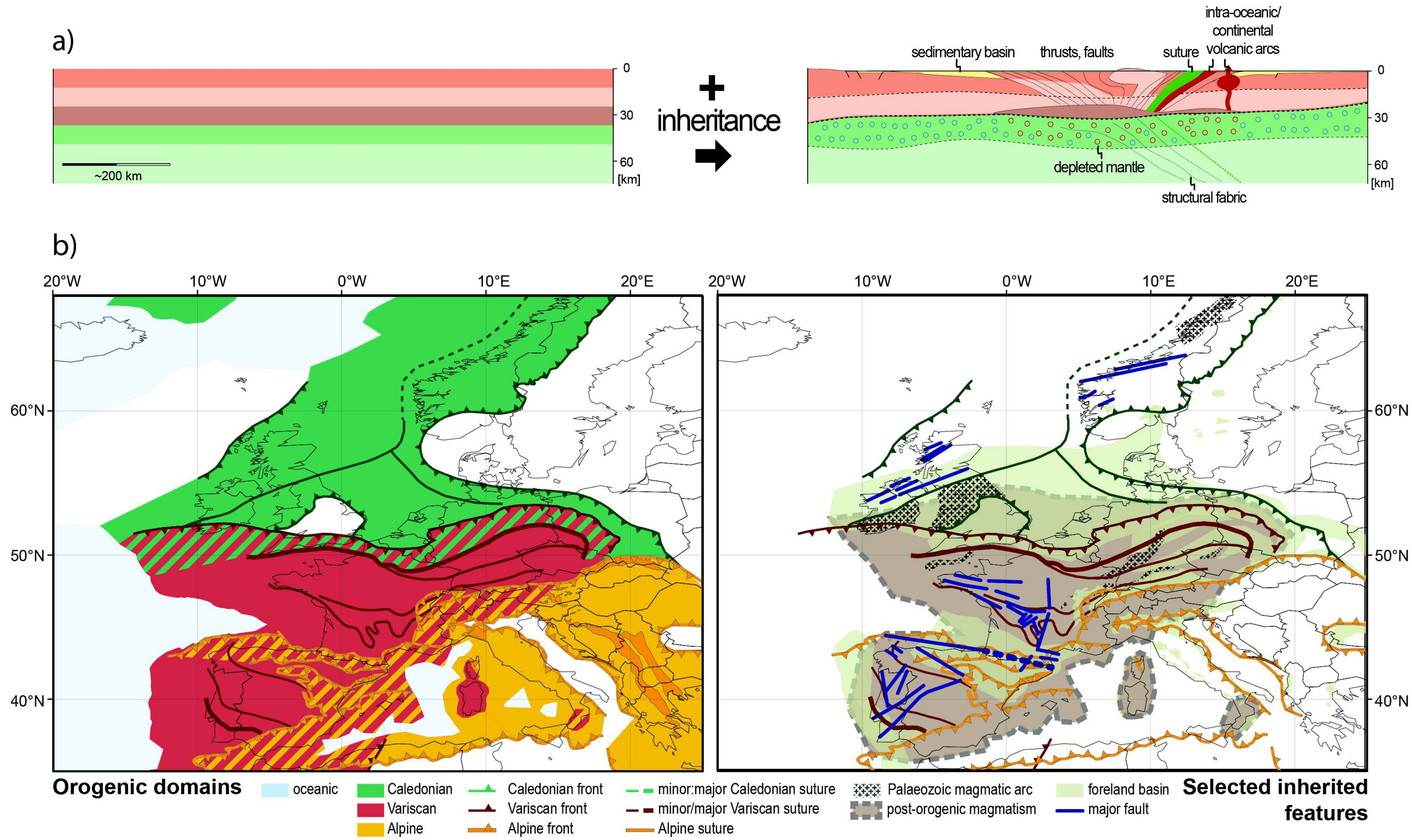

Figure 1 – (a) Definition of inheritance as the deviation between an ideal lithosphere with horizontally homogeneous physical properties and a natural lithosphere; (b) Maps showing the location of the Caledonian, Variscan and Alpine orogenic domains (left) and their corresponding major inherited features in Western Europe (right).

How to define and map the first-order structural architecture of rift systems?

In order to highlight the first-order architecture of rift systems, I distinguish between three rift domains, namely the *proximal*, *distal* and *oceanic* domains (Figure 2 a). I define these based on morphological criteria observable on seismic sections, following the methodology developed by Sutra et al. (2013) and Tugend et al. (2015). In addition, I use gravity and magnetic data to correlate the boundaries of these domains between seismic sections.

In the proximal domain, the crust is not significantly thinned ($\sim$ 30–35 km) and the basement is parallel to the Moho (Péron-Pinvidic et al., 2013; Sutra et al., 2013; Tugend et al., 2015). The boundary between the proximal domain and the distal domain is defined as the *necking point*, which marks the onset of basement deepening together with Moho shallowing on seismic sections in depth (Sutra et al., 2013). The necking point also appears as a prominent feature on Bouguer anomaly maps where low frequency signal were filtered (see Annex C). Indeed, high-pass filtering eliminates the long wavelengths induced by mantle density heterogeneities, thus highlights the high frequency signal from the crustal architecture. A filtered Bouguer anomaly map is therefore an efficient tool to extrapolate the location of the necking point between seismic sections on a large scale, provided that significant magmatic additions are absent or their gravity signal corrected.

The boundary between the distal domain and the oceanic domain is defined as the *lithospheric breakup point*, which corresponds to the onset of steady-state seafloor spreading (Sutra et al., 2013). On seismic sections, it is marked by an inflection in basement between, on one side, a more or less corrugated surface with a discontinuous or inexistent seismic Moho reflector (Whitmarsh et al., 2001) and syn-tectonic (sag) sedimentary deposits (Haupert et al., ress); and on the other side, a homogeneous $\sim$ 6 to 7 km/2 sTWT thick oceanic crust covered with essentially passive infill (Péron-Pinvidic et al., 2007; Sutra et al., 2013). Note that the inflection may be either up or down, depending on the magmatic budget associated with breakup. Indeed, the transition between exhumed mantle and normal oceanic crust translates as a step-up onto oceanic crust, since exhumed mantle is denser than a classical 'Penrose-type' oceanic crust. Conversely, the transition between a magma-rich margin with SDRs and normal oceanic crust is expressed by a step-down.

Because the basaltic rocks created at the ridge record the contemporary magnetic field, the lithospheric breakup point can *a priori* be correlated on a large scale between seismic sections, relying on magnetic anomaly maps. However, this method cannot be applied when the onset of seafloor spreading occurs during a so-called *quiet magnetic period*, i.e. times without inversion of the magnetic field. Note also that magnetic anomalies are not necessarily associated with steady-state seafloor spreading, as shown by Bronner et al. (2011) for the J-anomaly offshore Iberia and Newfoundland.

Importantly, care should be taken when there are significant magmatic additions, since they disrupt the seismic, gravimetric and magnetic signal, making the identification of rift domains difficult. It is for instance the case in the northern North Atlantic, where the lithospheric breakup is accompanied by an intense episode of magmatism. Thus, in order to locate areas where the limits of rift domains are questionable, I represented these magmatic additions on the map of rift domains (Figure 2 b), based on published studies (see section 4 in Chapter I for details).

Note that it is theoretically possible to map rift domains with a higher resolution, distinguishing between several subdomains within the distal domain as proposed by Sutra et al. (2013). However, such a mapping necessitates higher resolution seismic observations and further development of methods to correlate these domains through space (see Annex C). Indeed, applying the mapping method developed by Tugend et al. (2015) in the northern North Atlantic requires to eliminate the jamming of seismic and gravimetric signal caused by significant magmatic additions.

The map of rift domains achieved in the framework of this thesis is presented in Figure 2 (b). It highlights that: (1) Hyperextended rift systems are not always associated with lithospheric breakup (e.g. the North Sea, Rockall and Hatton troughs, Porcupine Basin and Flemish Pass); (2) The distal domain is comparably wide on both sides of the southern North Atlantic. Conversely, the eastern distal domain of the northern North Atlantic is significantly wider than its conjugate, and, unlike the latter, it contains ribbons of barely thinned continental crust (Rockall, Hatton and Porcupine banks); (3) The magmatic additions in the northern North Atlantic are broadly limited to the distal domain; in particular, their most distal limit usually corresponds to the transition to normal oceanic crust.

It is to be noted that the so-called *North Atlantic Igneous Province* is usually considered as an expression of the Iceland plume (Morgan (1971); Saunders et al. (1997) and more recently Buiter and Torsvik (2014)). Yet, this hypothesis is being increasingly questioned, in particular because the chemistry of the magma are not compatible with a unique plume source and because seismic tomography does not show indisputable evidence for a deep mantle plume (e.g. Brown and Lesher, 2014; Foulger and Jurdy, 2007; Kempton et al., 2000; Korenaga et al., 2000). In addition, the map on Figure 2 (b) highlights that magmatic additions are located along the entire hyperextended domain of the northern North Atlantic, but they become restricted to the Iceland region in the oceanic domain. Yet, it seems unlikely that a hotspot as local as the Iceland one could have caused such a widespread magmatic event, especially if the plume is rooted in the upper mantle as suggested by Foulger et al. (2001). Alternative explanations for the North Atlantic Igneous Province include inherited compositional heterogeneity in the upper mantle and rift-related small-scale convection (see review by Meyer et al., 2007).

How to define and map the timing of major rift events?

In order to assess the timing of rifting, I focus on two major rift events, namely: (1) the onset of necking, i.e. the transition between the *stretching* and *thinning* mode; and (2) the lithospheric breakup, i.e. the transition between *hyperextension/exhumation* and *steady-state seafloor spreading* (see Lavier and Manatschal (2006) for discussion of the different rift-related deformation modes). Note that this amounts to date the formation of the *necking point* and of the *lithospheric breakup point* described in the previous section, respectively.

Extension of a lithosphere containing weak heterogeneities in both the crust and the upper mantle forms initially rift basins at the crustal weak zones (see the numerical models by Chenin and Beaumont, 2013). In nature, this translates into widely distributed extension during the early stages of rifting (e.g. Bertotti, 1991; Tankard and Welsink, 1989). At the same time, faults/shear zones develop in the lower crust and/or in the lithospheric mantle, preferentially where the weakest heterogeneities are embedded. Because these layers have the strongest/stiffest rheology, the resulting *necking instabilities* grow very fast (Zuber et al., 1986), faster than thermal diffusion can re-equilibrate the resulting heat advection. Necking is therefore a weakening, self-reinforcing process (Buck et al., 1999), which may swiftly cause the localization of deformation. At the surface, the onset of necking translates into a shift from widely distributed extension to extension focused on a few faults, which accommodate a significant amount of extension (Mohn et al., 2012). The resulting abandonment and sealing of the most proximal sedimentary basins is recorded by the formation of a *necking unconformity* in the proximal domain, which separates syn-tectonic deposits from passive infill (see right insert in Figure 3 (a); Haupert et al., ress).

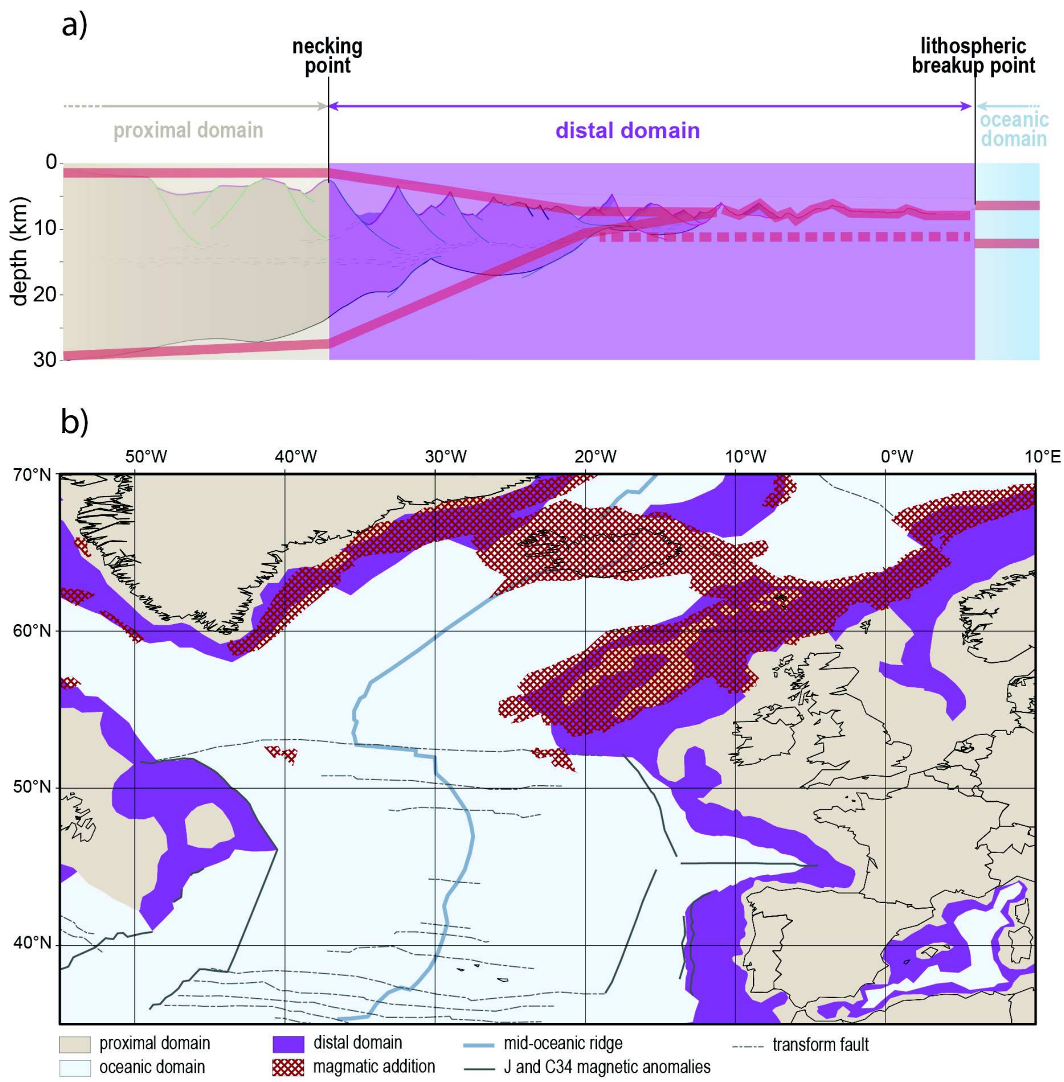

Figure 2 – (a) Definition of the three main rift domains considered in this study (simplified after Sutra et al., 2013) and their first-order morphology (red lines). The dotted line represents the seismic Moho, where it differs from the petrologic Moho. (b) Map of the rift domains and breakup-related to post-rift magmatism in the North Atlantic (see section 4 in Chapter I for details and discussion).

As extension progresses, continental crust is progressively thinned out to nothing and sub-continental mantle may be exhumed, until the lithospheric breakup is achieved. At the transition from hyperextension to steady-state seafloor spreading, active deformation of pre-existing material is replaced by accretion of newly-formed magmatic material. Therefore, the lithospheric breakup may also be recorded in the sediments as a transition from syn-tectonic deposits to passive infill, comparably to the necking unconformity (left insert in Figure 3 a). However, the breakup unconformity is younger than the necking unconformity and only exists in the distal domain, whereas the necking unconformity is restricted to the proximal domain.

Note that, although the term 'breakup unconformity' is abundantly used in the literature, its actual meaning remains a matter of debate. Indeed, the termination of the syn-tectonic phase is not necessarily coeval with the lithospheric breakup, since a phase of subcontinental mantle exhumation may occur in the meantime ('sag phase'; see Haupert et al., ress). In this case, the lithospheric breakup may not be expressed as an obvious unconformity. Moreover, during the exhumation stage, the play of successive mantle exhumation faults may form several comparable unconformities of different ages in the exhumation domain (see Gillard et al., 2015), all of which predate the actual lithospheric breakup. Therefore, to determine the age of lithospheric breakup, one must make sure to select the last/most distal unconformity. Alternatively, one could use the first sediments deposited on normal oceanic crust, however the latter are rarely sampled – thus dated. Therefore, the most convenient proxy remains the age of the first magnetic anomaly, given that the lithospheric breakup did not occur during a quiet magnetic period.

The map resulting from the compilation of published data according to this philosophy is shown on Figure 3 (b). It highlights that a phase of necking affected parts of both the northern and southern North Atlantic region during the Jurassic. However, lithospheric breakup occurred earlier in the south (Cretaceous) than in the north (Eocene). Thus, the time lag between the onset of necking and the lithospheric breakup is significantly longer in the northern North Atlantic (> 80 Myr) than in the southern North Atlantic (< 45 Myr).

How does orogenic inheritance impact the first-order architecture and evolution of rift systems?

Comparison between the different maps presented here-above highlights an abrupt and significant difference in the characteristics of the North Atlantic rift system on

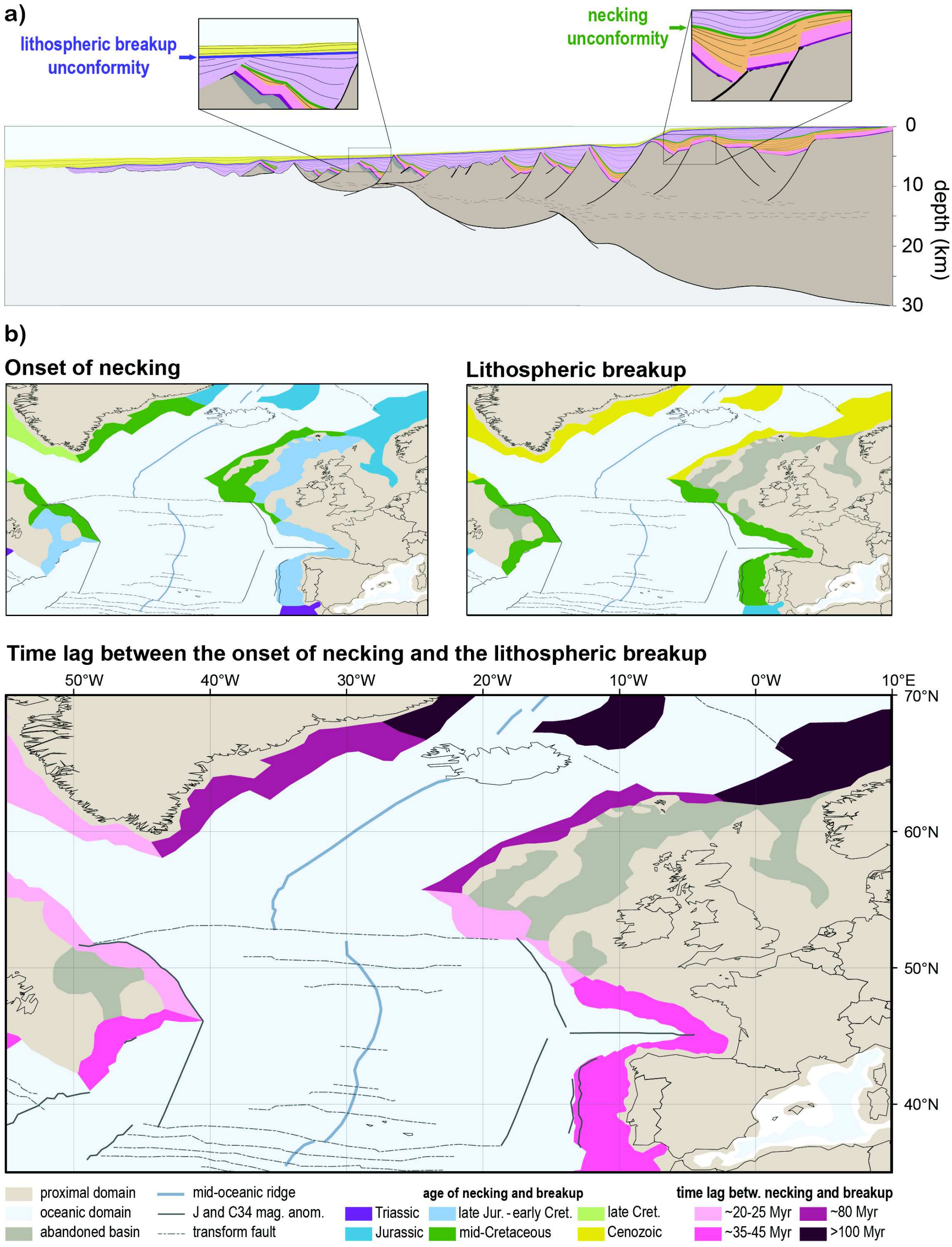

Figure 3 – a) Sedimentary record of the onset of necking (right-hand insert) and of the lithospheric breakup (left-hand insert); b) Maps displaying the age of (top left) the onset of necking; (top right) the lithospheric breakup; and (bottom) the time lag between these two events for the North Atlantic rift system.

either side of the Variscan front. Indeed, the rift cuts through the Caledonian orogenic lithosphere and parallels its structural grain north of the Variscan front, whereas to the south it circumvents the core of the Variscides of Western Europe. Moreover, rifting is protracted (> 80 Myr) and polyphase, marked by the development of a succession of 'failed rift basins' north of the Variscan front, while the duration of rifting is significantly shorter (< 50 Myr) and much less polyphase to the south. In addition, breakup is magma-rich north to the Variscan front, whereas it is apparently 'magma-poor' to the south.

Interestingly, the Charlie-Gibbs fracture zone seems to be the continuation offshore of the Variscan deformation front, or of the Rheic suture, or else, as suggested by Buiter and Torsvik (2014), of the Iapetus suture. It corresponds to the relatively sharp limit between a 'magma-rich' breakup to the north and a 'magma-poor' breakup to the south (Figure 2), in a similar way as the Colorado transfer zone in the South Atlantic (Franke et al., 2010) and as the Cape Range fracture zone offshore Northwest Australia (Hopper et al., 1992).

Besides, Roberts et al. (1999) described the opening of the North Atlantic in terms of one northward propagating Atlantic rift, initially terminating in the Porcupine basin, and a southward propagating Arctic rift, initially terminating in the North Sea. These two extended domains were abandoned in Late Cretaceous, as the two rifts systems became coalescent offshore United-Kingdom. Here again, the Variscan front is precisely located to the very end of each of these rifts, supporting the proposition that it is a major limit.

However, regardless of whether it affects Caledonian or Variscan terranes, the North Atlantic rift reactivates, at least partially, the sutures corresponding to former wide oceans (e.g. the Iapetus Ocean between Norway and Greenland and the Rheic Ocean in Central Atlantic). In contrast, the sutures corresponding to former 'narrow' (< 500–1,000 km) oceans (e.g. the Tornquist Seaway and Rhenohercynian, Saxothuringian and Medio-European 'oceans') are little affected by extension, both during the Alpine Tethys and North Atlantic rifting.

7.2 Chapter II

In the second chapter of my thesis, I characterize the first-order structural and lithological architecture of hyperextended rift systems (i.e. extensional systems that went beyond *coupling*; see Sutra et al., 2013 and Doré and Lundin, 2015) and study how they express in collisional orogens. In particular, I focus on orogens resulting from the closure of 'narrow oceans' (< 300 km wide), first to avoid the complexity induced by long-lasting subduction processes (formation of volcanic arcs and/or forearc- and/or backarc basins), and second because the impact of inheritance in such 'immature' collisional systems remains little studied to date. Note that I describe as 'mature' rift systems with self-sustained and steady-state seafloor spreading, as opposed to 'immature' or 'embryonic' rift systems which didn't go beyond hyperextension or mantle exhumation.

What is the first-order structural architecture of 'narrow' and 'wide oceans' and how can they be described quantitatively?

In order to characterize the architecture of rifted margins, I distinguish between three sub-domains within the *distal domain* (Figure 4 a), based on the morphological criteria described by Sutra et al. (2013) and Tugend et al. (2015), namely: (a) the *necking domain* is characterized by an abrupt thinning of the continental crust from $\sim$ 30 km down to $\sim$ 10 km, which translates into a deepening of basement and shallowing of the Moho on seismic sections in depth; (b) the *hyperextended domain* lies where the continental crust is thinned from $\sim$ 10 km down to 0 km. The transition between the necking domain and the hyperextended domain corresponds to a sudden decrease in the dip of the Moho on seismic sections in depth; (c) an *exhumation domain* may exist in so-called 'magma-poor' rifted margins, when subcontinental lithospheric mantle is exhumed at the seafloor and/or an 'embryonic' (as opposed to 'normal', Penrose-type) oceanic crust from a stuttering spreading system is emplaced (Gillard et al., 2015). On seismic sections, the exhumation domain usually appears as a more or less corrugated surface devoid of seismic Moho reflector – or with a discontinuous seismic Moho reflector if some magma is present (Whitmarsh et al., 2001).

The statistical analysis I undertook on a selection of seismic sections (see Chapter II section 2.2) highlights that, although the total width of continental margins may vary considerably, the width of the hyperextended domain seems relatively constant, with an average of 50 km (Figure II.2 (c) in Chapter II). In contrast, the necking and exhumation domains display a wider range of widths, although their average value is comparable (about 60 km).

The relatively constant width of the hyperextended domain amongst hyperextended rifted margins may be explained by the critical Coulomb wedge theory, as suggested by Nirrengarten et al., subm.). Indeed, the material comprising the hyperextended wedge is fully brittle (Pérez-Gussinyé et al., 2003; Sutra and Manatschal, 2012; Sutra et al., 2013; Figure 4) and is underlain by a low frictional décollement

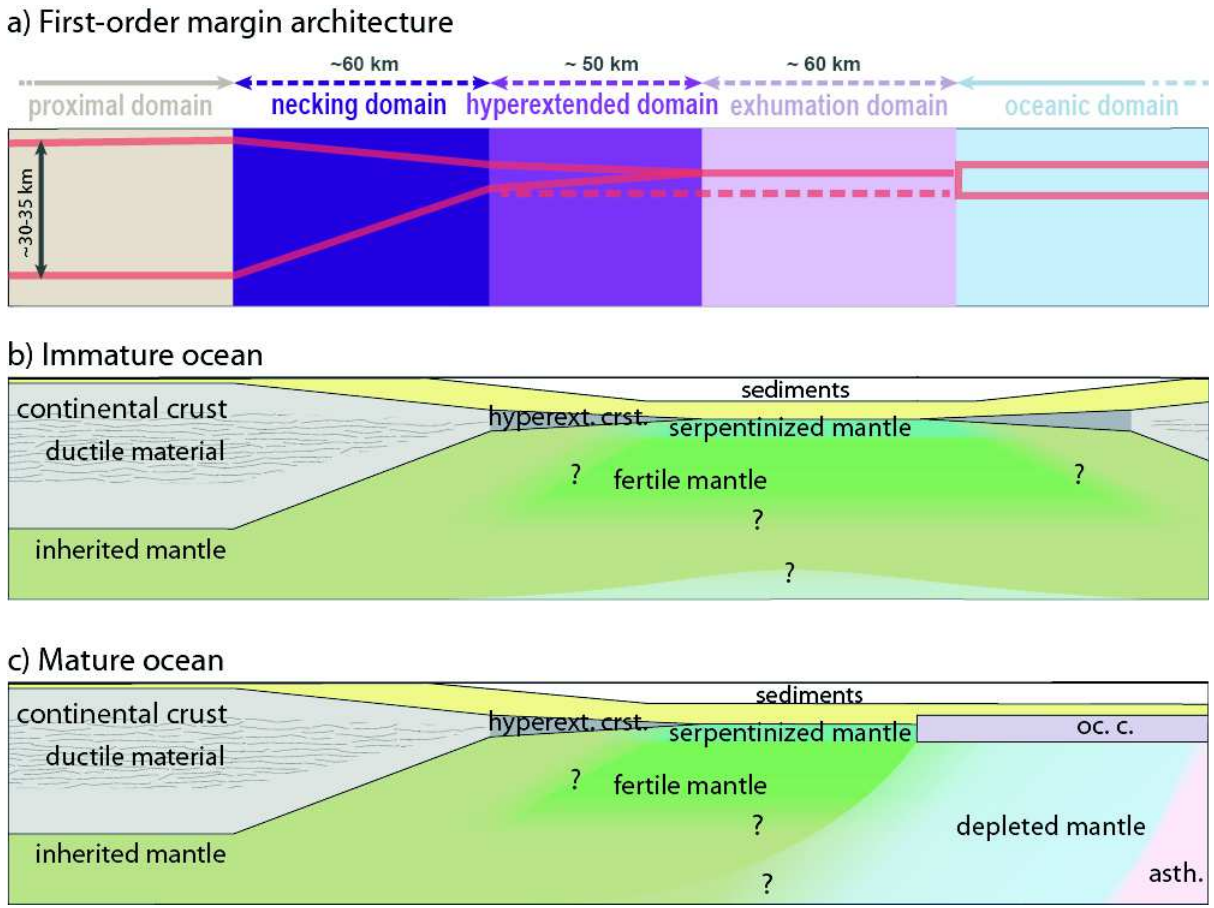

Figure 4 – (a) First-order structural architecture of rifted margins and average width of the distal sub-domains; (b) First-order lithological architecture of immature/embryonic oceans; (c) First-order lithological architecture of mature oceans. hyp. c.: hyperextended continental crust; oc. c.: oceanic crust; depl. m.: depleted mantle; asth.: asthenospheric mantle.

(mantle detachment fault). When such a system is submitted to extension, it deforms according to the same physical laws as a critical Coulomb wedge theory, which depend on the friction parameters of the material and the fluid pressure (Dahlen, 1984; Davis et al., 1983). By contrast, deformation of the necking domain may be dominantly controlled by the inherited architecture/rheology of the initial crust, in particular the amount of ductile material as suggested by Sutra and Manatschal (2012) and Manatschal et al. (2015).

Besides, the width of each specific rift domain appears to be unrelated to the total width of the margin (see Figure II.2 (b) in Chapter II), and the width of both the necking domain and hyperextended domain seems independent from the maturity of the rift system (Figure II.2 (d) in Chapter II).

What is the lithospheric-scale lithology of narrow and wide 'oceans'?

In the proximal domain and in the necking domain, neither the lithology of the crust, nor that of the mantle are significantly modified during rifting, therefore both retain most of their initial, inherited characteristics. On a global basis, the crust in these two domains can be approximated by a quartzo-feldspathic material and the underlying 'inherited mantle' with an average composition of 35–65% olivine, 7–30 % clinopyroxene, 25–30% orthopyroxene and $\sim$ 1% spinel (Picazo et al., 2015 and *in prep.*). Note, however, that in the necking domain, the crustal ductile layers are attenuated mechanically during extension, so that no ductile material is left in the hyperextended domain (Pérez-Gussinyé et al., 2003; Sutra et al., 2013.

By contrast, in the hyperextended and exhumation domains, fluid-rock interactions form a significant amount of hydrous minerals (sericite and illite in the remnants of continental crust (Picazo et al., 2013; Pinto, 2014); serpentinite, chlorite and talc in the shallowest part of the mantle (Christensen, 1970; Früh-Green et al., 2004; Hess, 1955; Picazo et al., 2013; Pinto, 2014). Although the hyperextended continental crust is never fully altered, its rheology is controlled by the weakest phase when its proportion is significant enough (Jammes et al., 2013, subm.). Thus the hyperextended crust and the top 6 km of the underlying or exhumed mantle can be approximated by a phyllosilicate material.

Besides, crustal thinning down to $\sim$ 10 km is associated with partial melting of the asthenosphere, which is initially stored in the overlying mantle (Müntener et al., 2010, 2004; Piccardo et al., 2014, and references therein). The average composition of this *fertile* mantle is about 51% olivine, 16% clinopyroxene, 25% orthopyroxene, 7% plagioclase, 1% spinel, and its density is significantly lower than that of the average inherited mantle ($\sim$ 3,250 kg.m^{-3} compared to $\sim$ 3,330 kg.m^{-3}; Picazo et al., 2015, in prep.).

When lithospheric breakup is achieved, steady-state seafloor spreading creates a Penrose-type' oceanic crust, homogeneous in both composition (about 50% plagioclase and 50% pyroxene) and thickness (5–6 km). This process extracts the most fusible elements from the underlying lower lithosphere and uppermost asthenosphere, leaving a depleted mantle with an average composition of about 57% olivine, 13% clinopyroxene, 28% orthopyroxene, 2% spinel (Workman and Hart, 2005). This depleted mantle is slightly lighter than the average inherited mantle ($\sim$ 3,305 kg.m^{-3} compared to $\sim$ 3,330 kg.m^{-3}; Picazo et al., 2015 and *in prep.*).

Figure 4 (b) and (c) provide visual summaries of the architecture of 'magma-poor' immature and mature 'oceans', respectively.

What are the first-order differences between narrow and wide 'oceans'?

Based on the data compilation presented in Table II.1 in Chapter II, I suggest that 'narrow' hyperextended rift systems (i.e. hyperextended rift systems for which the distance between the two conjugate points of necking is less than 300 km) usually lack a mature, self-sustained spreading system. Thus, they are devoid of normal oceanic crust and that their seafloor comprised of either thinned continental crust, exhumed mantle and/or embryonic oceanic crust. In contrast, oceans larger than 1,000 km often achieved their actual width because of their mature, self-sustained spreading system, which creates a smooth and homogeneous oceanic crust. Thus, the mantle underlying narrow hyperextended basins is likely to preserve the fertile composition resulting from the storage of asthenospheric melts during extension, unlike wide oceans which are underlain by a typical depleted mid-oceanic ridge mantle.

Besides, as there is no statistical difference in the architecture of the margins from a wide/mature and a narrow/immature rift system, I suggest that the main difference between these two end-members is the existence of a significant amount of normal oceanic crust and underlying depleted mantle (compare panels (b) and (c) in Figure 4).

How do the specificities of rifted margins impact orogenesis following the closure of a narrow 'ocean'? What are the differences compared to orogenesis produced by the closure of a wide ocean?

During the closure of narrow oceans, the slab remains usually at shallow angle

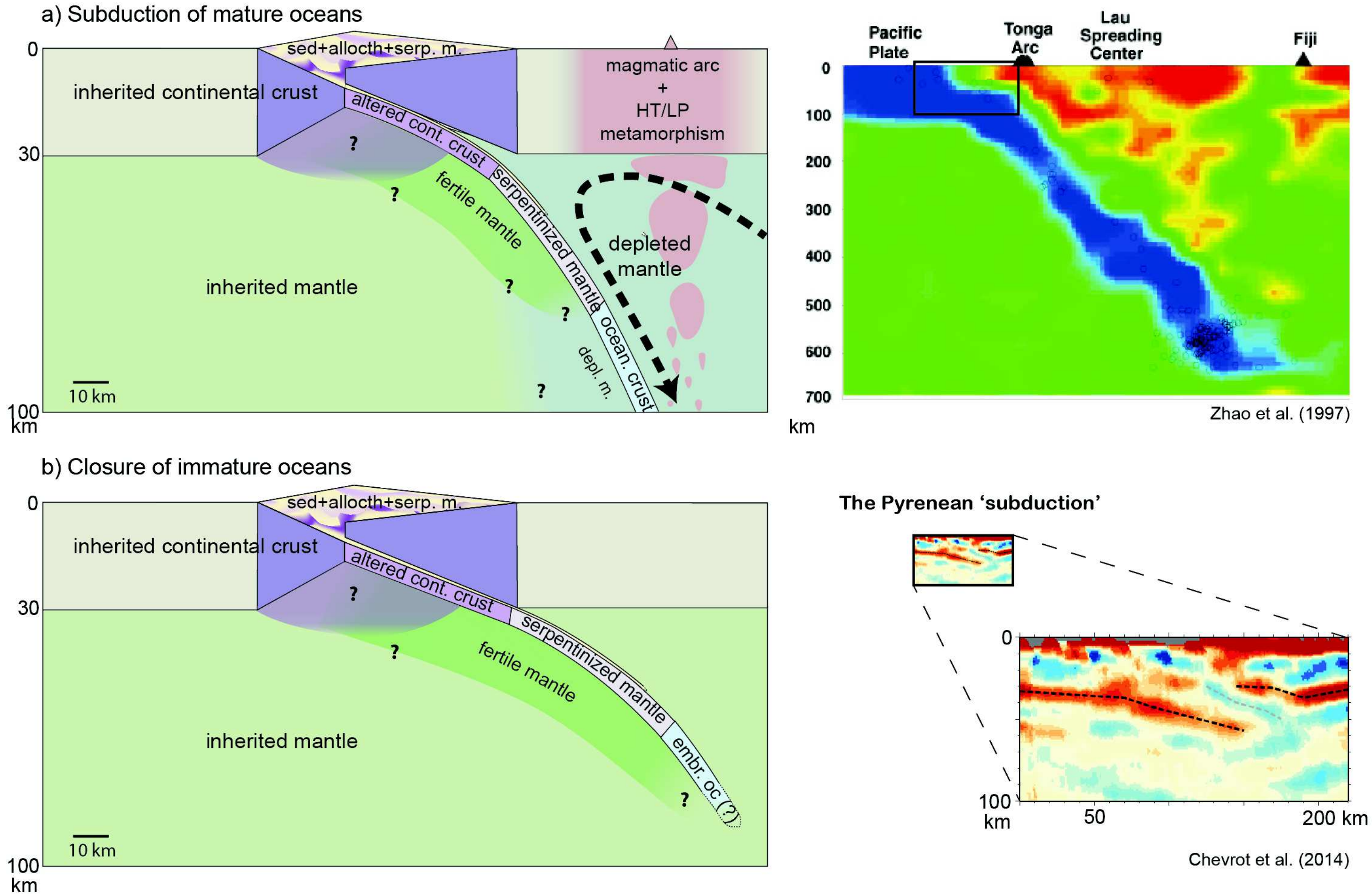

Figure 5 – Left-hand panels: Architecture of orogens following from the closure of (a) wide and mature oceans; (b) narrow and immature oceans. depl. m.: depleted mantle; embr. oc.: embryonic oceanic crust; HT/LP: high temperature/low pressure; oc. crust: oceanic crust; Right-hand panels: Seismic tomography across the Pacific subduction (mature ocean) after Zhao (1997) and the Pyrenean 'subduction' (immature ocean) after Chevrot et al. (2015). The inserts highlight the scale of the zone represented on the corresponding left-hand panel.

(Billen, 2008; Stevenson and Turner, 1977; Tovish et al., 1978). As a consequence, subduction is very unlikely to become self sustained (Gurnis et al., 2004; Hall et al., 2003) or to develop strong small-scale convection in the mantle wedge (Peacock et al., 1994), unlike subduction of wide oceans. Furthermore, the closure of narrow oceans does not induce significant magmatic activity, thus no mantle depletion, because not enough volatiles reach a sufficient depth to allow partial melting (Gaetani and Grove, 1998; Peacock, 1991; Rüpke et al., 2004). Therefore, hydration is likely to be the dominant process in the mantle wedge above such transitory subductions.

In addition, because of the low dip angle of the slab, both slab pull and the potential effect of mantle flow on the slab are very limited, making the development of back-arcs and associated partial melting unlikely (Heuret and Lallemand, 2005; Uyeda, 1981). Therefore the lithosphere underlying orogens resulting from the closure of narrow oceans is likely to be relatively fertile and hydrated (see Figure 5 b).

By contrast, protracted subductions associated with the closure of wide oceans are likely to become self-sustained, in particular due to the increasing density of the slab caused by its progressive eclogitization from a depth of about 50 km (Aoki and Takahashi, 2004; Doin and Henry, 2001). Long lasting subductions usually develop vigorous convection in the mantle wedge, which drives efficiently both volatiles from the dehydration of the slab to great depth and deep asthenospheric material toward the shallow part of the mantle wedge (Peacock et al., 1994). The resulting partial melting induced by both flux and decompression melting translates into the creation of thickened sialitic crust at the surface (volcanic arcs; Jagoutz et al., 2011), induces high grade metamorphism in the encompassing upper plate and depletes the underlying mantle in fusible elements (Bonatti and Michael, 1989; Uyeda, 1981).

When a significant amount of oceanic lithosphere is subducted, the strong slab pull, and potentially also the effect of dynamic mantle flow dragging on the slab may induce a backward migration of the lower plate with respect to the upper plate, which may result in the formation of a back-arc basin (Heuret and Lallemand, 2005; Uyeda, 1981). In such cases, extension may be associated with seafloor spreading and underlying mantle depletion as well. Note that, although the vigorous convection within the mantle wedge may tend to homogenize its composition, a lower mantle fertility is still to be expected beneath orogen resulting from the closure of wide oceans, as evidenced by the studies by Martinez and Taylor (2002); Woodhead et al. (1993). Therefore, the thermal and lithological architecture of orogens related to the closure of wide oceans differs much more from that of the initial margins involved compared to orogens produced by the closure of narrow oceans (Figure 5).

As a result, orogenesis resulting from the closure of narrow basins may be essentially controlled by mechanical processes, without significant compositional or thermal perturbation, and with a major influence of the inherited characteristics of the intervening margins (e.g. the Alps (Mohn et al., 2014); the Pyrenees (Tugend et al., 2014). In contrast orogenesis consequent to the closure of wide oceans may be significantly controlled by subduction-induced processes (Faccenda et al., 2008; Thompson et al., 2001).

The difference in mantle composition resulting from the closure of narrow/ embryonic oceans versus wide oceans may dictate the magmatic budget of subsequent extensional events such as post-orogenic collapse or rifting. Indeed, the depleted mantle beneath orogens related to mature subductions may not allow for voluminous magma production, in contrast to the fertile mantle underlying orogens produced by the closure of narrow oceans. This hypothesis may account for both the a-magmatic collapse of the Norwegian Caledonian range (Fossen et al., 2014; Meissner, 1999), which resulted from the closure of the large Iapetus Ocean (McKerrow and Cocks, 1976), and for the large amount of magmatism following the collapse of the Variscan range (Costa and Rey, 1995), which is essentially consequent to the closure of the narrow Rhenohercynian, Saxothuringian and Medio-European 'oceans', in addition to the suturing of the wide Rheic Ocean (Franke, 2006; see also section 3.2 in *General geological setting* and Chapter I).

Alternatively, the low magmatic budget of the Caledonian orogenic collapse may be explained by the depleted composition of the mantle underlying the two intervening continents, namely Laurentia and Baltica. Indeed, both are essentially comprised of Archean cratonic cores (the North American and East European craton, respectively), which are characterized by a thick, cold and depleted lithospheric mantle (Bernstein et al., 1998; Beyer et al., 2004; Griffin et al., 2003).

7.3 Chapter III

In the third chapter of my study, I investigate via numerical modelling how mafic underplating of the lower crust and associated underlying mantle depletion may impact a subsequent rifting event. In particular, I use the thermo-mechanical code FLAC (Cundall, 1989) to test how weak heterogeneities are reactivated during extension when embedded within a quartzite crust underlain by a 10 km thick gabbroic layer and a 40 km thick zone of depleted mantle (see Figure 6).

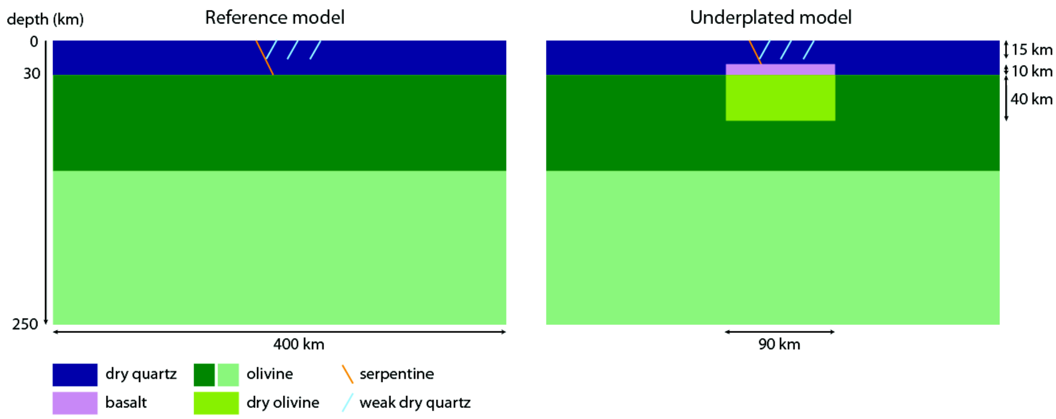

Figure 6 – Architecture of the reference (left) and underplated (right) models. The base of the lithosphere (dark green/light green boundary) is the isotherm 1300°C (no change in physical properties of the material on either sides). Its depth varies between 115 km in the model with a Moho at 400°C and 85 km when the Moho is 500°C.

How does crustal mafic underplating and/or underlying mantle depletion beneath a former orogenic suture impact the architecture and evolution of a subsequent rift system? How does the thermal state of such a lithosphere influence extensional processes?

The results of my numerical modelling experiments (Figure 7) support that the existence of a mafic lower crust and/or a zone of depleted mantle beneath a former, thermally equilibrated, orogenic area prevents the reactivation of the inherited weaknesses during a subsequent episode of extension (e.g. Models 2–4, and 6–8; see also the model in Annex E section E1). In contrast, when the underplating and its depleted mantle source are significantly hotter, thus weaker than the encompassing material, the inherited weaknesses concentrate the extensional deformation. In this case, breakup occurs within the former orogenic area (e.g. Model 5). In addition, the models show that a higher initial geotherm in such lithospheres contributes to a more protracted and delocalized rifting, comparably to when the lithosphere is horizontally homogeneous (e.g. Buck et al., 1999, for example).

When the geotherm of the lithosphere is high enough (here for Moho temperature > 450°C), strong heterogeneities within the lower crust and/or the upper mantle trigger the simultaneous development of several necking instabilities (Models3, 4 and 6–8 in Figure 7; see also the model in Annex E). This translates into the contemporaneous formation of several necked or hyperextended basins adjacent to little- or un-thinned regions of continental crust (including the underplated area), which may cause the *boudinage* of the continental crust.

It is also worthwhile to note that, in the reference model without underplating (Model 1 in Figure 7), hyperextension does not eventually localize at the suture zone, although it is the largest and the weakest heterogeneity embedded in our models (it crosscuts the whole crust and has a serpentine rheology; see Figure 6). Indeed, extension focuses between the two adjacent antithetic weak zones, which affects only the upper crust and have a dry quartzite rheology with reduced cohesion and internal angle of friction (the modelled 'fold-and-thrust belt'). The reason for this is that the extension of the crust is initially accommodated by the suture and the second adjacent conjugate 'fault', which induces the uplift of the underlying asthenosphere between these two structures. From the moment the rising of the asthenosphere becomes an active upwelling because of its lower density, it controls the location of extension. Note that in this model, the asymmetry of the conjugate margins seems to be essentially controlled by the initial distribution of the weak heterogeneities.

Of course, additional factors, such as the intensity of strain weakening within faults and the difference in density between the depleted mantle and the encompassing 'standard mantle' may have a significant impact on the architecture and evolution of rift systems. Yet both parameters are still relatively poorly constrained. Therefore, I ran some numerical models to test these parameters. The results of these preliminary tests are displayed in Annex D.

Is it possible to apply these results to the analysis of the North Atlantic rift system over the underplated Variscan lithosphere?

On the one hand, the results presented in the previous paragraph may explain why both the Alpine Tethys and southern North Atlantic rift systems circumvented the underplated Variscan lithosphere in Western Europe, while the northern North Atlantic rift reactivated the Caledonian Iapetus suture – and temporarily the Tornquist suture (Erratt et al., 1999) – in the regions where no significant post-orogenic magmatism is recorded (Figure 8). In addition, the development of both the Central Trough in the North Sea and of the Porcupine Basin southwest United-Kingdom seem to stop close to the edge of the underplated region (Figure 8), supporting the proposition that underplating may act as a barrier to the propagation of subsequent rifting.

However, the Bay of Biscay is a striking counterexample to this theory, since it opened apparently within a region thought to be underplated. In this case, the strike slip North Pyrenean fault inherited from the late Variscan evolution (Arthaud and

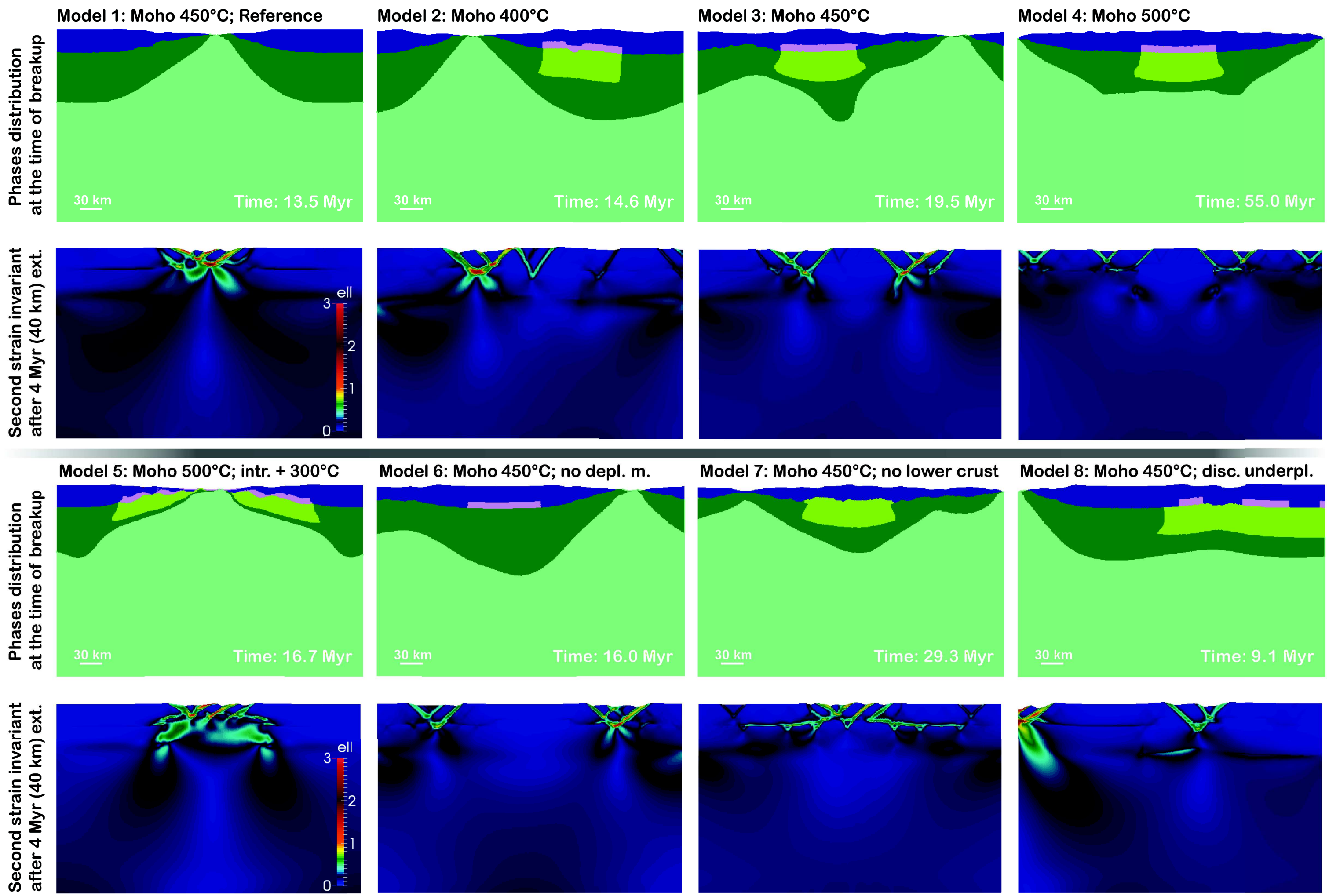

Figure 7 – Synthesis of the 8 numerical models presented in Chapter III. Top panels: phase distribution at the time of 'breakup'; bottom panels: second invariant of strain after 4 Myr (40 km) extension.

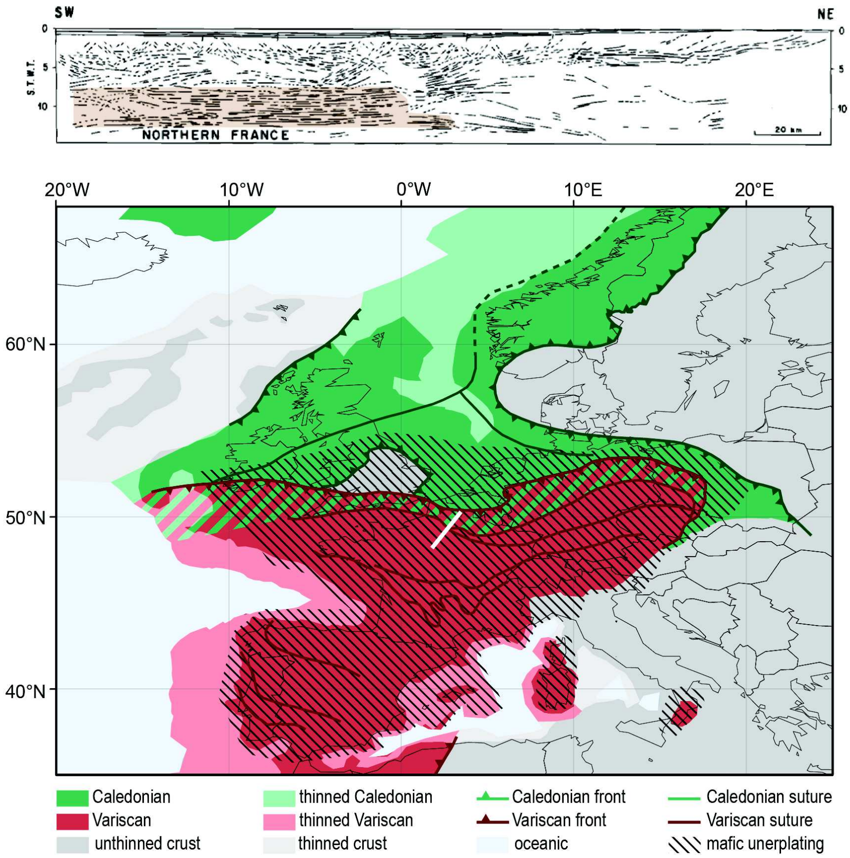

Figure 8 – Seismic section from Bois et al. (1989) through the Variscan orogenic area – see the map below for location; Map showing the distribution of orogenic domains, post-orogenic underplating and rift systems in Western Europe.

Matte, 1977; Burg et al., 1994) may have been reactivated during the initial transtensive, strike-slip opening of the Bay of Biscay (Jammes et al., 2009). Because major strike-slip faults are pervasive structures, which can crosscut the whole lithosphere (Vauchez et al., 1998), the North Pyrenean fault may have remained a weak zone despite the Variscan underplating. In particular, such structures are particularly sensitive to transcurrent motions.

On the other hand, the phenomenon of necking instability triggered by underplating may explain the formation of the continental ribbons offshore Iberia, Canada and United Kingdom (Galicia Bank, Flemish Cap, and Rockall and Hatton banks, respectively), as well as the 'failed' Porcupine and Celtic Sea rift basins. Indeed, the southern part of the North Atlantic rift system developed over orogenic lithosphere, which experienced a magma-rich orogenic collapse, as evidenced by the pre-rift mafic lower crust observable on seismic sections in these regions (e.g. Díaz and Gallart, 2009; Freeman et al., 1988; Van Avendonk et al., 2009).

In contrast, there is no evidence for post-orogenic underplating in Northern United Kingdom and Western Norway (Nirrengarten et al., 2014). There, the polyphase rifting punctuated by periods of relaxation (Doré et al., 1999) may account for the multiple rift basins architecture of this margin, since during extension, the thinned crust is replaced by lithospheric mantle, which is stronger once it has cooled down. Because such a material is harder to rift, extension will localize elsewhere during the next episode of rifting (Buck et al., 1999). An alternative explanation could involve zones of depleted mantle remaining from former magmatic arcs (and/or forearc/backarc basins) associated with the subduction of the Iapetus ocean. Indeed, Müntener and Manatschal (2006) interpreted the depleted peridotites drilled on the Newfoundland margin as residual mantle beneath a magmatic arc related to the subduction of this wide ocean. However, this hypothesis is tricky to test, since sampling the mantle underlying the Rockall, Hatton or Porcupine banks offshore United Kingdom is difficult.

Besides, in the model without underplating (Model 1 in Figure 7), the fact that breakup is not achieved directly at the location of the 'suture' but between two fault of the adjacent 'fold-and-thrust belt' could be compared with the northern North Atlantic rift. Indeed, between Norway and Greenland, extension affected the Iapetus suture but the eventual breakup is offset, occurring within the fold-and-thrust belt (Figure 8).

8 General discussion

The role of inheritance in controlling tectonic processes is a long-standing question in Earth Science. In particular, one may ask if the Wilson Cycle, the theory stating that oceans tend to open and close along the same lines, is somehow a consequence of orogenic and/or rift-related inheritance. The North Atlantic is a particularly suitable region to address this question, since it comprises two distinct orogenic domains with contrasting geologic histories, both overprinted by a same rifting event during the Mesozoic.

The impact of orogenic inheritance on the North Atlantic rifting

The comparison of the maps displaying orogenic inheritance, rift domains and rift timing (Figures 1, 2 and 3, respectively; see also Chapter I), highlights **major differences in the architecture, duration and amount of breakup-related magmatism in the North Atlantic, depending on whether the rift system affected the Caledonian or Variscan orogenic lithosphere** (Figure 9). Indeed, the rift cut through the Caledonian orogenic lithosphere, was protracted (> 80 Myr) and polyphase, and breakup was magma-rich north of the Variscan front. In contrast, the North Atlantic rift circumvented the core of the Variscides in Western Europe, had a 'short' duration (< 50 Myr) and 'magma-poor' lithospheric breakup was achieved after one, apparently continuous, episode of extension to the south.

These observations support the proposition that **orogenic inheritance impacts considerably subsequent rifting, but its influence may be significantly different depending on the characteristics of the orogenic lithosphere involved**. Note, however, that strictly speaking, the rift followed the former Iapetus suture only in the northernmost part of the North Atlantic, i.e. offshore Norway. The Jurassic southward propagating 'Arctic rift' (i.e. the southward-propagating part of the northern North Atlantic rift; see Roberts et al., 1999) followed initially the Iapetus and Tornquist sutures further south, which formed the Viking Graben and Central Trough in the North Sea. However, this part of the rift system was abandoned during the Cretaceous (Erratt et al., 1999), after which the mature, northward propagating Atlantic rift and the immature Arctic rift became coalescent offshore United Kingdom (Figure 7 in Chapter *General geological setting*; Roberts et al., 1999; Torsvik et al., 2002; Ziegler, 1988). The complex stress pattern induced by these two 'competing' rifts may have caused the deflection of the Arctic rift from its initial way along the suture.

Impact of the thermal state of the lithosphere

A first possible factor controlling the behaviour of the rift may be the thermal state of the lithosphere at the onset of rifting, which depends primarily on the time lag between the last orogenic event and the onset of rifting. In the North Atlantic region, ~ 200 Myr elapsed between the end of the Caledonian orogeny and the onset of necking, whereas this time lag was only ~ 100 Myr between the termination of the Variscides and the onset of necking in the southern North Atlantic. Note that, as horizontal thermal re-equilibration is usually achieved in less than 100 Myr (Jaupart and Mareschal, 2007), it is likely that no significant thermal heterogeneity existed

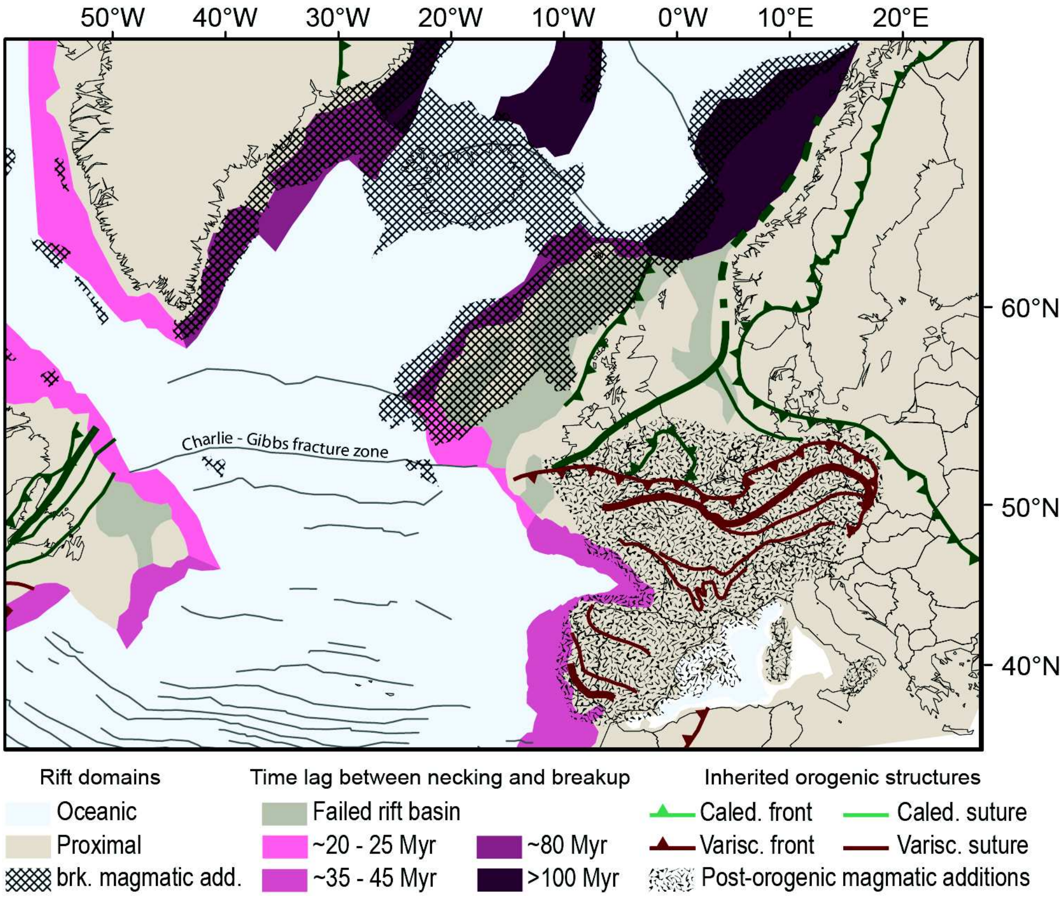

Figure 9 – Map synthesizing the location of Caledonian and Variscan sutures and deformations fronts, the area affected by significant post-orogenic magmatic activity, the location of the major rift domains, the extent of breakup-related and post-rift magmatic additions and the time lag between the onset of necking and the lithospheric breakup in the region of the North Atlantic. See text for discussion.

in either of these orogenic lithospheres. Thus, the major difference in the thermal structure of both orogenic lithosphere was presumably only a higher geothermal gradient in the Variscan area than in the Caledonian. According to Čermák and Bodri (1986), Moho temperatures were about $\sim$ 500–600°C and 350–500°C, respectively. Yet, as shown by Buck (1991) and evidenced by the numerical experiments described in Chapter III, higher initial geotherms result in more distributed extension and protracted rifting, which is the opposite to what is observed. Therefore, the thermal state cannot account for the different architecture and evolution of the North Atlantic rift with respect to the Caledonian and Variscan lithospheres.

Impact of the magmatic intensity of the post-orogenic collapse

The magma-rich versus magma-poor nature of the post-orogenic collapse is another potential explanation for the difference in rift characteristics between the Caledonian and Variscan lithospheres in Western Europe. Indeed, while the collapse of the Caledonian range is essentially controlled by mechanical processes, the significant magmatic event associated with the collapse of the Variscan range resulted in rejuvenation of the lower crust by mafic underplating (Costa and Rey, 1995; Rey, 1993). This event probably welded the different crustal blocks together and depleted the underlying mantle in the most incompatible elements.

Because thermal re-equilibration is usually achieved in less than 100 Myr (Jaupart and Mareschal, 2007), the Variscan lithosphere was presumably horizontally equilibrated, although its geotherm may have been still relatively high (Moho temperature up to $\sim 600°C$ according to Müntener and Manatschal, 2006). In such a framework, the numerical models described in Chapter III support the hypothesis that **the massive magmatic underplating underlying the Variscan range may be the cause for both the North Atlantic and the Alpine Tethys rift systems to have circumvented the Variscan orogenic area of Western Europe**.

This hypothesis may also explain why extension is localized at the edge of the orogenic area in the Basin and Range province in Western United States, as evidenced by the distribution of seismic activity published by Bennett (2003). Indeed, in this region, the orogenic collapse of the Laramide range was associated with an important magmatic episode, comparably to the Variscides. Like in Western Europe, it resulted in the emplacement of an up to 10 km thick mafic underplating, well-imaged on seismic sections (Bois et al., 1989; Rey, 1993).

Moreover, both the southward propagation of the initial Arctic rift system through the North Sea, and the northward propagation of the Atlantic rift through the Porcupine Basin seem to have stopped where they reach the underplated part of the orogenic lithosphere (see Figure 9). Indeed, the existence of mafic underplating can be inferred from the seismically layered and reflective lower crust imaged by the BIRPS survey in southern and eastern North Sea as well as in southwest United-Kingdom (Blundell et al., 1991; Bois et al., 1990). These observations support the hypothesis that underplating may act as a barrier to the propagation of future rifts.

The impact of paleogeography

It is likely that the pre-orogenic settings did significantly impact the construction of Caledonian and Variscan ranges. Indeed, the different number and size of the intervening oceans did presumably influence the thermal, structural and lithologic characteristics of the orogenic lithosphere, which in turn, probably controlled at least partially the subsequent rifting.

The Scandinavian Caledonides resulted from the closure of the wide Iapetus Ocean between two major cratonic shields of Laurentia and Baltica (Hossack and Cooper, 1986; Roberts, 2003; van Staal et al., 2012), while the Variscides were mainly formed by the accretion of several continental ribbons and/or microcontinents following the suturing of several 'narrow oceans', in addition to the closure of the wide Rheic Ocean (Franke, 2006; Kröner and Romer, 2013). Yet, as highlighted in Chapter II, major differences in the characteristics of orogens can be expected, depending on whether they arise from the closure of 'narrow' or 'wide oceans'. In the following, I use the term 'mature' to describe orogens resulting from the closure of wide oceans after protracted subduction of their oceanic lithosphere, as opposed to 'immature orogens' consequent to the closure of narrow oceans.

'Immature orogenies' are essentially controlled by mechanical processes, and no significant change in the lithology, composition or thermal state of the lithosphere is to be expected in the early stages of continental collision, except from hydration in the mantle wedge. **In contrast, both the composition and thermal state of the crust and mantle are strongly modified by the magmatic and metamorphic processes associated with long-lasting subductions** (Faccenda et al., 2008; Gerya and Meilick, 2011; Stern, 2002). Therefore, at least the continental margin on the upper plate has been significantly modified when continental collision following the closure of a wide ocean arises.

Furthermore, the considerably different compositions of both the lithospheric and asthenospheric mantle underlying short-lived versus long-lasting subductions may reverberate in the magmatic budget of the subsequent orogenic collapse. Indeed, as the **closure of narrow oceans** is unlikely to form a volcanic arc, the composition of the lithospheric mantle is little modified during subduction, and **the overlying asthenospheric mantle wedge is not depleted**. It may even be more or less fertilized by sediments and fluids, depending on the number and size of the basin(s) involved, the thickness of its (their) sedimentary cover, and the proportion of accreted versus subducted sediments (Clift et al., 2004). **In contrast,**

magmatic activity associated with volcanic arcs (and potentially also forearc- and backarc basins) in the case of a **protracted subduction may significantly deplete the asthenospheric mantle wedge** (Müntener and Manatschal, 2006). Although vigorous convection may tend to limit this imbalance, a lower fertility of the asthenospheric mantle is still to be expected in this region compared to a mantle wedge overlying an immature subduction (see Martinez and Taylor, 2002). Therefore, **the orogenic collapse of immature orogens is more likely to be accompanied with significant asthenospheric magmatism than that of mature orogens**.

This hypothesis may account for both the a-magmatic collapse of the mature Caledonian range in Scandinavia and for the large amount of magmatism during orogenic collapse of the largely immature Variscan orogen in Western Europe. Alternatively, the magma-poor orogenic collapse of the Caledonides may be explained by the significantly thicker, colder and more depleted mantle of the East-European and North American cratons involved in this orogeny (Bernstein et al., 1998; Beyer et al., 2004; Griffin et al., 2003).

Note, however, that the closure of one single narrow oceanic basin may be unlikely to create a topography important enough to trigger a large-scale orogenic collapse. Therefore asthenosphere-fed magmatic orogenic collapse (as opposed to only crustal partial melting) may be proper to orogens resulting from the closure of multiple narrow oceanic basins, or potentially to mature orogens with well-homogenized mantle wedge . Yet, this assumption is tricky to test, since, on the one hand, no orogen comparable to the Variscan one is known at present, and on the other hand, few rejuvenated lithospheres consequent to a magma-rich orogenic collapse have been indisputably identified in the world so far.

The architecture of narrow/immature versus wide/mature oceans

Because immature orogenies are essentially controlled by mechanical processes, rift-related inheritance plays presumably a dominant role in their development. Thus, understanding the resulting orogen requires to have a good knowledge of the initial architecture of the intervening rift systems. The statistical analysis presented in Chapter II suggests that some common features stand out in all rifted margins. Indeed, **on a first order, most rifted margins display a similar succession of comparable rift domains** (Péron-Pinvidic et al., 2013; Sutra et al., 2013). Moreover, **the width and rheology of the hyperextended domain seems to be relatively consistent amongst rifted margins**, independently from the length of the distal domain and the maturity of the rift system. In this respect, **the hyperextended domain may be considered as controlled by the same rift-induced processes in every rift systems, independently from its initial inheritance** (see Chapter II; Manatschal et al., 2015; Sutra and Manatschal, 2012, Nirrengarten et al., subm.).

In contrast, **the characteristics of the proximal and necking domains display a higher variability** in both their width and composition, probably because they remain **essentially controlled by (post-)orogenic inheritance** (Manatschal et al., 2015). Note that the exhumation domain may exist only in 'magma-poor' rifted margins, thus it cannot be considered as an ubiquitous characteristic.

From the observations exposed in the previous paragraph, it is interesting to note that, **in the architecture and lithology of rifted margins, 'inherited' seems to be tantamount to 'variability', whereas 'rift-induced' to 'consistency'**. Similarly, physico-chemical **processes associated with long-lasting, steady-state subductions seem to be quite consistent** (i.e. formation of magmatic arcs and associated magmatic processes and high T/low P metamorphism; see Stern, 2002; Uyeda, 1981), whereas nothing can be predicted for transient or short-lived subductions. As a consequence, **more variability can be expected in orogens resulting from the closure of narrow oceans compared to orogens consequent to the closure of wide oceans**.

Conclusion & Perspectives

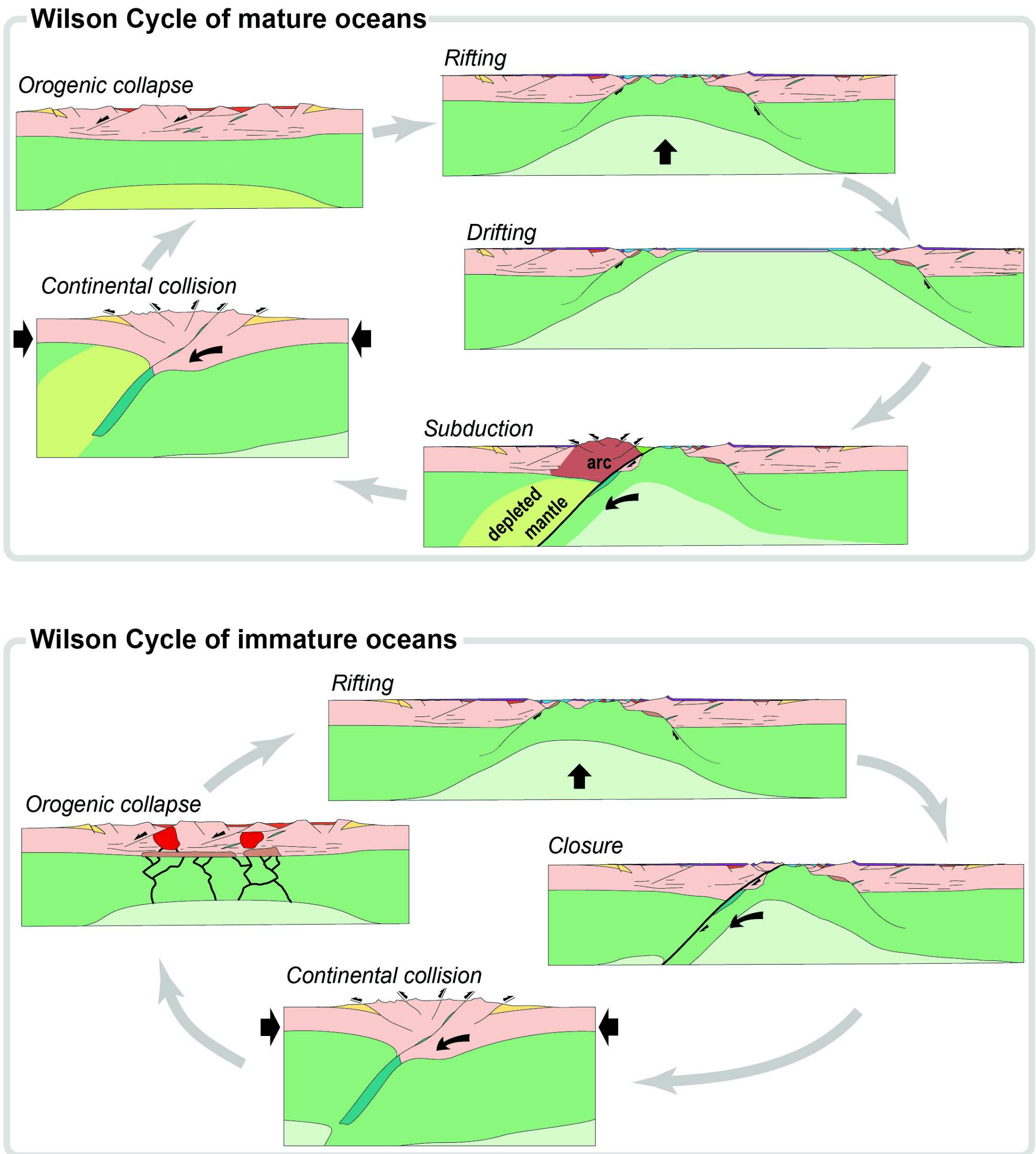

Figure 1 – Illustration of the two end-members of the Wilson Cycle as hypothesized in this study (modified after Petri, 2014).

Tectonic inheritance seems to significantly impact all the steps of the Wilson Cycle, and in a different way depending on the size and the maturity of the system involved. Therefore, it may be interesting to distinguish between two end-members for the Wilson Cycle (Figure 1): On the one hand, the transient subduction associated with the closure of a narrow and immature ocean may end up in an orogeny essentially controlled by mechanical processes. In such cases, the architecture of the resulting orogen may be primarily controlled by the initial (inherited) architecture of the intervening margins. Because of the variability of this inheritance, a high degree of variability between the different orogens of this type is to be expected as well. On the other hand, the protracted subduction associated with the closure of a wide and mature ocean usually forms magmatic arcs (and possibly also forearc- and/or backarc basins) and causes the depletion of the overlying mantle wedge. As these processes strongly modify the lithology and the thermal state of both the crust and the mantle, the final orogeny may be significantly controlled by the result of these subduction-induced processes. As a consequence, a certain consistency in the architecture of this type of orogens is to be expected.

In addition, because of mantle depletion caused by arc magmatism and also possible seafloor spreading in the forearc- and/or backarc basins, the magmatic budget available at the time of post-orogenic collapse may be relatively low for orogens resulting from the closure of wide, mature oceans. In contrast, the magmatic budget may be much higher for an orogen produced by the a-magmatic closure of one or several narrow, immature rift systems.

Yet, large-scale mafic underplating may possibly act as a barrier to rifting, thus control whether or not the subsequent ocean will form within the former orogenic area. In that framework, orogenic structures from immature orogens may not be reactivated during subsequent rifting events, in contrast to orogenic structures from mature orogens. However, further investigations are required in order to test these assumptions.

Stepping back leads to another first-order question: why do both wide/ mature and narrow/immature oceans exist? Although there is indisputable evidence for hyperextended rift systems, which failed in developing a mature accretionary system, what processes and/or inheritance initially control whether or not a rift system achieves lithospheric breakup and develops steady-state seafloor spreading remains, so far, an open question.

General references

General references

Abdelmalak, M. M., Andersen, T. B., Planke, S., Faleide, J. I., Corfu, F., Tegner, C., Shephard, G. E., Zastrozhnov, D., and Myklebust, R. (2015). The ocean-continent transition in the mid-Norwegian margin: Insight from seismic data and an onshore Caledonian field analogue. *Geology*, 43(11):G37086.1.

Afilhado, A., Matias, L., Shiobara, H., Hirn, A., Mendes-Victor, L., and Shimamura, H. (2008). From unthinned continent to ocean: The deep structure of the West Iberia passive continental margin at 38°N. *Tectonophysics*, 458:9–50.

Allègre, C. and Dars, R. (2009). *La géologie, passé, présent et avenir de la Terre*. Pour la Science, belin edition.

Amiguet, E., Van De Moortèle, B., Cordier, P., Hilairet, N., and Reynard, B. (2014). Deformation mechanisms and rheology of serpentines in experiments and in nature. *Journal of Geophysical Research*, 119:4640–4655.

Andersen, T. B. (1998). Extensional tectonics in the Caledonides of southern Norway, an overview. *Tectonophysics*, 285:333–351.

Andersen, T. B., Corfu, F., Labrousse, L., and Osmundsen, P.-T. (2012). Evidence for hyperextension along the pre-Caledonian margin of Baltica. *Journal of the Geological Society*, 169(5):601–612.

Anderson, D. L. (2006). Speculations on the nature and cause of mantle heterogeneity. *Tectonophysics*, 416(1-4):7–22.

Andreani, M., Mével, C., Boullier, A.-M., and Escartín, J. (2007). Dynamic control on serpentine crystallization in veins: Constraints on hydration processes in oceanic peridotites. *Geochemistry, Geophysics, Geosystems*, 8(2):n/a–n/a.

Andréasson, P. G., Gee, D. G., Whitehouse, M. J., and Schoberg, H. (2003). Subduction-flip during Iapetus Ocean closure and Baltica-Laurentia collision, Scandinavian Caledonides. *Terra Nova*, 15(6):362–369.

Anonymous (1972). Penrose field conference on ophiolites. In *Penrose Field Conference on ophiolites*, volume 17, pages 24–25. Geotimes.

Aoki, I. and Takahashi, E. (2004). Density of MORB eclogite in the upper mantle. *Physics of the Earth and Planetary Interiors*, 143-144:129–143.

Arenas, R., Martínez Catalán, J. R., Sánchez Martínez, S., Díaz García, F., Abati, J., Fernández-Suárez, J., Andonaegui, P., and Gómez-Barreiro, J. (2007). Paleozoic ophiolites in the Variscan suture of Galicia (northwest Spain): Distribution, characteristics, and meaning. In Hatcher, R. D. J., Carlson, M. P., McBride, J. H., and Martínez Catalán, J. R., editors, *4-D framework of Continental Crust*, volume 200, pages 1–20. Geological Society of America Memoir 200.

Arenas, R., Sánchez Martínez, S., Gerdes, A., Albert, R., Díez Fernández, R., and Andonaegui, P. (2014). Re-interpreting the Devonian ophiolites involved in the Variscan suture: U,ÄìPb and Lu,ÄìHf zircon data of the Moeche Ophiolite (Cabo Ortegal Complex, NW Iberia). *International Journal of Earth Sciences*, 103:1385–1402.

Artemieva, I. M. and Thybo, H. (2013). EUNAseis: A seismic model for Moho and crustal structure in Europe, Greenland, and the North Atlantic region. *Tectonophysics*, 609:97–153.

Artemieva, I. M., Thybo, H., and Kaban, K. K. (2006). Deep Europe today: geophysical synthesis of the upper mantle structure and lithospheric processes over 3.5 Ga. *Geological Society London Memoirs*, 32:11–41.

Arthaud, F. and Matte, P. (1977). Late Paleozoic strike-slip faulting in southern Europe and northern Africa: Result of a right-lateral shear zone between the Appalachians and the Urals. *Geological Society of America Bulletin*, 88(9):1305–1320.

Asher, J., Warren, M., Fox, R., Harding, P., Jeffcoate, G., and Jeffcoate, S. (2001). *The millennium atlas of butterflies in Britain and Ireland.* Oxford University Press.

Aslanian, D., Moulin, M., Olivet, J. L., Unternehr, P., Matias, L., Bache, F., Rabineau, M., Nouzé, H., Klingelheofer, F., Contrucci, I., and Labails, C. (2009). Brazilian and African passive margins of the Central Segment of the South Atlantic Ocean: Kinematic constraints. *Tectonophysics*, 468(1-4):98–112.

Audet, P. and Bürgmann, R. (2011). Dominant role of tectonic inheritance in supercontinent cycles. *Nature Geoscience*, 4(3):184–187.

Augier, R., Choulet, F., Faure, M., and Turrillot, P. (2015). A turning-point in the evolution of the Variscan orogen: the ca. 325 Ma regional partial-melting event of the coastal South Armorican domain (South Brittany and Vendee, France). *Bulletin de la Société Géologique de France*, 186(2-3):63–91.

Babeyko, A. and Sobolev, S. (2008). High-resolution numerical modeling of stress distribution in visco-elasto-plastic subducting slabs. *Lithos*, 103(1-2):205–216.

Bach, W., Garrido, C. J., Paulick, H., Harvey, J., and Rosner, M. (2004). Seawater-peridotite interactions: First insights from ODP Leg 209, MAR 15°N. *Geochemistry, Geophysics, Geosystems*, 5(9):n/a–n/a.

Ballèvre, M., Bosse, V., Ducassou, C., and Pitra, P. (2009). Palaeozoic history of the Armorican Massif: Models for the tectonic evolution of the suture zones. *Comptes Rendus Geoscience*, 341:174–201.

Bard, J. P., Maluski, H., Matte, P., and Proust, F. (1980). The Kohistan sequence: crust and mantle of an obducted island arc. *Geol. Bull. Univ. Peshawar*, 11:87–94.

Beltrando, M., Manatschal, G., Mohn, G., Dal Piaz, G. V., Vitale Brovarone, A., and Masini, E. (2014). Recognizing remnants of magma-poor rifted margins in high-pressure orogenic belts: The Alpine case study. *Earth-Science Reviews*, 131:88–115.

Bennett, V. C. (2003). Compositional Evolution of the Mantle. *Treatise on Geochemistry*, 2:493–519.

Bernstein, S., Kelemen, P. B., and Brooks, C. (1998). Depleted spinel harzburgite xenoliths in Tertiary dykes from East Greenland: Restites from high degree melting. *Earth and Planetary Science Letters*, 154(1-4):221–235.

Bertotti, G. (1991). Early Mesozoic extension and Alpine shortening in the western Southern Alps: The geology of the area between Lugano and Menaggio (Lombardy, Northern Italy). *Mem. Soc. Geol. Padova*, 43:17–123.

Beyer, E. E., Brueckner, H. K., Griffin, W. L., O'Reilly, S. Y., and Graham, S. (2004). Archean mantle fragments in Proterozoic crust, Western Gneiss Region, Norway. *Geology*, 32(7):609–612.

Billen, M. I. (2008). Modeling the Dynamics of Subducting Slabs. *Annual Review of Earth and Planetary Sciences*, 36(1):325–356.

Blundell, D. J., Hobbs, R. W., Klemperer, S. L., Scott-Robinson, R., Long, R. E., West, T. E., and Duin, E. (1991). Crustal structure of the central and southern North Sea from BIRPS deep seismic reflection profiling. *Journal of the Geological Society*, 148(3):445–457.

Blystad, P., Brekke, H., Færseth, R. B., Larsen, B. T., Skogseid, J., and Tørudbakken, B. (1995). Structural elements of the Norwegian continental shelf. part II: The Norwegian Sea region. *Norwegian Petroleum Directorate Bulletin*, 8:45.

Boillot, G., Féraud, G., Recq, M., and Girardeau, J. (1989). Undercrusting by serpentinite beneath rifted margins. *Nature*, 341(6242):523–525.

Boillot, G., Recq, M., Winterer, E., Meyer, A., Applegate, J., Baltuck, M., Bergen, J., Comas, M., Davies, T., Dunham, K., Evans, C., Girardeau, J., Goldberg, G., Haggerty, J., Jansa, L., Johnson, J., Kasahara, J., Loreau, J., Luna-Sierra, E., Moullade, M., Ogg, J., Sarti, M., Thurow, J., and Williamson, M. (1987). Tectonic denudation of the upper mantle along passive margins: a model based on drilling results (ODP leg 103, western Galicia margin, Spain). *Tectonophysics*, 132(4):335–342.

Bois, C., Lefort, J.-P., Le Gall, B., Sibuet, J.-C., Gariel, O., Pinet, B., and Cazes, M. (1990). Superimposed Variscan, Caledonian and Proterozoic features inferred from deep seismic profiles recorded between southern Ireland, Southwestern Britain and western France. *Tectonophysics*, 177(1-3):15–37.

Bois, C., Pinet, B., and Roure, F. (1989). Dating lower crustal features in france and adjacent areas from deep seismic profiles. *Geophysical Monograph Series*, 51:17–31.

Bonatti, E. and Michael, P. J. (1989). Mantle peridotites from continental rifts to ocean basins to subduction zones. *Earth and Planetary Science Letters*, 91(3-4):297–311.

Boschi, C., Früh-Green, G. L., Delacour, A., Karson, J. A., and Kelley, D. S. (2006). Mass transfer and fluid flow during detachment faulting and development of an oceanic core complex, Atlantis Massif (MAR 30°N). *Geochemistry, Geophysics, Geosystems*, 7(1):n/a–n/a.

Bosworth, W., Huchon, P., and McClay, K. (2005). The Red Sea and Gulf of Aden Basins. *Journal of African Earth Sciences*, 43(1-3):334–378.

Bronner, A., Sauter, D., Manatschal, G., Péron-Pinvidic, G., and Munschy, M. (2011). Magmatic breakup as an explanation for magnetic anomalies at magma-poor rifted margins. *Nature Geoscience*, 4:549–553.

Brown, E. L. and Lesher, C. E. (2014). North Atlantic magmatism controlled by temperature, mantle composition and buoyancy. *Nature Geoscience*, 7(11):820–824.

Brown, M. (2009). Metamorphic patterns in orogenic systems and the geological record. *Geological Society, London, Special Publications*, 318(1):37–74.

Buck, R., Lavier, L. L., and Poliakov, A. N. B. (1999). How to make a rift wide. *Philosophical Transactions of the Royal Society A: Mathematical, Physical and Engineering Sciences*, 357(1753):671–693.

Buck, W. R. (1991). Modes of continental lithospheric extension. *Journal of Geophysical Research*, 96(B12):20,161–20,178.

Buck, W. R., Lavier, L. L., and Babeyko, A. (2003). A Numerical Model of Lithospheric Extension Producing Fault-Bounded Basins and Ranges. *International Geology Review*, 45(8):712–723.

Buiter, S. J. H. and Torsvik, T. H. (2014). A review of Wilson Cycle plate margins: A role for mantle plumes in continental break-up along sutures? *Gondwana Research*, 26(2):627–653.

Burg, J.-P. (2011). Arc-Continent Collision. In *The Asia,ÄìKohistan,ÄìIndia Collision: Review and Discussion*, Frontiers in Earth Sciences, pages 279–309. Springer Berlin Heidelberg, Berlin, Heidelberg.

Burg, J.-P., Driessche, Van den, J., and Brun, J.-P. (1994). Syn- to post-thickening extension : mode and consequences. *Comptes rendus de l'Académie des sciences. Série 2. Sciences de la terre et des planètes*, 319(9):1019–1032.

Burov, E. and Yamato, P. (2008). Continental plate collision, P,ÄìT,Äìt,Äìz conditions and unstable vs. stable plate dynamics: Insights from thermo-mechanical modelling. *Lithos*, 103(1-2):178–204.

Bussy, F., Hernandez, J., and Von Raumer, J. (2000). Bimodal magmatism as a consequence of the post-collisional readjustment of the thickened Variscan continental lithosphere (Aiguilles Rouges,ÄìMont Blanc Massifs, Western Alps). *Geological Society of America Special Papers*, 350:221–233.

Butler, R. W. H. (2013). Area balancing as a test of models for the deep structure of mountain belts, with specific reference to the Alps. *Journal of Structural Geology*, 52(1):2–16.

Butler, R. W. H., Tavarnelli, E., and Grasso, M. (2006). Structural inheritance in mountain belts: An Alpine-Apennine perspective. *Journal of Structural Geology*, 28(11):1893–1908.

Buzzi, L. and Gaggero, L. (2008). Petrogenesis of post ,Äì orogenic Lower Permian andesites in southern Europe: insights into the collapse of the Variscan range. *Geodinamica Acta*, 21(5-6):273–290.

Cappelletti, A., Tsikalas, F., Nestola, Y., Cavozzi, C., Argnani, A., Meda, M., and Salvi, F. (2013). Impact of lithospheric heterogeneities on continental rifting evolution: Constraints from analogue modelling on South Atlantic margins. *Tectonophysics*, 608(0316):30–50.

Casteras, M. (1933). Recherches sur la structure du versant nord des Pyrénées centrales et orientales. *Bulletin du Service de la Carte Géologique de France*, 37:25.

Cawood, P. A., Kröner, A., Collins, W. J., Kusky, T. M., Mooney, W. D., and Windley, B. F. (2009). Accretionary orogens through Earth history. *Geological Society, London, Special Publications*, 318(1):1–36.

Cederbom, C., Larson, S., Tullborg, E.-L., and Stiberg, J.-P. (2000). Fission track thermochronology applied to Phanerozoic thermotectonic events in central and southern Sweden. *Tectonophysics*, 316:153–167.

Čermák, V. and Bodri, L. (1986). Two-dimensional temperature modelling along five East-European geotraverses. *Journal of Geodynamics*, 5(2):133–163.

Chalmers, J. a. and Pulvertaft, T. (2001). Development of the continental margins of the Labrador Sea: a review. *Geological Society, London, Special Publications*, 187(1):77–105.

Chenin, P. and Beaumont, C. (2013). Influence of offset weak zones on the development of rift basins: Activation and abandonment during continental extension and breakup. *Journal of Geophysical Research*, 118(4):1698–1720.

Chenin, P., Manatschal, G., Lavier, L. L., and Erratt, D. (2015). Assessing the impact of orogenic inheritance on the architecture, timing and magmatic budget of the North Atlantic rift system: a mapping approach. *Journal of the Geological Society*, 172(6):711–720.

Chevrot, S., Sylvander, M., Diaz, J., Ruiz, M., Paul, A., Cougoulat, G., Péquegnat, C., Wolyniec, D., Delmas, P., Grimaud, F., Benahmed, S., Pauchet, H., de Saint Blanquat, M., Lagabrielle, Y., and Manatschal, G. (2015). The Pyrenean architecture as revealed by teleseismic P-to-S converted waves recorded along two dense transects. *Geophysical Journal International*, 200(1):1096–1107.

Chian, D., Reid, I. D., and Jackson, H. R. (2001). Crustal structure beneath Orphan Basin and implications for nonvolcanic continental rifting. *Journal of Geophysical Research*, 106(B6):10,923–10,940.

Chopin, C. (1987). Very-High-Pressure Metamorphism in the Western Alps: Implications for Subduction of Continental Crust [and Discussion]. *Philosophical Transactions of the Royal Society A: Mathematical, Physical and Engineering Sciences*, 321(1557):183–197.

Christensen, N. I. (1970). Composition and evolution of the oceanic crust. *Marine Geology*, 8:139–154.

Clift, P. D., Dewey, J. F., Draut, A. E., Chew, D. M., Mange, M., and Ryan, P. D. (2004). Rapid tectonic exhumation, detachment faulting and orogenic collapse in the Caledonides of western Ireland. *Tectonophysics*, 384(1-4):91–113.

Clift, P. D. and Turner, J. (1998). Paleogene igneous underplating and subsidence anomalies in the rockall-Faeroe-Shetland area. *Marine and Petroleum Geology*, 15(3):223–243.

Cocks, L. R. M. and Fortey, R. A. (1982). Faunal evidence for oceanic separations in the Palaeozoic of Britain. *Journal of the Geological Society*, 139(4):465–478.

Cocks, L. R. M., McKerrow, W. S., and van Staal, C. R. (1997). The margins of Avalonia. *Geological Magazine*, 134(5):627–636.

Cocks, L. R. M. and Torsvik, T. H. (2005). Baltica from the late Precambrian to mid-Palaeozoic times: The gain and loss of a terrane's identity. *Earth-Science Reviews*, 72:39–66.

Cocks, L. R. M. and Torsvik, T. H. (2011). The Palaeozoic geography of Laurentia and western Laurussia: A stable craton with mobile margins. *Earth-Science Reviews*, 106:1–51.

Conder, J. A., Wiens, D. A., and Morris, J. (2002). On the decompression melting structure at volcanic arcs and back-arc spreading centers. *Geophysical Research Letters*, 29(15):17–1–17–4.

Connors, K. and Pryer, L. (2014). East Coast Magnetic Anomaly: Constraints, models and questions. In *4th Conjugate Margins Conference, 20,Äì22 August, St. John,Äôs, Canada*, pages 49–52.

Costa, S. and Rey, P. (1995). Lower crustal rejuvenation and growth during post-thickening collapse: Insights from a crustal cross section through a Variscan metamorphic core complex. *Geology*.

Coward, M. P., Enfield, M. A., and Fischer, M. W. (1989). Devonian basins of Northern Scotland: extension and inversion related to Late Caledonian – Variscan tectonics. *Geological Society, London, Special Publications*, 44(1):275–308.

Coward, M. P., Rex, D. C., Khan, M. A., Windley, B. F., Broughton, R. D., Luff, I. W., Petterson, M. G., and Pudsey, C. J. (1986). Collision tectonics in the NW Himalayas. *Geological Society, London, Special Publications*, 19(1):203–219.

Cundall, P. A. (1989). Numerical experiments on localization in frictional materials. *Ingenieur-Archiv*, 59(2):148–159.

Dadlez, R. (2000). Pomeranian Caledonides (NW Poland), fifty years of controversies: a review and a new concept. *Geological Quartely*, 44(3):221–236.

Dadlez, R., Kowalczewski, Z., and Znosko, J. (2013). Some key problems of the pre-Permian tectonics of Poland. *Geological Quarterly*, 38(2):169–190.

Dahlen, F. A. (1984). Noncohesive critical Coulomb wedges: An exact solution. *Journal of Geophysical Research*, 89(B12):10125.

Dal Piaz, G. V., Bistacchi, A., and Massironi, M. (2003). Geological outline of the Alps. *Episodes*, 26(3):175–180.

Davis, D., Dahlen, F. A., and Suppe, J. (1983). Mechanics of fold-and-thrust belts and accretionary wedges Cohesive Coulomb theory. *Journal of Geophysical Research*, 88(B2):1153–1172.

De Graciansky, P. C., Poag, C. W., Cunningham, R., Loubere, P., Masson, D. G., Mazzullo, J. M., Montadert, L., Müller, C., Otsuka, K., Reynolds, L. A., Sigal, J., Snyder, S. W., Townsend, H. A., Vaos, S. P., and Waples, D. (1985). The Goban Spur transect: Geologic evolution of a sediment-starved passive continental margin. *Geological Society of America Bulletin*, 96:58–76.

DeCelles, P. G. and Giles, K. A. (1996). Foreland basin systems. *Basin Research*, 8(2):105–123.

Desmurs, L., Müntener, O., and Manatschal, G. (2002). Onset of magmatic accretion within a magma-poor rifted margin: a case study from the Platta ocean-continent transition, eastern Switzerland. *Contributions to Mineralogy and Petrology*, 144(3):365–382.

Dewey, J. F. (1977). Suture zone complexities: a review. *Tectonophysics*, 40:53–67.

Dewey, J. F. (1988). Extensional collapse of orogens. *Tectonics*, 7(6):1123–1139.

Dewey, J. F. and Horsfield, B. (1970). Plate tectonics, orogeny and continental growth. *Nature*, 225:521–525.

Dewey, J. F., Ryan, P. D., and Andersen, T. B. (1993). Orogenic uplift and collapse, crustal thickness, fabrics and metamorphic phase changes: the role of eclogites. In Prichard, H. M., Alabaster, T., Harris, N. B. W., and Neary, C. R., editors, *Magmatic processes and plate tectonics*, pages 325–343. Geological Scociety Special Publication 76.

Díaz, J. and Gallart, J. (2009). Crustal structure beneath the Iberian Peninsula and surrounding waters: A new compilation of deep seismic sounding results. *Physics of the Earth and Planetary Interiors*, 173(1-2):181–190.

Dick, H. J. B., Lin, J., and Schouten, H. (2003). An ultraslow-spreading class of ocean ridge. *Nature*, 426(6965):405–412.

Direen, N. G., Stagg, H. M. J., Symonds, P. A., and Colwell, J. B. (2008). Architecture of volcanic rifted margins: new insights from the Exmouth–Gascoyne margin, Western Australia. *Australian Journal of Earth Sciences*, 55(3):341–363.

Doin, M.-P. and Henry, P. (2001). Subduction initiation and continental crust recycling : the roles of rheology and eclogitization. *Tectonophysics*, 342:163–191.

Domeier, M., Van Der Voo, R., and Torsvik, T. H. (2012). Paleomagnetism and Pangea: The road to reconciliation. *Tectonophysics*, 514-517:14–43.

Doré, A. G., Lundin, E. R., Fichler, C., and Olesen, O. (1997). Patterns of basement structure and reactivation along the NE Atlantic margin. *Journal of the Geological Society*, 154:85–92.

Doré, A. G., Lundin, E. R., Jensen, L. N., Birkelan, Ø., Eliassen, P. E., and Fichler, C. (1999). Principal tectonic events in the evolution of the northwest European Atlantic margin. In Fleet, A. J. and Boldy, S. A. R., editors, *Petroleum Geology of Northwest Europe: Proceedings of the 5th Conference*, pages 41–61. The Geological Society, London.

Doré, T. and Lundin, E. (2015). Hyperextended continental margins – Knowns and unknowns. *Geology*, 43(1):95–96.

Dörr, W. and Zulauf, G. (2010). Elevator tectonics and orogenic collapse of a Tibetan-style plateau in the European Variscides: the role of the Bohemian shear zone. *International Journal of Earth Sciences*, 99(2):299–325.

Drewes, H., Hornik, H., Ádám, J., and Rózsa, S. (2008). The Geodesist's Handbook. *Journal of Geodesy*, 82(11).

Dunbar, J. A. and Sawyer, D. S. (1989). How preexisting weaknesses control the style of continental breakup. *Journal of Geophysical Research*, 94(B6):7278–7292.

Ebbing, J. and Olesen, O. (2010). New compilation of top basement and basement thickness for the Norwegian continental shelf reveals the segmentation of the passive margin system. In Vining, B. A. and Pickering, S. C., editors, *Petroleum Geology: from mature basins to new frontiers - Proceedings of the 7th Conference*, number 6417, pages 885–897. The Geological Society, London.

Edel, J. B., Schulmann, K., Skrzypek, E., and Cocherie, A. (2013). Tectonic evolution of the European Variscan belt constrained by palaeomagnetic, structural and anisotropy of magnetic susceptibility data from the Northern Vosges magmatic arc (Eastern France). *Journal of the Geological Society*, 170:785–804.

Edwards, J. (2002). Development of the Hatton–Rockall Basin, North-East Atlantic Ocean. *Marine and Petroleum Geology*, 19(2):193–205.

Elliott, G. M. and Parson, L. M. (2008). Influence of margin segmentation upon the break-up of the Hatton Bank rifted margin, NE Atlantic. *Tectonophysics*, 457(3-4):161–176.

Enachescu, M. E. (2006). Structural setting and petroleum potential of the Orphan Basin, offshore Newfoundland and Labrador. *Recorder*, 31(2):5–13.

England, P., Engdahl, R., and Thatcher, W. (2004). Systematic variation in the depths of slabs beneath arc volcanoes. *Geophysical Journal International*, 156(2):377–408.

Ernst, W. G. (2005). Alpine and Pacific styles of Phanerozoic mountain building: subduction-zone petrogenesis of continental crust. *Terra Nova*, 17:165–188.

Ernst, W. G., Seki, Y., Onuki, H., and Gilbert, M. C. (1970). *Comparative Study of Low-Grade Metamorphism in the California Coast Ranges and the Outer Metamorphic Belt of Japan*, volume 124 of *Geological Society of America Memoirs*. Geological Society of America.

Erratt, D., Thomas, G. M., and Wall, G. R. T. (1999). The evolution of the Central North Sea Rift. In Fleet, A. J. and Boldy, S. A. R., editors, *Petroleum Geology of Northwest Europe: Proceedings of the 5th Conference*, pages 63–82. The Geological Society, London.

Escartín, J., Hirth, G., and Evans, B. (2001). Strength of slightly serpentinized peridotites: Implications for the tectonics of oceanic lithosphere. *Geology*, 29(11):1023–1026.

Faccenda, M., Gerya, T. V., and Chakraborty, S. (2008). Styles of post-subduction collisional orogeny: Influence of convergence velocity, crustal rheology and radiogenic heat production. *Lithos*, 103(1-2):257–287.

Faleide, J. I., Tsikalas, F., Breivik, A. J., Mjelde, R., Ritzmann, O., Engen, Ø., Wilson, J., and Eldholm, O. (2008). Structure and evolution of the continental margin off Norway and the Barents Sea. *Episodes*, 31(1):82–91.

Faure, M., Lardeaux, J.-M., and Ledru, P. (2009). A review of the pre-Permian geology of the Variscan French Massif Central. *Comptes Rendus Geoscience*, 341:202–213.

Finger, F. and Steyrer, H. P. (1990). I-type granitoids as indicators of a late Paleozoic convergent ocean-continent margin along the southern flank of the central European Variscan orogen. *Geology*.

Fletcher, R. C. and Hallet, B. (1983). Unstable extension of the lithosphere: A mechanical model for basin-and-range structure. *Journal of Geophysical Research*, 88(B9):7457.

Fossen, H., Gabrielsen, R. H., Faleide, J. I., and Hurich, C. A. (2014). Crustal stretching in the Scandinavian Caledonides as revealed by deep seismic data. *Geology*, 42(9):791–794.

Foulger, G. R. and Jurdy, D. M. (2007). *Plates, Plumes, and Planetary Processes*. The Geological Society of America special paper 430.

Foulger, G. R., Pritchard, M. J., Julian, B. R., Evans, J. R., Allen, R. M., Nolet, G., Morgan, W. J., Bergsson, B. H., Erlendsson, P., Jakobsdottir, S., Ragnarsson, S., Stefansson, R., and Vogfjörd, K. (2001). Seismic tomography shows that upwelling beneath Iceland is confined to the upper mantle. *Geophysical Journal International*, 146(2):504–530.

Franke, D., Ladage, S., Schnabel, M., Schreckenberger, B., Reichert, C., Hinz, K., Paterlini, M., de Abelleyra, J., and Siciliano, M. (2010). Birth of a volcanic margin off Argentina, South Atlantic. *Geochemistry, Geophysics, Geosystems*, 11(2):n/a–n/a.

Franke, W. (2000). The mid-European segment of the Variscides: tectonostratigraphic units, terrane boundaries and plate tectonic evolution. *Geological Society, London, Special Publications*, 179(1):35–61.

Franke, W. (2006). The Variscan orogen in Central Europe: construction and collapse. *Geological Society, London, Memoirs*, 32(1):333–343.

Franke, W. (2014). Topography of the Variscan orogen in Europe: failed,Äìnot collapsed. *International Journal of Earth Sciences*, 103(5):1471–1499.

Franke, W., Dallmayer, R. D., and Weber, K. (1995). Geodynamic evolution. In Dallmeyer, R. D., Franke, W., and Weber, K., editors, *Pre-Permian Geology of Central and Eastern Europe*, pages 579–593. Springer Berlin Heidelberg, Berlin, Heidelberg.

Franke, W. and Engel, W. (1988). Tectonic settings of synorogenic sedimentation in the Variscan belt of Europe. In Besly, B. M. and Kelling, G., editors, *Sedimentation in a synorogenic basin complex: the Upper Carboniferous of Northwest Europe*, pages 8–17. Blackie, Glasgow.

Freeman, B., Klemperer, S. L., and Hobbs, R. W. (1988). The deep structure of northern England and the Iapetus Suture zone from BIRPS deep seismic reflection profiles. *Journal of the Geological Society*, 145(5):727–740.

Frizon de Lamotte, D., Fourdan, B., Leleu, S., Leparmentier, F., and Clarens, P. (2015). Style of rifting and the stages of Pangea breakup. *Tectonics*, 34:1–21.

Frizon de Lamotte, D., Raulin, C., Mouchot, N., Wrobel-Daveau, J.-C., Blanpied, C., and Ringenbach, J.-C. (2011). The southernmost margin of the Tethys realm during the Mesozoic and Cenozoic: Initial geometry and timing of the inversion processes. *Tectonics*, 30(3):1–22.

Früh-Green, G. L., Connolly, J. A., Plas, A., Kelley, D. S., and Grobéty, B. (2004). The Subseafloor Biosphere at Mid-Ocean Ridges. *Geophysical Monograph Series*, 144:119–136.

Funck, T. (2003). Crustal structure of the ocean-continent transition at Flemish Cap: Seismic refraction results. *Journal of Geophysical Research*, 108(B11):1–20.

Funck, T., Andersen, M. S., Keser Neish, J., and Dahl-Jensen, T. (2008). A refraction seismic transect from the Faroe Islands to the Hatton-Rockall Basin. *Journal of Geophysical Research*, 113(B12):B12405.

Gabrielsen, R. H., Braathen, A., Dehis, J., and Roberts, D. (2002). Tectonic lineaments of Norway. *Norsk Geologisk Tidsskrift*, 82(3):153–174.

Gaetani, G. A. and Grove, T. L. (1998). The influence of water on melting of mantle peridotite. *Contributions to Mineralogy and Petrology*, 131(4):323–346.

Gaetani, M., Dercourt, J., and Vrielynck, B. (2003). The Peri-Tethys Programme: achievements and results. *Episodes*, 26(2):79–93.

Gaggero, L., Oggiano, G., Buzzi, L., Slejko, F., and Cortesogno, L. (2007). Post-variscan mafic dikes from the late orogenic collapse to the Tethyan rift : Evidence from Sardinia. *Ofioliti*, 32(1):15–37.

Gao, W. (2004). Upper mantle convection beneath the central Rio Grande rift imaged by P and S wave tomography. *Journal of Geophysical Research*, 109(B3):B03305.

Gee, D. G., Fossen, H., Henriksen, N., and Higgins, A. K. (2008). From the Early Paleozoic Platforms of Baltica and Laurentia to the Caledonide Orogen of Scandinavia and Greenland.

Gee, D. G., Janak, M., Majka, J., Robinson, P., and van Roermund, H. (2012). Subduction along and within the Baltoscandian margin during closing of the Iapetus Ocean and Baltica-Laurentia collision. *Lithosphere*, 5(2):169–178.

Gernigon, L., Gaina, C., Olesen, O., Ball, P., Péron-Pinvidic, G., and Yamasaki, T. (2012). The Norway Basin revisited: From continental breakup to spreading ridge extinction. *Marine and Petroleum Geology*, 35:1–19.

Gerya, T. V. and Meilick, F. I. (2011). Geodynamic regimes of subduction under an active margin: effects of rheological weakening by fluids and melts. *Journal of Metamorphic Geology*, 29:7–31.

Gillard, M., Autin, J., Manatschal, G., Sauter, D., Munschy, M., and Schaming, M. (2015). Tectonomagmatic evolution of the final stages of rifting along the deep conjugate Australian-Antarctic magma-poor rifted margins: Constraints from seismic observations. *Tectonics*, 34:753–783.

Gladczenko, T. P., Skogseid, J., and Eldhom, O. (1998). Namibia volcanic margin. *Marine Geophysical Researches*, 20(4):313–341.

Griffin, W., O'Reilly, S., Abe, N., Aulbach, S., Davies, R., Pearson, N., Doyle, B., and Kivi, K. (2003). The origin and evolution of Archean lithospheric mantle. *Precambrian Research*, 127(1-3):19–41.

Grove, T. L., Chatterjee, N., Parman, S. W., and Médard, E. (2006). The influence of H2O on mantle wedge melting. *Earth and Planetary Science Letters*, 249(1-2):74–89.

Gurnis, M., Hall, C., and Lavier, L. (2004). Evolving force balance during incipient subduction. *Geochemistry, Geophysics, Geosystems*, 5(7).

Hall, C. E., Gurnis, M., Sdrolias, M., Lavier, L. L., and Müller, R. (2003). Catastrophic initiation of subduction following forced convergence across fracture zones. *Earth and Planetary Science Letters*, 212(1-2):15–30.

Hall, R. (1976). Ophiolite emplacement and the evolution of the Taurus suture zone, southeastern Turkey. *Geological Society of America Bulletin*, 87(7):1078–1088.

Handy, M. R., M. Schmid, S., Bousquet, R., Kissling, E., and Bernoulli, D. (2010). Reconciling plate-tectonic reconstructions of Alpine Tethys with the geological-geophysical record of spreading and subduction in the Alps. *Earth-Science Reviews*, 102(3-4):121–158.

Haupert, I., Manatschal, G., Decarlis, A., and Unternehr, P. (in press.). Upper-plate magma-poor rifted margins: stratigraphic architecture and structural evolution. *Marine and Petroleum Geology*.

Haynes, S. J. and McQuillan, H. (1974). Evolution of the Zagros Suture Zone, Southern Iran. *Geological Society of America Bulletin*, 85(5):739–744.

Henk, A. (1997). Gravitational orogenic collapse vs plate-boundary stress: a numerical modelling approach to the Permo-Carboniferous evolution of Central Europe. *Geol Rundschau*, 86:39–55.

Hess, H. (1955). Serpentines, Orogeny, and Epeirogeny. *Geological Society of America Special Papers*, 62:391–408.

Heuret, A. and Lallemand, S. (2005). Plate motions, slab dynamics and back-arc deformation. *Physics of the Earth and Planetary Interiors*, 149(1-2 SPEC. ISS.):31–51.

Hirth, G. and Kohlstedt, D. L. (1996). Water in the oceanic upper mantle: implications for rheology, melt extraction and the evolution of the lithosphere. *Earth and Planetary Science Letters*, 144(1-2):93–108.

Hoffmann, N. and Franke, D. (1997). The Avalonia-Baltica suture in NE Germany-New constraints and alternative interpretations. *Zeitschrift für geologische Wissenschaften*, 25(3-14).

Hofmeister, A. M. (1999). Mantle Values of Thermal Conductivity and the Geotherm from Phonon Lifetimes. *Science*, 283(5408):1699–1706.

Holloway, N. H. (1982). North Palawan Block, Philippines; its relation to Asian mainland and role in evolution of South China Sea. *AAPG Bulletin*, 66(9):1355–1383.

Holtzman, B. K., Groebner, N. J., Zimmerman, M. E., Ginsberg, S. B., and Kohlstedt, D. L. (2003). Stress-driven melt segregation in partially molten rocks. *Geochemistry, Geophysics, Geosystems*, 4(5):n/a–n/a.

Hopper, J. R., Dahl-Jensen, T., Holbrook, W. S., Larsen, H. C., Lizarralde, D., Korenaga, J., Kent, G. M., and Kelemen, P. B. (2003). Structure of the SE Greenland margin from seismic reflection and refraction data: Implications for nascent spreading center subsidence and asymmetric crustal accretion during North Atlantic opening. *Journal of Geophysical Research*, 108(B5):2269.

Hopper, J. R., Funck, T., Tucholke, B. E., Christian Larsen, H., Holbrook, W. S., Louden, K. E., Shillington, D., and Lau, H. (2004). Continental breakup and the onset of ultraslow seafloor spreading off Flemish Cap on the Newfoundland rifted margin. *Geology*, 32(1):93.

Hopper, J. R., Mutter, J. C., Larson, R. L., and Mutter, C. Z. (1992). Magmatism and rift margin evolution: Evidence from northwest Australia. *Geology*, 20(9):853–857.

Horen, H., Zamora, M., and Dubuisson, G. (1996). Seismic waves velocities and anisotropy in serpentinized peridotites from Xigaze ophiolite: abundance of serpentine in slow spreading ridge. *Geophysical Research Letters*, 23(1):9–12.

Hossack, J. R. and Cooper, M. A. (1986). Collision tectonics in the Scandinavian Caledonides. *Geological Society, London, Special Publications*, 19(1):285–304.

Huigen, Y. D. and Andriessen, P. A. M. (2004). Thermal effects of Caledonian foreland basin formation, based on fission track analysis applied on basement rocks in central Sweden. *Physics and Chemistry of the Earth*, 29:683–694.

Isozaki, Y. (1997). Contrasting two types of orogen in Permo-Triassic Japan: Accretionary versus collisional. *The Island Arc*, 6:2–24.

Iwamori, H. (1998). Transportation of H2O and melting in subduction zones. *Earth and Planetary Science Letters*, 160(1-2):65–80.

Jagoutz, O., Müntener, O., Manatschal, G., Rubatto, D., Péron-Pinvidic, G., Turrin, B. D., and Villa, I. M. (2007). The rift-to-drift transition in the North Atlantic: A stuttering start of the MORB machine? *Geology*, 35(12):1087.

Jagoutz, O., Müntener, O., Schmidt, M. W., and Burg, J.-P. (2011). The roles of flux- and decompression melting and their respective fractionation lines for continental crust formation: Evidence from the Kohistan arc. *Earth and Planetary Science Letters*, 303:25–36.

Jammes, S. and Huismans, R. S. (2012). Structural styles of mountain building: Controls of lithospheric rheologic stratification and extensional inheritance. *Journal of Geophysical Research: Solid Earth*, 117(B10):n/a–n/a.

Jammes, S., Huismans, R. S., and Muñoz, J. A. (2014). Lateral variation in structural style of mountain building: Controls of rheological and rift inheritance. *Terra Nova*, 26(3):201–207.

Jammes, S., Lavier, L. L., and Reber, J. E. (2013). Effect of polymineralic crustal composition on deformation processes. In *AGU Fall Meeting Abstracts*, page 2519.

Jammes, S., Manatschal, G., Lavier, L., and Masini, E. (2009). Tectonosedimentary evolution related to extreme crustal thinning ahead of a propagating ocean: Example of the western Pyrenees. *Tectonics*, 28(4):TC4012.

Jarchow, C. M., Thompson, G. A., Catchings, R. D., and Mooney, W. D. (1993). Seismic evidence for active magmatic underplating beneath the Basin and Range Province, western United States. *Journal of Geophysical Research*, 98(B12):22095.

Jarrard, R. D. (1986). Relations among subduction parameters. *Reviews of Geophysics*, 24(2):217–284.

Jaupart, C. and Mareschal, J. C. (2007). Heat flow and thermal structure of the lithosphere. *Treatise on Geophysics*, 6:217–251.

Juhojuntti, N., Juhlin, C., and Dyrelius, D. (2001). Crustal reflectivity underneath the Central Scandinavian Caledonides. *Tectonophysics*, 334(3-4):191–210.

Jurdy, D. M., Stefanick, M., and Scotese, C. R. (1995). Paleozoic Plate Dynamics. *Journal of Geophysical Research*, 100(B9):17965–17975.

Keen, C. E., Dickie, K., and Dehler, S. a. (2012). The volcanic margins of the northern Labrador Sea: Insights to the rifting process. *Tectonics*, 31(TC1011).

Kempton, P., Fitton, J., Saunders, A., Nowell, G., Taylor, R., Hardarson, B., and Pearson, G. (2000). The Iceland plume in space and time: a Sr,ÄìNd,ÄìPb,ÄìHf study of the North Atlantic rifted margin. *Earth and Planetary Science Letters*, 177(3-4):255–271.

Keppie, J. D., Nance, R. D., Murphy, J. B., Dostal, J., and Braid, J. A. (2010). The high-pressure Iberian-Czech belt in the Variscan orogen: Extrusion into the upper (Gondwanan) plate? *Gondwana Research*, 17:306–316.

Kimbell, G., Ritchie, J., and Henderson, A. (2010). Three-dimensional gravity and magnetic modelling of the Irish sector of the NE Atlantic margin. *Tectonophysics*, 486:36–54.

Klingelhöfer, F., Edwards, R. A., Hobbs, R. W., and England, R. W. (2005). Crustal structure of the NE Rockall Trough from wide-angle seismic data modeling. *Journal of Geophysical Research*, 110(B11):B11105.

Korenaga, J., Holbrook, W. S., Kent, G. M., Kelemen, P. B., Detrick, R. S., Larsen, H., Hopper, J. R., and Dahl-Jensen, T. (2000). Crustal structure of the southeast Greenland margin from joint refraction and reflection seismic tomography. *Journal of Geophysical Research*, 105(B9):21,591–21,614.

Krabbendam, M. (2001). When the Wilson Cycle breaks down: how orogens can produce strong lithosphere and inhibit their future reworking. *Geological Society, London, Special Publications*, 184(1):57–75.

Krabbendam, M. and Barr, T. D. (2000). Proterozoic orogens and the break-up of Gondwana: why did some orogens not rift? *Journal of African Earth Sciences*, 31(1):35–49.

Krawczyk, C. M., McCann, T., Cocks, L. R. M., England, R. W., McBride, J. H., and Wibraniec, S. (2008). Caledonian tectonics. In McCann, T., editor, *The Geology of Central Europe, Volume 1: Precambrian and Palaeozoic*, pages 303–381. The Geological Society, London.

Kröner, U., Mansy, J. L., Mazur, S., Aleksandrowski, P., Hann, H. P., Huckriede, H., Lacquement, F., Lamarche, J., Ledru, P., Pharaoh, T. C., Zedler, H., Zeh, A., and Zulauf, G. (2008). Variscan tectonics. In McCann, T., editor, *The Geology of Central Europe, Volume 1: Precambrian and Palaeozoic*, chapter 11, pages 599–664. the Geological Society, London.

Kröner, U. and Romer, R. (2013). Two plates – Many subduction zones: The Variscan orogeny reconsidered. *Gondwana Research*, 24(1):298–329.

Kroner, U. and Romer, R. L. (2014). Anatomy of a diffuse cryptic suture zone: An example from the Bohemian Massif, European Variscides – comment. *Geology*, 42:e340.

Kvarven, T. (2013). *On the evolution of the North Atlantic - from continental collapse to oceanic accretion.* PhD thesis, University of Bergen.

Lagabrielle, Y. and Bodinier, J. L. (2008). Submarine reworking of exhumed subcontinental mantle rocks: Field evidence from the Lherz peridotites, French Pyrenees. *Terra Nova*, 20(1):11–21.

Larson, S. Å., Tullborg, E.-L., Cederbom, C., and Stiberg, J.-P. (1999). Sveconorwegian and Caledonian foreland basins in the Baltic Shield revealed by fission-track thermochronology. *Terra Nova*, 11(5):210–215.

Latin, D. and White, N. (1990). Generating melt during lithospheric extension: Pure shear vs. simple shear. *Geology*, 18:327–331.

Lavier, L. L., Buck, W. R., and Poliakov, A. N. B. (2000). Factors controlling normal fault offset in an ideal brittle layer. *Journal of Geophysical Research*, 105(B10):23431–23442.

Lavier, L. L. and Manatschal, G. (2006). A mechanism to thin the continental lithosphere at magma-poor margins. *Nature*, 440(7082):324–328.

Leat, P. T. and Larter, R. D. (2003). Intra-oceanic subduction systems: introduction. *Geological Society, London, Special Publications*, 219(1):1–17.

Lee, T.-Y. and Lawver, L. A. (1994). Cenozoic plate reconstruction of the South China Sea region. *Tectonophysics*, 235(1-2):149–180.

Leroy, S., Lucazeau, F., D'Acremont, E., Watremez, L., Autin, J., Rouzo, S., Bellahsen, N., Tiberi, C., Ebinger, C., Beslier, M. O., Perrot, J., Razin, P., Rolandone, F., Sloan, H., Stuart, G., Lazki, A. A., Al-Toubi, K., Bache, F., Bonneville, A., Goutorbe, B., Huchon, P., Unternehr, P., and Khanbari, K. (2010). Contrasted styles of rifting in the eastern Gulf of Aden: A combined wide-angle, multichannel seismic, and heat flow survey. *Geochemistry, Geophysics, Geosystems*, 11(7):1–14.

Lester, R., Van Avendonk, H. J. a., Mcintosh, K., Lavier, L., Liu, C.-S., Wang, T. K., and Wu, F. (2014). Rifting and magmatism in the northeastern South China Sea from wide-angle tomography and seismic reflection imaging. *Journal of Geophysical Research*, 119:2305–2323.

Li, X.-H., Faure, M., Lin, W., and Manatschal, G. (2013). New isotopic constraints on age and magma genesis of an embryonic oceanic crust: The Chenaillet Ophiolite in the Western Alps. *Lithos*, 160-161:283–291.

Li, X. H., Li, Z. X., Li, W. X., Liu, Y., Yuan, C., Wei, G., and Qi, C. (2007). U-Pb zircon, geochemical and Sr-Nd-Hf isotopic constraints on age and origin of Jurassic I- and A-type granites from central Guangdong, SE China: A major igneous event in response to foundering of a subducted flat-slab? *Lithos*, 96(1-2):186–204.

Linnemann, U., Pereira, F., Jeffries, T. E., Drost, K., and Gerdes, A. (2008). The Cadomian Orogeny and the opening of the Rheic Ocean: The diacrony of geotectonic processes constrained by LA-ICP-MS U-Pb zircon dating (Ossa-Morena and Saxo-Thuringian Zones, Iberian and Bohemian Massifs). *Tectonophysics*, 461(1-4):21–43.

Louden, K. E. and Chian, D. (1999). The deep structure of non-volcanic rifted. *Phil. Trans. R. Soc. London*, 357:767–805.

Lundin, E. R. and Doré, A. G. (1997). A tectonic model for the Norwegian passive margin with implications for the NE Atlantic: Early Cretaceous to break-up. *Journal of the Geological Society*, 154:545–550.

Lundin, E. R. and Doré, A. G. (2011). Hyperextension, serpentinization, and weakening: A new paradigm for rifted margin compressional deformation. *Geology*, 39(4):347–350.

Mac Niocaill, C., Van der Pluijm, B. A., and Van der Voo, R. (1997). Ordovician paleogeography and the evolution of the Iapetus ocean. *Geology*, 25(2):159–162.

Manatschal, G., Lavier, L., and Chenin, P. (2015). The role of inheritance in structuring hyperextended rift systems: Some considerations based on observations and numerical modeling. *Gondwana Research*, 27(1):140–164.

Manatschal, G. and Müntener, O. (2009). A type sequence across an ancient magma-poor ocean–continent transition: the example of the western Alpine Tethys ophiolites. *Tectonophysics*, 473:4–19.

Manatschal, G., Sauter, D., Karpoff, A. M., Masini, E., Mohn, G., and Lagabrielle, Y. (2011). The Chenaillet Ophiolite in the French/Italian Alps: An ancient analogue for an Oceanic Core Complex? *Lithos*, 124(3-4):169–184.

Martinez, F. and Taylor, B. (2002). Mantle wedge control on back-arc crustal accretion. *Nature*, 416(6879):417–420.

Martínez Catalán, J. R., Arenas, R., Diaz Garcia, F., and Abati, J. (1997). Variscan accretionary complex of northwest Iberia: Terrane correlation and succession of tectonothermal events. *Geology*, 25(12):1103–1106.

Martínez Catalán, J. R., Arenas, R., Díaz García, F., Cuadra, P. G., Gómez-Barreiro, J., Abati, J., Castiñeiras, P., Fernández-suárez, J., Sánchez Martínez, S., Andonaegui, P., González Clavijo, E., Díez Montes, A., Rubio Pascual, F. J., and Valle Aguado, B. (2007). Space and time in the tectonic evolution of the northwestern Iberian Massif : Implications for the Variscan belt. In Hatcher, R. D., Carlson, M. P., McBride, J. H., and Martínez Catalán, J. R., editors, *Space and time in the tectonic evolution of the north-western Iberian Massif: Implications for the Variscan belt*, volume 200, pages 403–423. The Gological Society of America Memoir 200.

Masini, E., Manatschal, G., and Mohn, G. (2013). The Alpine Tethys rifted margins: Reconciling old and new ideas to understand the stratigraphic architecture of magma-poor rifted margins. *Sedimentology*, 60:174–196.

Mattauer, M. (1968). Les traits structuraux essentiels de la chaîne pyrénéenne. *Revue de Géologie Dynamique et de Géographie physique*, 10:3–11.

Matte, P. (1986). Tectonics and plate tectonics model for the Variscan Belt of Europe. *Tectonophysics*, 126:329–360.

Matte, P. (1991). Accretionary history and crustal evolution of the Variscan belt in Western Europe. *Tectonophysics*, 196:309–337.

Matte, P. (2001). The Variscan collage and orogeny (480- 290 Ma) and the tectonic definition of the Armorica microplate: a review. *Terra Nova*, 13:122–128.

Maus, S., Barckhausen, U., Berkenbosch, H., Bournas, N., Brozena, J., Childers, V., Dostaler, F., Fairhead, J. D., Finn, C., von Frese, R. R. B., Gaina, C., Golynsky, S., Kucks, R., Lühr, H., Milligan, P., Mogren, S., Müller, R. D., Olesen, O., Pilkington, M., Saltus, R., Schreckenberger, B., Thébault, E., and Caratori Tontini, F. (2009). EMAG2: A 2-arc min resolution Earth Magnetic Anomaly Grid compiled from satellite, airborne, and marine magnetic measurements. *Geochemistry, Geophysics, Geosystems*, 10(8):n/a–n/a.

McCann, T., Pascal, C., Timmerman, M. J., Krzywiec, P., J, López-Gómez, J., Wetzel, A., Krawczyk, C. M., Rieke, H., and Lamarche, J. (2006). Post-Variscan (end Carboniferous ,Äì Early Permian) basin evolution in Western and Central Europe. In Gee, D. G. and Stephenson, R. a., editors, *European Lithosphere Dynamics*, pages 355–388. Gological Society, London, Memoirs.

McCarthy, A. and Müntener, O. (2015). Ancient depletion and mantle heterogeneity: Revisiting the Permian-Jurassic paradox of Alpine peridotites. *Geology*, 43(3):255–258.

McClay, K. R., Norton, M. G., Coney, P., and Davis, G. H. (1986). Collapse of the Caledonian orogen and the Old Red Sandstone. *Nature*, 323:147–149.

McDermott, K., Bellingham, P., Pindell, J., Graham, R., and Horn, B. (2014). Some insights into rifted margin development and the structure of the continent-ocean transition using a global deep seismic reflection database. In *4th Atlantic Conjugate Margins Conference*, pages 62–65, St John's.

McIntosh, K., Lavier, L., van Avendonk, H., Lester, R., Eakin, D., and Liu, C.-S. (2014). Crustal structure and inferred rifting processes in the northeast South China Sea. *Marine and Petroleum Geology*, 58:612–626.

Mckenzie, D. and Bickle, M. J. (1988). The volume and composition of melt generated by extension of the lithosphere. *Journal of Petrology*, 29(3):625–679.

McKerrow, W. S. (1988). The development of the Iapetus Ocean from the Arenig to the Wenlock. *Geological Society, London, Special Publications*, 38(1):405–412.

McKerrow, W. S. and Cocks, L. R. M. (1976). Progressive faunal migration accross the Iapetus Ocean. *Nature*, 263:304–306.

McKerrow, W. S., Mac Niocaill, C., Ahlberg, P. E., Clayton, G., Cleal, C. J., and Eagar, R. M. C. (2000a). The Late Palaeozoic relations between Gondwana and Laurussia. *Geological Society, London, Special Publications*, 179(1):9–20.

McKerrow, W. S., Mac Niocaill, C., and Dewey, J. F. (2000b). The Caledonian Orogeny redefined. *Journal of the Geological Society*, 157(6):1149–1154.

Meissner, R. (1999). Terrane accumulation and collapse in central Europe: seismic and rheological constraints. *Tectonophysics*, 305(1-3):93–107.

Meissner, R., Sadowiakl, P., and Thomas, S. A. (1994). East Avalonia, the third partner in the Caledonian collisions: evidence from deep seismic reflection data. *Geologische Rundschau*, 83(1):186–196.

Melankholina, E. N. (2008). Tectonotype of volcanic passive margins in the Norwegian-Greenland region. *Geotectonics*, 42(3):225–244.

Mengel, K. and Kern, H. (1992). Evolution of the petrological and seismic Moho-implications for the continental crust-mantle boundary. *Terra Nova*, 4(1):109–116.

Mével, C. (2003). Serpentinization of abyssal peridotites at mid-ocean ridges. *Comptes Rendus Geoscience*, 335(10-11):825–852.

Meyer, R., van Wijk, J., and Gernigon, L. (2007). The North Atlantic Igneous Province: A review of models for its formation. *Geological Society of America Special Paper*, 430:525–552.

Meyre, C. and Pusching, A. R. (1993). High-pressure metamorphism and deformation at Trescolmen, Adula nappe, Central Alps. *Schweizerische Mineralogische und Petrographische Mitteilungen*, 73(2):277–283.

Miller, D. J. and Christensen, N. I. (1997). Seismic velocities of lower crustal and upper mantle rocks from the slow-spreading Mid-Atlantic Ridge, south of the Kane Transform Zone (MARK). *Proceedings of the Ocean Drilling Program. Scientific results*, 153:437–454.

Milnes, A. G., Wennberg, O. P., Skar, O., and Koestler, A. G. (1997). Contraction, extension and timing in the South Norwegian Caledonides: the Sognefjord transect. *Geological Society, London, Special Publications*, 121(1):123–148.

Minshull, T. A. (2009). Geophysical characterisation of the ocean–continent transition at magma-poor rifted margins. *Comptes Rendus Geoscience*, 341(5):382–393.

Miyashiro, A. (1961). Evolution of Metamorphic Belts. *Journal of Petrology*, 2(3):277–311.

Miyashiro, A. (1967). Orogeny, regional metamorphism, and magmatism in the Japanese Islands. *Medd. fra Dansk Geol. Forening*, 17:390–446.

Mjelde, R., Breivik, a. A. J., Raum, T., Mittelstaedt, E., Ito, G., and Faleide, J. I. J. (2008). Magmatic and tectonic evolution of the North Atlantic. *Journal of the Geological Society, London*, 165(1):31–42.

Mohn, G., Manatschal, G., Beltrando, M., and Haupert, I. (2014). The role of rift-inherited hyper-extension in Alpine-type orogens. *Terra Nova*, 26(5):347–353.

Mohn, G., Manatschal, G., Beltrando, M., Masini, E., and Kusznir, N. (2012). Necking of continental crust in magma-poor rifted margins: Evidence from the fossil Alpine Tethys margins. *Tectonics*, 31(1):TC1012.

Mohn, G., Manatschal, G., Masini, E., and Müntener, O. (2011). Rift-related inheritance in orogens: a case study from the Austroalpine nappes in Central Alps (SE-Switzerland and N-Italy). *International Journal of Earth Sciences*, 100(5):937–961.

Mooney, W. D. and Brocher, T. M. (1987). Coincident seismic reflection/refraction studies of the continental lithosphere: a global review. *Geophys. J. R. astr. Soc.*, 89:1–6.

Morgan, W. J. (1971). Convection Plumes in the Lower Mantle. *Nature*, 230(5288):42–43.

Mosar, J. (2003). Scandinavia,Äôs North Atlantic passive margin. *Journal of Geophysical Research*, 108(B8, 2360).

Muñoz, J. A. (2002). The Pyrenees. In Gibbons, W. and Moreno, M. T., editors, *The Geology of Spain*, pages 370–385. Journal of the Geological Society.

Müntener, O., Hermann, R. G., and Trommsdorff, V. (2000). Cooling History and Exhumation of Lower- Crustal Granulite and Upper Mantle (Malenco, Eastern Central Alps). *Journal of Petrology*, 41(2):175–200.

Müntener, O. and Manatschal, G. (2006). High degrees of melt extraction recorded by spinel harzburgite of the Newfoundland margin: The role of inheritance and consequences for the evolution of the southern North Atlantic. *Earth and Planetary Science Letters*, 252:437–452.

Müntener, O., Manatschal, G., Desmurs, L., and Pettke, T. (2010). Plagioclase Peridotites in Ocean-Continent Transitions: Refertilized Mantle Domains Generated by Melt Stagnation in the Shallow Mantle Lithosphere. *Journal of Petrology*, 51(1-2):255–294.

Müntener, O., Pettke, T., Desmurs, L., Meier, M., and Schaltegger, U. (2004). Refertilization of mantle peridotite in embryonic ocean basins: trace element and Nd isotopic evidence and implications for crust,Äìmantle relationships. *Earth and Planetary Science Letters*, 221:293–308.

Murphy, J. B., Gutierrez-Alonso, G., Nance, R. D., Fernandez-Suarez, J., Keppie, J. D., Quesada, C., Strachan, R. a., and Dostal, J. (2006). Origin of the Rheic Ocean: Rifting along a Neoproterozoic suture? *Geology*, 34(5):325.

Murphy, J. B., Keppie, J. D., Nance, R. D., and Dostal, J. (2010). Comparative evolution of the Iapetus and Rheic Oceans: A North America perspective. *Gondwana Research*, 17:482–499.

Murray, C. G., Scheibner, E., and Walker, R. N. (1989). Regional geological interpretation of a digital coloured residual Bouguer gravity image of eastern Australia with a wavelength cut,Äêoff of 250 km. *Australian Journal of Earth Sciences*, 36(3):423–449.

Muttoni, G., Kent, D. V., Garzanti, E., Brack, P., Abrahamsen, N., and Gaetani, M. (2003). Early Permian Pangea 'B' to Late Permian Pangea 'A'. *Earth and Planetary Science Letters*, 215:379–394.

Nance, R. D., Gutiérrez-Alonso, G., Keppie, J. D., Linnemann, U., Murphy, J. B., Quesada, C., Strachan, R. A., and Woodcock, N. H. (2010). Evolution of the Rheic Ocean. *Gondwana Research*, 17:194–222.

Nance, R. D. and Linnemann, U. (2008). The Rheic Ocean: Origin, Evolution, and Significance. *GSA Today*, 18(12):4.

Neubauer, F. and Handler, R. (2000). Variscan orogeny in the Eastern Alps and Bohemian Massif: How do these units correlate? *Mitteilungen der Österreichischen Geologischen Gesellschaft*, 92:35–59.

Nikolaeva, K., Gerya, T. V., and Marques, F. O. (2010). Subduction initiation at passive margins: Numerical modeling. *Journal of Geophysical Research: Solid Earth*, 115(3):1–19.

Nirrengarten, M., Gernigon, L., and Manatschal, G. (2014). Nature, structure and age of Lower Crustal Bodies in the Møre volcanic rifted margin: facts and uncertainties. *Tectonophysics*, 636:143–157.

Nirrengarten, M., Manatschal, G., Yan, X., Kusznir, N., and Millot, B. (subm.). Application of the critical Coulomb wedge theory to hyper-extended, magma-poor rifted margins. *Earth and Planetary Science Letters*.

Nissen, S. S., Hayes, D. E., Buhl, P., Diebold, J., Bochu, Y., Zeng, W., and Chen, Y. (1995). Deep penetration seismic soundings across the northern margin of the South China Sea. *Journal of Geophysical Research*, 100(B11):22,407–22,433.

Oncken, O., Plesch, A., Weber, J., Ricken, W., and Schrader, S. (2000). Passive margin detachment during arc-continent collision (Central European Variscides). *Geological Society, London, Special Publications*, 179(1):199–216.

Osmundsen, P. T. and Ebbing, J. (2008). Styles of extension offshore mid-Norway and implications for mechanisms of crustal thinning at passive margins. *Tectonics*, 27(6).

Peacock, S. M. (1991). Numerical Simulation of Subduction Zone Pressure-Temperature-Time Paths: Constraints on Fluid Production and Arc Magmatism. *Philosophical Transactions of the Royal Society of London A: Mathematical, Physical and Engineering Sciences*, 335(1638):341–353.

Peacock, S. M., Rushmer, T., and Thompson, A. B. (1994). Partial melting of subducting oceanic crust. *Earth and Planetary Science Letters*, 121(1-2):227–244.

Pereira, M., Chichorro, M., Johnston, S., Gutiérrez-Alonso, G., Silva, J., Linnemann, U., Hofmann, M., and Drost, K. (2012). The missing Rheic Ocean magmatic arcs: Provenance analysis of Late Paleozoic sedimentary clastic rocks of SW Iberia. *Gondwana Research*, 22:882–891.

Pérez-Gussinyé, M., Ranero, C. R., and Reston, T. J. (2003). Mechanisms of extension at nonvolcanic margins: Evidence from the Galicia interior basin, west of Iberia. *Journal of Geophysical Research*, 108(B5).

Péron-Pinvidic, G. and Manatschal, G. (2009). The final rifting evolution at deep magma-poor passive margins from Iberia-Newfoundland: A new point of view. *International Journal of Earth Sciences*, 98(7):1581–1597.

Péron-Pinvidic, G. and Manatschal, G. (2010). From microcontinents to extensional allochthons: witnesses of how continents rift and break apart? *Petroleum Geoscience*, 16(3):189–197.

Péron-Pinvidic, G., Manatschal, G., Minshull, T. a., and Sawyer, D. S. (2007). Tectonosedimentary evolution of the deep Iberia-Newfoundland margins: Evidence for a complex breakup history. *Tectonics*, 26(2):n/a–n/a.

Péron-Pinvidic, G., Manatschal, G., and Osmundsen, P. T. (2013). Structural comparison of archetypal Atlantic rifted margins: A review of observations and concepts. *Marine and Petroleum Geology*, 43:21–47.

Petri, B. (2014). *Formation et exhumation des granulites permiennes*. PhD thesis, Université de Strasbourg.

Pharaoh, T. C. (1999). Palaeozoic terranes and their lithospheric boundaries within the Trans-European Suture Zone (TESZ): a review. *Tectonophysics*, 314:17–41.

Picazo, S., Cannat, M., Delacour, A., Escartín, J., Rouméjon, S., and Silantyev, S. (2012). Deformation associated with the denudation of mantle-derived rocks at the Mid-Atlantic Ridge 13°-15°N: The role of magmatic injections and hydrothermal alteration. *Geochemistry, Geophysics, Geosystems*, 13(9):n/a–n/a.

Picazo, S., Manatschal, G., Cannat, M., and Andréani, M. (2013). Deformation associated to exhumation of serpentinized mantle rocks in a fossil Ocean Continent Transition: The Totalp unit in SE Switzerland. *Lithos*, 175-176:255–271.

Picazo, S., Müntener, O., and Manatschal, G. (2015). Recognizing mantle domains related to an extensional cycle: the record from Western Europe. In *AGU Fall Meeting Abstracts*, San Francisco.

Piccardo, G. B., Padovano, M., and Guarnieri, L. (2014). The Ligurian Tethys: Mantle processes and geodynamics. *Earth-Science Reviews*, 138(October):409–434.

Pinto, V. H. (2014). *Linking tectonic evolution with fluid history in hyperextended rifted margins: Examples from the fossil Alpine and Pyrenean rift systems and the present-day Iberia rifted margin.* PhD thesis, Université de Strasbourg.

Piqué, A. and Laville, E. (1996). The central Atlantic rifting: Reactivation of Palaeozoic structures? *Journal of Geodynamics*, 21(3):235–255.

Popov, A. and Sobolev, S. (2008). SLIM3D: A tool for three-dimensional thermomechanical modeling of lithospheric deformation with elasto-visco-plastic rheology. *Physics of the Earth and Planetary Interiors*, 171(1-4):55–75.

Poprawa, P., Šliaupa, S., Stephenson, R., and Lazauskien,âê, J. (1999). Late Vendian,ÄìEarly Palæozoic tectonic evolution of the Baltic Basin: regional tectonic implications from subsidence analysis. *Tectonophysics*, 314(1-3):219–239.

Radhakrishna, M., Twinkle, D., Nayak, S., Bastia, R., and Rao, G. S. (2012). Crustal structure and rift architecture across the Krishna-Godavari basin in the central Eastern Continental Margin of India based on analysis of gravity and seismic data. *Marine and Petroleum Geology*, 37(1):129–146.

Rampone, E. (2004). Mantle dynamics during Permo-Mesozoic extension of the Europe-Adria lithosphere: insights from the Ligurian ophiolites. *Per. Minearal.*, 73:215–230.

Rast, N. (1988). Variscan–Alleghanian orogen. In *Triassic-Jurassic Rifting: Continental Breakup and the Origin of the Atlantic Ocean and Passive Margins, Part A*, chapter 1, pages 1–27. Elsevier, New York.

Reston, T., Gaw, V., Pennell, J., Klaeschen, D., Stubenrauch, A., and Walker, I. (2004). Extreme crustal thinning in the south Porcupine Basin and the nature of the Porcupine Median High: implications for the formation of non-volcanic rifted margins. *Journal of the Geological Society*, 161:783–798.

Reston, T. J. (2009). The structure, evolution and symmetry of the magma-poor rifted margins of the North and Central Atlantic: A synthesis. *Tectonophysics*, 468(1-4):6–27.

Rey, P. (1993). Seismic and tectono-metamorphic characters of the lower continental crust in Phanerozoic areas: a consequence of post-thickening extension. *Tectonics*, 12(2):580–590.

Rey, P., Burg, J.-P., and Casey, M. (1997). The Scandinavian Caledonides and their relationship to the Variscan belt contractional tectonics. In Burg, J.-P. and Ford, M., editors, *Orogeny trough time*, pages 179–200. Geological Society Special Pubication No. 121, London.

Rey, P., Vanderhaeghe, O., and Teyssier, C. (2001). Gravitational collapse of the continental crust: Definition, regimes and modes. *Tectonophysics*, 342(3-4):435–449.

Ring, U. (1994). The influence of preexisting structure on the evolution of the Cenozoic Malawi rift (East African rift system). *Tectonics*, 13(2):313–326.

Robardet, M. (2003). The Armorica 'microplate': fact or fiction? Critical review of the concept and contradictory palaeobiogeographical data. *Palaeogeography, Palaeoclimatology, Palaeoecology*, 195:125–148.

Roberts, D. (2003). The Scandinavian Caledonides: event chronology, palaeogeographic settings and likely modern analogues. *Tectonophysics*, 365:283–299.

Roberts, D. G., Thompson, M., Mitchener, B., Hossack, J., Carmichael, S., and Bjørnseth, H.-M. (1999). Palaeozoic to Tertiary rift and basin dynamics: mid-Norway to the Bay of Biscay – a new context for hydrocarbon prospectivity in the deep water frontier. In Fleet, A. J. and Boldy, S. A. R., editors, *Petroleum Geology of Northwest Europe: Proceedings of the 5th Conference*, pages 7–40. The Geological Society, London.

Rosas, F. M., Marques, F. O., Ballèvre, M., and Tassinari, C. (2008). Geodynamic evolution of the SW Variscides: Orogenic collapse shown by new tectonometamorphic and isotopic data from western Ossa-Morena Zone, SW Iberia. *Tectonics*, 27(6):n/a–n/a.

Rosenbaum, G. and Lister, G. S. (2005). The Western Alps from the Jurassic to Oligocene: Spatio-temporal constraints and evolutionary reconstructions. *Earth-Science Reviews*, 69(3-4):281–306.

Rosenbaum, G., Lister, G. S., and Duboz, C. (2002). Relative motions of Africa, Iberia and Europe during Alpine orogeny. *Tectonophysics*, 359(1-2):117–129.

Rossi, P., Cocherie, A., and Fanning, C. M. (2015). Evidence in Variscan Corsica of a brief and voluminous Late Carboniferous to Early Permian volcanic-plutonic event contemporaneous with a high-temperature/low-pressure metamorphic peak in the lower crust. *Bulletin de la Société Géologique de France*, 186(2-3):171–192.

Ru, K. and Pigott, J. D. (1986). Episodic Rifting and Subsidence in the South China Sea. *AAPG Bulletin*, 70(9):1136–1155.

Rüpke, L. H., Morgan, J. P., Hort, M., and Connolly, J. A. D. (2004). Serpentine and the subduction zone water cycle. *Earth and Planetary Science Letters*, 223(1-2):17–34.

Sandwell, D. T. and Smith, W. H. F. (2009). Global marine gravity from retracked Geosat and ERS-1 altimetry: Ridge Segmentation versus spreading rate. *Journal of Geophysical Research*, 114(B01411).

Saunders, A. D., Fitton, J. G., Kerr, A. C., Norry, M. J., and Kent, R. W. (1997). The North Atlantic Igneous Province. In *Large Ignous Province: Continental, Oceanic, and Planetary Flood Volcanism*, pages 45–93. Geophysical Monograph 100.

Schaltegger, U. (1997). Magma pulses in the Central Variscan Belt: episodic melt generation and emplacement during lithospheric thinning. *Terra Nova*, 9(5/6):242–245.

Schaltegger, U. and Brack, P. (2007). Crustal-scale magmatic systems during intra-continental strike-slip tectonics: U, Pb and Hf isotopic constraints from Permian magmatic rocks of the Southern Alps. *International Journal of Earth Sciences*, 96:1131–1151.

Schaltegger, U. and Corfu, F. (1995). Late Variscan ‚ÄúBasin and Range‚Äù magmatism and tectonics in the Central Alps: evidence from U-Pb geochronology. *Geodinamica Acta*, 8(2):82–98.

Schaltegger, U. and Gebauer, D. (1999). Pre-Alpine geochronology of the Central, Western and Southern Alps. *Schweiz. Mineral. Petrogr. Mitt.*, 79:79–87.

Schettino, A. and Turco, E. (2009). Breakup of Pangaea and plate kinematics of the central Atlantic and Atlas regions. *Geophysical Journal International*, 178(2):1078–1097.

Schilling, F. R., Trumbull, R. B., Brasse, H., Haberland, C., Asch, G., Bruhn, D., and Vietor, T. (2006). Partial melting in the Central Andean crust: a review of geophysical, petrophysical, and petrologic evidence. In Oncken, O., Chong, G., Franz, G., Giese, P., Gotze, H.-J., Ramos, V. a., Strecker, M. R., and Wigger, P., editors, *The Andes*, pages 459–474. Springer, Berlin Heidelberg.

Schmid, S. M., Bernoulli, D., Fügenschuh, B., Matenco, L., Schefer, S., Schuster, R., Tischler, M., and Ustaszewski, K. (2008). The Alpine-Carpathian-Dinaridic orogenic system: correlation and evolution of tectonic units. *Swiss Journal of Geosciences*, 101:139–183.

Schmid, S. M., Fgenschuh, B., Kissling, E., Schuster, R., and Fügenschuh, B. (2004). Tectonic map and overall architecture of the Alpine orogen. *Eclogae Geologicae Helvetiae*, 97:93–117.

Schulmann, K., Konopásek, J., Janoušek, V., Lexa, O., Lardeaux, J.-M., Edel, J.-B., Štípská, P., and Ulrich, S. (2009). An Andean type Palaeozoic convergence in the Bohemian Massif. *Comptes Rendus Geoscience*, 341(2-3):266–286.

Schulmann, K., Lexa, O., Janoušek, V., Lardeaux, J. M., and Edel, J. B. (2014a). Anatomy of a diffuse cryptic suture zone: An example from the Bohemian Massif, European Variscides. *Geology*, 42(4):275–278.

Schulmann, K., Lexa, O., Janoušek, V., Lardeaux, J. M., and Edel, J. B. (2014b). Anatomy of a diffuse cryptic suture zone: An example from the Bohemian Massif, European Variscides – Reply. *Geology*, 42(4):275–278.

Schuster, R. and Stüwe, K. (2008). Permian metamorphic event in the Alps. *Geology*, 36(8):603–606.

Séranne, M. and Seguret, M. (1987). The Devonian basins of western Norway: tectonics and kinematics of an extending crust. *Geological Society, London, Special Publications*, 28(1):537–548.

Shannon, P. M., Jacob, A. W. B., O'Reilly, B. M., Hauserr, F., Readman, P. W., and Makris, J. (1999). Structural setting, geological development and basin modelling in the Rockall Trough. *Petroleum Geology Conference series*.

Shillington, D. J., Holbrook, W. S., Van Avendonk, H. J. A., Tucholke, B. E., Hopper, J. R., Louden, K. E., Larsen, H. C., and Nunes, G. T. (2006). Evidence for asymmetric nonvolcanic rifting and slow incipient oceanic accretion from seismic reflection data on the Newfoundland margin. *Journal of Geophysical Research*, 111(B9):B09402.

Sibson, R. H. (1985). A note on fault reactivation. *Journal of Structural Geology*, 7(6):751–754.

Sibuet, J., Srivastava, S. P., Enachescu, M., and Karner, G. D. (2007). Early Cretaceous motion of Flemish Cap with respect to North America: implications on the formation of Orphan Basin and SE Flemish Cap–Galicia Bank conjugate margins. In Karner, G. D., Manatschal, G., and Pinhiero, L. M., editors, *Imaging, Mapping and Modelling Continental Lithosphere Extension and Breakup, Geological Society, London, Special Publications, 282*, pages 59–72. The Geological Society of London.

Sintubin, M., Debacker, T. N., and Van Baelen, H. (2009). Early Palaeozoic orogenic events north of the Rheic suture (Brabant, Ardenne): A review. *Comptes Rendus Geoscience*, 341(2-3):156–173.

Skelton, A., Whitmarsh, R., Arghe, F., Crill, P., and Koyi, H. (2005). Constraining the rate and extent of mantle serpentinization from seismic and petrological data: implications for chemosynthesis and tectonic processes. *Geofluids*, 5(3):153–164.

Smith, W. H. F. and Sandwell, D. T. (1997). Global seafloor topography from satellite altimetry and ship depth soundings. *Science*, 277:1957–1962.

Soper, N. J., Strachan, R. A., Holdsworth, R. E., Gayer, R. A., and Greiling, R. O. (1992). Sinistral transpression and the Silurian closure of Iapetus. *Journal of the Geological Society*, 149(6):871–880.

Stahle, V., Frenzel, G., Hess, J. C., Saupé, F., Schmidt, S. T., and Schneider, W. (2001). Permian metabasalt and Triassic alkaline dykes in the northern Ivrea zone: clues to the post-Variscan geodynamic evolution of the Southern Alps. *Schweizerische Mineralogische und Petrographische Mitteilungen*, 81(1):1–21.

Stampfli, G., Mosar, J., Marquer, D., Marchant, R., Baudin, T., and Borel, G. (1998). Subduction and obduction processes in the Swiss Alps. *Tectonophysics*, 296(1-2):159–204.

Stampfli, G. M. and Borel, G. D. (2002). A plate tectonic model for the Paleozoic and Mesozoic constrained by dynamic plate boundaries and restored synthetic oceanic isochrons. *Earth and Planetary Science Letters*, 196:17–33.

Stampfli, G. M., Von Raumer, J. F., and Borel, G. D. (2002). Paleozoic evolution of pre-Variscan terranes; from Gondwana to the Variscan collision. In Martínez Catalán, J. R., Hatcher, R. D. J., Arenas, R., and Díaz García, F., editors, *Variscan-Appalachian dynamics: The building of the late Paleozoic basement*, volume 364, pages 263–280. Geological Society of America Special Paper 364, Boulder, Colorado.

Stephens, M. B. (1988). The Scandinavian Caledonides: a complexity of collisions. *Geology Today*, 4(1):20–26.

Stern, C. R. (2011). Subduction erosion: Rates, mechanisms, and its role in arc magmatism and the evolution of the continental crust and mantle. *Gondwana Research*, 20:284–308.

Stern, R. J. (2002). Subduction zones. *Reviews of Geophysics*, 40(4):–.

Stern, R. J. (2004). Subduction initiation: spontaneous and induced. *Earth and Planetary Science Letters*, 226:275–292.

Stevenson, D. J. and Turner, J. S. (1977). Angle of subduction. *Nature*, 270(5635):334–336.

Stica, J. M., Zalán, P. V., and Ferrari, A. L. (2014). The evolution of rifting on the volcanic margin of the Pelotas Basin and the contextualization of the Paraná‚ÄìEtendeka LIP in the separation of Gondwana in the South Atlantic. *Marine and Petroleum Geology*, 50:1–21.

Storey, M., Duncan, R. a., and Tegner, C. (2007). Timing and duration of volcanism in the North Atlantic Igneous Province: Implications for geodynamics and links to the Iceland hotspot. *Chemical Geology*, 241:264–281.

Strachan, R. A. (1994). Evidence in North-East Greenland for Late Silurian-Early Devonian regional extension during the Caledonian orogeny. *Geology*, 22(10):913–916.

Sutra, E. and Manatschal, G. (2012). How does the continental crust thin in a hyper-extended rifted margin? Insights from the Iberia margin. *Geology*, 40(2):139–142.

Sutra, E., Manatschal, G., Mohn, G., and Unternehr, P. (2013). Quantification and restoration of extensional deformation along the Western Iberia and Newfoundland rifted margins. *Geochemistry, Geophysics, Geosystems*, 14(8):2575–2597.

Tait, J., Bachtadse, V., and Soffel, H. (1995). Upper Ordovician palaeogeography of the Bohemian Massif: implications for Armorica. *Geophysical Journal International*, 122(1):211–218.

Tait, J., Schätz, M., Bachtadse, V., and Soffel, H. (2000). Palaeomagnetism and Palaeozoic palaeogeography of Gondwana and European terranes. *Geological Society, London, Special Publications*, 179(1):21–34.

Talwani, M. and Eldholm, O. (1977). Evolution of the Norwegian- Greenland Sea. *Geological Society of America Bulletin*, 88:969–999.

Tan, E., Lavier, L. L., Van Avendonk, H. J. A., and Heuret, A. (2012). The role of frictional strength on plate coupling at the subduction interface. *Geochemistry, Geophysics, Geosystems*, 13(10):n/a–n/a.

Tankard, A. J. and Welsink, H. J. (1989). Mesozoic extension and styles of basin formation in Atlantic Canada. In Tankard, A. J. and Balkwill, H. R., editors, *Extensional tectonics and stratigraphy of the North Atlantic margins; Am. Assoc. Petroleum Geol. Mem. 46*, pages 175–195.

Thinon, I., Matias, L., Réhault, J. P., Hirn, A., Fidalgo-González, L., and Avedik, F. (2003). Deep structure of the Armorican Basin (Bay of Biscay): a review of Norgasis seismic reflection and refraction data. *Journal of the Geological Society of London*, 160:99–116.

Thompson, A., Schulmann, K., Jezek, J., and Tolar, V. (2001). Thermally softened continental extensional zones (arcs and rifts) as precursors to thickened orogenic belts. *Tectonophysics*, 332(1-2):115–141.

Thöni, M. and Jagoutz, E. (1993). Isotopic constraints for eo-Alpine high-P metamorphism in the Austroalpine nappes of the Eastern Alps: bearing on Alpine olrogenesis. *Schweizerische Mineralogische und Petrographische Mitteilungen*, 73(2):177–189.

Timmerman, M. J. (2004). Timing, geodynamic setting and character of Permo-Carboniferous magmatism in the foreland of the Variscan Orogen, NW Europe. *Geological Society, London, Special Publications*, 223:41–74.

Timmerman, M. J., Heeremans, M., Kirstein, L. A., Larsen, B. T., Spencer-Dunworth, E.-A., and Sundvoll, B. (2009). Linking changes in tectonic style with magmatism in northern Europe during the late Carboniferous to latest Permian. *Tectonophysics*, 473(3-4):375–390.

Tommasi, A. and Vauchez, A. (2001). Continental rifting parallel to ancient collisional belts: an effect of the mechanical anisotropy of the lithospheric mantle. *Earth and Planetary Science Letters*, 185:199–210.

Torsvik, T. H. (1998). Palaeozoic palaeogeography: A North Atlantic viewpoint. *GFF*, 120:109–118.

Torsvik, T. H., Carlos, D., Mosar, J., Cocks, L. R. M., and Malme, T. N. (2002). Global reconstructions and North Atlantic paleogeography 440 Ma to recent. *BATLAS,ÄîMid Norway plate reconstruction atlas with global and Atlantic perspectives*, pages 18–39.

Torsvik, T. H. and Cocks, L. R. M. (2011). The Palaeozoic palaeogeography of central Gondwana. *Geological Society London Special Publication*, 357:137–166.

Torsvik, T. H. and Cocks, L. R. M. (2013a). Gondwana from top to base in space and time. *Gondwana Research*, 24:999–1030.

Torsvik, T. H. and Cocks, L. R. M. (2013b). New global palaeogeographical reconstructions for the Early Palaeozoic and their generation. *Geological Society, London, Memoirs*, 38(1):5–24.

Torsvik, T. H. and Rehnström, E. F. (2003). The Tornquist Sea and Baltica–Avalonia docking. *Tectonophysics*, 362(1-4):67–82.

Torsvik, T. H., Van der Voo, R., Preeden, U., Mac Niocaill, C., Steinberger, B., Doubrovine, P. V., van Hinsbergen, D. J., Domeier, M., Gaina, C., Tohver, E., Meert, J. G., McCausland, P. J. A., and Cocks, L. R. M. (2012). Phanerozoic polar wander, palaeogeography and dynamics. *Earth-Science Reviews*, 114:325–368.

Tovish, A., Schubert, G., and Luyendyk, B. P. (1978). Mantle flow pressure and the angle of subduction: Non-Newtonian corner flows. *Journal of Geophysical Research*, 83(B12):5892.

Tucholke, B. E., Sawyer, D. S., Sibuet, J., and Brest, I. C. D. (2007). Breakup of the Newfoundland–Iberia rift. In Karner, G. D., Manatschal, G., and Pinheiro, L. M., editors, *Imaging, Mapping and Modelling Continental Lithosphere Extension and Breakup; Geological Society, London, Special Publications, 282*, volume 3, pages 9–46. The Geological Society of London.

Tucholke, B. E. and Sibuet, J.-C. (2007). Leg 210 synthesis: tectonic, magmatic, and sedimentary evolution of the Newfoundland rift. *Proceeding of the Ocean Drilling Program, Scientific Results*, 210:1–51.

Tugend, J., Manatschal, G., and Kusznir, N. (2015). Spatial and temporal evolution of hyperextended rift systems: implication for the nature, kinematics and timing of the Iberian-European plate boundary. *Geology*, 43(1):15–18.

Tugend, J., Manatschal, G., Kusznir, N. J., Masini, E., Mohn, G., and Thinon, I. (2014). Formation and deformation of hyperextended rift systems: Insights from rift domain mapping in the Bay of Biscay-Pyrenees. *Tectonics*, 33(7):1239–1276.

Unternehr, P., Péron-Pinvidic, G., Manatschal, G., and Sutra, E. (2010). Hyper-extended crust in the South Atlantic: in search of a model. *Petroleum Geoscience*, 16(3):207–215.

Uyeda, S. (1981). Subduction zones and back arc basins - A review. *Geologische Rundschau*, 70(2):552–569.

Van Avendonk, H. J., Lavier, L. L., Shillington, D. J., and Manatschal, G. (2009). Extension of continental crust at the margin of the eastern Grand Banks, Newfoundland. *Tectonophysics*, 468(1-4):131–148.

Van Staal, C. R. and Barr, S. M. (2012). Lithospheric architecture and tectonic evolution of the canadian appalachians and associated atlantic margin. In Percival, J. A., Cook, F. A., and Clowed, R. M., editors, *Tectonic styles in Canada: The LITHOPROBE perspective*, chapter 2, pages 41–95. Geological Association of Canada, Special Paper 49.

van Staal, C. R., Barr, S. M., and Murphy, J. B. (2012). Provenance and tectonic evolution of Ganderia: Constraints on the evolution of the Iapetus and Rheic oceans. *Geology*, 40(11):987–990.

van Staal, C. R., Dewey, J. F., Niocaill, C. M., and McKerrow, W. S. (1998). The Cambrian-Silurian tectonic evolution of the northern Appalachians and British Caledonides: history of a complex, west and southwest Pacific-type segment of Iapetus. *Geological Society, London, Special Publications*, 143(1):197–242.

van Wijk, J., van Hunen, J., and Goes, S. (2008). Small-scale convection during continental rifting: Evidence from the Rio Grande rift. *Geology*, 36(7):575.

Vanderhaeghe, O. and Teyssier, C. (2001). Crustal-scale rheological transitions during late-orogenic collapse. *Tectonophysics*, 335:211–228.

Vauchez, A., Barruol, G., and Tommasi, A. (1997). Why do continents break-up parallel to ancient orogenic belts? *Terra Nova*, 9(2):62–66.

Vauchez, A., Tommasi, A., and Barruol, G. (1998). Rheological heterogeneity, mechanical anisotropy and deformation of the continental lithosphere. *Tectonophysics*, 296(1-2):61–86.

Vavra, G., Gebauer, D., Schmid, R., and Compston, W. (1996). Multiple zircon growth and recrystallization during polyphase Late Carboniferous to Triassic metamorphism in granulites of the Ivrea Zone (Southern Alps): an ion microprobe (SHRIMP) study. *Contributions to Mineralogy and Petrology*, 122(4):337–358.

Veevers, J. J. (2004). Gondwanaland from 650–500 Ma assembly through 320 Ma merger in Pangea to 185–100 Ma breakup: supercontinental tectonics via stratigraphy and radiometric dating. *Earth-Science Reviews*, 68:1–132.

von Raumer, J. F. and Stampfli, G. M. (2008). The birth of the Rheic Ocean ‚Äî Early Palaeozoic subsidence patterns and subsequent tectonic plate scenarios. *Tectonophysics*, 461:9–20.

von Raumer, J. F., Stampfli, G. M., and Bussy, F. (2003). Gondwana-derived microcontinents – the constituents of the Variscan and Alpine collisional orogens. *Tectonophysics*, 365:7–22.

Warr, L. N. (2009). The Variscan orogeny: the welding of Pangea. In Woodcock, N. H. and Strachan, R. A., editors, *Geological History of Britain and Ireland*, chapter 15, pages 271–294. Blackwell Publishing Ltd.

Welford, J. K., Shannon, P. M., O'Reilly, B. M., and Hall, J. (2010). Lithospheric density variations and Moho structure of the Irish Atlantic continental margin from constrained 3-D gravity inversion. *Geophysical Journal International*, 183:79–95.

Welford, J. K., Shannon, P. M., O'Reilly, B. M., and Hall, J. (2012). Comparison of lithosphere structure across the Orphan Basin‚ÄìFlemish Cap and Irish Atlantic conjugate continental margins from constrained 3D gravity inversions. *Journal of the Geological Society, London*, 169(4):405–420.

White, R. S., Mckenzie, D., and O'Nions, K. (1992). Oceanic crustal thickness from seismic measurements and rare earth inversions. *Journal of Geophysical Research*, 97(B13):19683–19715.

White, R. S., Smallwood, J. R., Fliedner, M. M., Boslaugh, B., Maresh, J., and Fruehn, J. (2003). Imaging and regional distribution of basalt flows in the Faeroe-Shetland Basin. *Geophysical Prospecting*, 51:215–231.

White, R. S. and Smith, L. K. (2009). Crustal structure of the Hatton and the conjugate east Greenland rifted volcanic continental margins, NE Atlantic. *Journal of Geophysical Research*, 114(B2):B02305.

Whitmarsh, R. B., Manatschal, G., and Minshull, T. a. (2001). Evolution of magma-poor continental margins from rifting to seafloor spreading. *Nature*, 413(6852):150–154.

Whittaker, J. M., Goncharov, A., Williams, S. E., Müller, R. D., and Leitchenkov, G. (2013). Global sediment thickness data set updated for the Australian-Antarctic Southern Ocean. *Geochemistry, Geophysics, Geosystems*, 14(8):3297–3305.

Willett, S., Beaumont, C., and Fullsack, P. (1993). Mechanical model for the tectonics of doubly vergent compressional orogens. *Geology*.

Williamson, J. P., Pharaoh, T. C., Banka, D., Thybo, H., Laigle, M., and Lee, M. K. (2002). Potential field modelling of the Baltica ‚Äì Avalonia (Thor ‚Äì Tornquist) suture beneath the southern North Sea. *Tectonophysics*, 360:47–60.

Wilson, D., Aster, R., West, M., Ni, J., Grand, S., Gao, W., Baldridge, W. S., Semken, S., and Patel, P. (2005). Lithospheric structure of the Rio Grande rift. *Nature*, 433:851–855.

Wilson, J. T. (1966). Did the Atlantic close and then re-open? *Nature*, 211:676–681.

Winchester, J. A., Pharaoh, T. C., and Verniers, J. (2002). Palaeozoic amalgamation of Central Europe: an introduction and synthesis of new results from recent geological and geophysical investigations. In Winchester, J. A., Pharaoh, T. C., and Verniers, J., editors, *Palaeozoic Amalgamation of Central Europe*, volume 201, pages 1–18. Geological Society, London, Special Publications, 201.

Wintsch, R. P., Yang, H. J., Li, X. H., and Tung, K. A. (2011). Geochronologic evidence for a cold arc-continent collision: The Taiwan orogeny. *Lithos*, 125(1-2):236–248.

Withjack, M. O., Schilsche, R. W., and Olsen, P. E. (2012). Development of the passive margin of eastern North America: Mesozoic rifting, igneous activity, and breakup. In Roberts, D. G. and Bally, A. W., editors, *Regional Geology and Tectonics: Phanerozoic Rift Systems and Sedimentary Basins*, chapter 13, pages 301–335. Elsevier.

Woodcock, N., Soper, N., and Strachan, R. (2007). A Rheic cause for the Acadian deformation in Europe. *Journal of the Geological Society*, 164(5):1023–1036.

Woodcock, N. H. and Strachan, R. A. (2009). The Caledonian Orogeny: a multiple plate collision. In Woodcock, N. H. and Strachan, R. A., editors, *Geological History of Britain and Ireland*, chapter 12, pages 187–206. Blackwell Publishing Ltd.

Woodhead, J., Eggins, S., and Gamble, J. (1993). High field strength and transition element systematics in island arc and back-arc basin basalts: Evidence for multiphase melt extraction and a depleted mantle wedge. *Earth and Planetary Science Letters*, 114(4):491–504.

Workman, R. K. and Hart, S. R. (2005). Major and trace element composition of the depleted MORB mantle (DMM). *Earth and Planetary Science Letters*, 231(1-2):53–72.

Yamazaki, D. and Karato, S.-i. (2001). Some mineral physics constraints on the rheology and geothermal structure of Earth‚Äôs lower mantle. *American Mineralogist*, 86:385–391.

Žák, J., Dragoun, F., Verner, K., Chlupáčová, M., Holub, F. V., and Kachlík, V. (2009). Forearc deformation and strain partitioning during growth of a continental magmatic arc: The northwestern margin of the Central Bohemian Plutonic Complex, Bohemian Massif. *Tectonophysics*, 469(1-4):93–111.

Zalán, P. V., Severino, M. D. C. G., Rigoti, C. A., Magnavita, L. P., Bach de Oliveira, J. A., and Viana, A. R. (2012). 3D crustal architecture of a magma-poor passive margin, Santos, Campos and Espírito Santo Basins ‚Äì Comparisons with a volcanic passive margin, Pelotas Basin ‚Äì Offshore Brazil. *Marine and Petroleum Geology*.

Zhao, D. (1997). Depth Extent of the Lau Back-Arc Spreading Center and Its Relation to Subduction Processes. *Science*, 278(5336):254–257.

Ziegler, P. A. (1988). Evolution of the Arctic-North Atlantic and the Western Tethys. *American Association of Petroleum Geologists Memoir*, 43:164–196.

Ziegler, P. a. and Cloetingh, S. (2004). Dynamic processes controlling evolution of rifted basins. *Earth-Science Reviews*, 64(1-2):1–50.

Ziegler, P. A. and Dèzes, P. (2006). Crustal Evolution of Western and Central Europe. In Gee, D. G. and Stephenson, R. A., editors, *European Lithosphere Dynamics*, pages 43–56. Geological Society, London, Memoir 32.

Zuber, M. T., Parmentier, E. M., and Fletcher, R. C. (1986). Extension of continental lithosphere - A model for two scales of Basin and Range deformation. *Journal of Geophysical Research*, 91(4):4826–4838.

Annex A

The role of inheritance in structuring hyperextended rift systems: some considerations based on observations and numerical modelling

Gianreto Manatschal[*,1], Luc L. Lavier[2], Pauline Chenin[1]
[1] IPGS - EOST, Université de Strasbourg, 1 rue Blessig, 67084 Strasbourg, France
[2] Institute for Geophysics, J.J. Pickle Research Campus, Bldg. 196, 10100 Burnet Rd., Austin, Texas, 78758, USA
[*] Corresponding author (email: gianreto.manatschal@unistra.fr)

Published in *Gondwana Research* in January 2015
Volume: 27; issue 1; pages: 140–164

Abstract

A long-standing question in Earth Sciences is related to the importance of inheritance in controlling tectonic processes. In contrast to physical processes that are generally applicable, assessing the role of inheritance suffers from two major problems: firstly, it is difficult to appraise without having insights into the history of a geological system; and secondly all inherited features are not reactivated during subsequent deformation phases. Therefore, the aim of this paper is to give some conceptual framework about how inheritance may control the architecture and evolution of hyperextended rift systems.

In this paper, we use the term inheritance to refer to the difference between an "ideal" layer-cake type lithosphere and a "real" lithosphere containing heterogeneities. The underlying philosophy of this work is that the evolution of hyperextended rift systems reflects the interplay between their inheritance (innate/"genetic code") and the physical processes at play (acquired/external factors). Thus, by observing the architecture and evolution of hyperextended rift systems and integrating the physical processes, one my get hints on what may have been the original inheritance of a system.

We first define 3 types of inheritance, namely structural, compositional and thermal inheritance and develop a simple and robust terminology able to describe and link observations made at different scales using geological, geophysical and modelling approaches. To this, we add definition of rift-induced processes, i.e. processes leading to compositional changes during rifting (e.g. seprentinization or decompression melting). Using this approach, we focus on 3 well-studied rift systems that are the Alpine Tethys, Pyrenean-Bay of Biscay and Iberia-Newfoundland rift systems. However, as all these examples are magma-poor, hyperextended rift systems that evolved over Variscan lithosphere the concepts developed in this paper cannot be applied universally. For the studied examples we can show that:

1. the inherited structures did not significantly control the location of breakup and the structures in the southern North Atlantic example
2. the inherited thermal state may control the mode and architecture of rift systems, in particular the architecture of the necking zone

3. the architecture of the necking zone may be influenced by the distribution and importance of ductile layers during decoupled deformation and is consequently controlled by the thermal structure and/or the inherited composition of the curst
4. conversely, the deformation in hyperextended domains is strongly controlled by weak hydrated minerals (e.g. clay, serpentinite) that result form the breakdown of feldspar and olivine due to fluid and reaction assisted deformation
5. inherited structures, in particular weaknesses, are important in controlling strain localization on a local scale and during early stages of rifting
6. inherited mantle composition and rift-related mantle processes may control the rheology of the mantle, the magmatic budget, the thermal structure and the localization of final rifting

These key observations show that both inheritance and rift-induced processes played a significant role in the development of the magma-poor southern North Atlantic and Alpine Tethys rift systems and that the role of inheritance may change as the physical conditions vary during the evolving rifting and as rift-induced processes (serpentinization; magma) become more important. Thus, it is not only important to determine the "genetic code" of a rift system, but also to understand how it interacts and evolves during rifting. Understand how far these new ideas and concepts derived from the well-studied hyperextended rift systems of the southern North Atlantic and Alpine Tethys can be translated to other less explored hyperextended rift systems will be one of the challenges of the future research in rifted margins.

Annex B

Mapping orogenic inheritance in Western Europe: the Palaeozoic and Mesozoic orogenic domains

In this appendix, I detail the orogenic inheritance map presented in Chapter I, distinguishing between the features relative to the Caledonian and Variscan orogens and adding the orogenic features inherited from the Alpine orogeny. I remind that I define inheritance as the deviation between an ideal, horizontally thermally and lithologically homogeneous, and a real lithosphere with structural complexity and lithological and thermal heterogeneities (Figure B1). In my mapping, an orogenic domain is the area limited by the trace of its corresponding deformation fronts at the surface. For each, I map suture zones, deformation fronts and foreland basins.

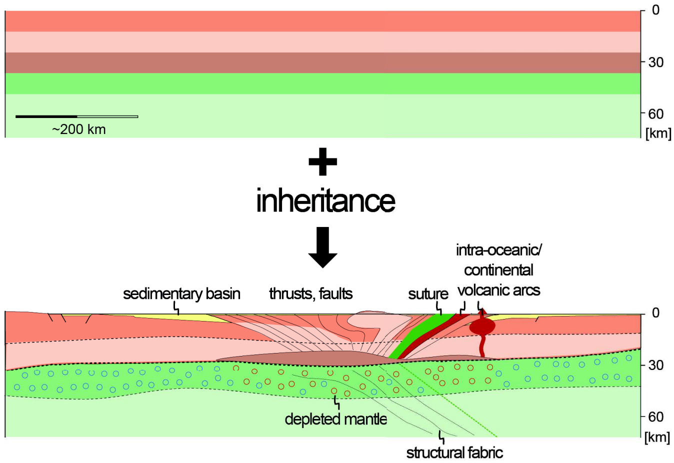

Figure B1 – Definition of inheritance as the deviation between an ideal 'layer-cake'-type lithosphere and a real, heterogeneous lithosphere.

1 The Caledonian orogenic domain

The map presented in Figure B2 shows the extent of the Caledonian orogen and the location of its corresponding sutures, deformation fronts and foreland basin. Data are compiled after Asher et al. (2001); Dadlez et al. (2013); Larson et al. (1999); Mosar (2003); Roberts (2003); Ziegler and Dèzes (2006); see Chapter I for details and discussion.

2 The Variscan orogenic domain

The map presented in Figure B3 shows the extent of the Variscan orogen and the location of its corresponding sutures, deformation fronts and foreland basin. Data are compiled after Ballèvre et al. (2009); Edel et al. (2013); Franke (2006); Franke

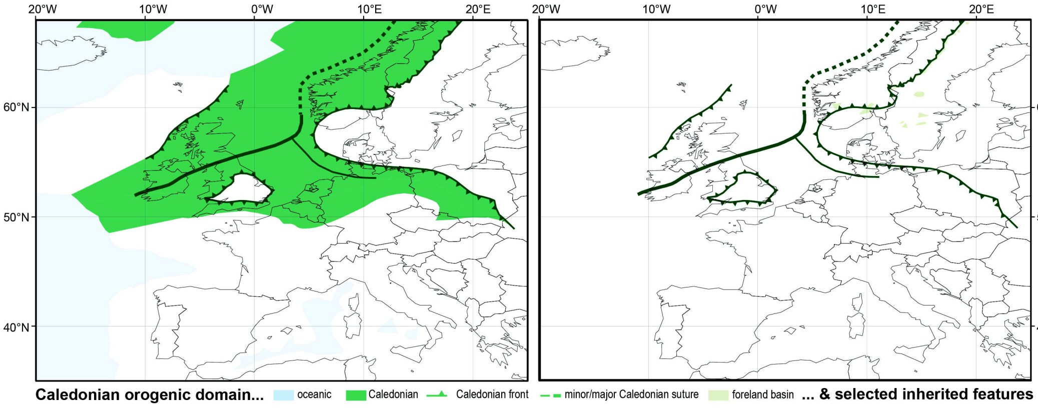

Figure B2 – Map of the Caledonian orogenic domain and its corresponding major inherited features western Europe.

and Engel (1988); Frizon de Lamotte et al. (2011); Ziegler (1988); Ziegler and Dèzes (2006); see Chapter I for details and discussion.

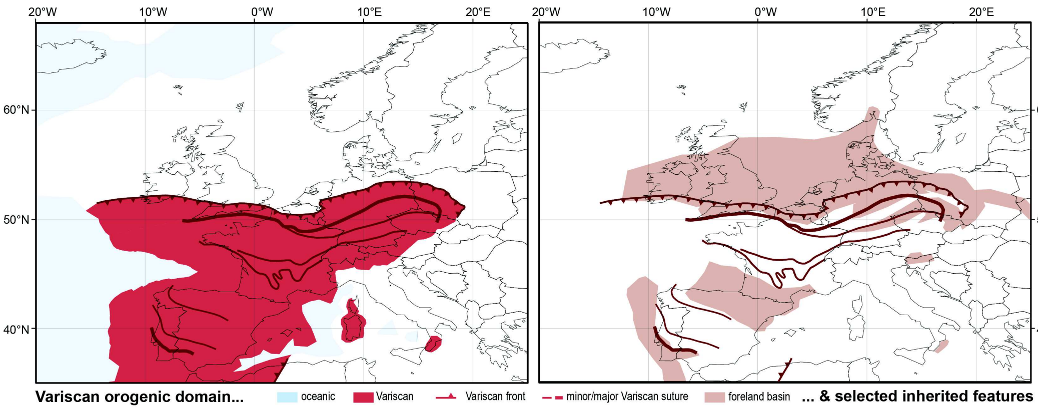

Figure B3 – Map of the Variscan orogenic domain and its corresponding major inherited features western Europe.

3 The Alpine orogenic domain

In addition to mapping Palaeozoic orogenic inheritance, I compiled the same inherited features for the Mesozoic Alpine domain. I consider the suture zones and deformation fronts as mapped by Ziegler and Dèzes (2006) for western part of the Alpine domain. The Alpine deformation front in eastern Spain is from Verges and Sabat (1999) and the Alpine foreland after Gawfôda and Golonka (2011). Ophiolites in western Alps are from Schmid et al. (2004), Greek ophiolites from Robertson et al. (2013) and Carpathian ophiolites from Stojadinovic et al. (2013). These are summarized in the map presented in Figure B4.

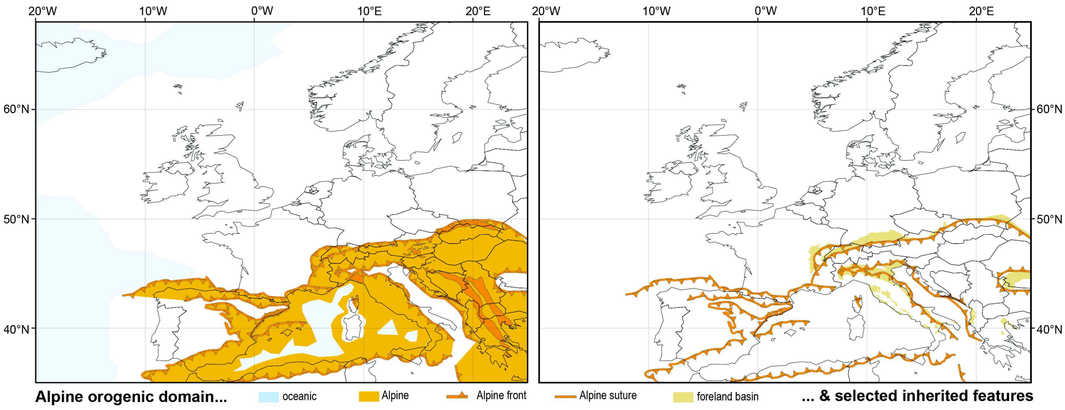

Figure B4 – Map of the Alpine orogenic domain and its corresponding major inherited features western Europe.

4 The extent of post-orogenic underplating

I assessed the extent of the widespread Permo-Triasic magmatic event in Western Europe based using a combination of seismic data and data from field studies (Figure B5). The seismic sections published by Rey (1993) and Blundell et al. (1991) show a very reflective lower crust over most of Western Europe and in the North Sea. Furthermore, in several places in the Alps such as Sondalo, Fedoz and Braccia, pre-rift mafic magmatic bodies located in the lower crust crop out. With regard to their contemporaneous age and their associated granulitic metamorphism, these have been interpreted as emplaced during a large-scale post-orogenic thermal event (see Petri, 2014 for a review). Samples from drill-holes as well as xenoliths suggest that this event did affect most of Western Europe.

5 Summary: Palaeozoic and Mesozoic orogenic inheritance

The map compiling the selected inherited features for all the Palaeozoic and Mesozoic orogens, including post-orogenic collapse magmatic intrusions/underplating and pre-orogenic magmatic arcs, is presented on Figure B6.

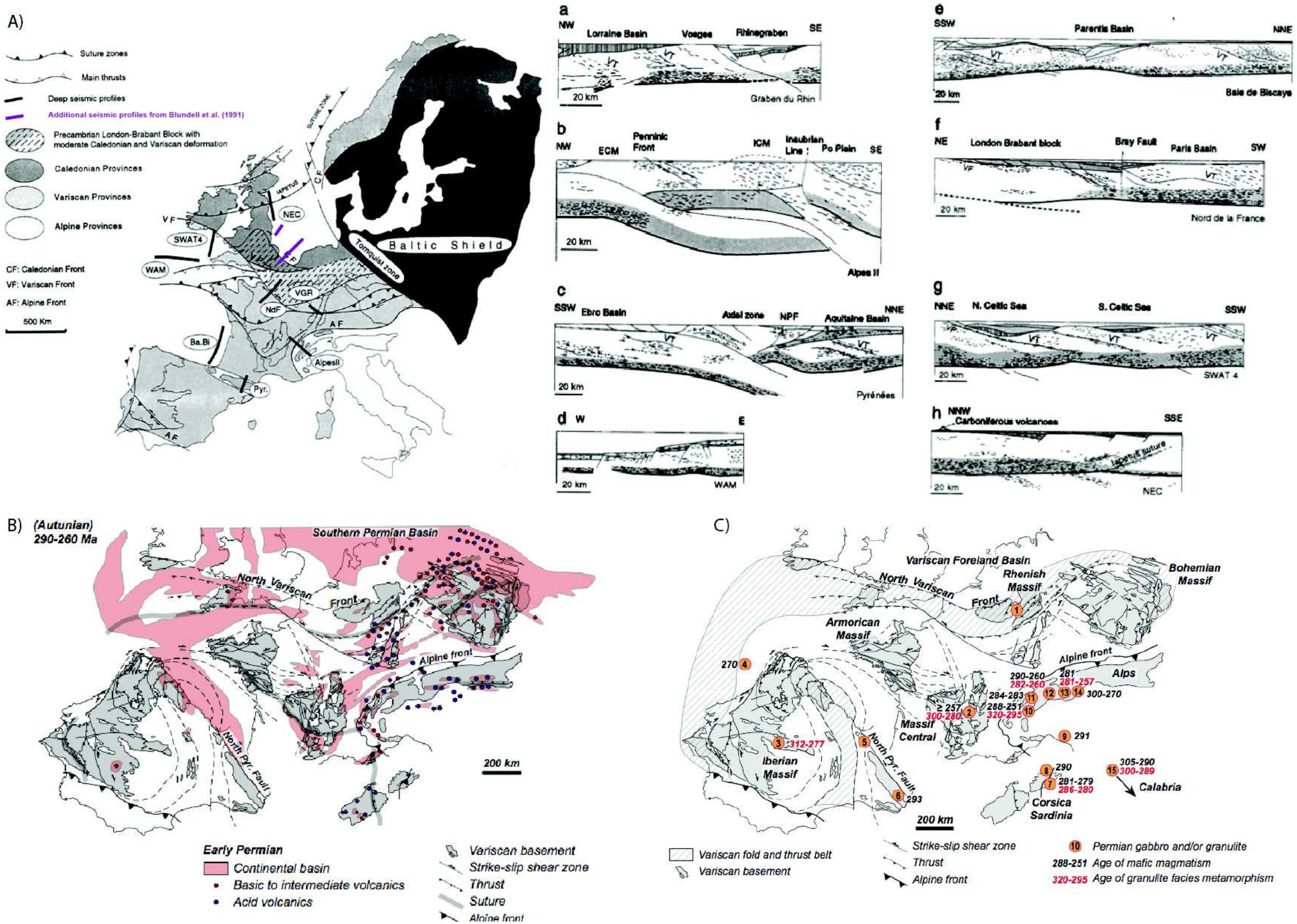

Figure B5 – Data used to assess the extent of underplating in Western Europe. A) Seismic sections from Rey (1993) and Blundell et al. (1991). B) and C) Outcrops, xenoliths and drilling of massive magmatic intrusions, mafic lower crust and granulite facies metamorphism from Petri (2014).

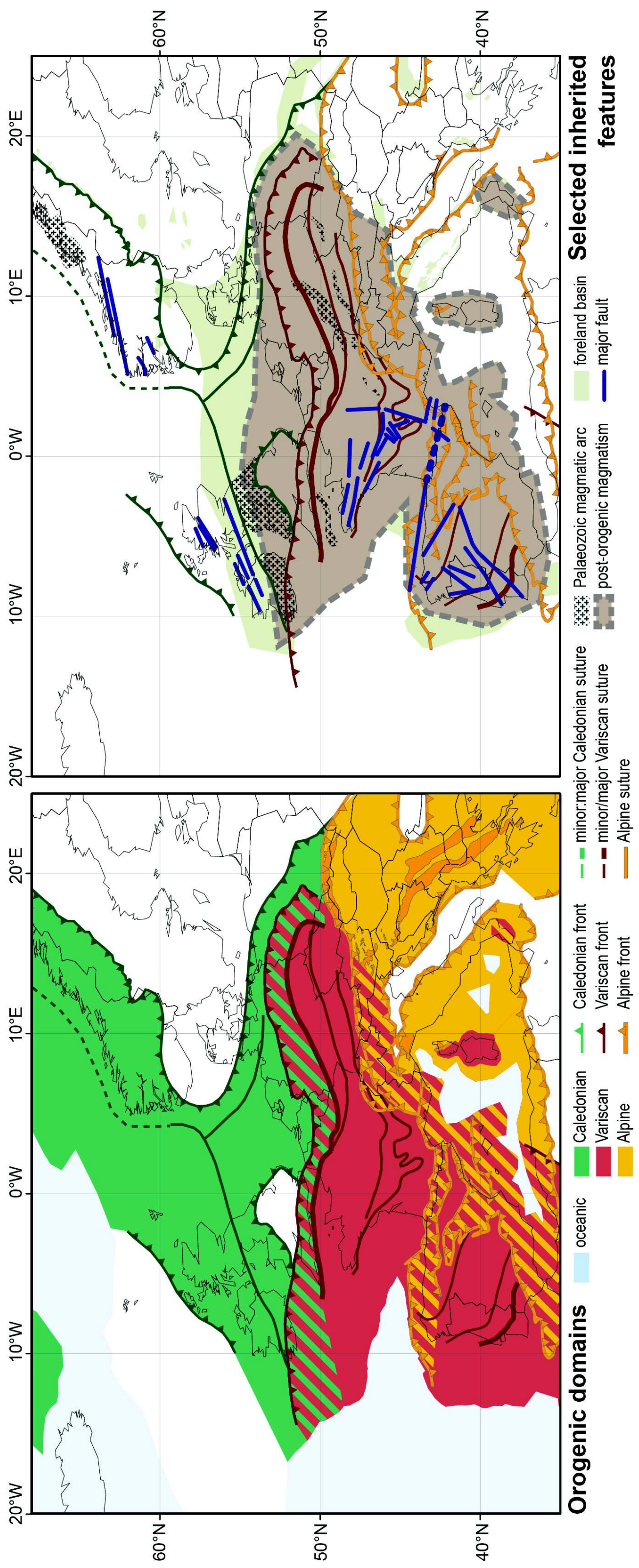

Figure B6 – Map of orogenic inheritance in western Europe.

Annex C

Mapping the necking, hyperextended and exhumation domains in the North Atlantic and in Western Europe: a failed attempt

1 Initial objectives

My initial goal was to map the necking, hyperextended and exhumation domains as defined by Sutra et al. (2013) – see Figure C1 – at the scale of the North Atlantic region. At first, I attempted to synthesize the results published studies and to rely on public cross sections in order to identify these. However, I quickly reached a deadlock due to the scarcity and insufficient quality of data, thus the impossibility to correlate these domains through space (Figure C2).

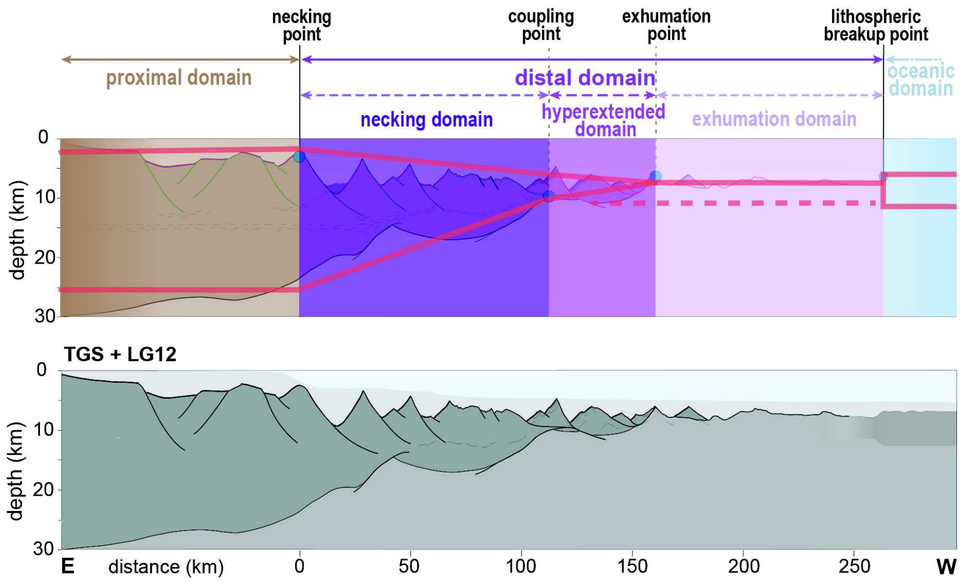

Figure C1 – Definition of rift domains by Sutra et al. (2013). The necking point corresponds to the limit of significant crustal thinning. From the coupling point, the whole crust is embrittled, thus coupled to the lithospheric mantle. The exhumation point stands at the first occurrence of exhumed mantle and the lithospheric breakup point corresponds to the onset of steady-state seafloor spreading.

My second attempt consisted in applying the same method as (Tugend et al., 2014) in the North Atlantic in order to extend their mapping offshore Iberia and in the Bay of Biscay to the whole North Atlantic. However, as this method used to highlight crustal architecture is primarily based on gravity data inversion, it required to correct the topography of the seafloor from the amount of sediment, but also from magma where it exists. However, the thickness of the extensive magmatic additions that exist North of the Charlie–Gibbs fracture zone is very poorly known, and the resolution of seismic section in this region is insufficient to constrain it better.

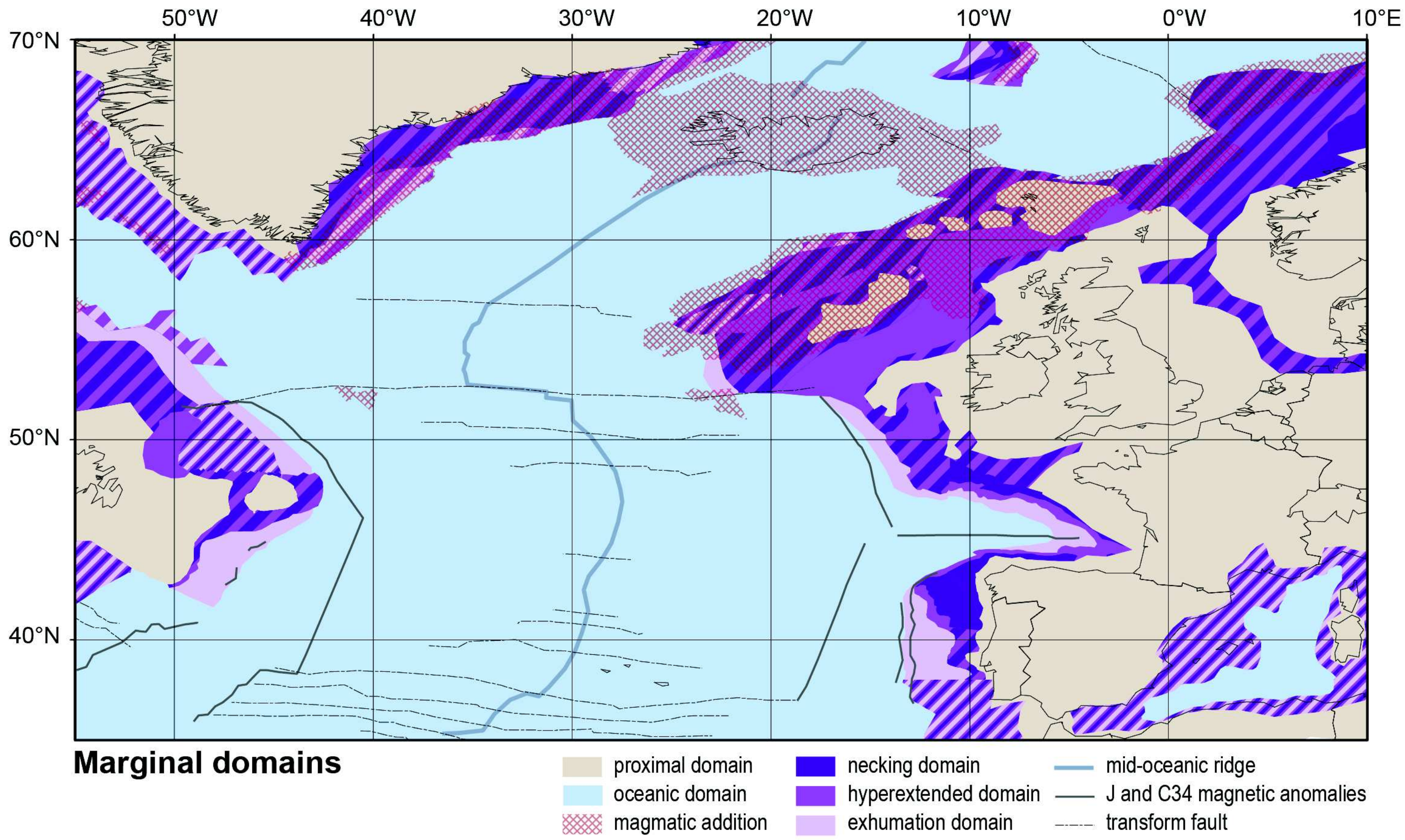

Figure C2 – The result of my first attempt to map rift domains as defined in Figure C1.

At the same time, I also worked on extending the mapping of rift domains to the former Tethyan rift system, now exposed in the Alps. To identify the different domains onshore, I used the criteria developed by Tugend et al. (2014a) – see Figure C3. These include (1) the nature and thickness of sediments, which depends on the paleo-depth and the total accommodation space; (2) the nature of top basement (continental crust, exhumed mantle or oceanic crust); and (3) the geometry and kinematics of extensional system, which is recorded in the architecture of the sedimentary deposits. I relied on published studies, especially the tectonic maps by Schmid et al. (2004) and the study by Mohn et al. (2010) to create the map shown in Figure C3. However, as I decided to focus my PhD thesis on the North Atlantic rift system, I didn't extent this mapping further.

2 Method actually developed

Because my primary aim was to create a robust but first-order map highlighting crustal architecture, I decided to simplify my definition of rift domains (Figure C4), in order to use other geophysical methods to correlate domains boundaries through space. In particular I combined observation of published seismic section and / or gravity models (see Figure C5 for location and Chapter I for references) with a filtered Bouguer anomaly map (see Figure C6 and next section for further details) and the magnetic anomaly map EMAG2 by Maus et al. (2009) – see Figure C7.

2.1 Filtered Bouguer anomaly map

Because the necking point (see Figure C4) represents an abrupt change in crustal thickness, gravimetry is a tool particularly appropriate to locate and correlate this limit on a large scale. We used the bathymetry and gravimetry data grid by Sandwell and Smith (2009); Smith and Sandwell (1997). From these, I calculated the Bouguer anomaly and corrected it from the sedimentary thickness using the grid from Divins (2003). In order to highlight the behavior of the crust with respect to the large-scale variation in the mantle, I filtered the Bouguer anomaly passing wavelengths < 200 km and removing wavelengths > 400 km. The resulting map is shown in Figure C6, and the GMT code is available at the end of this chapter.

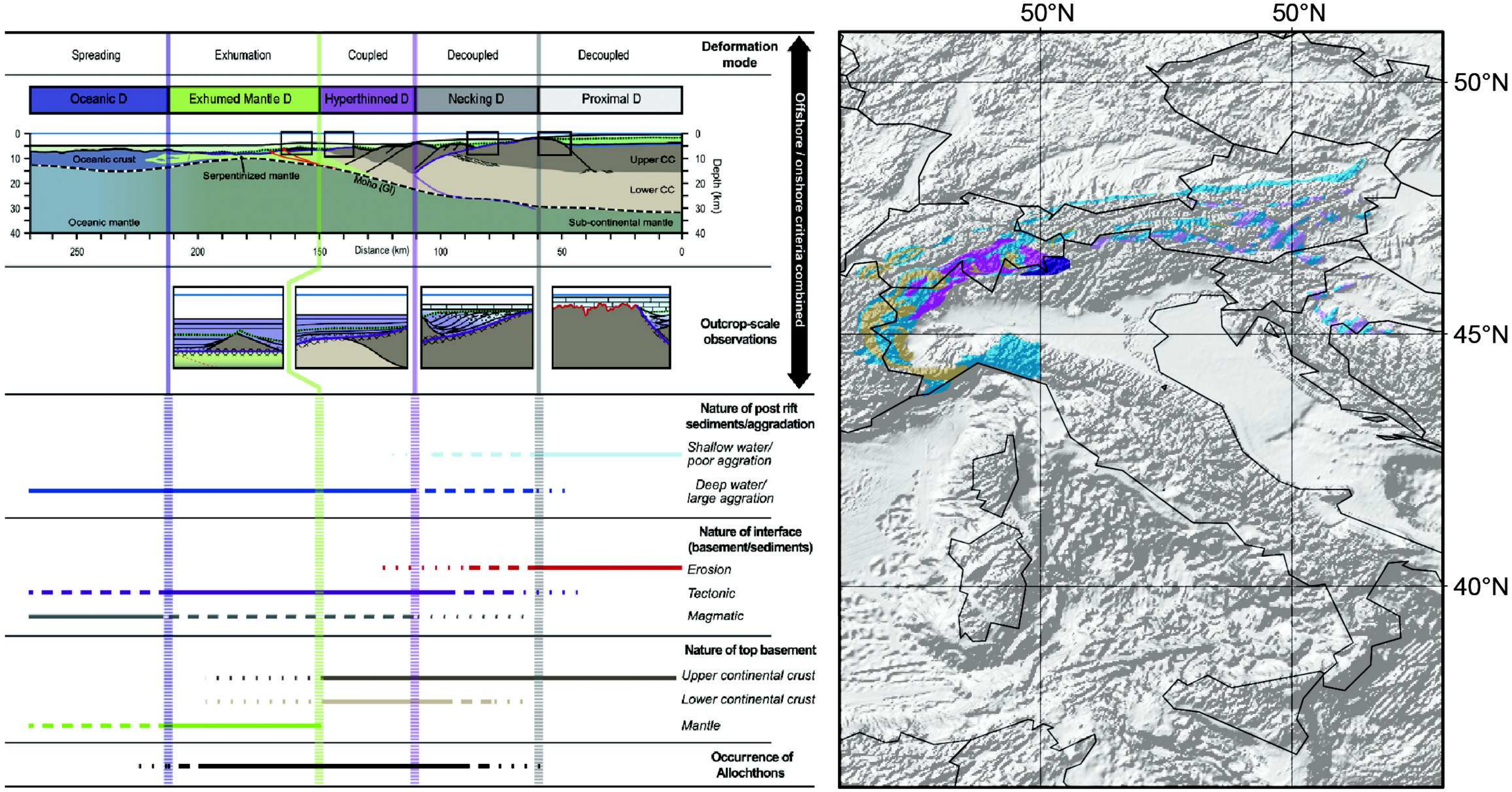

Figure C3 – Left: Geological criteria used to identify the different domains onshore (Tugend et al., 2014a); Right: Map of the former Tethyan rift domains in western Alps.

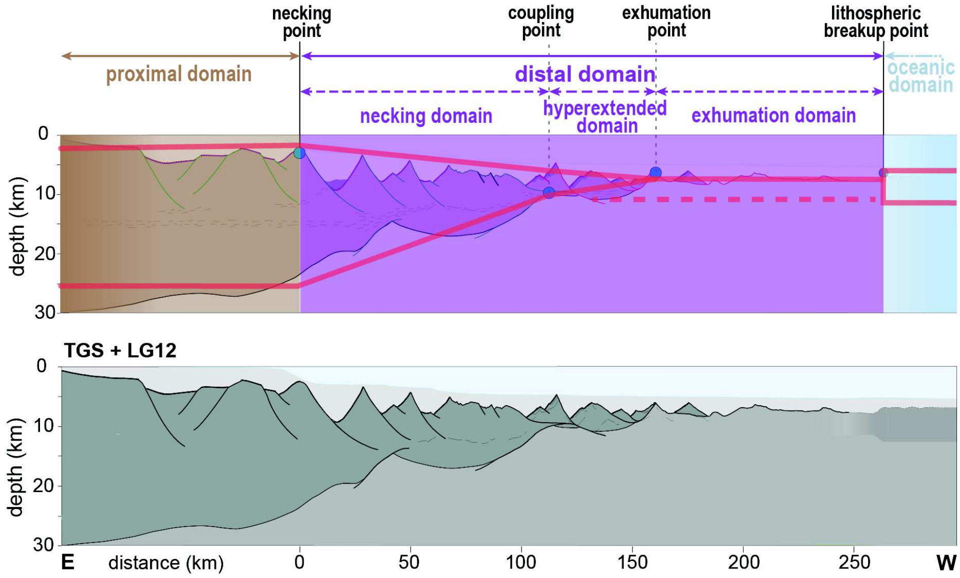

Figure C4 – Definition of the simplified rift domains I actually used in my study. The necking point corresponds to the limit of significant crustal thinning and the lithospheric breakup point to the onset of steady-state seafloor spreading.

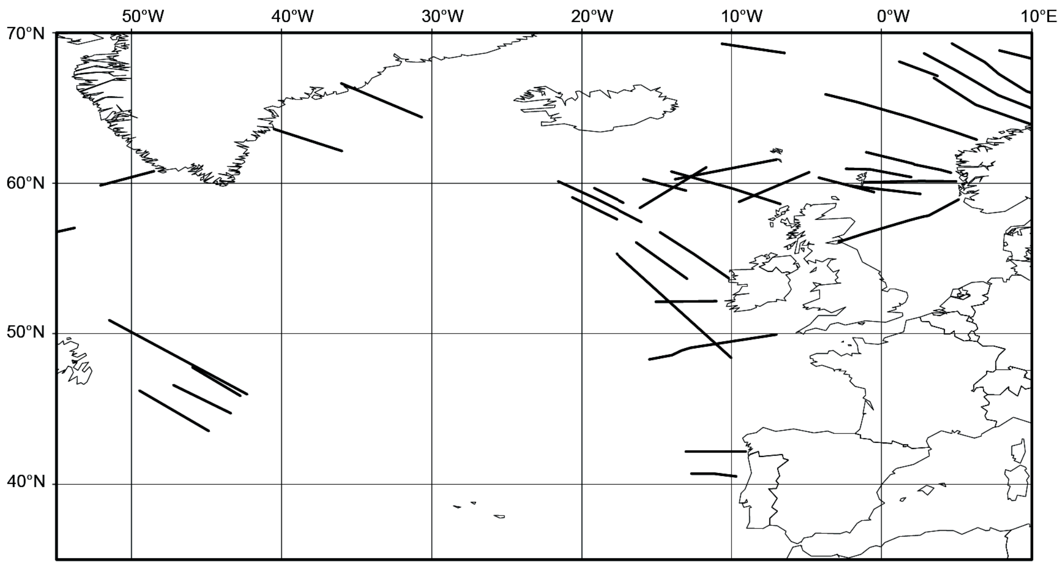

Figure C5 – Location of published cross sections used to highlight crustal architecture in this study.

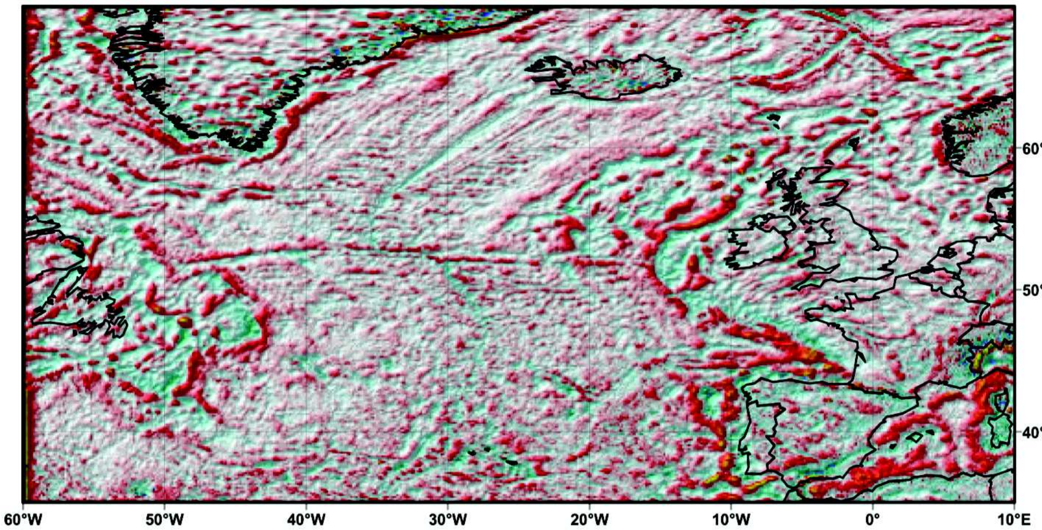

Figure C6 – The filtered Bouguer anomaly map created to correlate the necking point between the cross sections of Figure C5.

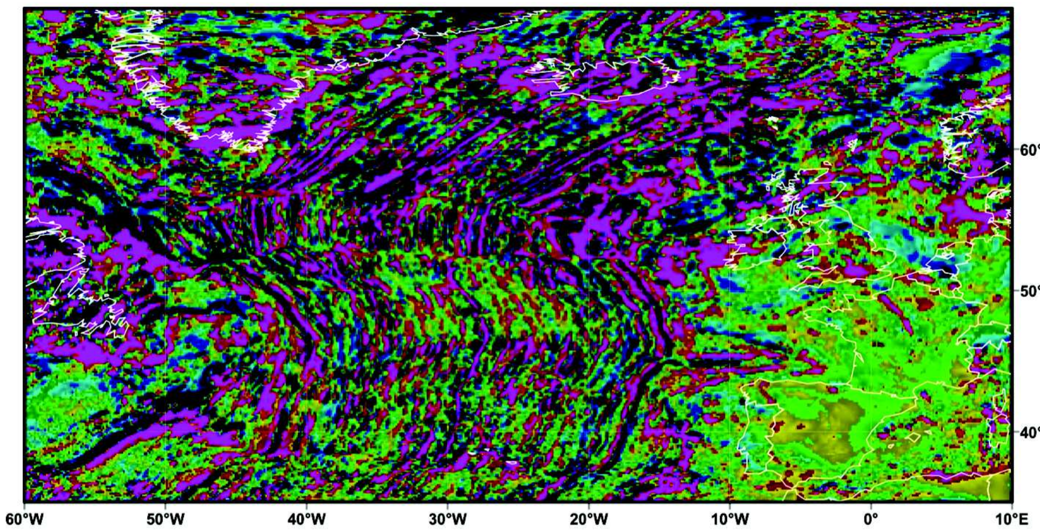

Figure C7 – The magnetic anomaly map EMAG2 (Maus et al., 2009) used to correlate the lithospheric breakup point between the cross sections of Figure C5.

GMT code to generate the filtered Bouguer anomaly map presented here-above

```
#!/bin/bash

# COMPUTATION OF THE BOUGUER ANOMALY: SUBTRACTION OF THE WATER ANOMALY TO THE FREE AIR GRAVITY ANOMALY
GMT grdmath ../00_Gravi/G_-15_50_35_0.grd ../00_Water_correction/W2_-15_50_35_0.grd SUB = BW2_-15_50_35_0.grd
GMT grdmath ../00_Gravi/G_-15_70_65_-5.grd ../00_Water_correction/W2_-15_70_65_-5.grd SUB = BW2_-15_70_65_-5.grd
GMT grdmath ../00_Gravi/G_-25_65_50_0.grd ../00_Water_correction/W2_-25_65_50_0.grd SUB = BW2_-25_65_50_0.grd
GMT grdmath ../00_Gravi/G_-40_70_60_-20.grd ../00_Water_correction/W2_-40_70_60_-20.grd SUB = BW2_-40_70_60_-20.grd
GMT grdmath ../00_Gravi/G_-55_70_40_-40.grd ../00_Water_correction/W2_-55_70_40_-40.grd SUB = BW2_-55_70_40_-40.grd
GMT grdmath ../00_Gravi/G_0_70_60_15.grd ../00_Water_correction/W2_0_70_60_15.grd SUB = BW2_0_70_60_15.grd

# COMPUTATION OF THE BOUGUER ANOMALY: SUBTRACTION OF THE SEDIMENT GRAVITY ANOMALY TO THE FREE AIR GRAVITY - WATER ANOMALY
GMT grdmath BW2_-15_50_35_0.grd ../00_Sediments/SedEffect_-15_50_35_0.grd SUB = B2_-15_50_35_0.grd
GMT grdmath BW2_-15_70_65_-5.grd ../00_Sediments/SedEffect_-15_70_65_-5.grd SUB = B2_-15_70_65_-5.grd
GMT grdmath BW2_-25_65_50_0.grd ../00_Sediments/SedEffect_-25_65_50_0.grd SUB = B2_-25_65_50_0.grd
GMT grdmath BW2_-40_70_60_-20.grd ../00_Sediments/SedEffect_-40_70_60_-20.grd SUB = B2_-40_70_60_-20.grd
GMT grdmath BW2_-55_70_40_-40.grd ../00_Sediments/SedEffect_-55_70_40_-40.grd SUB = B2_-55_70_40_-40.grd
GMT grdmath BW2_0_70_60_15.grd ../00_Sediments/SedEffect_0_70_60_15.grd SUB = B2_0_70_60_15.grd


# HIGHPASS FILTER PASSING WAVELENGTH <200 KM AND REMOVING WAVELENGTH > 400 KM
GMT grdfft B2_-15_50_35_0.grd -GB2F_-15_50_35_0.grd -F400000/200000/-/- -fg -V
GMT grdfft B2_-15_70_65_-5.grd -GB2F_-15_70_65_-5.grd -F400000/200000/-/- -fg -V
GMT grdfft B2_-25_65_50_0.grd -GB2F_-25_65_50_0.grd -F400000/200000/-/- -fg -V
GMT grdfft B2_-40_70_60_-20.grd -GB2F_-40_70_60_-20.grd -F400000/200000/-/- -fg -V
GMT grdfft B2_-55_70_40_-40.grd -GB2F_-55_70_40_-40.grd -F400000/200000/-/- -fg -V
GMT grdfft B2_0_70_60_15.grd -GB2F_0_70_60_15.grd -F400000/200000/-/- -fg -V

# CREATION OF A COLORBAR
GMT grd2cpt B2F_-15_50_35_0.grd -Z > colorbarB2F_-15_50_35_0.cpt
GMT grd2cpt B2F_-15_70_65_-5.grd -Z > colorbarB2F_-15_70_65_-5.cpt
GMT grd2cpt B2F_-25_65_50_0.grd -Z > colorbarB2F_-25_65_50_0.cpt
GMT grd2cpt B2F_-40_70_60_-20.grd -Z > colorbarB2F_-40_70_60_-20.cpt
```

```
GMT grd2cpt B2F_-55_70_40_-40.grd -Z > colorbarB2F_-55_70_40_-40.cpt
GMT grd2cpt B2F_0_70_60_15.grd -Z > colorbarB2F_0_70_60_15.cpt

# CREATION OF THE MAP
GMT grdimage B2F_-15_50_35_0.grd -R345/360/35/50 -CcolorbarB2F_-15_50_35_0.cpt -Jm0/0/1 -P -V -B1 -K > B2F_-15_50_35_0.ps
GMT grdimage B2F_-15_70_65_-5.grd -R345/355/65/70 -CcolorbarB2F_-15_70_65_-5.cpt -Jm0/0/1 -P -V -B1 -K > B2F_-15_70_65_-5.ps
GMT grdimage B2F_-25_65_50_0.grd -R335/360/50/65 -CcolorbarB2F_-25_65_50_0.cpt -Jm0/0/1 -P -V -B1 -K > B2F_-25_65_50_0.ps
GMT grdimage B2F_-40_70_60_-20.grd -R320/360/60/70 -CcolorbarB2F_-40_70_60_-20.cpt -Jm0/0/1 -P -V -B1 -K > B2F_-40_70_60_-20.ps
GMT grdimage B2F_-55_70_40_-40.grd -R305/320/40/70 -CcolorbarB2F_-55_70_40_-40.cpt -Jm0/0/1 -P -V -B1 -K > B2F_-55_70_40_-40.ps
GMT grdimage B2F_0_70_60_15.grd -R0/15/60/70 -CcolorbarB2F_0_70_60_15.cpt -Jm0/0/1 -P -V -B1 -K > B2F_0_70_60_15.ps

# COLORING WITH THE CREATED SCALE
gmt psscale -D6.4i/2i/7.5c/0.5c -O -K -CcolorbarB2F_-15_50_35_0.cpt >> B2F_-15_50_35_0.ps
gmt psscale -D6.4i/2i/7.5c/0.5c -O -K -CcolorbarB2F_-15_70_65_-5.cpt >> B2F_-15_70_65_-5.ps
gmt psscale -D6.4i/2i/7.5c/0.5c -O -K -CcolorbarB2F_-25_65_50_0.cpt >> B2F_-25_65_50_0.ps
gmt psscale -D6.4i/2i/7.5c/0.5c -O -K -CcolorbarB2F_-40_70_60_-20.cpt >> B2F_-40_70_60_-20.ps
gmt psscale -D6.4i/2i/7.5c/0.5c -O -K -CcolorbarB2F_-55_70_40_-40.cpt >> B2F_-55_70_40_-40.ps
gmt psscale -D6.4i/2i/7.5c/0.5c -O -K -CcolorbarB2F_0_70_60_15.cpt >> B2F_0_70_60_15.ps

# PLOTTING COASTLINES
GMT pscoast -R345/360/35/50 -Jm0/0/1 -O -Na -B1 >> B2F_-15_50_35_0.ps
GMT pscoast -R345/355/65/70 -Jm0/0/1 -O -Na -B1 >> B2F_-15_70_65_-5.ps
GMT pscoast -R335/360/50/65 -Jm0/0/1 -O -Na -B1 >> B2F_-25_65_50_0.ps
GMT pscoast -R320/360/60/70 -Jm0/0/1 -O -Na -B1 >> B2F_-40_70_60_-20.ps
GMT pscoast -R305/320/40/70 -Jm0/0/1 -O -Na -B1 >> B2F_-55_70_40_-40.ps
GMT pscoast -R0/15/60/70 -Jm0/0/1 -O -Na -B1 >> B2F_0_70_60_15.ps

exit
```

Annex D

Additional numerical modelling results: tests on parameters

In this appendix, I present the additional numerical models I ran in order to test various parameters.

1 Constraining the wavelength of the necking instability for high Moho temperatures

In Chapter III, I presented a series of models testing the impact of the initial thermal state of a lithosphere affected by mafic underplating of the continental crust and underlying depleted mantle). In the model with the highest geothermal gradient (Model 4 with a Moho temperature of 500°C in Chapter III – the top one in Figure D1), rifting occurs at the very edge of the model, suggesting that the wavelength of the necking instability is larger than 200 km (= half of the model total width). In order to estimate this wavelength, we increased the width of the model from 400 km to 600 km and 1,000 km (Figure D1).

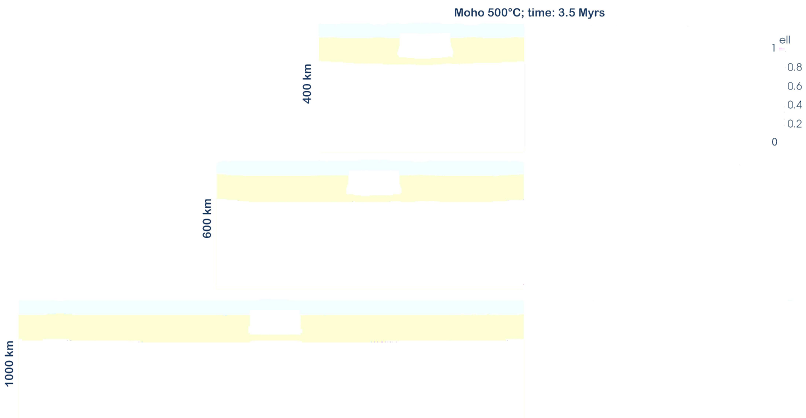

Figure D1 – Models with a similar geothermal gradient and lithological architecture as Model 4 in Chapter III (Moho temperature at 500°C), but with different width; from top to bottom 400 km; 600 km; and 1,000 km; left-hand panels show phase distribution and right-hand panels the second invariant of strain.

This series of models highlights that the wavelength of the necking instability becomes larger (i.e. from 90 km to 200 km and 370 km) when the width of the model is increased (from 400 km to 600 km and to 1,000 km, respectively). Thus, the wavelength of the necking instability depends on the size of the model, at least when the model is less than 1,000 km, in addition to the thermal structure and the strength ratio between the different layer.

Indeed, in all cases, extension localizes eventually at one of the model edges, where stress is applied. A possible cause may relate to the different wavelengths of stress propagation, depending on the rheological properties of the intervening materials. Wider models may allow superimpositions of waves, which wouldn't occur in smaller ones.

Yet, a natural lithosphere is never a infinite homogeneous material since it may be comprised of different terranes with various lithologies and/or thermal states. Therefore, in nature, the wavelength of the *boudinage* triggered by the existence of mafic underplating of the continental crust and/or underlying depleted mantle may essentially be controlled by lateral variations in the rheology of the lithosphere.

2 Impact of fault strength

The rheology of faults is poorly constrained and their strength is most likely highly variable (Ikari et al., 2011). For instance, faults containing phyllosilicates may have an internal angle of friction as low as 11° (Ikari et al., 2011), and even 0° when there is fluid overpressure (Huismans and Beaumont, 2007). Therefore, I ran a series of models with a strain weakening more intense than in the models described in Chapter III, namely ϕ 30° → 5° instead of ϕ 30° → 15°. I reproduced the settings of Models 2–4, i.e. lithospheres with both mafic underplating and depleted mantle, and with Moho temperature of 400°C, 450°C and 500°C (see Figure D2 and D3).

The comparison between the final stages of these two series of models can be compared between Figures D2 and D3. It highlights significant changes in the architecture of the rift depending on the intensity of strain softening. In particular, in our models with cold thermal states (Moho at 400°C and 450°C), the strong strain weakening allow protracted reactivation of the inherited weaknesses above the underplated area, which leads to the final 'breakup' within the former orogenic area (Figure D2). In both cases, the architecture of the rift is very similar, suggesting that the inherited structures are the dominant controlling factor. Conversely, in the equivalent models with a lower strain weakening, extension localizes outside the underplated area while the inherited weaknesses are little or not reactivated (Figure D3).

When the thermal state is higher (Moho at 500°C), the eventual 'breakup' occurs outside the underplated zone in both cases. However, the margins are much shorter and no boudinage of the crust occurs in the model with intense strain softening, although a set of shear zones forms initially on the left-hand side of the model (Figure D2). Indeed, due to the intense strain softening, deformation localizes very early on the right-hand set of shear zones, preventing the formation of any other rift basin. Thus, the architecture of the rift systems is very different from the comparable model with moderate strain softening, and 'breakup' is achieved much earlier.

The major conclusion of this preliminary work is that the rheology of faults may be a major controlling factor in the localization of deformation, thus in the architecture of margins and in the timing of rifting. Appraising the behaviour of faults on a large-scale is therefore of primary importance for the comprehension of rift systems.

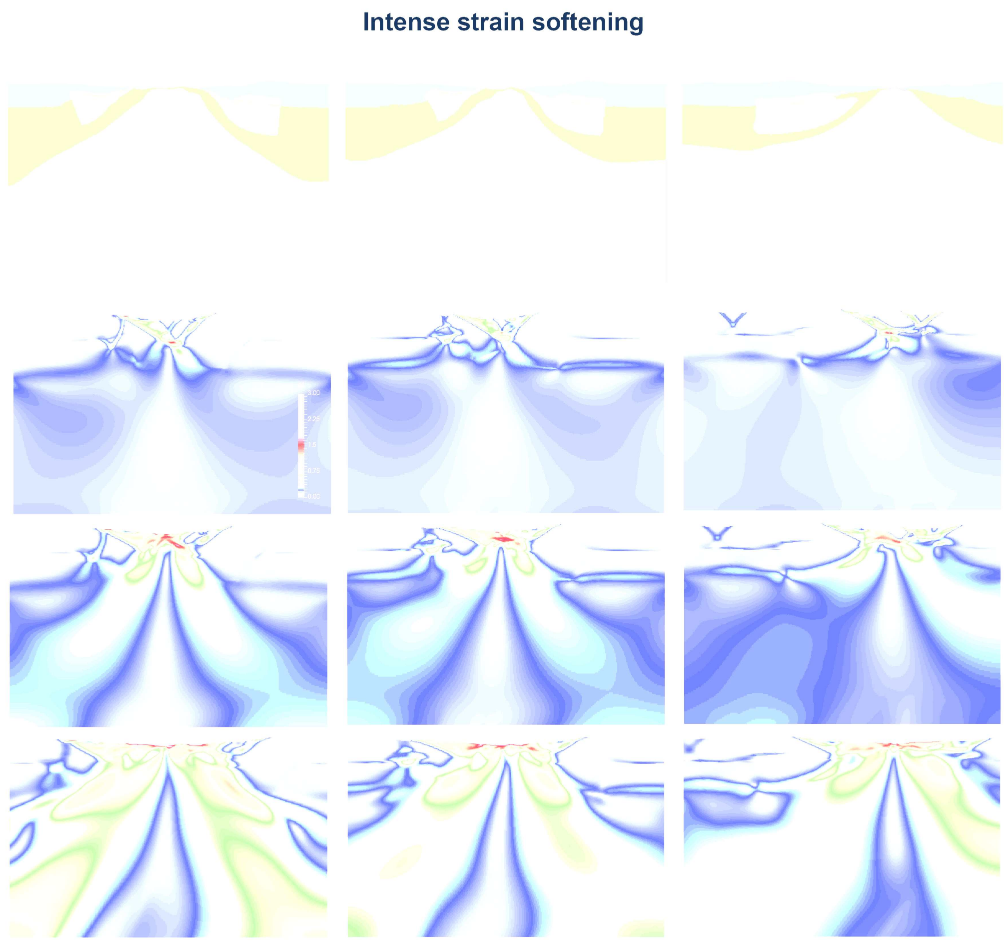

Figure D2 – Top: Phase distribution at the time of 'breakup' for models with a high strain softening (ϕ 30° → 5°); Lower panels: second invariant of strain at different times for Moho temperature of 400°C (left), 450°C (middle) and 500°C (bottom).

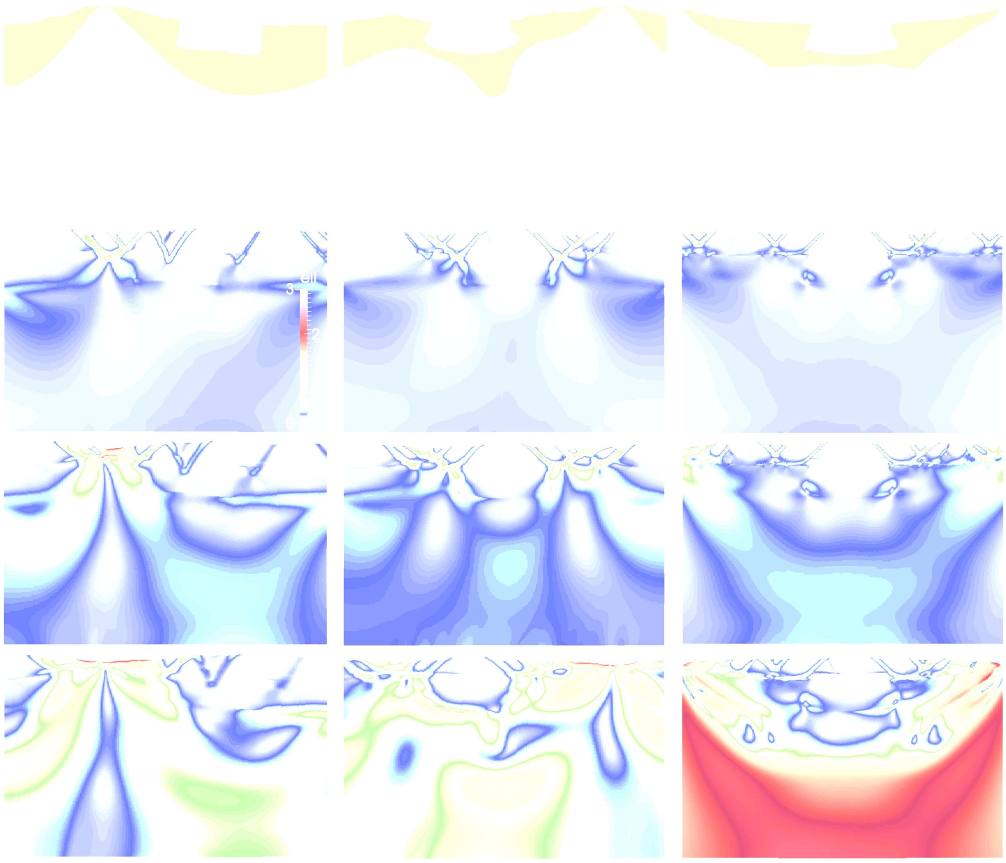

Figure D3 – Top: Phase distribution at the time of 'breakup' for models with a moderate strain softening (ϕ 30° $\rightarrow$ 15°); Lower panels: second invariant of strain at different times for Moho temperature of 400°C (left), 450°C (middle) and 500°C (bottom).

3 The impact of large-scale mantle density contrasts

Subcontinental mantle is likely to be highly heterogeneous, with variations in composition at all scales (Anderson, 2006). In particular, large-scale heterogeneities are associated with mid-oceanic ridges, mantle plumes, subducting slabs and partial melting associated to lithospheric thinning. Yet, differences in mantle composition express as more or less important density variations, as highlighted by (Picazo et al., in prep.). For instance, the density of a fertile mantle associated to crustal thinning down to 10 km or less may be about 3,250 kg.m^{-3}, the density of depleted post-orogenic collapse mantle 3,305 kg.m^{-3} and the density of depleted mid-oceanic ridge mantle 3,320 kg.m^{-3}. In contrast, an average 'inherited' mantle has a density of 3,330 kg.m^{-3} (Picazo et al., in prep), and a typical asthenospheric mantle ranges

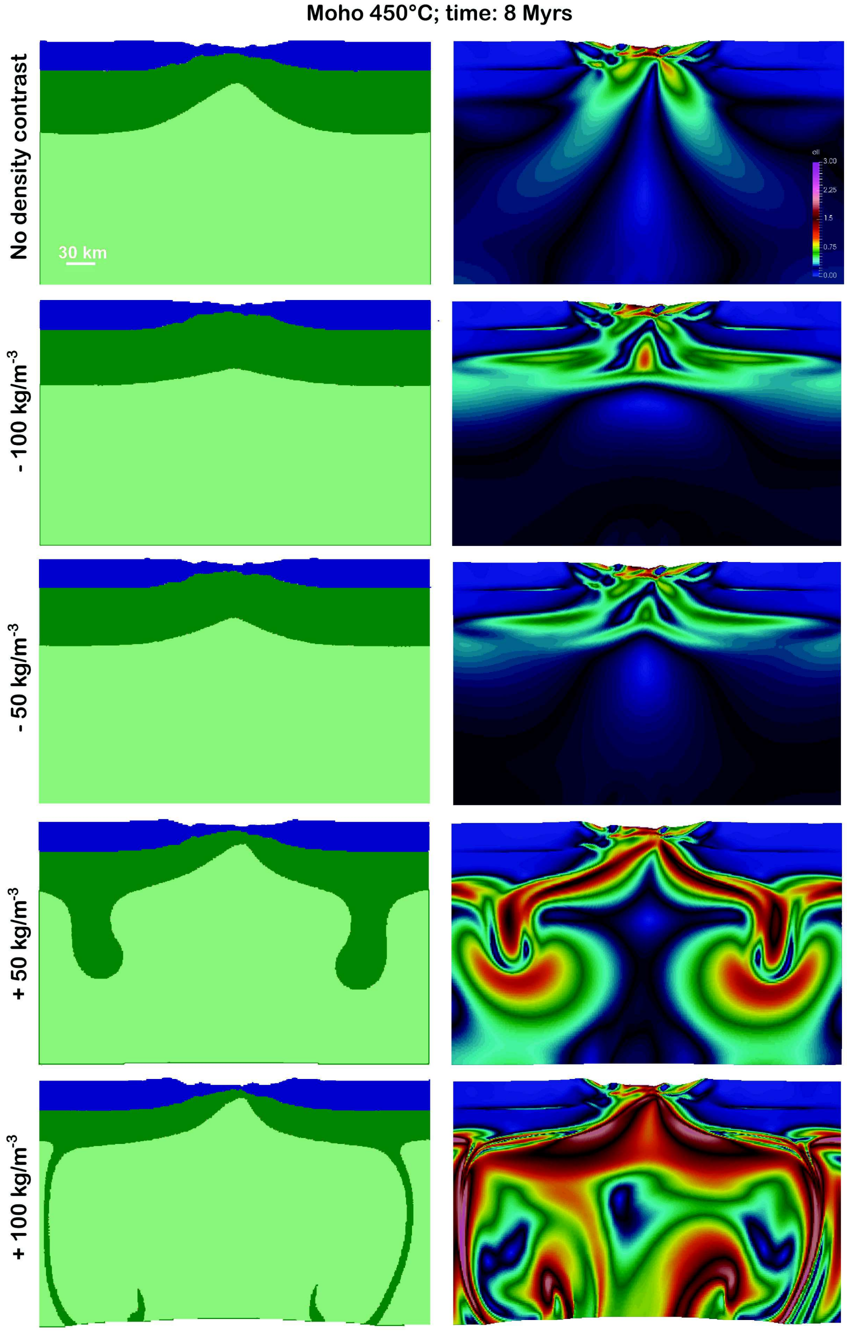

Figure D4 – Models with Moho at 450°C and different density of the lithospheric mantle, compared to the 3,300kg.m^{-3} asthenospheric mantle. Results after 8 Myrs (80 km) extension. Left: phase distribution; Right: second invariant of strain; From top to bottom: No density contrast; 3,400 kg.m^{-3}; 3,350 kg.m^{-3}; 3,250 kg.m^{-3}; and 3,200 kg.m−3.

from about 3,340 to 3,440 kg.m^{-3} between 100 and 250 km. Therefore, I ran some preliminary models in order to test how density contrasts between the lithospheric and asthenospheric mantle may reflect during a rifting event.

This series of models highlight that lower densities of the lithospheric mantle result in more protracted rifting, because the density contrast plays against the upwelling of the asthenospheric mantle. Conversely, when the density of the lithospheric mantle is higher, rifting evolves faster and large-scale convection may be triggered by the delamination of the denser mantle within the asthenosphere.

Note that, in every models of this series, hyperextension localizes within the 'fold-and-thrust belt' (i.e. the series of weaknesses with a reduced internal angle of friction and cohesion from top to middle crustal levels) rather than at the 'suture' (which is a lithospheric-scale structure with serpentine rheology, weaker than the other weaknesses – see Table III.1 in Chapter III for the rheological parameters). The initial asymmetric distribution of the inherited weaknesses reverberates more or less markedly in the architecture of the margins, depending on the density contrast between the lithospheric and asthenospheric mantle.

Appraising the first-order density architecture of the mantle is therefore a key point to understand the behaviour of rift systems on a large scale.

Annex E

Additional numerical modelling results: testing others lithospheric architectures

1 An alternative Variscan lithosphere architecture

The amount, continuity and distribution of depleted mantle beneath a region affected by massive underplating is very poorly constrained. Yet, as the intervening melt is primarily sourced from the underlying asthenospheric mantle (Costa and Rey, 1995; Petri, 2014), part of the latter may be integrated into the lithosphere after the collapse and isostatic re-equilibration of the orogen (Petri, 2014). The composition of the overlying lithosphere may be only little modified by the percolation of melts, thus its rheology mar remain relatively close to that of the surrounding 'inherited mantle' (Müntener et al., 2000; Müntener and Manatschal, 2006; Petri, 2014). Therefore, in this model, we analyze the behaviour of a lithosphere, whose thermal and lithological architecture is comparable to that of Model 3 in Chapter III, except that the 40 km thick depleted mantle is at the base of the lithosphere, thus separated from the mafic underplating by a layer of 'inherited mantle' (Figure E1).

The deformation pattern within the crust is comparable the initial stages of extension (compare Figures E1 and E2 at 4 Myr and 8 Myr), forming two about 80 km wide and 5 km deep basins. However, the depleted mantle zone is intensely deformed, essentially by pure shear, when it is separated from the mafic lower crust by a layer of inherited mantle. This behaviour contrasts with that of Model 3, where the crust and the depleted mantle zone remain in one, largely undeformed block. Interestingly, although the depleted mantle is stronger than the inherited mantle (see Table III.1 in Chapter III), the former is more intensely deformed when it is deeper (Figure E1). This may be explained by a 'grey zone' in stress beneath the mafic underplating, which protects the inherited mantle from the stress induced by the two sets of shear zones on either sides of the underplated domain.

The zone of depleted mantle is progressively stretched and uplifted as extension progresses (Figure E1), while the crust in the two basins is thinned down to less than 3 km. Depleted mantle is eventually exhumed at the seafloor in the right-hand side basin, just prior to the 'breakup' after 27.5 Myr extension. this much more protracted extension compared to Model 3 (19.5 Myr; see Figure E2) may be explained by both its stronger rheology and its lower density (see section 3 in Annex D).

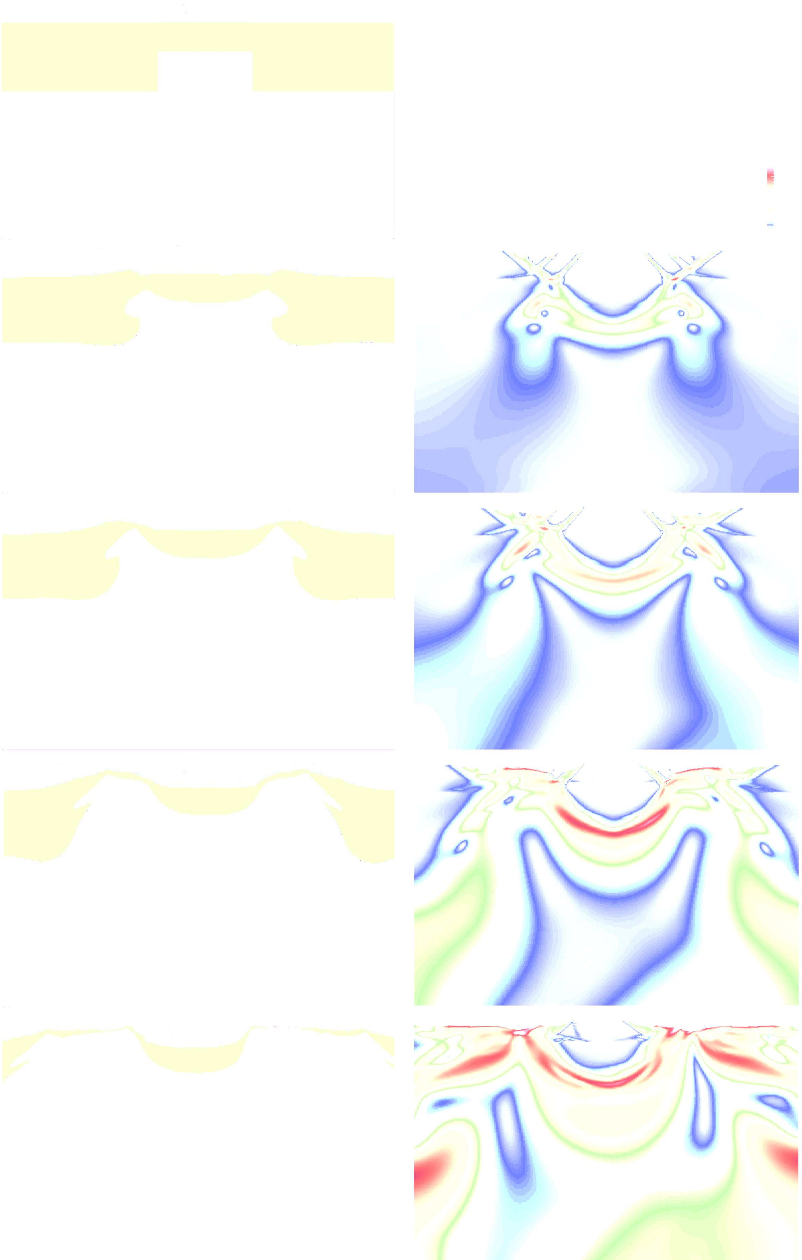

Figure E1 – Results of the numerical model with an alternative Variscan-type lithosphere (see text for details). Left-hand panels: phase distribution; Right-hand panels: second invariant of strain.

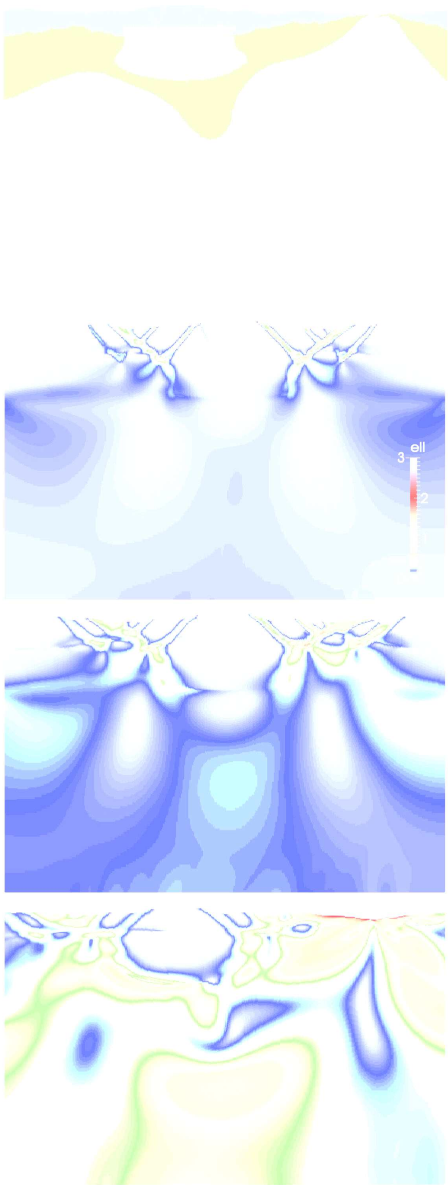

Figure E2 – Results of the Model 3 described in Chapter III. The Moho temperature is 450°C.

2 Caledonian architecture

The architecture of a post-orogenic lithosphere following the closure of a wide oceanic domain may be much more complex than that of the 'reference model' described in Chapter III (Model 1 in Figure III.4). Indeed, orogenesis usually involves the formation of an accretionary prism and the creation of magmatic arcs on the upper plate of the subduction(Uyeda, 1981). Furthermore, the mantle may be highly heterogeneous as well, with remnants of the slab after its breakoff and possibly a zone hydrated mantle above the uppermost part of the slab (Figure E3).

In this model, I test how a simplified post-orogenic lithosphere, which integrates rheological contrasts mimicking a strong magmatic arc (basalt rheology; see Table III.1 in Chapter III), a weak accretionary wedge (same dry quartzite as the continental crust except from the activation energy, which is 200 kJ.mol^{-1} instead of 300 kJ.mol^{-1}), a strong slab remnant (dry olivine rheology; see Table III.1 in Chapter III) and a weak hydrated mantle wedge (wet olivine rheology after Hirth and Kohlstedt (1996)) may impact the architecture of the subsequent rift system. Although the architecture is largely simplified and mostly tentative – especially in the mantle, this model provides areas for further research on the impact of rheological architecture on rift systems.

When extension starts, deformation localizes immediately along the suture zone, down to the hydrated mantle wedge and on the rigth-hand side of the accretionary wedge (Figure E3). As the arc has a stronger rheology, it is harder to deform, thus the necking of the right-hand side margin is much sharper (15 km) than the left-hand one (40 km). The weak accretionary wedge and hydrated mantle are intensively extended and deformed. Rifting is highly asymmetrical, and breakup will most likely be achieved within the accretionary wedge, at the edge of the depleted mantle region.

As a conclusion, rheological contrasts inherited from pre- and syn-orogenic processes are likely to significantly impact both the localization of extension and the architecture of the margins during subsequent rifting.

Figure E3 – Results of the numerical model with a Caledonian-type orogenic lithosphere (see text for details). Left-hand panels: phase distribution; Right-hand panels: second invariant of strain.

References Annex 2 – 5

Anderson, D. L. (2006). Speculations on the nature and cause of mantle heterogeneity. *Tectonophysics*, 416(1-4):7–22.

Asher, J., Warren, M., Fox, R., Harding, P., Jeffcoate, G., and Jeffcoate, S. (2001). *The millennium atlas of butterflies in Britain and Ireland.* Oxford University Press.

Ballèvre, M., Bosse, V., Ducassou, C., and Pitra, P. (2009). Palaeozoic history of the Armorican Massif: Models for the tectonic evolution of the suture zones. *Comptes Rendus Geoscience*, 341:174–201.

Blundell, D. J., Hobbs, R. W., Klemperer, S. L., Scott-Robinson, R., Long, R. E., West, T. E., and Duin, E. (1991). Crustal structure of the central and southern North Sea from BIRPS deep seismic reflection profiling. *Journal of the Geological Society*, 148(3):445–457.

Costa, S. and Rey, P. (1995). Lower crustal rejuvenation and growth during post-thickening collapse: Insights from a crustal cross section through a Variscan metamorphic core complex. *Geology*.

Dadlez, R., Kowalczewski, Z., and Znosko, J. (2013). Some key problems of the pre-Permian tectonics of Poland. *Geological Quarterly*, 38(2):169–190.

Divins, D. L. (2003). Total Sediment Thickness of the World's Oceans & Marginal Seas.

Edel, J. B., Schulmann, K., Skrzypek, E., and Cocherie, A. (2013). Tectonic evolution of the European Variscan belt constrained by palaeomagnetic, structural and anisotropy of magnetic susceptibility data from the Northern Vosges magmatic arc (Eastern France). *Journal of the Geological Society*, 170:785–804.

Franke, W. (2006). The Variscan orogen in Central Europe: construction and collapse. *Geological Society, London, Memoirs*, 32(1):333–343.

Franke, W. and Engel, W. (1988). Tectonic settings of synorogenic sedimentation in the Variscan belt of Europe. In Besly, B. M. and Kelling, G., editors, *Sedimentation in a synorogenic basin complex: the Upper Carboniferous of Northwest Europe*, pages 8–17. Blackie, Glasgow.

Frizon de Lamotte, D., Raulin, C., Mouchot, N., Wrobel-Daveau, J.-C., Blanpied, C., and Ringenbach, J.-C. (2011). The southernmost margin of the Tethys realm during the Mesozoic and Cenozoic: Initial geometry and timing of the inversion processes. *Tectonics*, 30(3):1–22.

Gawfôda, A. and Golonka, J. (2011). Variscan plate dynamics in the circum-carpathian area. *Geodinamica Acta*, 24(3-4):141–155.

Hirth, G. and Kohlstedt, D. L. (1996). Water in the oceanic upper mantle: implications for rheology, melt extraction and the evolution of the lithosphere. *Earth and Planetary Science Letters*, 144(1-2):93–108.

Huismans, R. S. and Beaumont, C. (2007). Roles of lithospheric strain softening and heterogeneity in determining the geometry of rifts and continental margins. In Karner, G. D., Manatschal, G., and Pinhiero, L. M., editors, *Imaging, Mapping and Modelling Continental Lithosphere Extension and Breakup*, pages 107–134. Geological Society, London, Special Publications, 282.

Ikari, M. J., Marone, C., and Saffer, D. M. (2011). On the relation between fault strength and frictional stability. *Geology*, 39(1):83–86.

Larson, S. Å., Tullborg, E.-L., Cederbom, C., and Stiberg, J.-P. (1999). Sveconorwegian and Caledonian foreland basins in the Baltic Shield revealed by fission-track thermochronology. *Terra Nova*, 11(5):210–215.

Maus, S., Barckhausen, U., Berkenbosch, H., Bournas, N., Brozena, J., Childers, V., Dostaler, F., Fairhead, J. D., Finn, C., von Frese, R. R. B., Gaina, C., Golynsky, S., Kucks, R., Lühr, H., Milligan, P., Mogren, S., Müller, R. D., Olesen, O., Pilkington, M., Saltus, R., Schreckenberger, B., Thébault, E., and Caratori Tontini, F. (2009). EMAG2: A 2-arc min resolution Earth Magnetic Anomaly Grid compiled from satellite, airborne, and marine magnetic measurements. *Geochemistry, Geophysics, Geosystems*, 10(8):n/a–n/a.

Mohn, G., Manatschal, G., Müntener, O., Beltrando, M., and Masini, E. (2010). Unravelling the interaction between tectonic and sedimentary processes during lithospheric thinning in the Alpine Tethys margins. *International Journal of Earth Sciences*, 99(SUPPL. 1):75–101.

Mosar, J. (2003). Scandinavia,Äôs North Atlantic passive margin. *Journal of Geophysical Research*, 108(B8, 2360).

Müntener, O., Hermann, R. G., and Trommsdorff, V. (2000). Cooling History and Exhumation of Lower- Crustal Granulite and Upper Mantle (Malenco, Eastern Central Alps). *Journal of Petrology*, 41(2):175–200.

Müntener, O. and Manatschal, G. (2006). High degrees of melt extraction recorded by spinel harzburgite of the Newfoundland margin: The role of inheritance and consequences for the evolution of the southern North Atlantic. *Earth and Planetary Science Letters*, 252:437–452.

Petri, B. (2014). *Formation et exhumation des granulites permiennes*. PhD thesis, Université de Strasbourg.

Rey, P. (1993). Seismic and tectono-metamorphic characters of the lower continental crust in Phanerozoic areas: a consequence of post-thickening extension. *Tectonics*, 12(2):580–590.

Roberts, D. (2003). The Scandinavian Caledonides: event chronology, palaeogeographic settings and likely modern analogues. *Tectonophysics*, 365:283–299.

Robertson, A. H., Trivić, B., fêerić, N., and Bucur, I. I. (2013). Tectonic development of the Vardar ocean and its margins: Evidence from the Republic of Macedonia and Greek Macedonia. *Tectonophysics*, 595-596:25–54.

Sandwell, D. T. and Smith, W. H. F. (2009). Global marine gravity from retracked Geosat and ERS-1 altimetry: Ridge Segmentation versus spreading rate. *Journal of Geophysical Research*, 114(B01411).

Schmid, S. M., Fgenschuh, B., Kissling, E., Schuster, R., and Fügenschuh, B. (2004). Tectonic map and overall architecture of the Alpine orogen. *Eclogae Geologicae Helvetiae*, 97:93–117.

Smith, W. H. F. and Sandwell, D. T. (1997). Global seafloor topography from satellite altimetry and ship depth soundings. *Science*, 277:1957–1962.

Stojadinovic, U., Matenco, L., Andriessen, P. A. M., Toljić, M., and Foeken, J. P. (2013). The balance between orogenic building and subsequent extension during the Tertiary evolution of the NE Dinarides: Constraints from low-temperature thermochronology. *Global and Planetary Change*, 103:19–38.

Sutra, E., Manatschal, G., Mohn, G., and Unternehr, P. (2013). Quantification and restoration of extensional deformation along the Western Iberia and Newfoundland rifted margins. *Geochemistry, Geophysics, Geosystems*, 14(8):2575–2597.

Tugend, J., Manatschal, G., Kusznir, N. J., and Masini, E. (2014a). Characterizing and identifying structural domains at rifted continental margins: application to the Bay of Biscay margins and its Western Pyrenean fossil remnants. *Geological Society London Special Publication*, 413:SP413—-3.

Tugend, J., Manatschal, G., Kusznir, N. J., Masini, E., Mohn, G., and Thinon, I. (2014b). Formation and deformation of hyperextended rift systems: Insights from rift domain mapping in the Bay of Biscay-Pyrenees. *Tectonics*, 33(7):1239–1276.

Uyeda, S. (1981). Subduction zones and back arc basins - A review. *Geologische Rundschau*, 70(2):552–569.

Verges, J. and Sabat, F. (1999). Constraints on the Neogene Mediterranean kinematic evolution along a 1000 km transect from Iberia to Africa. *Geological Society, London, Special Publications*, 156(1):63–80.

Ziegler, P. A. (1988). Evolution of the Arctic-North Atlantic and the Western Tethys. *American Association of Petroleum Geologists Memoir*, 43:164–196.

Ziegler, P. A. and Dèzes, P. (2006). Crustal Evolution of Western and Central Europe. In Gee, D. G. and Stephenson, R. A., editors, *European Lithosphere Dynamics*, pages 43–56. Geological Society, London, Memoir 32.

Pauline CHENIN

Unravelling the impact of inheritance on the Wilson Cycle: A combined mapping and numerical modelling approach applied to the North Atlantic rift system

Résumé

Au travers de cette thèse, j'analyse l'influence de l'*héritage* sur le Cycle de Wilson de l'Atlantique Nord : (1) Je développe des méthodes de cartographie pour mettre en évidence les structures orogéniques majeures, ainsi que l'architecture premier ordre et l'évolution temporelle des systèmes de rift ; (2) Je synthétise l'architecture premier-ordre des systèmes extensifs hyper-étendus et océaniques ; (3) J'étudie, via la modélisation numérique, les conséquences d'un sous-plaquage magmatique sur un système de rift subséquent.

Mes résultats suggèrent que : (1) Les caractéristiques du rift Nord Atlantique diffèrent significativement selon qu'il affecte la lithosphère Calédonienne ou Varisque; (2) Deux types extrêmes de systèmes de rift peuvent être mis en évidence : (a) étroits et immatures (i.e. sans système d'accrétion océanique stable), dont la fermeture mène à des orogenèses essentiellement contrôlées par des processus mécaniques ; et (b) larges et matures, dont la fermeture mène à des orogenèses largement affectées par des processus magmatiques; (3) L'existence de sous-plaquage mafique de la croûte continentale et/ou de manteau appauvri à l'aplomb d'une ancienne zone orogénique peut peut empêcher la réactivation des structures faibles héritées et entraîner le boudinage de la croûte continentale, et par conséquent la formation de micro-continents.

Mots clés : Cycle de Wilson ; Héritage ; Système de rift hyper-étendu ; Atlantique Nord ; Orogenèses Calédonienne et Varisque.

Abstract

In this thesis, I analyse the impact of inheritance on the Wilson Cycle in the North Atlantic: (1) I develop mapping methods to highlight large-scale orogenic structures, the first-order architecture of hyperextended rift systems and the timing of major rifting events; (2) I describe the first-order architecture of hyperextended and oceanic extensional systems; (3) I study, via numerical modelling, the impact of underplating on subsequent rifting events.

My results show that: (1) The characteristics of the North Atlantic rift system varies significantly depending on whether it affects the Caledonian or Variscan orogenic lithosphere; (2) Two end-members for rift systems can be distinguished : (a) narrow and immature (i.e. devoid of steady-state seafloor spreading system), whose closure results in orogenesis essentially controlled by mechanical processes; and (b) wide and mature, whose closure leads to orogenesis largely affected by magmatic processes; (3) The existence of mafic underplating and/or mantle depletion beneath a former orogenic area may prevent the re-activation of the inherited weaknesses and may trigger the *boudinage* of the continental crust, resulting in the formation of micro-continents.

Keywords: Wilson Cycle; Inheritance; Hyperextended rift system; North Atlantic; Caledonian and Variscan orogens.